Denison Mines

Wheeler River Project

Final Environmental Impact Statement

November 2024

Powering
PEOPLE, PARTNERSHIPS AND PASSION.

NUMERICAL MODELLING: POST-DECOMMISSIONING EVALUATION

REPORT PREPARED FOR:

DENISON MINES
345 4TH Avenue South
Saskatoon, SK Canada S7K 1N3

REPORT PREPARED BY:

Ecometrix Incorporated
www.ecometrix.ca
Mississauga, ON

Ref. 19-2649
17 July 2024

Ecometrix | Environmental INTELLIGENCE

NUMERICAL MODELLING: POST-DECOMMISSIONING EVALUATION

PAUL J. MARTIN, M.Sc., P.Eng.
Technical Lead, Groundwater Modelling
Aqua Insight Inc.

PATRICIA MEYER, M.Sc., P.Geo.
Reviewer, Groundwater Modelling
Aqua Insight Inc.

ELIZABETH HAACK, Ph.D., P. Chem.
Technical Lead, Geochemical Modelling
Ecometrix Inc.

R.V. (RON) NICHOLSON, Ph.D., P.Geo.
Review and Approver, Geochemical Modelling
Mine Water Matters Inc.

EXECUTIVE SUMMARY

Denison has collected geological, geotechnical, hydrogeological, geophysical, mineralogical, chemical, and hydrological data for over 16 years as part of their exploration and characterization efforts. From a hydrogeological standpoint, these data were subsequently analyzed and interpreted by Denison, Ecometrix and other consultants and were documented in the Baseline Hydrogeology Report. As additional data were collected, the Conceptual Site Model was refined, and in 2021, groundwater flow and reactive transport modelling tools were constructed to help understand the migration and attenuation of constituents dissolved in groundwater from the Phoenix ore zone, toward Whitefish Lake. This report describes the modelling results which evaluate the transport and fate of the neutralized recovered solution post-decommissioning.

A three-dimensional groundwater flow model was developed at the regional scale and was calibrated to observed water level and stream baseflow data. The groundwater flow patterns in the calibrated groundwater flow model are consistent with the Conceptual Model and observed hydrochemistry in the Upper and Lower Sandstone Aquifers systems. Groundwater flow at the site is dominated by flow through the Upper Aquifer system. Groundwater discharge to Whitefish Lake is primarily through the Upper Aquifer (overburden and upper sandstone aquifer), with a lesser component flowing from the Lower Sandstone Aquifer, through the Desilicified Zone, into the base of Whitefish Lake near its eastern shore.

Groundwater flow from the vicinity of the ore body is observed and simulated in the calibrated groundwater model to travel eastward within the Lower Sandstone Aquifer before moving upward through the Desilicified Zone in the Athabasca Supergroup sandstone units and overlying overburden deposits toward Whitefish Lake. The Desilicified Zone is described as a porous media rather than a fractured rock environment and it facilitates the connection between the Upper and Lower groundwater flow systems in the area east of the Phoenix deposit.

Transport of dissolved constituents was simulated using a three-dimensional geochemical reactive transport approach whereby the chemical reactions were computed using PHREEQC and the transport was computed using FEFLOW. In this manner, dissolved constituents interact with the geologic media through which they are flowing. The modelling approach is complex as numerous constituents in groundwater were considered and chemical reactions included sorption to a limited number of well-understood sorbing phases that were verified through geochemical modelling in other In-Situ Recovery (ISR) projects. Precipitation of mineral phases was also included using learnings from the other ISR projects. This geochemical modelling approach considered sensitivity analysis that included attenuation through redox-driven processes, including reduction of U(VI) (i.e., hexavalent uranium, U^{+6}) to U(IV) (i.e., tetravalent uranium, U^{+4}) and re-immobilization as uraninite downgradient of the mineralized zone. Transport analysis incorporated background conditions that were derived from groundwater quality observations throughout the Site, geochemical reactions sites based on solid phase constituent concentrations and mineralogical assemblages from core analyses, and source conditions consistent with those observed during lab core leaching and flushing experiments.

Transport of dissolved constituents generally follows the predicted groundwater flow paths, with additional spreading due to dispersion, and retardation due to sorption reactions. Dispersion reduces the concentrations as time progresses and the dissolved plume spreads, leading to lower concentrations reaching Whitefish Lake than those that are left in the sub-surface at the mined ore zone. In addition to the dispersion, constituents adsorb to available reaction sites on mineral surfaces (i.e., quartz, goethite, and clay) as the dissolved constituents reach these sites. Sorption removes mass from the dissolved phase and retards its migration through the sub-surface, which effectively reduces the dissolved mass and concentrations that are available to be transported toward Whitefish Lake.

By accounting for these reactions, the simulated dissolved constituent plumes emanating from the ore zone reach their maximum extents within the deeper units (i.e., Lower Sandstone Aquifer and deeper parts of the Desilicified Zone) after approximately 10,000 years. Consequently, concentrations at Whitefish Lake throughout the future centuries are simulated to be similar to background concentrations. Under the base case scenario, which represents a conservative estimate of the conditions present, no exceedances of the groundwater quality screening criteria protective of freshwater aquatic life in the receiving environment were predicted.

A suite of parameter and process uncertainty scenarios were performed to evaluate the potential for concentrations to reach Whitefish Lake above the groundwater quality screening criteria (GQSC) threshold values. A suite of 16 additional scenarios is presented; all scenarios indicated that concentrations of most constituents would not exceed GQSC thresholds. The exceptions include constituents with naturally elevated concentrations or naturally outside of the GQSC range (e.g., iron, manganese, and pH), and a scenario with conservative dispersivity values wherein selenium and cobalt concentrations were simulated to exceed the GQSC by a factor of 1.1 and 1.2, respectively.

The simulated conditions indicate that the natural setting has a large assimilative capacity, such that the mass left in solution within the Phoenix ore zone will be naturally sorbed to available mineral sites within the sub-surface, limiting the potential to be transported to Whitefish Lake throughout the future centuries. Sorption and geochemical reaction, coupled with dispersion is predicted to reduce the concentrations of constituents reaching Whitefish Lake to relatively minor variations from background conditions.

Table of Contents

1.0 INTRODUCTION 1.1

1.1 Scope of Work 1.5

1.2 Organization of Report 1.6

2.0 THREE-DIMENSIONAL GROUNDWATER MODEL DEVELOPMENT 2.1

2.1 Modelling Code Selection 2.1

2.2 Model Structure 2.2
2.2.1 Model Domain 2.2
2.2.2 Model Mesh and Hydrostratigraphic Layers 2.2
2.2.3 Hydrostratigraphic Layers 2.4

2.3 Model Properties 2.6
2.3.1 Hydraulic Conductivity Values 2.6
2.3.2 Storage Values 2.15
2.3.3 Exploration Coreholes 2.17

2.4 Model Boundary Conditions 2.20
2.4.1 Groundwater Recharge 2.20
2.4.2 Surface Water Features 2.22
2.4.3 Perimeter Boundary Conditions 2.24

2.5 Groundwater Model Calibration 2.26
2.5.1 Calibration Targets 2.26
2.5.2 Calibration Results 2.28
2.5.3 Overall Calibration Assessment 2.37

2.6 Enhanced Groundwater Flow Understanding 2.37
2.6.1 3D Groundwater Flow Patterns 2.37
2.6.2 Evaluation of Potential Receiving Bodies 2.40
2.6.3 Groundwater Flow Quantity 2.41
2.6.4 Water Budget for Whitefish Lake 2.42

2.7 Groundwater Conditions During Mine Operations 2.42
2.7.1 Groundwater Demand 2.42
2.7.2 Groundwater Recharge 2.43
2.7.3 Hydrogeological Change Due to Mine Operations 2.43

2.8 Parameter Uncertainty Assessment 2.50
2.8.1 Parameter Uncertainty within the 3D Model 2.50
2.8.2 Focus of Parameter Uncertainty Assessment 2.50
2.8.3 Parameter Uncertainty Assessment Approach and Results 2.52

3.0 GEOCHEMICAL REACTIONS AND MODELLING 3.1

3.1 Important Concepts in Subsurface Assessment for ISR Projects 3.1
3.1.1 Groundwater Remediation 3.1

3.1.2 Assimilative Capacity 3.2
3.1.3 Geochemical Assessment Framework 3.2

3.2 Pre-Mining Existing Conditions 3.3
3.2.1 Mineralogical Composition 3.3
3.2.2 Hydrochemistry 3.9

3.3 Source Condition: Remediated Mining Area Water Quality 3.18

3.4 Expected Geochemical Reactions Along Flow Paths 3.21

3.5 Geochemical Modelling Approach 3.22
3.5.1 Discussion of Solid Liquid Partition Coefficients (K_ds) 3.23
3.5.2 One-Dimensional Geochemical Evaluation 3.24
3.5.3 Thermodynamic Database 3.28
3.5.4 Initial Solutions 3.28
3.5.5 Subsurface Conditions Incorporated 3.30
3.5.6 Evaluation of Geochemical Processes 3.31

3.6 Understanding Gained through 1D Geochemical Modelling 3.55

3.7 Control Files for Three-Dimensional Modelling Analysis 3.56

4.0 POST-DECOMMISSIONING REACTIVE TRANSPORT MODELLING 4.1

4.1 Post Decommissioning Source Zones 4.1

4.2 Simulated COPCs in 3D Reactive Transport Model 4.4

4.3 Groundwater Quality Screening Criteria 4.4

4.4 3D Sub-Domain Model Development 4.6
4.4.1 Sub-Domain Model Area and Mesh 4.6
4.4.2 Sub-Domain Model Hydrogeologic Parameters 4.6
4.4.3 Sub-Domain Model Flow Boundary Conditions 4.7
4.4.4 Sub-Domain Model Transport Boundary Conditions 4.7
4.4.5 Sub-Domain Model Calibration Check 4.8

4.5 3D Geochemical Reactive Transport Simulation: PiChem 4.13

4.6 3D Sub-Domain Model: Base Case Scenario Predictions 4.15
4.6.1 Advective Transport of Dissolved Constituents 4.15
4.6.2 Advection and Dispersion of Dissolved Constituents 4.16
4.6.3 Advection, Dispersion, and Geochemical Reactions 4.20
4.6.4 Matrix Diffusion 4.31
4.6.5 Constituents Reaching Whitefish Lake 4.31
4.6.6 Summary of Base Case Transport Analysis 4.37

4.7 Prediction Uncertainty Analysis 4.37
4.7.1 Prediction Uncertainty Results 4.43

4.8 Summary of Reactive Transport Results 4.48

4.9 Output for Effects Assessment at Whitefish Lake 4.49

5.0 SUMMARY AND CONCLUSIONS 5.1
5.1.1 Understanding of Post-Decommissioning Fate and Transport 5.2
5.2 Limitations 5.3
5.2.1 Simplifications 5.3
5.2.2 Assumptions 5.4
5.2.3 Limitations 5.5

6.0 REFERENCES 6.1

APPENDIX A CREATION OF NUMERICAL MODEL SURFACES A.1

APPENDIX B CALIBRATED HYDRAULIC CONDUCTIVITY DISTRIBUTIONS BY MODEL LAYER B.1

APPENDIX C MODEL LAYER ELEVATIONS C.1

APPENDIX D GROUNDWATER CHEMISTRY D.1

APPENDIX E 1D MODEL SUPPORTING INFORMATION E.1

APPENDIX F SUMMARY OF RESULTS FROM METALLURGICAL TESTING F-1

LIST OF TABLES

Table 2-1: Conceptual and Numerical Hydrostratigraphic Layers 2.4
Table 2-2: Calibrated Hydraulic Conductivity and Anisotropy Values 2.7
Table 2-3: Storage Values Applied in the Model 2.15
Table 2-4: Effective Porosity Values Applied in the Model 2.17
Table 2-5: Model Simulated Lake Stage Elevations 2.22
Table 2-6: Water Level Calibration Statistics 2.33
Table 2-7: Observed and Simulated Vertical Gradients at Available Well Clusters 2.35
Table 2-8: Baseflow Calibration Results 2.37
Table 2-9: Regional Water Budget (Average Annual Rates) 2.41
Table 2-10: Groundwater Discharge to Surface Water Bodies 2.42
Table 3-1: Mineralogy by Unit 3.6
Table 3-2: CaO, Fe Oxide and Clay Content of the Athabasca Supergroup sandstones and Paleoweathered Zone 3.7
Table 3-3: Existing Groundwater Monitoring Network for the Wheeler River Project 3.9

Table 3-4: Summary Statistics, Groundwater and Surface Water Quality, Wheeler River Project 3.12
Table 3-5: UBS Constituent Concentrations at end of mining, Restored Solutions and Representative Groundwater Composition by Hydrostratigraphic Unit....3.20
Table 3-6: Summary of Key Geochemical Processes for Transport of Uranium, other Radionuclides and Trace Elements (US EPA 1999)....3.21
Table 3-7: Progressive Geochemical Evaluation using the 1D Model....3.32
Table 3-8: Saturation Indices for Select Solid Phases in Groundwater Representative of Hydrostratigraphic Units....3.36
Table 3-9: Solid Phase Speciation of Uranium, Existing Conditions (after Percival, 1989)....3.43
Table 3-10: Properties of Adsorbing Mineral Phases....3.45
Table 3-11: Solid-Phase Concentrations and Partitioning Constants for COPCs, measured and simulated....3.47
Table 3-12: Distribution Coefficients (Coefficients (K_d) Used in the IMPACT Model....3.48
Table 3-13: Sorbent Properties of Chlorite....3.51
Table 4-1: Groundwater Quality Screening Criteria....4.5
Table 4-2: Geochemical Zones in 3D Reactive Transport Model....4.14
Table 4-3: Peak Concentrations in Groundwater Reaching Whitefish Lake Base Case....4.35
Table 4-4: Mass Flux to Whitefish Lake: Base Case....4.36
Table 4-5: Predictive Uncertainty Simulations....4.42
Table 4-6: Uncertainty Results: Groundwater Concentrations at Whitefish Lake....4.47

LIST OF FIGURES

Figure 1-1: Ground Surface Topography and Surface Water Features....1.3
Figure 1-2: Project Studies and Key Deliverables....1.4
Figure 2-1: Model Domain and Finite Element Mesh....2.3
Figure 2-2: Three-dimensional View of Elevated Friability Values in the Desilicified Zone....2.5
Figure 2-3: Fracture Frequency Data to Define the Desilicification Zone....2.9
Figure 2-4: RQD Data to Define the Desilicification Zone in Plan View....2.10
Figure 2-5: Model Structure and Hydraulic Conductivity Zones....2.11
Figure 2-6: Representation of Exploration Coreholes within the Groundwater Model....2.19
Figure 2-7: Boundary Conditions – Groundwater Recharge Rates....2.21
Figure 2-8: Boundary Conditions – Surface Water Features....2.23
Figure 2-9: Boundary Conditions – Lateral In/Outflow to Lower Sandstone Aquifer....2.25
Figure 2-10: Location of Model Calibration Targets....2.27
Figure 2-11: Model Simulated Water Level Elevations in the Upper Sandstone Aquifer....2.29
Figure 2-12: Model Simulated Water Level Elevations in the Lower Sandstone Aquifer....2.30
Figure 2-13: Model Calibration Scatterplot....2.31
Figure 2-14: Qualitative Calibration – Lower Sandstone Aquifer Water Level Trends....2.32
Figure 2-15: Spatial Distribution of Model Residuals at All Locations....2.36
Figure 2-16: Groundwater Flow toward Whitefish Lake (A) Plan View, (B) Cross Section....2.39

Figure 2-17: Simulated Pumping Well Drawdown During Mine Operations 2.46
Figure 2-18: Simulated Change in Groundwater Discharge and Flow through Whitefish Lake.. 2.47
Figure 2-19: Groundwater Flow Paths Pre-Mining 2.48
Figure 2-20: Groundwater Flow Paths During Operation 2.49
Figure 2-21: Parameter Zones Included in the Uncertainty Analysis 2.51
Figure 2-22: Hydraulic Conductivity Range Satisfying Calibration Constraints 2.54
Figure 2-23: Calibrated Parameter Values and Realizations Applied for Prediction Uncertainty Analysis 2.55
Figure 3-1: Downgradient Desilicified Zone, Corehole Locations 3.5
Figure 3-2: Regional Groundwater Monitoring Well Clusters 3.10
Figure 3-3: Hydrochemical Type by Hydrostratigraphic Unit, Piper Diagram 3.16
Figure 3-4: Pourbaix Diagrams, Select Monitoring Wells 3.17
Figure 3-5: Schematic of Transport in PHREEQC 3.26
Figure 3-6: 1D Transport, Conceptual Models 3.27
Figure 3-7: Authigenic Mineral Formation: Influence on Peak Uranium Concentrations in Groundwater at Whitefish Lake 3.40
Figure 3-8: Authigenic Mineral Formation: Influence on Peak ^{226}Radium Concentrations in Groundwater at Whitefish Lake 3.41
Figure 3-9: Iron Oxidation: Influence on pH of Groundwater at Whitefish Lake 3.52
Figure 3-10: Sorption and pH-tail: Influence on Peak Uranium Concentrations in Groundwater at Whitefish Lake 3.53
Figure 3-11: Sorption and pH-tail: Influence on pH of Groundwater at Whitefish Lake 3.54
Figure 4-1: Post Decommissioning: Restored Water Source Zones 4.3
Figure 4-2: Sub-Domain Model Extents and Finite Element Mesh 4.10
Figure 4-3: Sub-Domain Model Property Zones 4.11
Figure 4-4: Transport Boundary Conditions and Particle Paths from the Ore Zone to Whitefish Lake 4.12
Figure 4-5: Cross-Section Following Flow Path from the Ore Zone to Whitefish Lake 4.18
Figure 4-6: Example Transport of a Non-Reactive Species: Chloride 4.19
Figure 4-7a: Example Transport of a Reactive Species: Selenium First 1000 Years 4.23
Figure 4-7b: Example Transport of a Reactive Species: Selenium After 1000 Years 4.24
Figure 4-8a: Example of Sorption onto Mineral Phases: Cadmium First 5,000 Years 4.25
Figure 4-8b: Example of Sorption onto Mineral Phases: Cadmium After 10,000 Years 4.26
Figure 4-9a: Example of Sorption onto Mineral Phases: Uranium First 5,000 Years 4.27
Figure 4-9b: Example of Sorption onto Mineral Phases: Uranium First 10,000 Years 4.28
Figure 4-10: Example of Partitioning to Mineral Phases: Uranium 4.29
Figure 4-11: 3D Views of Dissolved Uranium Plume Extent 4.30
Figure 4-12: Representative COPC Concentrations Reaching Whitefish Lake: Base Case 4.33
Figure 4-13: Simulated Mass Loading To Whitefish Lake: Base Case 4.34
Figure 4-14: Simulated Peak Exceedance at Whitefish Lake: Selenium 4.45
Figure 4-15: Simulated Peak Exceedance at Whitefish Lake: Cobalt 4.46

ACRONYMS AND ABBREVIATIONS

1D	One-dimensional
3D	Three-dimensional
7Q10	Seven-day average low streamflow with a return frequency of once in 10-years
AECL	Atomic Energy Canada Limited
BC MOE	British Columbia Ministry of Environment
CCME	Canadian Council of Ministers of the Environment
CEC	Cation Exchange Coefficient
COPC	constituent of potential concern
DEM	Digital elevation model
EA	Environmental Assessment
EIA	Environmental Impact Assessment
EIS	Environmental Impact Statement
ERA	environmental risk assessment
FEFLOW	Finite element groundwater modelling code
GQSC	Groundwater quality screening criteria
GWMP	Groundwater Monitoring Plan
IAEA	International Atomic Energy Agency
IC	Initial condition
IMPACT	Integrated Model for the Probabilistic Assessment of Contaminant Transport
IES	Iterative Ensemble Smoother
ISS	Intermediate Sandstone
ISR	in-situ recovery
Kd	Distribution (i.e., Partitioning) coefficient between a solid and liquid form
Kv, Kvertical	Vertical hydraulic conductivity
Kh, Khorizontal	Horizontal hydraulic conductivity
K_xx	Hydraulic conductivity in the X-direction (i.e., horizontal)
LSA	local study area
LSS	Lower Sandstone
MFa, MFb, MFc, and MFd	Sub-units of the Athabasca Supergroup sandstones
Minteq	Geochemical reaction database
MOE	Ministry of Environment
NRMS	Normalized Root Mean Squared
ORP	Oxidation-reduction potential
PEST	Parameter Estimation modelling code
pe	REDOX potential
PIMA	Portable Infrared Mineral Analyzer
pH	A measure of the acidity of a solution.
PHREEQC	Geochemical reaction modelling code (pH-REdox-EQuilibrium)
QEMSCAN	Quantitative Evaluation of Materials by Scanning Electron Microscopy

REDOX	REDuction / OXidation
RMS	Root Mean Squared
RSA	regional study area
RS1	Restored solution 1
RQD	Rock quality designation
SEQG	Saskatchewan environmental quality guidelines
Ss	Specific Storage
Sy	Specific Yield
TDS	Total Dissolved Solids
US EPA	United States Environmental Protection Agency
w/w	Weight by weight

Units of Measure

%	percent
a	annum (year)
µg/L	Micrograms per litre
µg/m3	micrograms per cubic metre
µg/kg/d	micrograms per kilogram per day
Bq/L	becquerels per litre
g	grams
g/d	grams per day
g/m2/yr	grams per square metre per year
km	kilometre
km2	square kilometre
L/s	Litres per second
L/kg	Litres per kilogram
m	Metre
m asl	metres above sea level
min	Minute
m/a or m/yr	Metres per annum or metres per year
m2/s	Metres squared per second
m3/hr	cubic metre per hour
m3/d	cubic metre per day
m3/s	cubic metre per second
m/s	metres per second
m/d	Metres per day
mg/L	milligrams per litre
mg CaCO3/L	milligrams of calcium carbonate per litre
mg/cm2/30 days	milligrams per square centimetre per 30 days
mg/d	milligrams per day
mg/kg	milligrams per kilogram
mg/kg/d	milligrams per kilogram per day

mm/yr	millimeters per year
yr	Year

1.0 Introduction

Denison Mines Corp. (Denison) is the operator of the Wheeler River Joint Venture that has proposed the development of the high-grade Phoenix uranium deposit located approximately 35 km north-northeast of Cameco's Key Lake Operation and 35 km southwest of Cameco's McArthur River Operation in the eastern portion of the Athabasca Basin region in northern Saskatchewan (See Figure 1-1). The Phoenix uranium deposit is proposed to be mined through an in-situ recovery (ISR) mining operation with on-site processing.

This Groundwater Modelling Report is part of the Environmental Impact Statement (hereafter referred to as "the EIS") submission (Denison, 2024a). The objective of the groundwater flow modelling tasks within the Wheeler River Project EIA is to identify and predict the potential influence of groundwater quality achieved through remediation of the IRS mining area in Decommissioning on the hydrogeological system and nearby surface water features. Groundwater modelling was used to inform our professional judgement regarding the attenuation of constituents in groundwater during transport from the remediated mining area. Consistent with other impact assessments at neighbouring mine sites which have been successfully evaluated and permitted, numerical models are used as predictive tools to understand and evaluate potential impacts from operations. Models are the only appropriate means of evaluating future conditions, as they facilitate bringing proven scientific principles and processes (e.g., groundwater flow, contaminant transport, and geochemical reaction processes) into the evaluation. Not all parameter values will be known *a priori*; as such, models are used as tools to inform professional judgement (i.e., using conservative approaches and through evaluation of uncertainty realizations).

The Baseline Geology and Hydrogeology Report (Ecometrix, 2024a) describes the conceptual understanding of the current physical environment, and hydrogeologic setting present in the study area and the data and information contained in that report are not reiterated herein. As such, the reader is encouraged to review the Baseline Hydrogeology Report for information on the Conceptual Site Model that is numerically represented in the groundwater flow model. The Baseline Hydrogeology Report forms the technical foundation of the groundwater flow modelling undertaken in this study. The Baseline Hydrogeological Report reflects the conceptual hydrogeologic understanding based on the dataset of sub-surface conditions developed from over 16 years of exploration, analysis, and interpretation by Denison, as well as the results of hydrogeologic field investigations carried out in recent years.

This Groundwater Modelling Report describes the development and calibration of the numerical groundwater model and insights gained from application of that model. Figure 1-2 illustrates how the groundwater modelling assessment, and this report, fits into the EIS scope; the groundwater modelling assessment addresses effects post-decommissioning and extending into the future centuries. The results and predictions from the groundwater modelling assessment inform the development of the Groundwater Monitoring Plan (GWMP). The GWMP is an iterative process, that is designed at each Project stage (Pre-Construction through to Post-Decommissioning) to demonstrate compliance with regulations and predictions and protection

of the environment, and to monitor for any changes in groundwater conditions during operations relative to current baseline conditions.

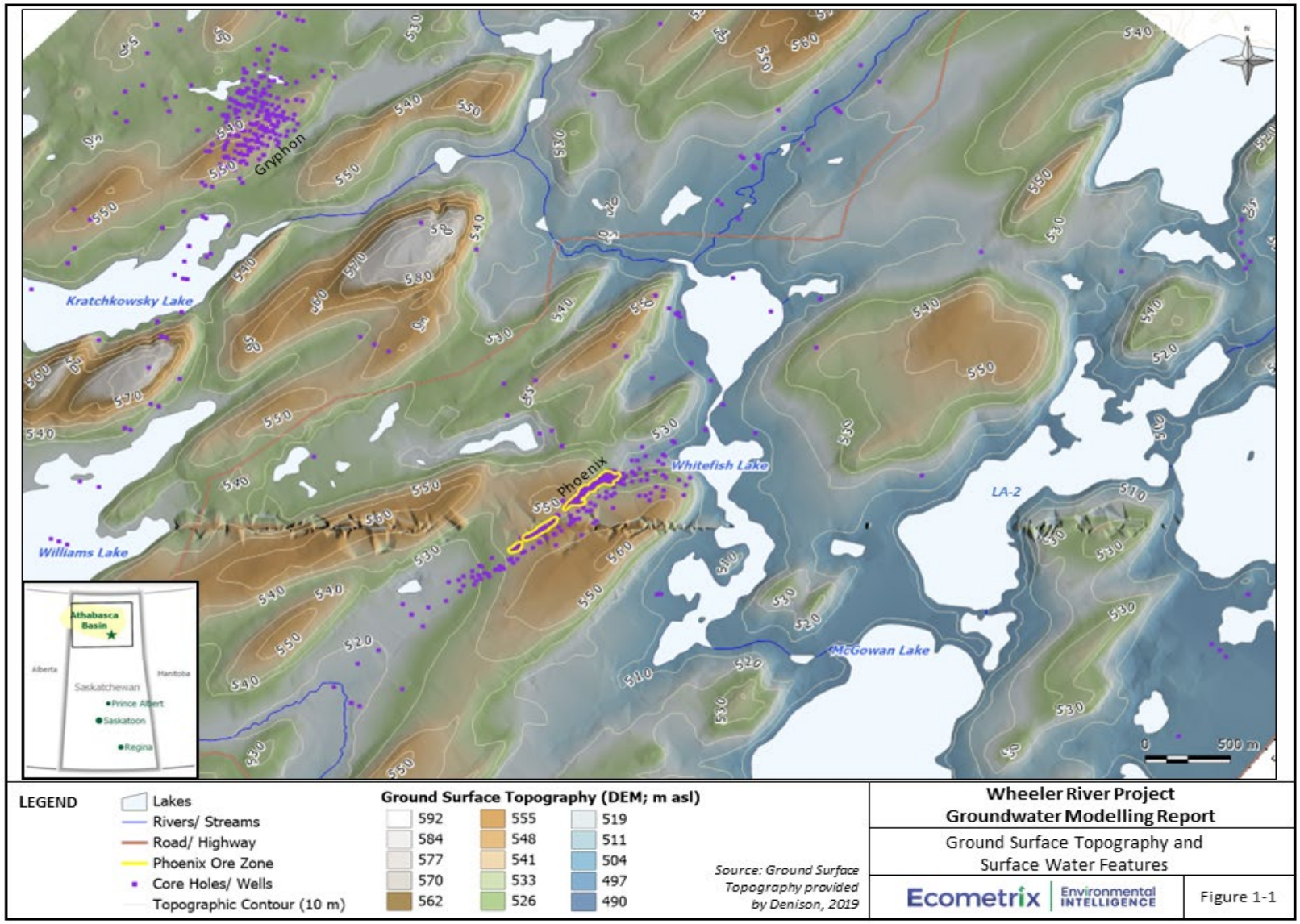

Figure 1-1: Ground Surface Topography and Surface Water Features

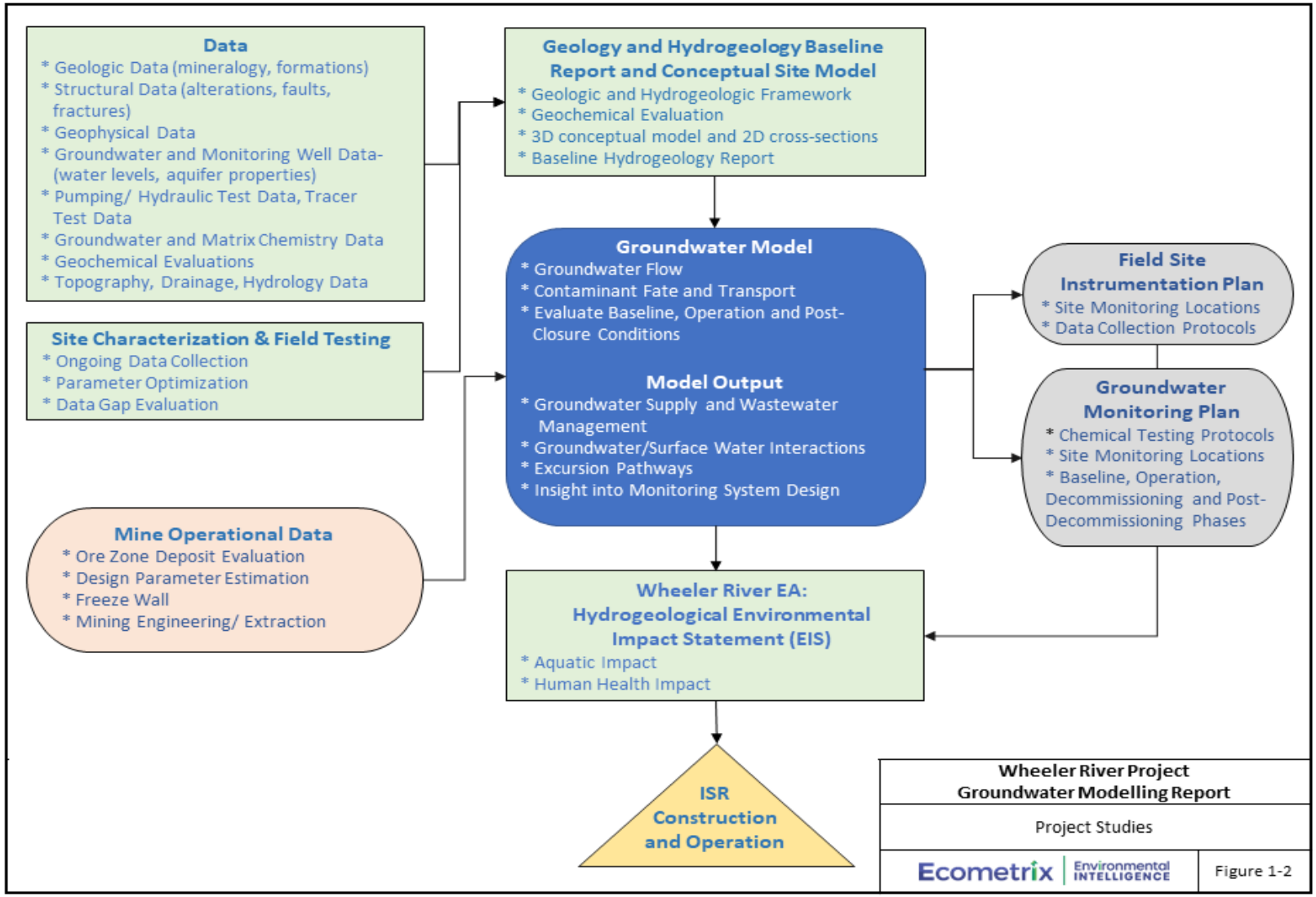

Figure 1-2: Project Studies and Key Deliverables

1.1 Scope of Work

The scope of work for this project involved the development, calibration and application of groundwater flow and contaminant transport modelling tools to support Environmental Assessment (EA) and the (EIS) for the Wheeler River Project. The objective of the modelling completed was to predict potential changes to groundwater quality and quantity following remediation of groundwater quality in the mining area during Decommissioning. Predicted changes in groundwater quantity were evaluated against baseline conditions and in groundwater quality were evaluated against groundwater quality screening criteria. Screening-Level criteria applied were for the protection of aquatic life within the receiving environment (surface water bodies). Potential risks to humans and ecological receptors were further evaluated through environmental risk assessment (Ecometrix, 2024b).

The approach developed to predict groundwater conditions (quality and quantity) associated with the Project was to use a three-dimensional (3D) numerical groundwater flow and transport model (developed using FEFLOW), coupled with a geochemical model (developed using PHREEQC) to complete reactive transport evaluations. This type of approach has been shown to provide advanced insights into complex geochemical reactions involving uranium (Miller, 1993; Bain et al. 2001; Appello and Dimer 2004; U.S.EPA 2012; Bea et al. 2013, Nicholai, 2015; Moore 2020). The modelling approach, although complex in that numerous constituents in groundwater are considered, is relatively straightforward in that the primary interaction of those constituents with the rock matrix is through sorption. The sorbing phases included in the model reflect the mineral composition of the rock matrix and the well-understood sorptive capacities for these minerals. Precipitation of key mineral phases was also included. The modelling approach is one that has been used for several ISR projects (e.g., Johnson et al., 2016; Lagneau et al., 2019; Reimus et al., 2019; de Boissezon et al., 2020).

The 3D numerical model was calibrated to existing groundwater flow conditions beneath and surrounding the Phoenix deposit under current (i.e., 2021) hydrogeologic conditions and then applied to evaluate fate and transport of groundwater migrating from the mining area toward surface water features following remediation of the mining area in Decommissioning. Geochemical reactions were developed to reflect observed geochemical conditions, expected geochemical reactions, and the understanding of groundwater flow patterns. The 3D numerical model is considered conservative as not all potential attenuating processes are simulated, including matrix diffusion, and chemical reactions that include redox transformations of COPCs.

This report outlines the development of modelling tools, their calibration to represent observed conditions at the Site, and modelling applications to develop the understanding required to support conclusions made in the EIS, extending into the future centuries. The modelling was specifically designed to:

- Characterize current (baseline) conditions regarding groundwater flow around and through the Phoenix uranium deposit, and document potential migration pathways for COPCs under existing conditions.

- Simulate post-decommissioning changes to the groundwater flow system and identify potential migration pathways for uranium and other COPCs.

- Simulate post-decommissioning fate and transport of dissolved constituents in groundwater following remediation of the mining area in Decommissioning.

Pathways from the Phoenix deposit toward potential environmental receiving bodies at the surface, such as wetlands, streams, and lakes of ecological importance, were evaluated in support of the EIS. Surface water is considered the appropriate media for evaluation of environmental effects as groundwater is not currently used for domestic purposes based on the following insights:

- there are no non-industrial potable wells listed in the Saskatchewan Groundwater Well Database within the regional study area (100 km radius) surrounding the Wheeler River Project (Ecometrix 2024a). A single domestic well is listed in the search area; this is a shallow well drilled by Cameco Corporation in 1969 to a depth of approximately 72 m bgs, installed in sand. There is also a shallow drinking water well at the existing Wheeler River Project camp, located over two kilometres southwest of the Phoenix deposit. There are no records in the database of groundwater wells for non-industrial use (i.e., being used by residents in the area as a potable water source);

- groundwater use for potable water has not been documented throughout Denison's public engagement process; and

- Existing (baseline) water quality in the deep groundwater beneath the Phoenix area is characterized by several groundwater constituents exceeding drinking water guidelines (Ecometrix, 2024a).

As a result, this study is focused on evaluating groundwater quality that would reach surface water bodies during future centuries for areas where groundwater is interpreted and predicted to be at least partly sourced from the mining area.

1.2 Organization of Report

This report is organized into the following sections:

Section 1.0: Introduction describes the modelling objectives and approach to achieve the defined objectives.

Section 2.0: Three-Dimensional Groundwater Model Development describes the three-dimensional groundwater flow and contaminant transport model, including the input parameters, boundary conditions, and calibration of the groundwater flow model. Analysis of parameter uncertainty is also described.

Section 3.0: Geochemical Reactions and Modelling describes the data and understanding applied to characterize the expected geochemical reactions affecting fate and transport of minerals post-decommissioning.

Section 4.0.: Post-Decommissioning Reactive Transport Modelling describes the modelling predictions for the potential effects on the surface water environment, including the effect of parameter uncertainty on model predictions.

Section 5.0: Summary and Conclusions outlines the summary and conclusions of the modelling work completed, as well as the limitations of the work.

2.0 Three-Dimensional Groundwater Model Development

The numerical groundwater flow and transport model was developed from the Conceptual Model described in the Wheeler River Project Baseline Geology and Hydrogeology report (EcoMetrix, 2024a; hereafter referred to herein as "the Baseline Report"). The groundwater flow model was designed to encompass potential ecological receptors, including the lakes surrounding, upgradient and down-gradient of the Phoenix mining operation area. The model structure is outlined in Section 2.2, the Model Properties in Section 2.3 and model boundary conditions in Section 2.4.

Model calibration is outlined in Section 2.5 and was completed by varying model input parameters and boundary conditions until: 1) the model simulated water level elevations in wells and lakes were a reasonable match to those observed in the area, and 2) the groundwater discharge volume was consistent with estimated stream baseflow. Initial model calibration was completed manually using insights gained through the conceptual model development.

Beyond manual model calibration to groundwater flow conditions, parameter optimization tools were employed to determine parameter combinations that yield an equivalent match to observed conditions. Such alternative, calibrated parameter sets are used to evaluate prediction uncertainty in subsequent simulations, as outlined in Section 2.8.

The 3D groundwater modelling tool developed was subsequently used to complete reactive transport simulations and evaluate fate and transport of dissolved constituents remaining in groundwater (porewater) within the mining area after Decommissioning.

The understanding gained through modelling analyses has been used to inform a groundwater monitoring network and sampling plan over the life of the Project (the EIS, Section 7). Monitoring changes in groundwater levels, gradients and water quality will act as an early-warning system to identify potential excursions from the mining area (i.e., within the freeze wall) and facilitate fine-tuning of mining operations to mitigate any potential identified risks.

2.1 Modelling Code Selection

The code FEFLOW (Diersch, 2014) was selected for use in this assessment because it offers the flexibility to represent complex spatial features at surface and within the subsurface and can represent saturated and unsaturated flow and transport. The modelling code was applied without any modifications to the processes simulated in the code.

FEFLOW is a finite element code whereby the model area (domain) is subdivided horizontally and vertically into a set of triangular prisms called elements that represent a unit of porous media. Each element has specified hydraulic properties such as hydraulic conductivity and storage values that are assigned. FEFLOW simulates the flow of groundwater using the properties assigned within the elements, water level elevations (hydraulic heads) at known locations such as surface water features like lakes and rivers (i.e., boundary conditions) and specified flow through the domain (i.e., groundwater recharge).

2.2 Model Structure

2.2.1 Model Domain

The model domain was designed to simulate the groundwater flow at and surrounding the Phoenix deposit and is illustrated on Figure 2-1. The outer reaches of the model were extended a sufficient distance away from the Phoenix ore zone so the boundaries applied at the perimeter of the model do not influence the simulated groundwater flow conditions in the vicinity of the Phoenix ore zone where model predictions will be made. The model domain extends from Kratchkowsky Lake in the northwest, approximately 5 km east to Whitefish and McGowan Lakes. The model domain is approximately 4.5 kilometers from north to south (Figure 2-1).

The Local Study Area (LSA) for the Geology and Groundwater Valued Components in the EIS was defined by the Model Domain presented in Figure 2-1. The "model domain" and the LSA are referred to interchangeably within this document.

2.2.2 Model Mesh and Hydrostratigraphic Layers

As noted in Section 2.1, FEFLOW is a finite element groundwater modelling software package that simulates groundwater flow by solving mathematical equations governing groundwater flow, contaminant and/or heat transport at discrete node points within the model domain. The first step in building a groundwater flow model using the finite element method is to subdivide the model domain into elements that are collectively referred to as the finite element mesh. Figure 2-1 illustrates a plan view of the model mesh, which consists of triangular elements with nodes at the vertices of the elements. The triangular shaped elements can be of any size; the use of variably shaped elements throughout the domain allows model boundary conditions to accurately conform to natural features such as streams and lakes. The spacing between finite element nodes and the size of the elements is smallest in areas of the model where a more detailed simulation of groundwater levels and contaminant transport is desired. These include the areas around pumping wells and surface water features, such as lakes and rivers.

In this project, the mesh was refined in areas where the representation of drawdown or changes in water levels or chemistry under current or future conditions are expected. Specifically, the mesh was refined to an element size of approximately 5 to 15 m along the Phoenix ore deposit, and to less than 15 m along the margins of the local surface water features in the area. The largest element sizes (less than 200 m) were defined at the periphery of the model further away from the areas of hydrogeologic interest.

The model is flexible and if an additional area of interest, such as a new pumping well, is identified within the model domain, the mesh can readily be refined at that location without negatively impacting the model or its predictions.

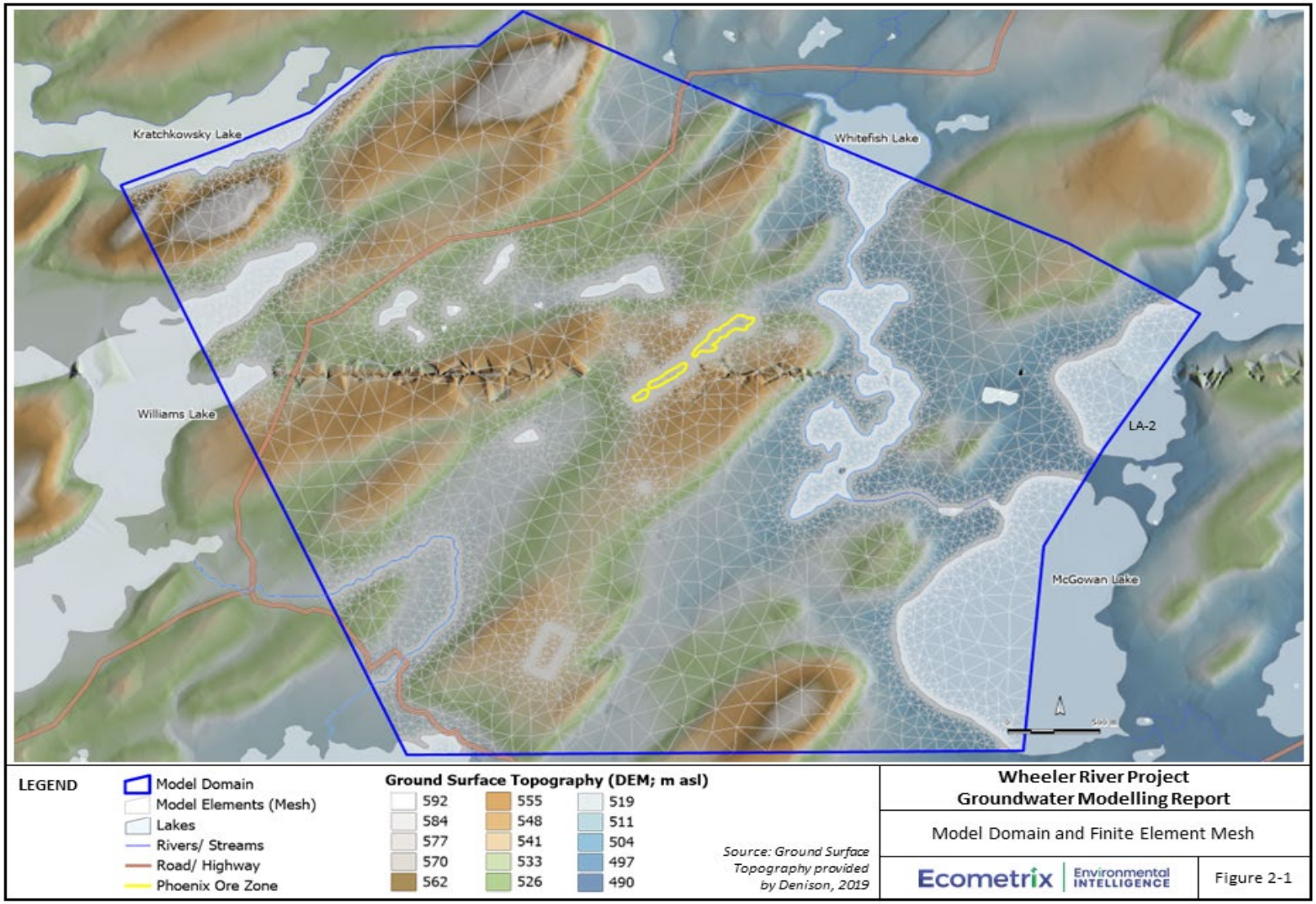

Figure 2-1: Model Domain and Finite Element Mesh

2.2.3 Hydrostratigraphic Layers

In addition to the mesh discretization horizontally, the model domain is also discretized vertically into layers that represent the changing hydrogeologic conditions with depth. As discussed in the Baseline Report, several hydrostratigraphic units were identified and mapped in three dimensions within the Phoenix area. Table 2-1 and Appendix A outlines how each of the numerical model layers assigned within the groundwater flow model were created. The bedrock and basement aquifers and aquitards were subdivided into multiple numerical model layers to capture the changes in groundwater flow directions and gradients with depth.

Table 2-1: Conceptual and Numerical Hydrostratigraphic Layers

Conceptual Model Layer Number	Numerical Model Layer Number	Hydrostratigraphic Unit	Description
1	1	Overburden	Upper Aquifer (Aquitard where Till is present)
2	2, 3, 4	Upper Sandstone Aquifer	Manitou Falls Group; Dunlop Fm unit and upper portion of Collins Fm
3	5 to 9	Intermediate Sandstone Aquitard	Manitou Falls Fm; Collins Fm, lower portion of Bird Fm and upper portion of Read Fm
4	10 to 13	Lower Sandstone Aquifer	Lower portion of Read Fm
5	14	Upper Barrier Zone Aquitard	Upper clay cap and sulphide cemented rock
6	15	Ore Zone Aquifer	Ore Zone
	16	Lower Barrier Zone Aquitard	Lower clay cap and sulphide cemented rock
7	17, 18	Upper Basement Aquitard	Paleoweathered Basement
8	19	Basement Aquitard	Competent Basement

The numerical model layers in this model are continuous across the model domain; however, some of the model layers, such as the clay cap are only present in the vicinity of the ore zone. In these cases, where the layer is interpreted to be absent it is assigned a minimum layer thickness that varies from 0.5 to 5 m, and the hydraulic properties of the overlying unit are applied so the properties of the clay cap are only assigned where it is present. Where multiple layers are "pinched out", the hydraulic properties of the overlying unit are applied to the underlying minimally thick layers, so the numerical model closely replicates the conceptual model. Figure 2-2 illustrates a vertical cross-section through the model where the vertical discretization (i.e., elements) and the hydrostratigraphic model layers listed in Table 2-1 are evident.

The base of the model was specified to lie at a uniform elevation corresponding to sea level (i.e., 0 m asl). Due to the low hydraulic conductivity of the basement rock, vertical leakage was not simulated to occur in or out of the base of the model.

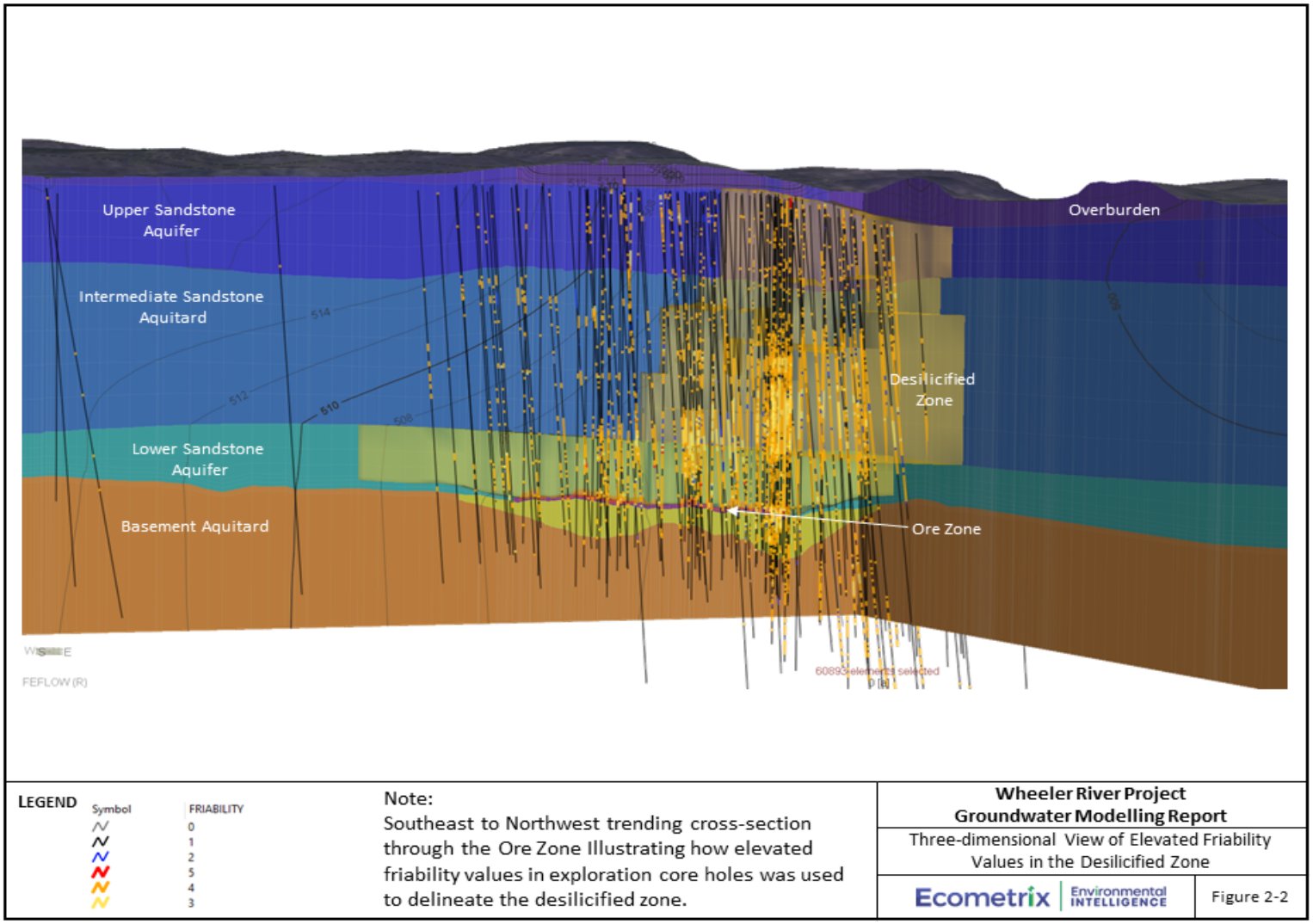

Figure 2-2: Three-dimensional View of Elevated Friability Values in the Desilicified Zone

2.3 Model Properties

Hydrogeologic properties assigned within the FEFLOW model included hydraulic conductivities and storage values (i.e., specific storage and specific yield) as outlined in the following subsections.

2.3.1 Hydraulic Conductivity Values

Hydraulic conductivity values represent the ability of a hydrostratigraphic unit to transmit water. Geologic materials that are highly permeable and able to transmit large volumes of water (e.g., gravel) have high hydraulic conductivity values, while geologic materials that are not as transmissive (e.g., clay) have low hydraulic conductivity values.

Hydraulic conductivities tend to be anisotropic, meaning groundwater travels more easily in one direction than another. Often hydraulic conductivity values in the vertical direction are lower than the horizontal direction as a result horizontal bedding or layering in sedimentary units. Based on literature and professional judgement, an anisotropy ratio of 10 horizontal to 1 vertical was assigned in the model for the unaltered overburden and sandstone hydrostratigraphic units. An anisotropy ratio of 1:1 was assigned to the desilicified sandstone and basement hydrostratigraphic units as the bedding orientations in these units are not expected to be horizontal like the overlying sedimentary layers.

When developing groundwater flow models, initial hydraulic conductivity values are assigned to zones within the various hydrostratigraphic units based on conductivity estimates from field tests conducted in the area (see Appendix B of the Baseline Report), and local knowledge and conceptualization. Literature values (Freeze and Cherry 1979; Anderson and Woessner 2002) were also consulted to ensure the initial and calibrated hydraulic conductivity values were reasonable.

After the initial hydraulic conductivity values are assigned, they are adjusted through the model calibration process (Section 2.5) before arriving at a set of values that produced the best overall simulation of groundwater levels as compared to the observed field data. The range of field-based hydraulic conductivity values are outlined on Table 2-2 alongside the final calibrated hydraulic conductivity values applied in the model. The underlying sections describe the calibrated conductivity values assigned in the model. Appendix B contains plan view maps illustrating the hydraulic conductivity values applied in each model layer.

Table 2-2: Calibrated Hydraulic Conductivity and Anisotropy Values

Hydrostratigraphic Units	Calibrated Horizontal Hydraulic Conductivity Value (m/s)	Anisotropy ($K_{horizontal}$: $K_{vertical}$)
Overburden Aquifer/ Aquitard	$5x10^{-7}$ (till) to $8x10^{-5}$ (sand)	10:1
Upper Sandstone Aquifer	$5x10^{-6}$ (competent rock) to $5x10^{-5}$ (desilicified rock)	10:1 in competent; 1:1 in desilicified
Intermediate Sandstone Aquitard	$1x10^{-8}$ (competent rock) to $5x10^{-6}$ (desilicified rock)	
Lower Sandstone Aquifer	$2x10^{-7}$ to $1x10^{-5}$	
Desilicified Zone Aquifer	$5x10^{-6}$	1:1
Upper Barrier Zone (overlying Ore Zone)	$1x10^{-9}$ to $1x10^{-8}$	10:1
Ore Zone	$7x10^{-10}$ to $2x10^{-5}$	1:1
Lower Barrier Zone (underlying Ore Zone)	$1x10^{-9}$	1:1
Basement Aquitards	$1x10^{-9}$ to $5x10^{-9}$	1:1

2.3.1.1 Overburden

Overburden in the area is a mixture of sand and gravel outwash, and coarse-grained sandy till with 2 - 30% fine grained material (i.e., silt and clay). Coarse-grained sand till is interpreted to lie in the centre and on the surface of the drumlins in the area and horizontal hydraulic conductivity values of $5x10^{-7}$ to $1x10^{-6}$ m/s were assigned to represent this unit (Figure B1, Appendix B). These values are comparable but slightly lower than the interpreted results of hydraulic testing in the Gryphon area ($3.2x10^{-6}$ to $6.3x10^{-6}$ m/s; Golder, 2018), and the Phoenix area ($3x10^{-6}$ m/s; as provided in the Baseline Report) for sand-rich tills.

Outwash sediments flank the sides of the drumlins and in some lowland areas, so higher horizontal hydraulic conductivity values ($5x10^{-5}$ to $8x10^{-5}$ m/s) were applied to represent these silty sands. These values are consistent with the hydraulic testing in the Gryphon area of $3.3x10^{-5}$ m/s, and by Ecometrix (2024a) of $2x10^{-4}$ m/s. The horizontal hydraulic conductivity values applied in the uppermost layer of the model are illustrated on Figure B1 of Appendix B.

2.3.1.2 Upper Sandstone Aquifer

The Upper Sandstone Aquifer consists of fine to medium-grained sandstone with low (less than 3%) normative clay content. Groundwater flow within the sandstone is controlled by the fracture spacing, orientation, connectivity, and aperture thickness, as well as the permeability of the matrix, which in some places has been influenced by diagenesis and alteration.

The calibrated horizontal hydraulic conductivity values of this unit vary depending on the cementation, alteration and fracturing of the sandstone (Figure B2; Appendix B). The Desilicified Zone that extends northeast of the Phoenix deposit to Whitefish Lake consists of fractured and highly friable sandstone and was assigned a horizontal and vertical hydraulic conductivity value of approximately $5x10^{-5}$ m/s. Outside this Desilicified Zone, the more competent and less

fractured sandstone was assigned a lower horizontal conductivity value of $5x10^{-6}$ m/s. These values are consistent with hydraulic conductivity values interpreted from hydraulic tests completed in this aquifer unit that ranged from $4x10^{-7}$ to $2x10^{-4}$ m/s, with a geomean of $3.7x10^{-6}$ m/s (as provided in the Baseline Report).

As the Desilicified Zone is interpreted to have a higher hydraulic conductivity value as compared to the competent Upper Sandstone Aquifer (and Intermediate Sandstone Aquitard) care was taken when mapping the three-dimensional extent of the unit within the groundwater flow model. Three dimensional boreholes illustrating zones of friability were imported into the FEFLOW model to help visualize the location of the Desilicified Zone, as illustrated on Figure 2-2. In addition, four geotechnical parameters (i.e., friability, fracture frequency, normative clay, and Rock Quality Designation) were also mapped in three-dimensions (Figure 2-3) and plan view for each model layer (Figure 2-4) onto the model elements to illustrate the changes in geotechnical properties of the rock. The geotechnical datasets were used to define the spatial extent of the Desilicified Zone through the Lower Sandstone Aquifer, Intermediate Sandstone Aquitard, and Upper Sandstone Aquifer (Figure 2-5).

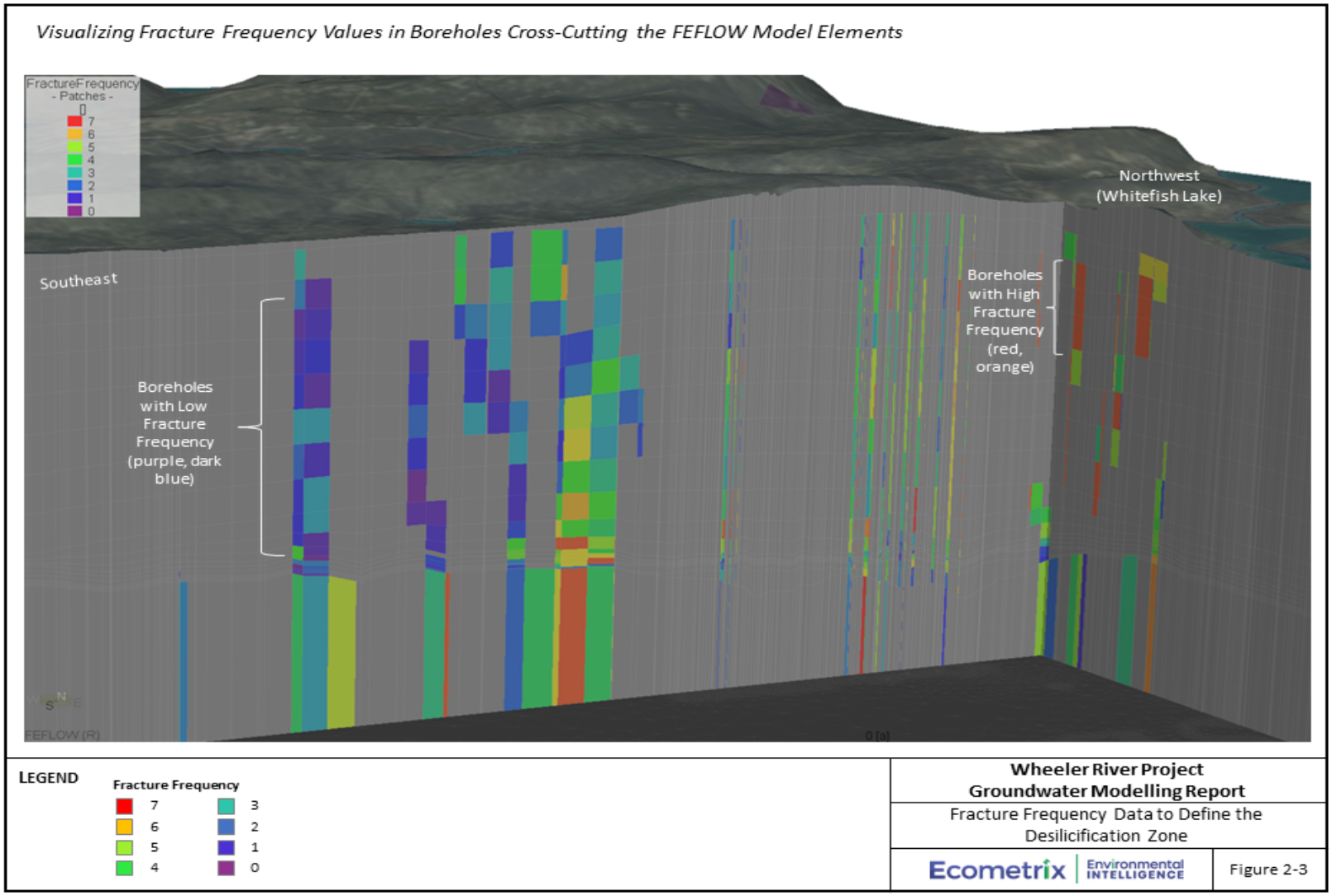

Figure 2-3: Fracture Frequency Data to Define the Desilicification Zone

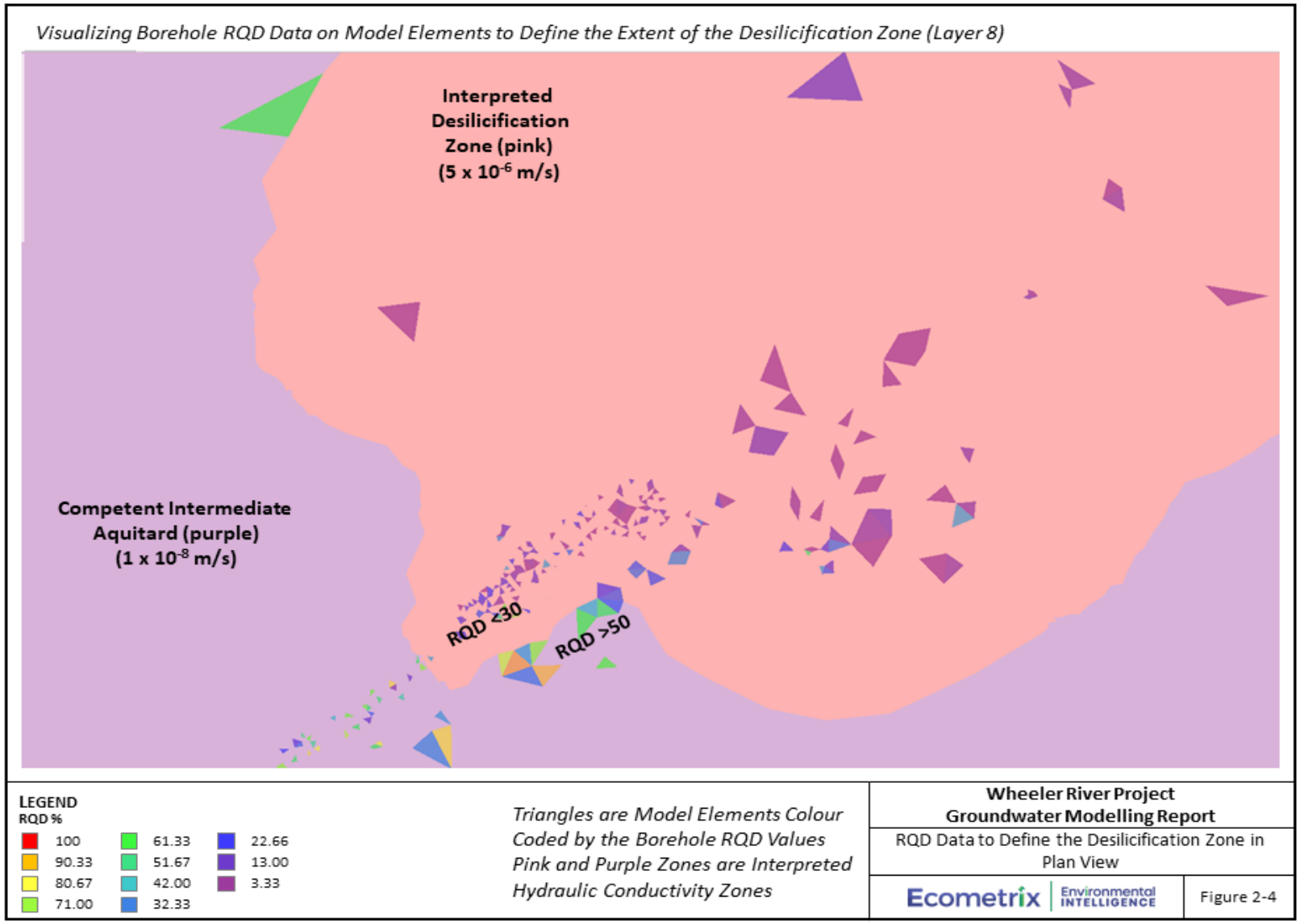

Figure 2-4: RQD Data to Define the Desilicification Zone in Plan View

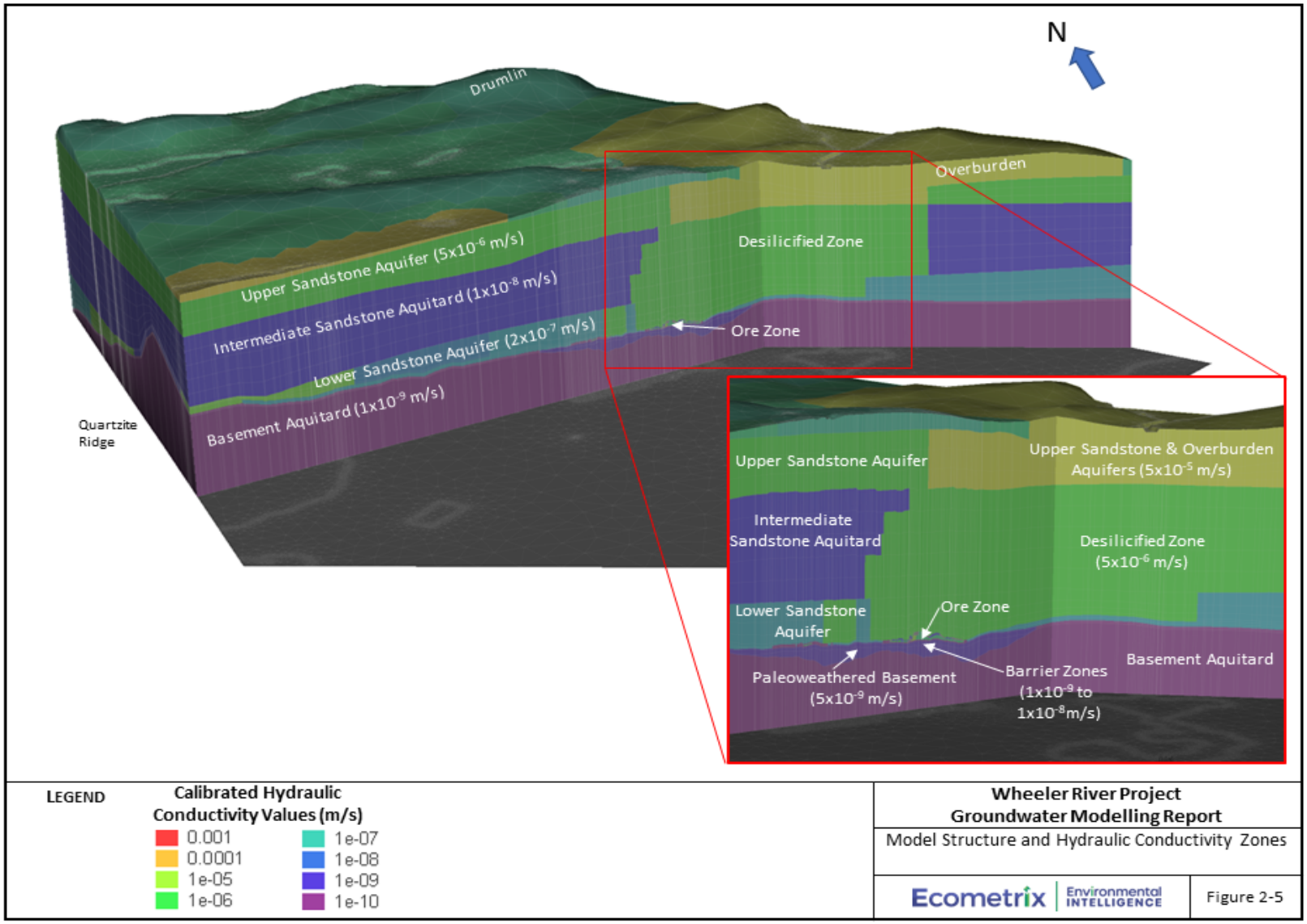

Figure 2-5: Model Structure and Hydraulic Conductivity Zones

2.3.1.3 Intermediate Sandstone Aquitard

The Intermediate Sandstone Aquitard is comprised of competent fractured sandstone with a normative clay content that varies from 4 to 10%. Groundwater flow in this unit is controlled by fracture spacing, orientation, connectivity, and aperture thickness; however, the normative clay is conceptualized to reduce or heal the fractures, reduce their connectivity, and reduce the hydraulic conductivity of this unit.

The calibrated horizontal hydraulic conductivity values of the Intermediate Sandstone Aquitard vary depending on the cementation, alteration and fracturing of the sandstone (Figures B3 and B4; Appendix B). Hydraulic conductivity typically assigned in the model for this unit was $1x10^{-8}$ m/s, which is consistent with values estimated from field-based studies on the competent rock that ranged from $1x10^{-10}$ to $3.8x10^{-6}$ m/s, with a geomean of $8.4x10^{-9}$ m/s (as provided in the Baseline Report).

2.3.1.4 Desilicified Zone

The Desilicified Zone is a distinct zone in the area overlying and east of the Phoenix deposit where the bedrock was subject to hydrothermal alternation resulting in desilicification of the sandstone. The Desilicified Zone is most noticeable in the Intermediate Sandstone Aquitard as the Desilicified Zone is characterized by poor RQD values, and enhanced fracture and friability which are in sharp contrast to the rock qualities of the Intermediate Sandstone Aquitard.

A hydraulic conductivity value of $5x10^{-6}$ m/s was uniformly assigned to the model layers representing the Desilicified Zone. This value is consistent with packer and pumping tests screened in this unit that have interpreted hydraulic conductivity values ranging from $1x10^{-6}$ to $2x10^{-5}$ m/s, with a calculated geomean value of $4.8x10^{-6}$ m/s. As within other units, the geomean value was not applied directly, but rather a rounded value slightly higher than the geomean was applied throughout the entire desilicified zone. The value applied within the desilicified zone is considered conservative as it is a factor of 1.9 higher than the most-reliable hydraulic conductivity estimates (i.e., values obtained through pumping tests measured the conductivity as $2.7x10^{-6}$ m/s) and is equivalent to the geomean value.

Given these differences in the hydraulic conductivity values between the Desilicified Zone ($5x10^{-6}$ m/s) and the Intermediate Sandstone Aquitard ($1x10^{-8}$ m/s), the Desilicified Zone is considered a natural preferential pathway for groundwater to flow from the ore zone and Lower Sandstone Aquifer to Whitefish Lake.

2.3.1.5 Lower Sandstone Aquifer

The Lower Sandstone Aquifer is comprised of fractured and faulted sandstone that overlies the Canadian Shield basement rocks. This unit has a consistently low normative clay content (< 4%), and this trend of low clays is observed in corehole data across the Phoenix and nearby Gryphon areas.

As the normative clay content in this aquifer unit is low, the horizontal hydraulic conductivity value assigned in the model to unfaulted areas is $2x10^{-7}$ m/s, which is higher than the value assigned to the unaltered zone in the overlying Intermediate Sandstone Aquitard ($1x10^{-8}$ m/s). This value is consistent with the range of field values for the Lower Sandstone Aquifer.

Where the fracture spacing and friability are observed to be high, including within the Desilicified Zone, a higher hydraulic conductivity value of $5x10^{-6}$ m/s was assigned (Figure B5; Appendix B). The geomean of hydraulic test values calculated for wells screened in the Desilicified Zone was $4.8x10^{-6}$ m/s and $2.2x10^{-6}$ m/s for wells screened in the Lower Sandstone Aquifer. The desilicified portion of the Lower Sandstone Aquifer is interpreted to follow the trajectory of the WS Shear fault in the basement rock; the interpretation is that there is enhanced fracturing associated with the faulting that follows the WS shear. Cross-faults associated with the WS shear were not interpreted to cause hydrogeologic parameter changes at the scale of the model elements.

The Lower Sandstone Aquifer thins north of the Phoenix deposit where a ridge of quartzite rock protrudes through the sandstone unit. Figure B5 illustrates the zone of low hydraulic conductivity ($1x10^{-8}$ m/s) that corresponds to the quartzite ridge and an area where the Lower Sandstone Aquifer pinches out and has zero thickness.

2.3.1.6 Upper Barrier Zone (Clay Cap and Sulphide Cemented Rock) Aquitard

The deposits associated with the mineralized zone were mapped by Denison (2021) and include a permeable and friable high-grade zone (Unit 2b), with surrounding units that are clay-rich (Unit 2a and 2e), or sulphide-cemented (Unit 1b and 2d). Each unit is interpreted to be discontinuous based on the core data. Clay features are mapped as extending laterally beyond the ore zone by as much as 25 m in some areas, while less than 5 m in other areas; the thickness is interpreted between or beyond coreholes (Denison, 2022b). The combination of clay-rich and sulphide-cemented regions provide a natural barrier between the friable, high-grade ore zone and the overlying sandstone. This barrier has isolated the high-grade ore from groundwater flowing past it (i.e., natural leaching) during the millions of years since deposition of the uranium mineralization. This inference - regarding the natural barrier unit's role to limit migration of chemical constituents away from the ore zone – is the authors' professional opinions on the present-day conditions which includes persistence of the ore body over geologic time and differences in groundwater chemistries within and outside the ore body. The information reviewed and used to formulate this inference is presented in detail in Ecometrix (2024a).

The Upper Barrier Zone includes clay-rich and sulphide cemented rock that overlies the uranium ore zone (Units 1b and 2a). Permeameter-based hydraulic conductivity measurements for the Upper Barrier Zone units ranged from $4x10^{-8}$ to $3x10^{-10}$ m/s.

The percentage of clay within this unit is variable, and as such the hydraulic conductivity value represented in the model is also variable. A Leapfrog model was developed by Petrotek (2020) using available core data. Layers that represent the interpreted percentage of clays and values ranged from 1% to over 50% (Petrotek, 2020). The distribution of the percentage of clay was

used to guide the assignment of hydraulic conductivity values in this layer. Zones in the Leapfrog model where the percentage of clays ranged from 25 to 50% were assigned a hydraulic conductivity of $1x10^{-9}$ m/s in the groundwater model. Zones where the percentage of clays was 9 to 25% were assigned a hydraulic conductivity value of $1x10^{-8}$ m/s in the groundwater model. Zones where the percentage of clays was less than 9% were assumed to be absent and were conservatively assigned the same conductivity value as the ore zone ($1x10^{-6}$ m/s). The Upper Barrier Zone only exists in the area surrounding the ore zone; therefore, the thickness of the model layer representing this unit is minimally thin outside the ore zone. Figure B6 (Appendix B) illustrates the hydraulic conductivity values applied in the model for this unit.

2.3.1.7 Ore Zone

The deposits associated with the mineralized zone were mapped by Denison (2021) and include a permeable and friable high-grade zone (Unit 2b). Permeameter-based hydraulic conductivity measurements for the high-grade zone are reported to have a median of $2x10^{-7}$ m/s and an upper quartile conductivity of $7x10^{-7}$ m/s (Denison, 2022b); those measures are biased low as they are focused on the rock core rather than the fractured media, but they provide an indication of the background matrix hydraulic conductivity.

Hydraulic conductivity values within the ore zone were assigned in the groundwater flow model using the hydraulic conductivity values applied in a detailed MODFLOW groundwater flow model of the ore zone in Phases 1 and 2 (Petrotek, 2020). The horizontal hydraulic conductivity zones and values from the Petrotek groundwater flow model ranged from $2x10^{-5}$ to $7x10^{-10}$ m/s, and these zones were applied in the regional scale groundwater flow model. The values applied are consistent with interpreted hydraulic conductivity results from pumping tests screened within Phases 1 and 2 of the Phoenix deposit (Figure B7; Appendix B). A hydraulic conductivity value of $1x10^{-6}$ m/s was uniformly applied in the ore zone within Phases 3 and 4 as these zones had not been subject to additional hydrogeologic characterization at the time of this report.

2.3.1.8 Lower Barrier Zone Aquitard

The deposits associated with the Lower Barrier Zone Aquitard were also mapped by Denison (Denison, 2022b) and included a clay-rich unit (2e), and a sulphide-cemented unit (2d). Permeameter-based hydraulic conductivity measurements for the lower barrier units ranged from $3x10^{-8}$ to $8x10^{-13}$ m/s.

To be conservative, the Lower Barrie Zone aquitard is interpreted to have the same properties as the Upper Barrier Zone. The Lower Barrier Zone aquitard lies within the basement rock where the percentage of clay minerals is much higher. The thickness of the Lower Barrier Zone Aquitard was provided by Denison (Denison, 2022b) and assigned a horizontal hydraulic conductivity of $1x10^{-9}$ m/s (Figure B8, Appendix B). This value is consistent with the hydraulic conductivity values estimated from permeameter testing conducted by Denison (Denison, 2022b).

2.3.1.9 Paleoweathered and Competent Basement Aquitard

The upper Paleoweathered Basement Aquitard is comprised of more fractured and faulted basement rocks as compared to the lower competent basement rock. The more fractured portion is interpreted to be limited to the area surrounding the WS Shear fault. A horizontal hydraulic conductivity value for the paleoweathered zone was estimated at $5x10^{-9}$ m/s. This value is consistent with the geomean of interpreted hydraulic testing of the Basement Aquitard, which was $4.8x10^{-9}$ m/s. The paleoweathered zone extends in a southwest to northeast direction along the trend of the WS Shear as illustrated on Figure B9 (Appendix B).

The Competent Basement Aquitard is comprised of competent basement rocks with little to no fracturing. Where unfractured, the basement rocks have very low permeability and porosity values. A hydraulic conductivity value of $1x10^{-9}$ m/s was applied in the model to represent the competent basement rock, which is within the range of field-based values ($1.1x10^{-11}$ m/s to $1.1x10^{-5}$ m/s, with a geomean of $4.8x10^{-9}$ m/s).

The low hydraulic conductivity assigned to the competent basement aquitard is consistent with observed water quality and dissolved minerals.

2.3.2 Storage Values

Groundwater storage is defined as the quantity of water released from storage due to a unit change in pressure head. Specific storage and yield values are not used in calculating water level elevations in steady-state (i.e., long term average annual simulations), but are used in simulating or predicting time varying (transient) conditions. Specific yield and specific storage values control the timing and response of the groundwater system to external stresses such as pumping and injection.

The storage coefficient used during FEFLOW calculations varies depending on if the aquifer is unconfined or confined. Where confined, the storage coefficient is referred to as Specific Storage (Ss), which for bedrock aquifer materials ranges from $1x10^{-6}$ to $5x10^{-4}$ /m. In an unconfined aquifer, the storage is referred to as specific yield (Sy) where the predominant source of water is gravity drainage from pores at the water table.

Storage estimates assigned to the model layers in the groundwater flow model were within the ranges of values outlined in the Baseline Report. Specific yield and specific storage values were assigned to zones coincident with the hydraulic conductivity zones and are listed in Table 2-3 and illustrated on the figures in Appendix B.

Table 2-3: Storage Values Applied in the Model

Hydrostratigraphic Units	Specific Yield (Unconfined Aquifers)	Specific Storage (1/m)
Overburden Aquifer	0.2	$1x10^{-4}$
Upper Sandstone Aquifer	0.2	$1x10^{-4}$
Intermediate SandstoneAquitard	(Units are confined,	$1x10^{-5}$

Hydrostratigraphic Units	Specific Yield (Unconfined Aquifers)	Specific Storage (1/m)
Lower Sandstone Aquifer	Sy values not assigned)	$1x10^{-4}$
Desilicified Zone Aquifer		$1x10^{-4}$
Upper and Lower Barrier Zone Aquitards		$1x10^{-6}$
Ore Zone Aquifer		$3x10^{-4}$
Basement Aquitard		$1x10^{-6}$

2.3.2.1 Porosity Values

Groundwater flow models provide estimates of the Darcy flux, or flow rate of groundwater per unit cross-sectional area through porous media (i.e., overburden or rock). To estimate the linear groundwater velocity, representing the speed at which a particle of water might travel, the Darcy flux is divided by the effective porosity of the porous media. Effective porosity is less than the total porosity of a porous media, as it represents only the portion of pores that are interconnected. While a fractured rock may have a high proportion of pore space, many of those pores may not be interconnected. Disconnected pores do not act as pathways for groundwater to travel, but rather act as storage locations.

As outlined in the Baseline Hydrogeology Report, the overburden aquifer is estimated to have an effective porosity of 0.25 on the coarse-grained sand outwash, 0.20 on silty sands and 0.18 on silty sand tills (Table 2-4).

In fractured bedrock, porosity consists of the space between grains (primary porosity), and fractures and dissolution features (secondary porosity). A proportion of the primary and secondary porosity features will be disconnected and will not act as pathways for groundwater flow or contaminant transport. Based on permeameter testing completed on rock core samples (Scibek, 2019), the total porosity within the sandstone units is estimated to average from 10 to 40%, whereas the fracture volume that leads to effective porosity is estimated to be much lower (i.e., 0.01%).

As tracer test results to estimate effective porosity were unavailable at the time of modelling, effective porosity values for the sandstone bedrock and basement units were sourced from literature values (Table 2-4). The Cigar Lake uranium mine is located approximately 75 kilometres northeast of the Phoenix deposit and has similar geologic and hydrogeologic properties as the Phoenix deposit. The effective porosities from the Cigar Lake study (AECL, 1994) are a suitable analogue for this study and are listed on Table 2-4 alongside effective porosity values applied in the numerical model in this study.

Table 2-4: Effective Porosity Values Applied in the Model

Hydrostratigraphic Units	Effective Porosity (%)	
	This Study	AECL (1994)
Overburden Aquifer	18% (till) to 25% (sand)	30%
Upper Sandstone Aquifer	1 to 3%	2% to 5%
Intermediate Sandstone Aquitard	1% to 3% (10 to 20% in Desilicified Zone)	1% to 5% (20% in "weathered sandstone")
Lower Sandstone Aquifer	1%, 10 to 20% in Desilicified Zone	20% in "fractured/ altered sandstone"
Upper and Lower Barrier Zone Aquitards	20%	5%
Desilicified Zone	20%	20%
Ore Zone Aquifer	1%	5%
Basement Aquitard	0.1%	0.1%

Effective porosity does not affect the simulated groundwater water level elevations, or the flux of water computed to move through an aquifer or discharging to a boundary condition. Linear groundwater velocities are required for particle tracking and calculating travel time, for example, advective travel time from the ore zone to nearby receptors.

2.3.3 Exploration Coreholes

Exploration coreholes drilled in the Phoenix area, where not decommissioned, have the potential to act as preferential flow paths between the Upper and Lower Sandstone Aquifers. Most exploration boreholes were partially plugged with grout approximately 10 to 20 m above and below the ore zone, while the remainder of the corehole was left to naturally collapse, to protect surficial aquifers. In areas where the Rock Quality Designation (RQD) is low, such as in the Desilicified Zone, the coreholes are expected to have readily collapsed and are thus interpreted to be infilled with sand from the area surrounding the corehole. In areas where the RQD was high, indicating dense intact rock core was recovered, less infill is expected to have occurred. Infill is expected to be sand from the Desilicified, or more friable portions of the Athabasca sandstone.

There are over 400 boreholes that lie along the WS Shear in the vicinity of the Phoenix deposit, most of which were drilled as NQ diameter holes (diameter = 75 mm). The hydraulic impact of these exploration coreholes was evaluated in the model using one-dimensional line elements superimposed on the three-dimensional finite element mesh. Clusters of exploration coreholes were grouped together based on location and represented in the model as one line element. Figure 2-6 illustrates the locations of grouped coreholes represented in the model, along with the number of exploration coreholes represented at each location, and the relative hydraulic conductivity assigned to the line element. The cross-sectional area specified in the model was increased to reflect the number of coreholes represented by each cluster, as labeled on Figure 2-6. The hydraulic conductivity was assigned based on a review of the RQD for each cluster of

coreholes; coreholes with high RQD were assigned a higher hydraulic conductivity, and conversely lower RQD areas were assigned a lower hydraulic conductivity. The corehole hydraulic conductivity simulated was a factor of 2 to 100 times greater than the surrounding host media, based on the background conductivity and the expected infill characteristics.

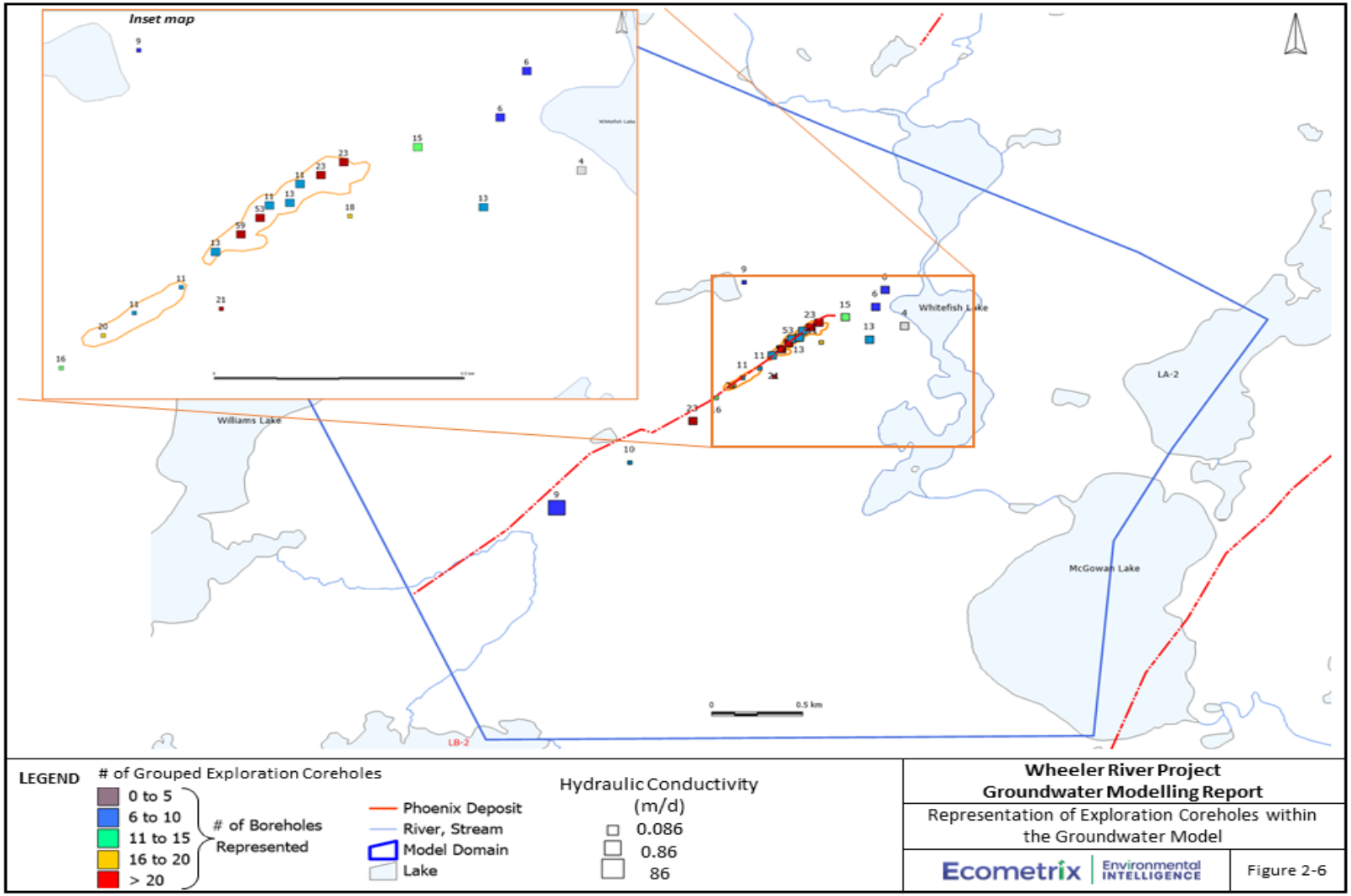

Figure 2-6: Representation of Exploration Coreholes within the Groundwater Model

2.4 Model Boundary Conditions

Boundary conditions applied in the groundwater flow model were chosen to approximate the regional groundwater flow patterns and to approximate the major groundwater fluxes in the model domain. Boundary conditions applied in the model consisted of two types:

- Specified head boundary conditions are boundaries where the value of the hydraulic head is assigned to nodes within the model, and the amount of discharge into or out of the model fluctuates to satisfy the head condition. Physically, these boundary conditions (specified heads) are commonly used to simulate areas where hydraulic potentials are expected to remain at a constant level. This is commonly used to simulate flow to and from large rivers, lakes, or areas where water enters or exits the model domain.

- Specified flux boundary conditions are boundary conditions for which a flux value is assigned to specific nodes. The hydraulic head within the surrounding elements is computed to meet that flux condition. These boundary conditions are used to represent groundwater extraction or injection wells, and recharge to the groundwater system. No flow boundaries are one type of specified flux boundary where the rate of lateral flow across the boundary is assumed to be negligible or equal to zero. In general, no flow boundaries are applied to simulate groundwater divides or impermeable geologic units.

Boundary conditions applied in this model include groundwater recharge, flow into and out of surface water features such as rivers and lakes, groundwater pumping wells, and flow into and out of the model along the perimeter of the model. The boundary conditions applied are described in the following subsections.

2.4.1 Groundwater Recharge

Groundwater recharge refers to the amount of water that infiltrates through the unsaturated zone and reaches the underlying watertable. The rate of groundwater recharge is dependent on precipitation, vegetation, surficial soil type (geology), physiography, and ground surface topography. Recharge is enhanced in areas where the ground surface is hummocky as the potential for overland flow to nearby creeks and rivers is reduced.

As noted in the Baseline Report, the estimated average annual recharge rate for the Phoenix site is approximately 156 mm/year. The groundwater recharge rates applied in the model are illustrated on Figure 2-7 and range from a low of 100 mm/year on the drumlins and areas where tills are interpreted to lie at surface, to a high of 165 mm/year where sands are interpreted to lie at surface.

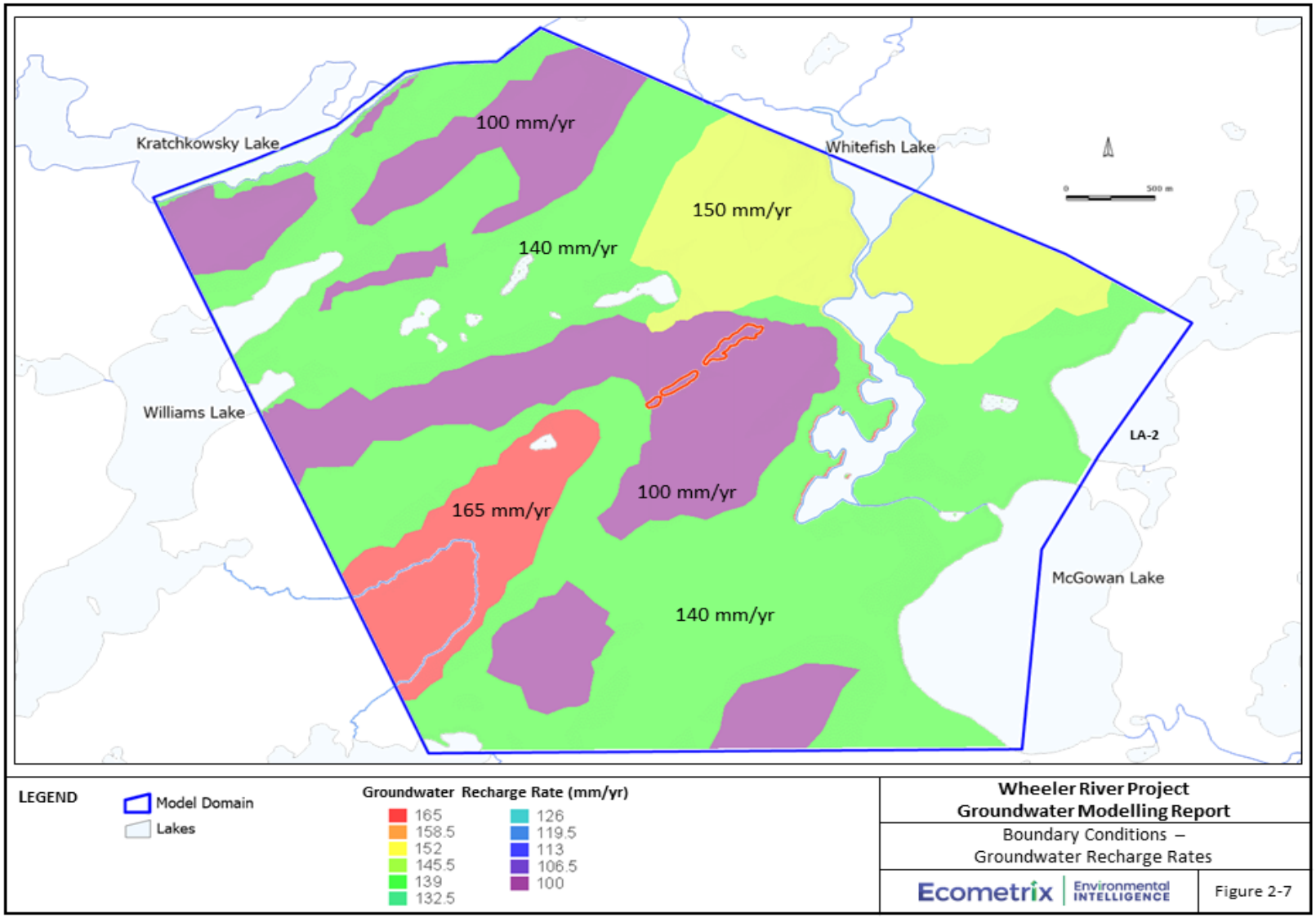

Figure 2-7: Boundary Conditions – Groundwater Recharge Rates

2.4.2 Surface Water Features

Interaction between groundwater and surface water features are simulated in the model using specified head boundary conditions. Based on the model simulated groundwater level, and the water level assigned to represent the surface water stage, groundwater may be simulated to discharge into the surface water body or recharge the underlying aquifer.

Several lakes located within the model domain were modelled using specified head boundary conditions. The water level elevations of these lakes were assigned based on observed water level elevations (within the Baseline Report), as outlined in Table 2-5 and Figure 2-8.

Table 2-5: Model Simulated Lake Stage Elevations

Lake Name	Lake Stage Elevation (m asl)
Whitefish Lake	500.0
McGowan Lake	494.2
Kratchkowsky Lake	520.8
Williams Lake	518.4
LA-2	494.4

Several smaller lakes were also assigned using specified head boundary conditions and where water level data were unavailable, the ground surface elevation represented in the Digital Elevation Model (DEM) was applied (Figure 2-8).

In addition to the boundary conditions represented for the lakes and ponds, two rivers and streams were simulated in the model by assigning declining specified head boundary conditions along each stream segment. The specified head assigned in the model to represent the stream or river stage elevation was estimated using the DEM. These surface water boundary conditions are illustrated on Figure 2-8.

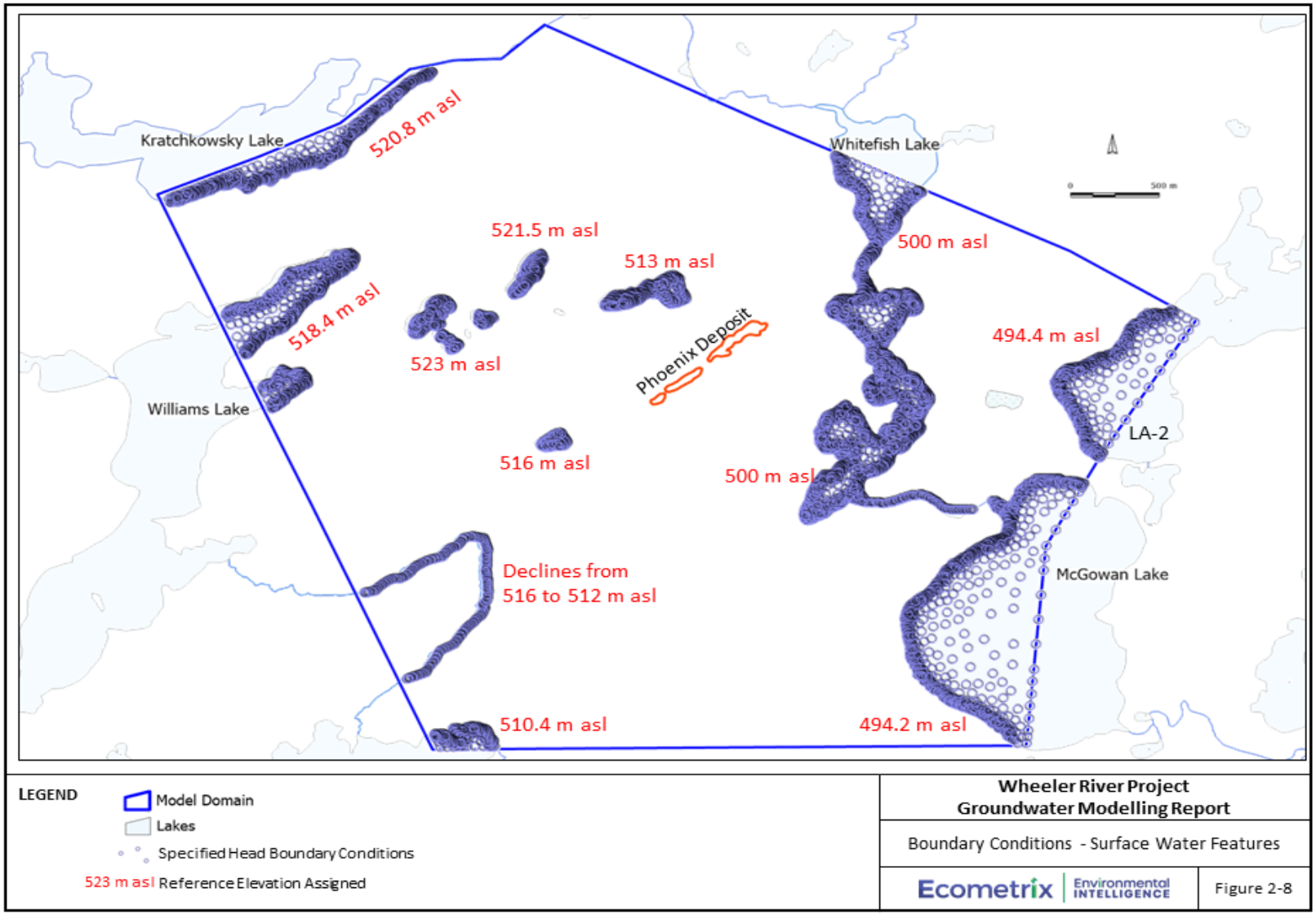

Figure 2-8: Boundary Conditions – Surface Water Features

2.4.3 Perimeter Boundary Conditions

The model domain extends from Kratchkowsky and Williams Lakes in the west to Whitefish, McGowan, and LA-2 Lakes in the east. Aside from these natural boundaries, additional boundary conditions were applied to simulate the flow of groundwater into and out of the model domain along the perimeter of the model domain (Figure 2-9).

Specified head boundary conditions were assigned in the Lower Sandstone Aquifer along the northwestern and southwestern edges of the model domain to allow water to enter the model; an elevation of 520 m asl was selected for the area near Kratchkowsky Lake based on observed water level elevations in the Gryphon area, while the area near Williams Lake was assigned an elevation of 516 m asl based on water levels within the overlying stream.

A specified head boundary condition was also assigned in the Lower Sandstone Aquifer along the south edge the model domain to allow groundwater to flow out of the model domain toward Russell Lake (Figure 2-9). For this boundary condition, the hydraulic gradient between the Phoenix deposit and Russell Lake was used to linearly estimate an appropriate hydraulic head value at the model boundary.

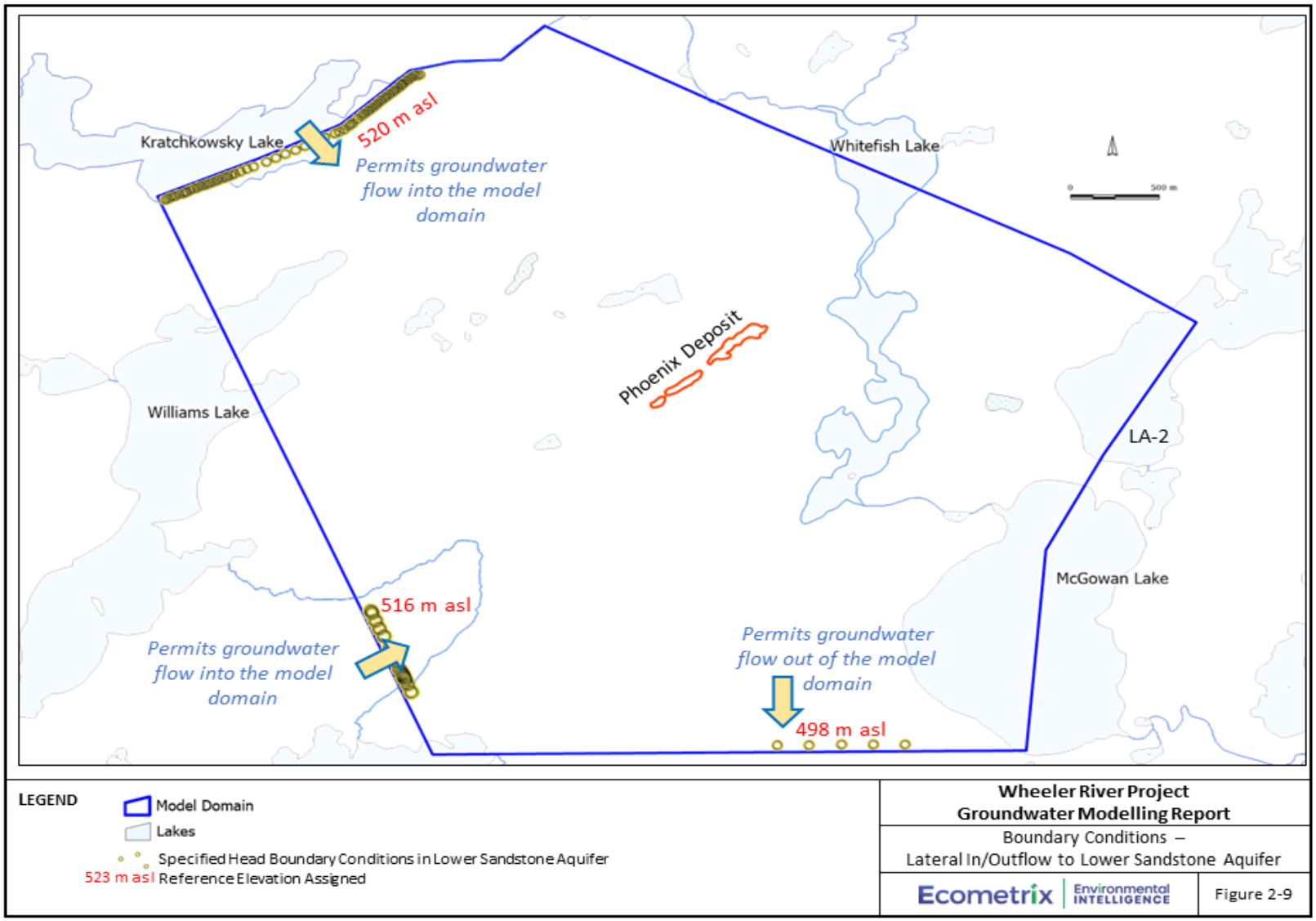

Figure 2-9: Boundary Conditions – Lateral In/Outflow to Lower Sandstone Aquifer

2.5 Groundwater Model Calibration

The purpose of model calibration is to determine a set of parameter and boundary condition values such that the groundwater flow model can reproduce field-measured water level elevations in wells, and groundwater discharge estimated in surface water features. Numerical groundwater flow models are typically calibrated by systematically adjusting the model input parameters and boundary conditions to determine the optimum match (within an acceptable margin of error) between the model predicted results and field observations. The model's ability to represent observed conditions is assessed qualitatively by comparing to trends in water levels and distribution of groundwater discharge and quantitatively through statistical measures of fit to field-measured water levels and stream baseflow.

The model calibration approach included calibration to long term, average annual (i.e., steady state) water level elevations collected in monitoring wells and exploration boreholes across the model domain. The model was also calibrated to estimated groundwater discharge (i.e., stream baseflow) values.

2.5.1 Calibration Targets

Calibration targets are measurements of hydraulic heads or flows that are compared to the model-predicted values during the model calibration process. The steady-state groundwater flow model was calibrated to water level measurements reported in GWR monitoring wells, as well as lower-quality water level measurements collected in exploration boreholes. The model was also calibrated to a range of streamflow measurements collected for stream reaches within the model domain.

2.5.1.1 Water Level Elevations

Groundwater level elevations observed in the GWR monitoring wells represent the highest quality water level data in the study area and attempts were made to match these water levels as closely as possible using the groundwater flow model. The locations of the GWR monitoring wells that had available water level data are illustrated as pink circles on Figure 2-10. Of the 21 monitoring wells available at the time of model calibration, seven were screened in the Overburden and Upper Sandstone Aquifers, six were screened in the Sandstone Aquitard, and eight were screened in the Lower Sandstone, Basement Aquitards and the ore zone.

Observed water levels in 172 exploration boreholes within the model domain were also used as lower quality calibration targets as there is much more data and it extends spatially across the model domain (Figure 2-10; orange squares). Most of the boreholes do not contain a screened interval and are able to exchange water along their entire open length (i.e., from the top of bedrock to the basement aquitard); as such observed water levels represent a blended water level for the length of open interval. The observed water levels in the exploration boreholes were interpreted to be representative of the Lower Sandstone Aquifer as the water levels in these wells closely matched observed water level elevations in nearby GWR wells that are screened in this aquifer unit.

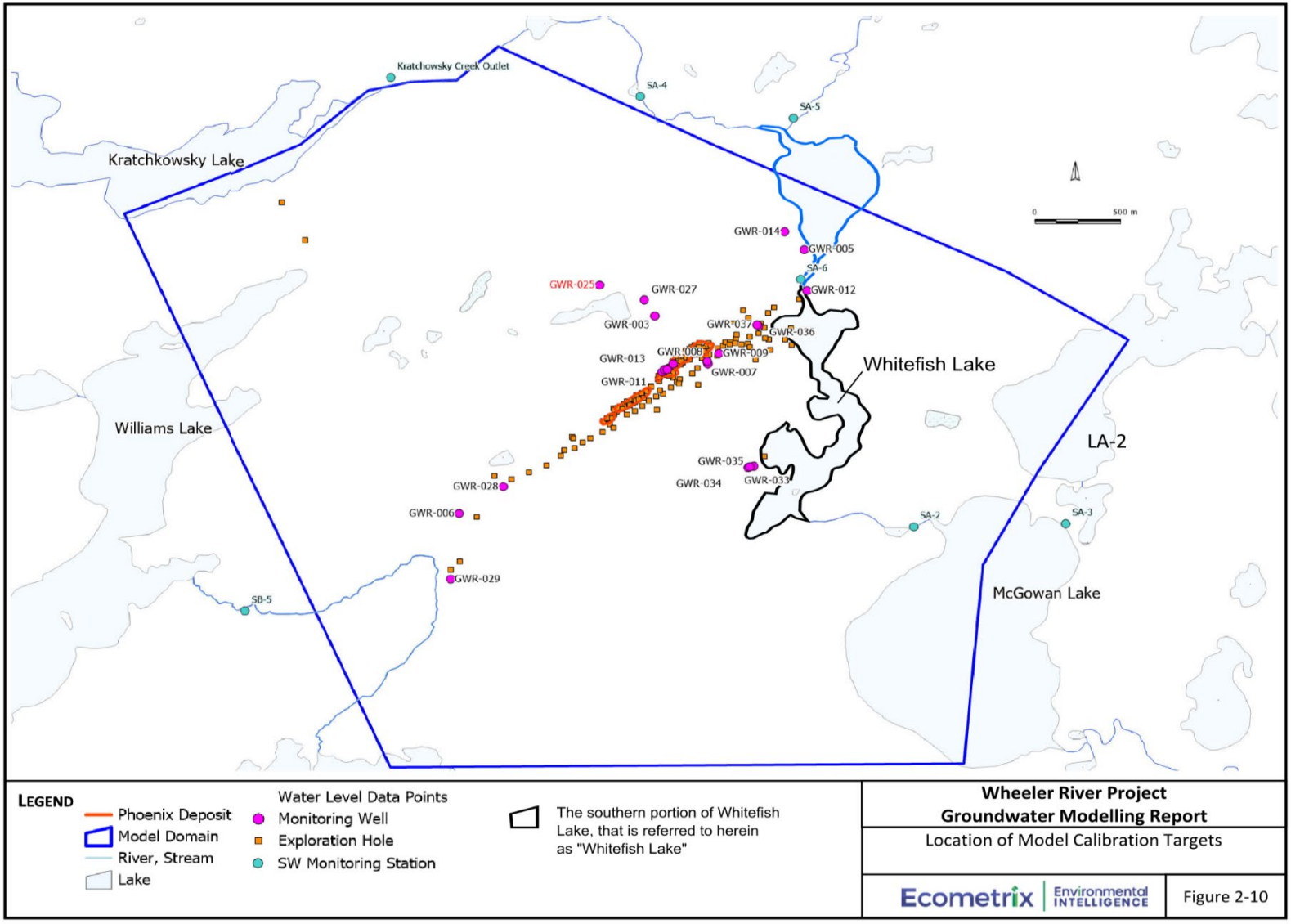

Figure 2-10: Location of Model Calibration Targets

2.5.1.2 Groundwater Discharge Data

In addition to calibrating against water level elevation data, the model was also calibrated to groundwater discharge (i.e., stream baseflow) data. Stream baseflow refers to the slow release of water in a watershed. Baseflow calibration targets were developed using spot flow measurement data. Spotflow measurements refer to instantaneous measurement of streamflow collected during interpreted baseflow conditions.

2.5.2 Calibration Results

The following subsections provide an overview of the model calibration results and establish that the three-dimensional numerical model designed to assess potential environmental change under future scenarios is suitably calibrated. The calibration achieved is evaluated as follows:

- Quantitative error, based on the difference between observed and simulated water levels, is minimal and there are no spatial trends in this error.
- Locally within the vicinity of the ore zone, the simulated water levels and hydraulic head patterns are close to observed conditions.
- Simulated groundwater discharge rates agree favourably with measured flow differences between monitoring stations upstream and downstream of Whitefish Lake.

2.5.2.1 Water Level Elevations – Quantitative Calibration

Figures 2-11 and 2-12 illustrate the simulated water level elevations in the Upper Sandstone and Lower Sandstone Aquifers, respectively. The calibration residuals in the monitoring wells are illustrated on the maps and illustrate the excellent fit between the model-predicted and observed water levels.

The model simulated fit to observed water levels is illustrated in a scatterplot (Figure 2-13), which illustrates the level of fit between observed (horizontal axis) and model-simulated (vertical axis) water levels. The line of ideal fit, which corresponds to an exact match between observed and simulated values, is illustrated as a 45-degree line extending through the origin. A deviation of ±2 m is shown on the plots as parallel lines offset from the line of ideal fit, which illustrates that most of the simulated water levels are within 2 m of the observed values. Points that lie outside may be due to generalization of modelled hydrogeologic parameters or errors associated with the field-observed data such as incorrect location coordinates, ground surface elevation, or water level readings.

The scatterplot also illustrates that there is no bias towards over-estimating or under-estimating groundwater levels. These trends appear to be consistent throughout the targets with the range in scatter being constant across the range of observed water levels.

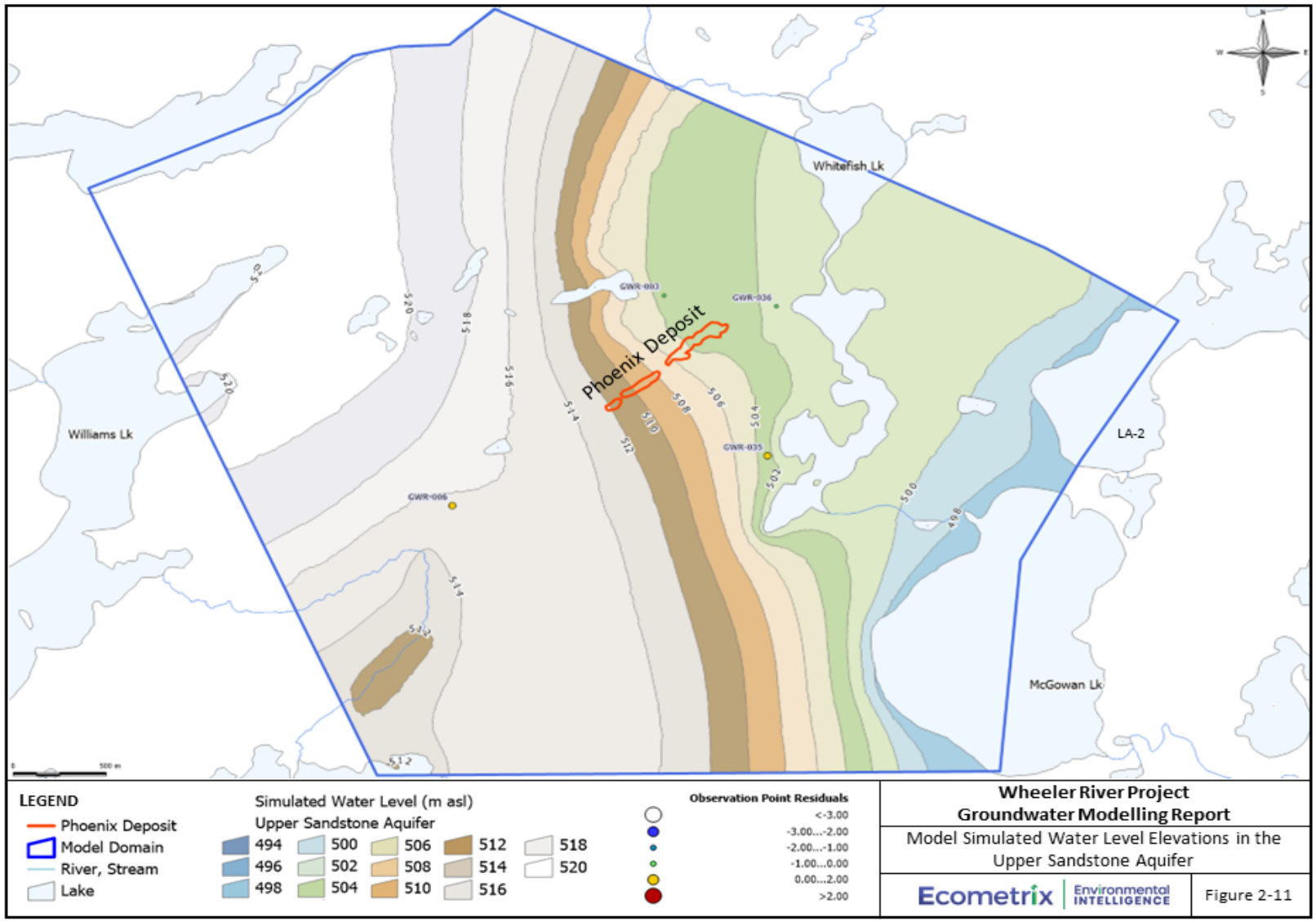

Figure 2-11: Model Simulated Water Level Elevations in the Upper Sandstone Aquifer

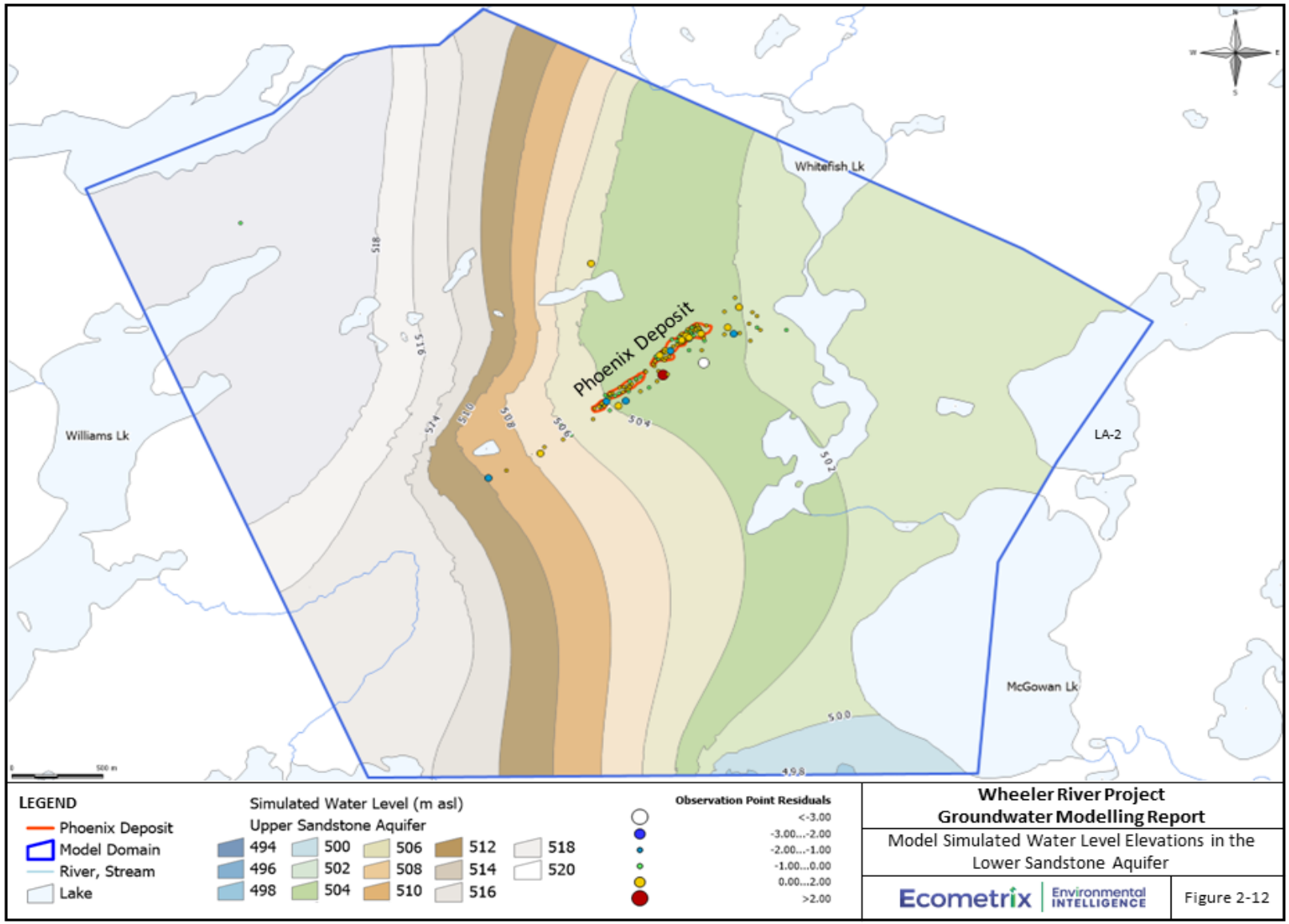

Figure 2-12: Model Simulated Water Level Elevations in the Lower Sandstone Aquifer

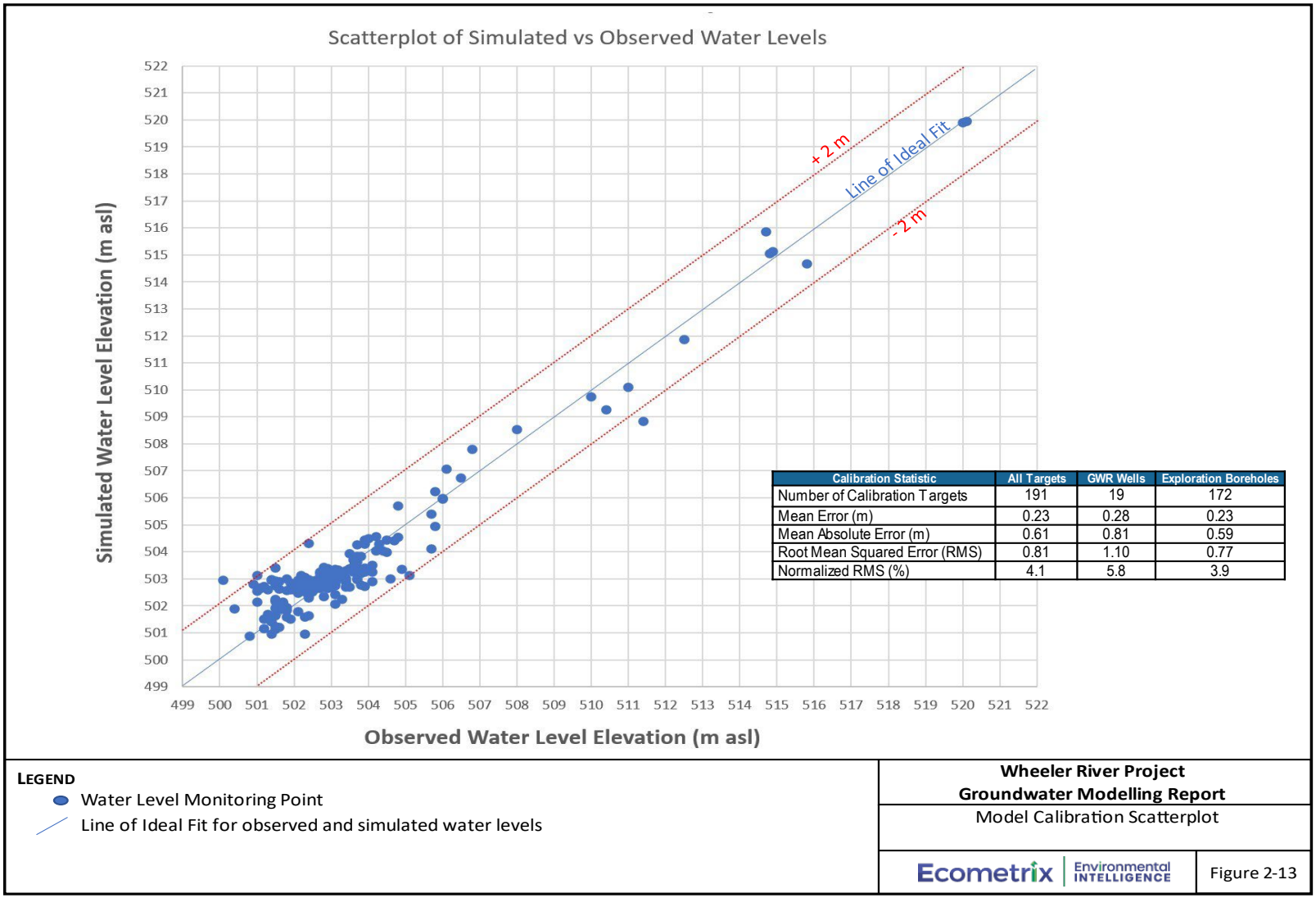

Calibration Statistic	All Targets	GWR Wells	Exploration Boreholes
Number of Calibration Targets	191	19	172
Mean Error (m)	0.23	0.28	0.23
Mean Absolute Error (m)	0.61	0.81	0.59
Root Mean Squared Error (RMS)	0.81	1.10	0.77
Normalized RMS (%)	4.1	5.8	3.9

LEGEND
- Water Level Monitoring Point
- Line of Ideal Fit for observed and simulated water levels

Wheeler River Project
Groundwater Modelling Report
Model Calibration Scatterplot
Ecometrix Environmental INTELLIGENCE
Figure 2-13

Figure 2-13: Model Calibration Scatterplot

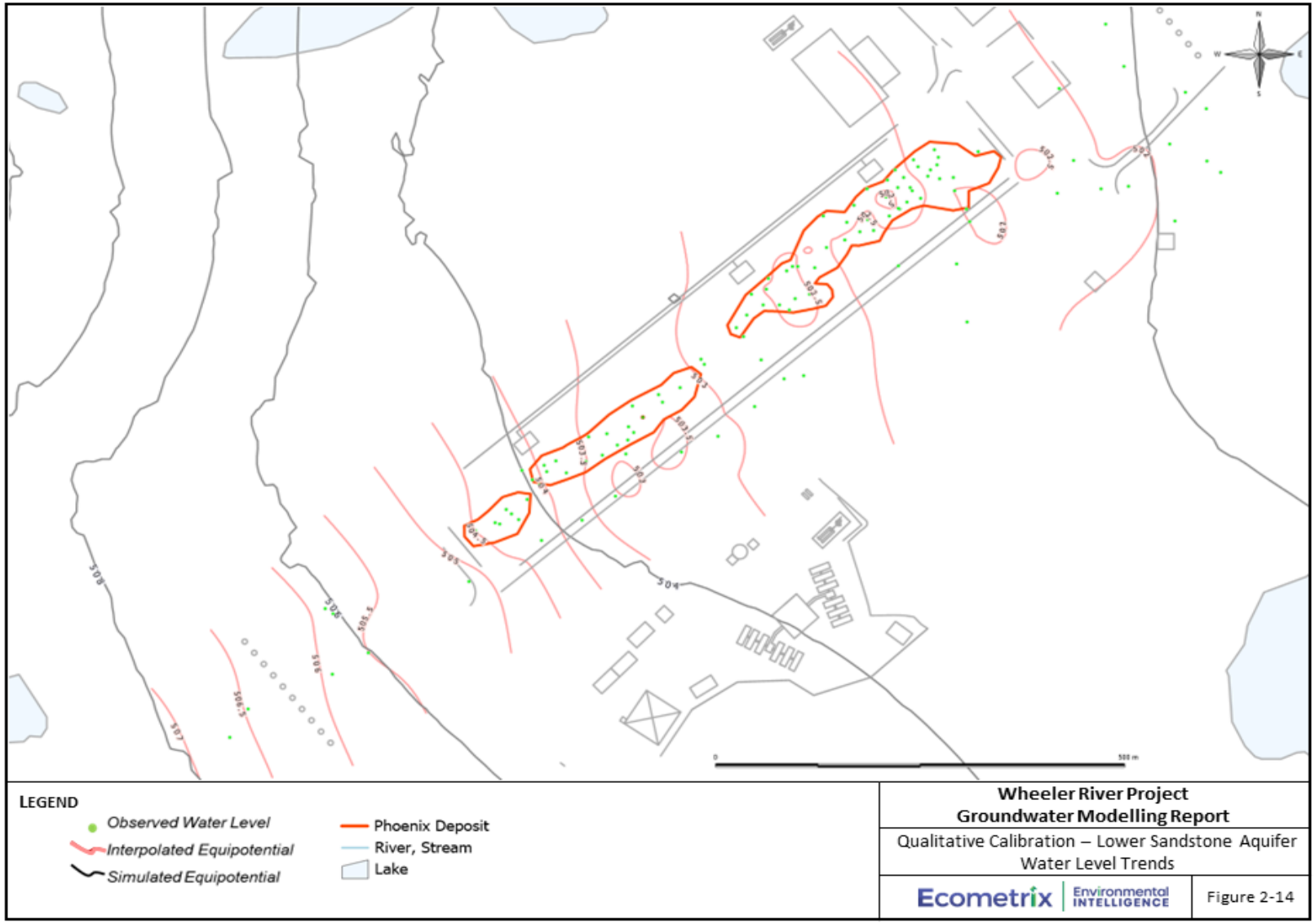

Figure 2-14: Qualitative Calibration – Lower Sandstone Aquifer Water Level Trends

2.5.2.2 Water Level Elevations – Qualitative Calibration

Figure 2-14 illustrates the match between contoured water level trends within the Lower Sandstone Aquifer and those simulated within the groundwater flow model. As shown, there is an excellent match between the contoured water levels and the simulated water levels in the immediate vicinity of the observation well locations. In many cases, throughout the ore zone the corresponding simulated and interpolated water level contours are within 50 meters of one another. It is important to note that the simulated water levels are achieved using idealized, simplified parameter zones, and as such simulated water levels are generally smoother and intended to represent the general patterns of observed conditions. In this case, the match achieved is excellent.

2.5.2.3 Statistical Measures of Calibration to Water Levels

Calibration statistics were calculated as a measure of the statistical goodness of fit between the model-simulated and observed water level elevations and are outlined in Table 2-6.

Table 2-6: Water Level Calibration Statistics

Calibration Statistic	All Targets	GWR Wells	Exploration Boreholes
Number of Calibration Targets	191	19	172
Mean Error (m)	0.23	0.28	0.23
Mean Absolute Error (m)	0.61	0.81	0.59
Root Mean Squared Error (RMS)	0.81	1.10	0.77
Normalized RMS (%)	4.1%	5.8%	3.9%
Range of Observed Water Levels	20.0	20.0	20.0

- Mean Error = 0.23 m for all targets. The mean error is a measure of whether, on average, simulated water levels are higher or lower than those observed. Ideally, the Mean Error should be as close as possible to zero. This statistic indicates that on average the simulated water levels are higher than the observed values by 0.23 m. This represents an excellent match to the observed water levels.

- Root Mean Squared Error = 0.81 m. The root mean squared error is comparable to a standard deviation and provides a measure of the degree of scatter about the 1:1 line. It is calculated by averaging the squares of each residual error (i.e., difference between simulated and observed) and then taking the square root of that average. It is most desirable to have a low RMSE, especially for high-quality data. The model RMSE indicates that most predicted water levels in the model domain lie within 0.81 m of the observed values.

- Normalized Root Mean Squared (NRMS) Error is calculated by dividing the Root Mean Squared Error by the maximum range in observed water level elevations. This percentage value allows the goodness-of-fit in one model to be compared to another model regardless of the scale of the model. Typically, a groundwater flow model is considered calibrated when the NRMS is less than or equal to 10% (Spitz and Moreno, 1996); however,

the NRMS error is dependent on the range of observed water levels. The NRMSE for all targets in the current model is 4.1% which is very good, especially considering the total range in observed water levels is only 20 m across the model domain.

The spatial distribution of the residuals (difference between simulated and observed water levels at each well) are illustrated on Figure 2-15. The lack of a trend in residual values (colours) reflects that there is no trend in the calibration residuals (i.e., they are randomly distributed).

2.5.2.4 Simulated Vertical Gradients

Observed and simulated vertical gradients at available the well clusters presented in Appendix 7-A (Table 3-1), are summarized in Table 2-7. Observed static water levels are presented as there were issues with the barometric pressure correction for transient water levels. Vertical gradients are implicitly incorporated into the 3D model calibration as water levels from all observation wells are incorporated as calibration targets using their coordinates in 3D space.

As indicated by the results presented in Figure 2-7 , the model provides an excellent representation of the observed gradients estimated using these monitoring well clusters.

- At the northwest (NW) cluster, the observed and simulated gradients are virtually identical.

- At the southeast (SE) cluster, the gradient from the shallow overburden (OVB) to the intermediate sandstone aquitard (ISA) is under-estimated in the model, however the water level at GWR-007 is believed to be perched above the regional water table, and therefore not a good representation of vertical gradients; regardless both the model and observed data indicate a downward vertical gradient. The gradient between the ISA and the lower sandstone aquifer (LSA) is negligible, which is replicated within the model.
- At the up-gradient cluster, the observed are very well represented by the simulated gradients, including the flow directions.

- At the down-gradient cluster, the gradient between the ISA and the LSA is negligible, which is replicated within the model. The gradient between the OVB and ISA is observed to be downward. However, GWR-005 is located near the shore of Whitefish Lake but has an observed water level 2 m higher than the average lake level. Consequently, the simulated upward is considered reasonable.

- At the Whitefish Lake Bay, the simulated and observed gradients between the upper sandstone aquifer (USA) and the overburden (OVB) are both upward and of similar magnitude. It is noted that he hydraulic head difference between the two observation wells is rounded to 0.1 m.

Table 2-7: Observed and Simulated Vertical Gradients at Available Well Clusters

Cluster	Well	Hydrostratigraphic Unit	Observed Water Level (static) (m asl)	Simulated Water Level (m asl)	Screen mid-point Elevation (m asl)	Observed Gradient (m/m)[a]	Simulated Gradient (m/m)[a]	Notes
NW	GWR-003	Overburden	503.97	503.87	467.8			
	GWR-027	ISA	500.91	501.00	246.3	0.0138	0.0130	
	GWR-025	LSA	502.34	502.40	146.3	-0.0143	-0.0140	
SE	GWR-007	Overburden	514.12	503.48	515.2			perched aquifer at GWR-007 impacts gradient calculation
	GWR-009	ISA	502.20	502.57	285.5	0.0519	0.0039	
	GWR-008	LSA	502.40	502.37	166.2	-0.0017	0.0017	
Up- gradient	GWR-006	Overburden	514.70	515.81	504.75			
	GWR-028	ISA	511.00	510.40	241	0.0140	0.0205	Wells GWR-028 and GWR-029 are 520 m apart.
	GWR-029	LSA	514.80	515.07	172.25	-0.0553	-0.0680	
Down-gradient	GWR-005	Overburden	501.99	500.94	382.55			
	GWR-014	ISA	501.60	501.21	348.05	0.0113	-0.0079	Wells GWR-014 and GWR-012 are 430 m apart.
	GWR-012	LSA	501.27	501.40	166.5	0.0018	-0.0010	
Whitefish Lake Bay	GWR-036	Overburden	502.3	501.59	459.9			
	GWR-037	USA	502.4	501.62	441.3	-0.0054	-0.0017	

Notes:

[a] – Downward gradients are indicated by positive values and upward gradients by negative values.

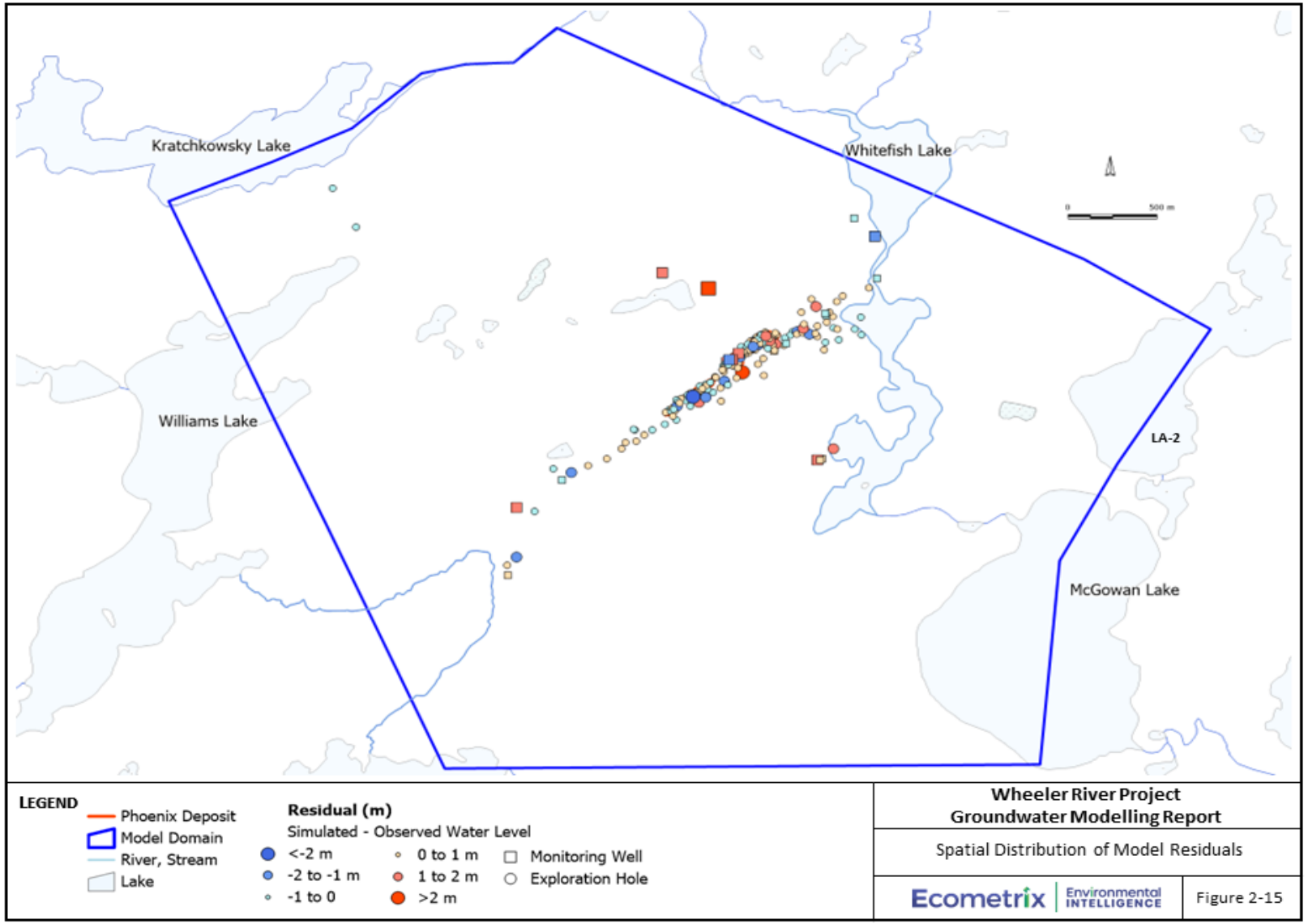

Figure 2-15: Spatial Distribution of Model Residuals at All Locations

2.5.2.5 Baseflow Calibration Results

In addition to calibrating to water level elevations targets, the model was calibrated to estimates of groundwater discharge to Whitefish Lake. A match between simulated and observed flows helps to support that groundwater recharge rates are reasonable, and to provide validation for water budget assessments. Baseflow calibration targets were developed using point streamflow measurements collected upstream and downstream of Whitefish Lake. Figure 2-10 shows the locations of the baseflow calibration targets, and Table 2-8 illustrates the model-simulated groundwater discharge rates in relation to the estimated range of baseflow from stream measurements. The simulated baseflow to Whitefish Lake is in good agreement with the estimated representative baseflow.

Table 2-8: Baseflow Calibration Results

Surface Water Stations	Feature Monitored	Range of Observed Baseflow (L/s)			Simulated Baseflow (l/s)
		Low	Representative	High	
SA-6 to SA-2	Flow through the Southern portion of Whitefish Lake as indicated on Figure 2-10	29.3	40	50.6	40.6

2.5.3 Overall Calibration Assessment

Overall, the calibration assessment indicates that the model is well calibrated, and the model can be used as a tool to guide predictions of groundwater flow directions and gradients. The differences between observed and simulated water levels at monitoring wells (i.e., residuals) were minimized, and there are no spatial trends in residuals that are expected to impact the groundwater flow model predictions. The simulated heads at monitoring wells are close to observed values, and simulated groundwater discharge rates agree favourably with the available baseflow estimates.

2.6 Enhanced Groundwater Flow Understanding

2.6.1 3D Groundwater Flow Patterns

Groundwater flow contours within the Upper and Lower Sandstone Aquifers are presented on Figures 2-11 and 2-12. Regionally, groundwater flow extends from the area near Kratchkowsky Lake in the west, where the highest water levels and lake levels are present, to the southeast towards McGowan Lake. This creates a regional groundwater gradient from the northwest to the southeast. Near the Phoenix Deposit, the local hydraulic gradient is from the southwest to the northeast. Within the Upper Sandstone Aquifer, the local hydraulic gradient is influenced by the Desilicified Zone and the thick coarse-grained overburden deposits underlying Whitefish Lake. Within the Lower Sandstone Aquifer, the hydraulic gradient is influenced by the presence of 1) the Desilicified Zone, and 2) an area of higher hydraulic conductivity along the trajectory of the WS Shear which is interpreted to have been caused by enhanced fracturing along the fault trajectory and thermal alteration.

The flow patterns for groundwater discharging to Whitefish Lake are illustrated in plan and cross-section view on Figure 2-16, based on backward-tracking particles that were started at Whitefish Lake (orange dots) and tracked backward in time toward their source area. Particle traces illustrate that while Whitefish Lake receives groundwater from all directions, most groundwater starts in areas west of Whitefish Lake. Review of the cross-section illustrates that most of the groundwater flow to Whitefish Lake is sourced from waters flowing through the Upper Sandstone Aquifer and Overburden units, with a lesser contribution flowing from the Lower Sandstone Aquifer through the Desilicified Zone. Review of the hydraulic head isolines illustrates the lateral hydraulic gradients within the Upper and Lower Sandstone Aquifers, and the predominantly vertical gradient through the Intermediate Sandstone Aquitard. Downward gradients from the Upper Sandstone Aquifer are found near the western (i.e., upgradient) edge of the Desilicified Zone where flow from the Upper Sandstone Aquifer expands to flow through the permeable Desilicified Zone; the gradient transitions to upward beneath Whitefish Lake. Similarly, slight upward flow paths from the Lower Sandstone Aquifer are also experienced near the western (i.e., upgradient) edge of the Desilicified Zone, where flow through the Lower Sandstone Aquifer also extends vertically to flow into the overlying Desilicified Zone (Figure 2-16). This transitions to dominantly upward hydraulic gradients and groundwater flow throughout the eastern (i.e., downgradient) portion of the Desilicified Zone.

The colours on the particle traces (Figure 2-16) illustrate that groundwater discharging to Whitefish Lake through the Upper Sandstone Aquifer requires less than 50 years of travel time for groundwater recharging near the Phoenix site; groundwater recharge west of the Phoenix site would require 50 to 500 years (i.e., groundwater discharge to Whitefish Lake is generated from precipitation hundreds of years earlier). Groundwater travel time from the Lower Sandstone Aquifer through the Desilicified Zone to Whitefish Lake requires 250 to 400 years of travel time.

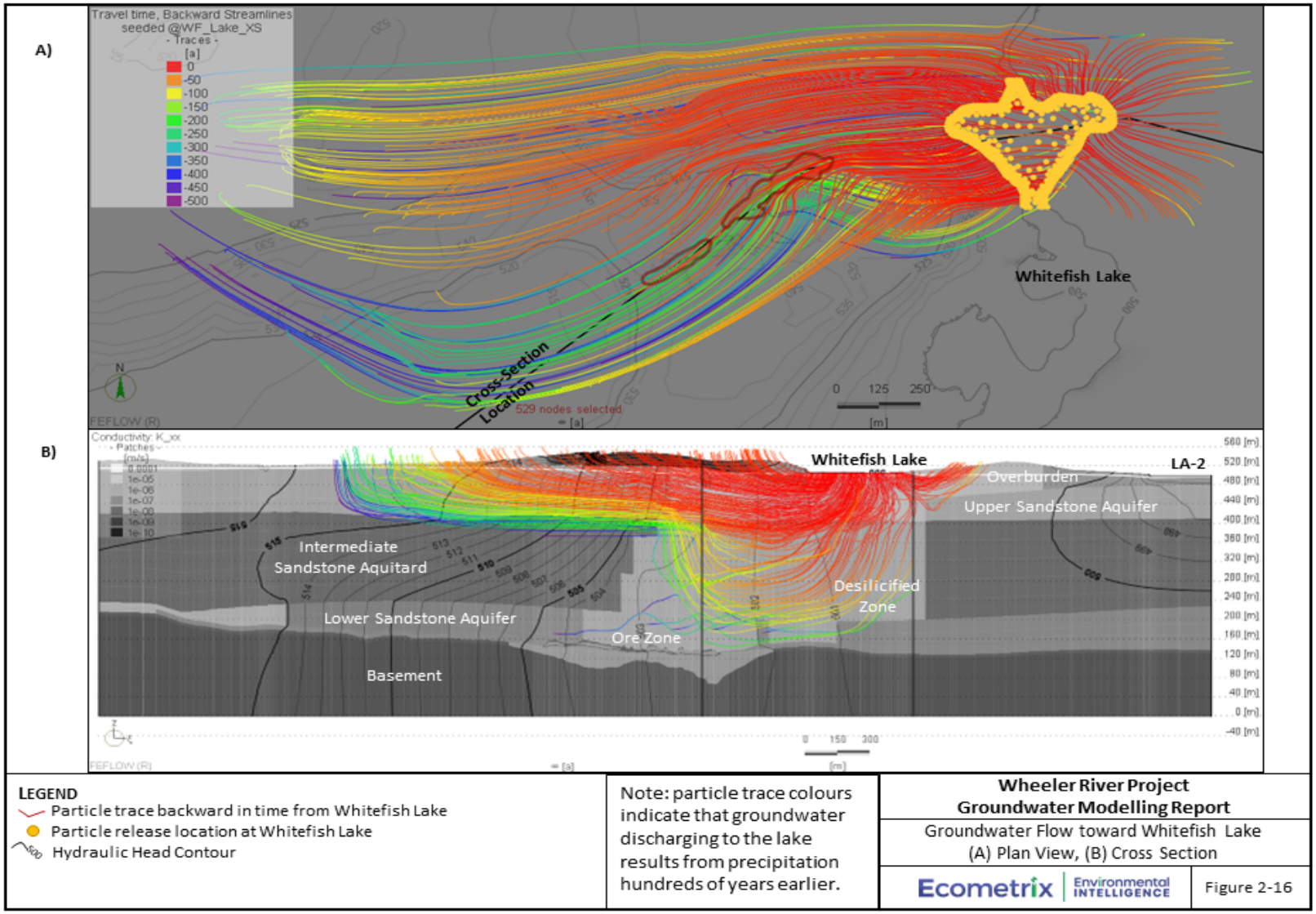

Figure 2-16: Groundwater Flow toward Whitefish Lake (A) Plan View, (B) Cross Section

2.6.2 Evaluation of Potential Receiving Bodies

Identification of potential receiving bodies involved review of available groundwater level, streamflow, and stream or lake level elevation data. The potential hydraulic gradients and flow rates were also evaluated to identify the potential for groundwater to migrate from the ore zone to each potential receiving body. The observed (and calibrated) groundwater flow patterns identify a primarily west to east groundwater flow direction at the Phoenix deposit, which suggests that surface water bodies east of the site are the most likely downgradient receiving water bodies. Water bodies located east of the site (Figure 2-8 and 2-9) include Whitefish Lake (500 m east), McGowan Lake (2 km southeast) and an un-named lake (LA-2) east of McGowan Lake (1.9 km east). Russell Lake, located 6 km south of the Phoenix deposit, was also considered a potential regional discharge location.

Hydraulic gradients were estimated based on water level differences between the ore zone and each potential surface water receptor. In addition, calculations of potential groundwater flow rates to each surface water receptor were evaluated for a range of interpreted hydraulic conductivity values. Hydraulic gradients toward McGowan Lake and Lake LA-2 are 50% larger than the gradient toward Whitefish Lake. However, the groundwater flow rate through the Desilicified Zone where a relatively high hydraulic conductivity is conservatively interpreted to exist, is estimated to be more than ten times greater than other areas where the intermediate sandstone aquitard is unaltered. As a result, the groundwater flow rate potential is estimated to be highest (i.e., by an order of magnitude or more) toward Whitefish Lake than any other surface water body in the area. Groundwater flow potential toward Russell Lake is the lowest of any surface water feature evaluated. Groundwater discharge to Whitefish Lake is also most conservative from a predictive perspective as groundwater flow and discharge into other nearby surface water bodies such as McGowan or Russell Lakes, would predict lower concentrations due to dispersion along those longer flow paths.

Given this potential flow rate evaluation, Whitefish Lake is considered the most likely receiving body of groundwater flowing through and around the Phoenix deposit. Additionally, as Whitefish Lake represents the shortest potential transport distance, evaluation of this lake as the receptor-of-interest is conservative.

Despite the physical evaluation of potential receiving bodies highlighting Whitefish Lake as the most likely receiving body, boundary conditions applied in the model (Figures 2-8 and 2-9) were designed to permit groundwater to migrate toward, and discharge at, any of the surface lakes (including flow south toward Russell Lake). However, calibration to the horizontal and vertical gradients evident at the site, coupled with the interpretation of the Desilicified Zone as a higher hydraulic conductivity zone, supports the upward migration of groundwater toward Whitefish Lake from the ore zone area. Upward flow from the ore zone toward Whitefish Lake is also consistent with geochemical and mineralogical trends. The implication of this interpretation is that the primary potential receiving body, for groundwater constituents of potential concern associated with the ore body, is Whitefish Lake.

2.6.3 Groundwater Flow Quantity

The calibrated model was utilized to evaluate the regional groundwater budget (Table 2-9). The water budget is presented for steady-state, pre-mining conditions, and as such represents what is expected to occur within a typical year.

Groundwater inflow to the model area is dominated by groundwater recharge, which is supplied through annual precipitation (i.e., infiltration of rainfall, runoff, and snowmelt). Additional inflow is provided via a) recharge from some of the surface ponds within the model footprint (e.g., near GWR-025 and west toward the Gryphon deposit), and b) deep regional groundwater flow entering the model in the Lower Sandstone Aquifer near Kratchkowsky (north) and Williams (west) Lakes. Water supplied through surface ponds is also expected to be derived from rainfall runoff and snowmelt. Deep regional groundwater flow is estimated to be a relatively minor (i.e., <1% of total inflow) part of the groundwater flow budget. Similarly, deep regional outflow south toward Russell Lake is also estimated to be minor (i.e., 0.2% of total outflow).

Groundwater leaving the model is dominantly simulated to exit as groundwater discharge (seepage) to surface water bodies. Such groundwater discharge supports stream baseflow in otherwise dry conditions. As noted above, there is a minor component of deep groundwater flow out of the model south toward Russell Lake.

Table 2-9: Regional Water Budget (Average Annual Rates)

Element	Water In (m^3/d)	Water Out (m^3/d)	Comment
Groundwater Recharge from Precipitation	6,365		Inflow at Ground Surface
Interaction with Lakes	510	6,903	In/Outflow at Ground Surface
North Inflow	22		Lateral Inflow to Lower Sandstone Aquifer
South Outflow		15	Lateral Outflow from Lower Sandstone Aquifer toward Russell Lake
West Inflow	21		Lateral Inflow to Lower Sandstone Aquifer
Sum	6,918	6,918	

The distribution of groundwater discharge to the various lakes is presented in Table 2-10. Here the discharge is presented as a percentage of the groundwater discharging at each lake relative to the total flow through the model domain (i.e., 6,918 m^3/d).

Through this analysis, Whitefish Lake is simulated to receive 51% of the groundwater flowing through the model domain, with smaller amounts discharging to lakes in the southeast (McGowan and LA-2) and southwest (LB-2 and the river between Williams Lake and LB-2), respectively. Kratchkowsky and Williams Lakes receive relatively small amounts of the groundwater recharged within the model domain; they are expected to dominantly receive groundwater discharge from further upgradient areas (i.e., northwest), which are outside of the model domain.

Table 2-10: Groundwater Discharge to Surface Water Bodies

Element	Water In (m^3/d)	Water Out (m^3/d)	% of Groundwater Inflow which Discharges to Each Surface Feature within the Model
Whitefish Lake		3,517	51%
McGowan & LA-2		1,938	28%
Kratchkowsky & Williams Lakes		445	6%
LB-2 & Inflowing River		1,003	14%
Interior Ponds	510		
Sum	510	6,903	

As indicated through this water budget analysis, most of the groundwater flow through the model occurs within the shallow portions of the model domain (i.e., the Overburden and Upper Sandstone Aquifer). Additional sub-domain water budgeting suggests that 99% of the groundwater flow occurs through the Upper Sandstone Aquifer and Overburden deposits, extending from the groundwater recharge areas to discharge areas at the respective lakes and rivers. Similarly, it is calculated that flow from the Lower Sandstone Aquifer migrating up through the Desilicified Zone, accounts for < 1% of the groundwater discharge to Whitefish Lake. This suggests that any deep groundwater discharge from the vicinity of the ore zone will be a small proportion of the groundwater discharging into Whitefish Lake.

2.6.4 Water Budget for Whitefish Lake

As noted above in Section 2.6.3, it is estimated that 99% of the groundwater discharge to Whitefish Lake is derived from groundwater that has only flowed through shallow deposits (i.e., Overburden and Upper Sandstone Aquifers). Contribution of deep groundwater flow through the Desilicified Zone within the Intermediate Sandstone Aquitard is estimated to be less than 1% of the groundwater discharging to Whitefish Lake.

Groundwater discharge to Whitefish Lake is estimated to be 40 L/s (3,456 m^3/d or 0.04 m^3/s), which is a small component (~ 3%) of the average surface flow through the lake (average of 1.4 m^3/s). The component of groundwater discharge emanating from the Lower Sandstone Aquifer is 1% of the total groundwater discharge, or 0.03% of the total flow through Whitefish Lake. At low flow conditions (i.e., 7Q10), the estimated flow through Whitefish Lake is 0.81 m^3/s, indicating that the portion of deep groundwater discharge could reach a maximum level of 0.05% of the flow through Whitefish Lake.

2.7 Groundwater Conditions During Mine Operations

2.7.1 Groundwater Demand

Mining operations will include the use of groundwater for several purposes, including supply make-up water to the ISR plant, support freeze wall development, wash bay requirements, and drilling activities (pre-development). Pumping demand was estimated and provided by Denison as follows:

a) 20 m^3/hr (5.6 L/s) during mine construction (Years 1-3) to support drilling activities and development of the freeze wall,

b) 31.3 m^3/hr (8.7 L/s) during mine operation (Years 3-18), and

c) 35.5 m^3/hr (9.9 L/s) during mine decommissioning (18-23 years).

Groundwater pumping was simulated in the model to be derived from three pumping wells located outside the ore zone and proximal to the mine operations. The wells were simulated to pump water from the Upper Sandstone Aquifer.

2.7.2 Groundwater Recharge

In addition to this water demand, groundwater recharge is also anticipated to be reduced (estimated at 50%) within the freeze wall area during the mine construction and ISR phases and enhanced within the borrow pit area (20%). In addition, groundwater inflow from the septic effluent pond is estimated at 2.5 m^3/hr (0.7 L/s) during all mine construction, operation, and decommissioning phases. The reduced hydraulic conductivity associated with the vertical freeze walls was also incorporated within the model simulations.

The calibrated, steady-state model was used as the basis for the transient model used to evaluate drawdown during operations. Only conditions immediately at the mining zone were altered within the transient model to reflect the proposed changes during mine operations. All boundary conditions that drive regional groundwater flow were unchanged for the transient model, and all hydrogeologic properties outside of the mining area were left unchanged. Changes made to the hydrogeologic properties were implemented transiently to represent the phased implementation of the freeze wall. Groundwater recharge changes were made to reflect alterations to surficial land use and the implication to groundwater recharge, and transient well boundary conditions were added to simulate the planned pumping demand for camp and ISR water requirements.

The transient version of the model was used to evaluate changes to the groundwater discharge occurring at Whitefish Lake. The model simulation was started at the beginning of mine construction, with initial conditions taken from the calibrated model. The simulation period was extended for 40 years to include the entire period of construction, operation, and decommissioning, and extending through 17 years post-decommissioning.

2.7.3 Hydrogeological Change Due to Mine Operations

Figure 2-17 illustrates the predicted change in water levels due to planned pumping at the mine relative to current conditions, as simulated in the base case model. Three groundwater wells for water supply are planned and their proposed locations are shown in Figure 2.2-1 of the EIS. The wells are shown as freshwater wells “A”, “B” and “C” in (Figure 2-20). The expected drawdown ranges from a high of 9 m at Well B to a low of 2.4 m at Well C; predicted drawdown is proportional to the estimated hydraulic conductivity value applied in the model at the pumping well locations.

Figure 2-18 illustrates the predicted changes that will occur within Whitefish Lake during mine construction, operation, and decommissioning periods. Groundwater discharge to Whitefish Lake is predicted to be reduced by as much as 25% (from 41 to 31 L/s), with a 10% reduction lasting from the start of operation to 1-year into the post-decommissioning period. The reduction in groundwater discharge is interpreted to be due to the Mine groundwater demand (Section 2.7.1) from the Upper Sandstone Aquifer.

The simulated decommissioning phase ends at year 23 on the graph (Figure 2-18), and full recovery of groundwater discharge is asymptotically approached and achieved by year 34 (i.e., 9-years later); 90% recovery is achieved within 4 years (by the end of year 26). However, because groundwater discharge to Whitefish Lake is a small component of the flow through the Lake (i.e., average flow estimated as 1.41 m^3/s or 1,410 L/s), the change in water quantity conditions within Whitefish Lake are predicted to be negligible and too small to measure (Figure 2-18; blue line).

Consequently, the water quantity impact on Whitefish Lake is expected to be of low magnitude, and for a moderate length of time. This outcome is considered likely as the onsite water use is small relatively to the surface flow through the Lake which has been measured over several years of streamflow monitoring (2011 to 2019).

Effect of Freeze Wall

The effect of the freeze wall on groundwater flow conditions within the LSA was simulated using the regional groundwater flow model. Hydraulic conductivity of the freeze wall was simulated as a reduction of the baseline hydraulic conductivity by four (4) orders of magnitude, which was consistent with expected hydraulic conductivity changes as reported by Newmans (2020). The recharge reduction on top of the ore zone was estimated at 50% of the pre-development recharge based on the expected regrading and surface drainage at the site to accommodate all of the surficial operations. The simulated effect of the active freeze walls is illustrated through Figure 2-19 and Figure 2-20, which illustrate the change in groundwater flow paths resulting from the freeze wall and operational groundwater pumping.

Figure 2-19 illustrates the pre-mining (and pre-pumping) groundwater flow paths toward Whitefish Lake. The particle traces shown were released at Whitefish Lake and tracked backward in time / space to their recharge area. They provide an understanding of the west-east groundwater flow toward Whitefish Lake, with local recharge creating the driving force for that groundwater flow. On this figure, the groundwater level contours are shown in black, while the flowlines (particle traces) are shown in blue. Note the flowlines closest to the pumping wells (red circles; three freshwater wells "A", "B" and "C") and the ore body (light brown outline). The colours in the background reflect the shallow hydraulic conductivity zones, which help to explain inflections in the hydraulic head contours and flowlines.

Figure 2-20 illustrates the same groundwater flow paths toward Whitefish Lake during mining operations, while pumping will occur at the three freshwater wells and the freeze walls for (mining/ore zone) Phases 1 through 5 are in place. From this figure, the effect of the freeze walls

on groundwater flow can be seen to be limited to the immediate area around the freeze walls. The addition of the freeze walls creates a cluster of water level contours consistent with the freeze wall locations, representing the change in water levels between the area inside and outside of the freeze wall. Note that the water levels outside the freeze wall are simulated to be relatively unchanged during freeze wall operations.

Also evident in Figure 2-20 are the water level drawdown contours, which deflect around the pumping wells. Note the additional level of drawdown experienced at wells simulated to pump from the lower hydraulic conductivity zone (i.e., green area, as opposed to the yellow area).

The flowlines in Figure 2-20 indicate how the groundwater flow patterns will change due to the addition of the freeze wall and the onsite pumping. Flowlines are noted to travel around the freeze wall and in between the pumping wells to discharge at the lake. The pumping wells will capture water flowing from the west which would otherwise discharge to Whitefish Lake.

The impact of the freeze wall on the local and semi-regional groundwater flow regimes is minor. The footprint of the freeze walled area represents < 0.04% of the area of the regional groundwater flow model, and as described above, the freeze walled area is a relatively small disruption to the regional groundwater flow system. Post mining, the groundwater flow path patterns would return to a condition similar to that simulated for pre-mining.

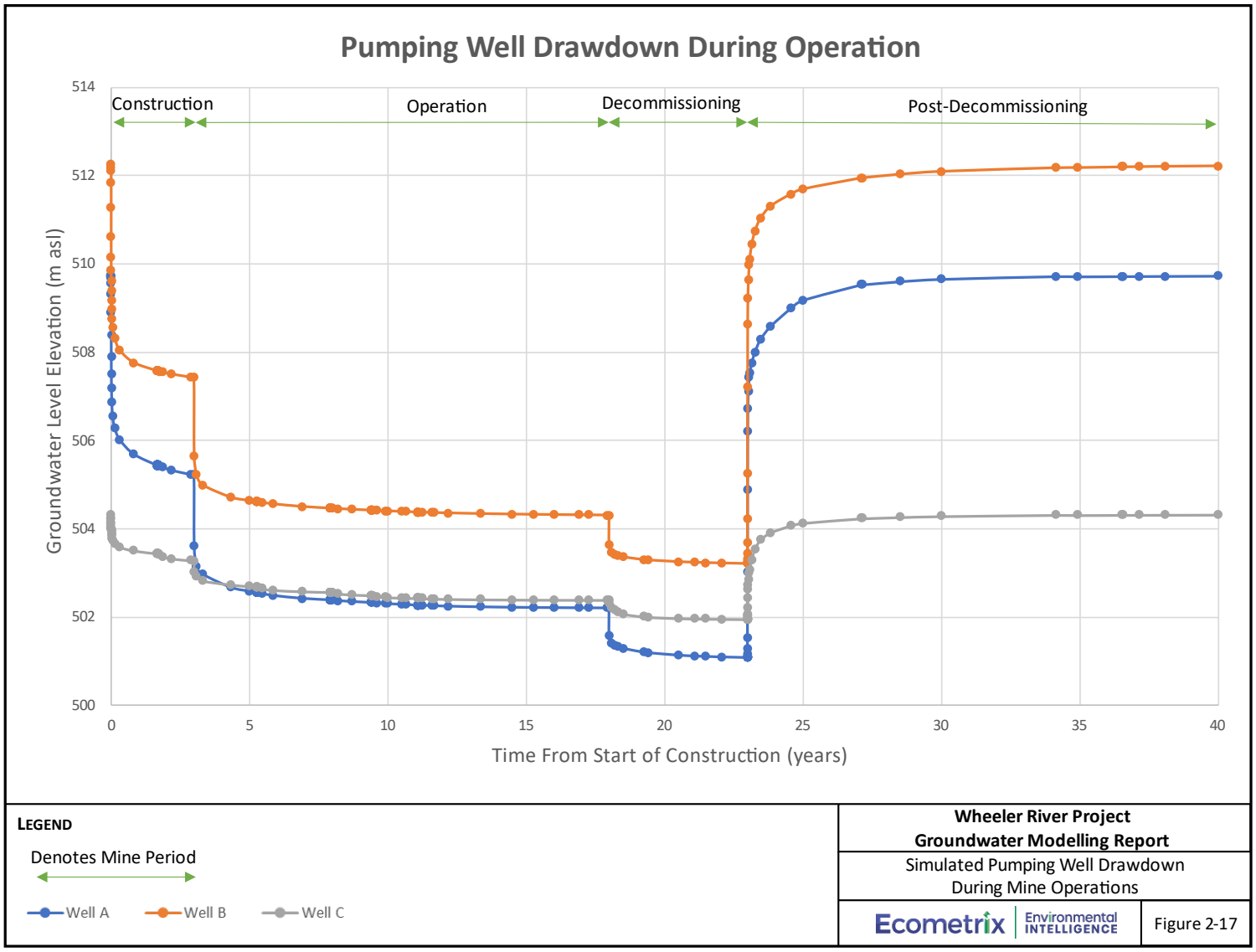

Figure 2-17: Simulated Pumping Well Drawdown During Mine Operations

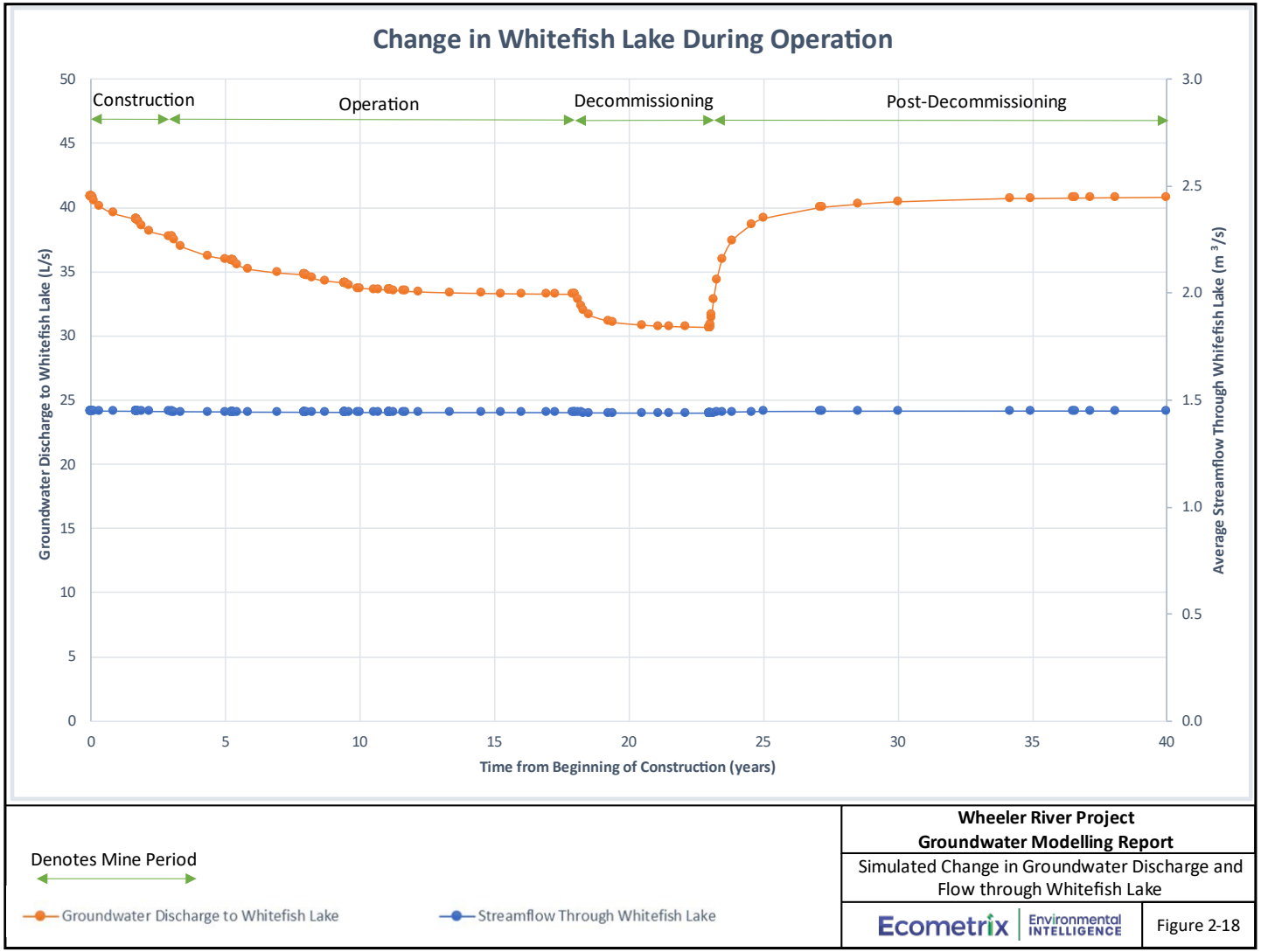

Figure 2-18: Simulated Change in Groundwater Discharge and Flow through Whitefish Lake

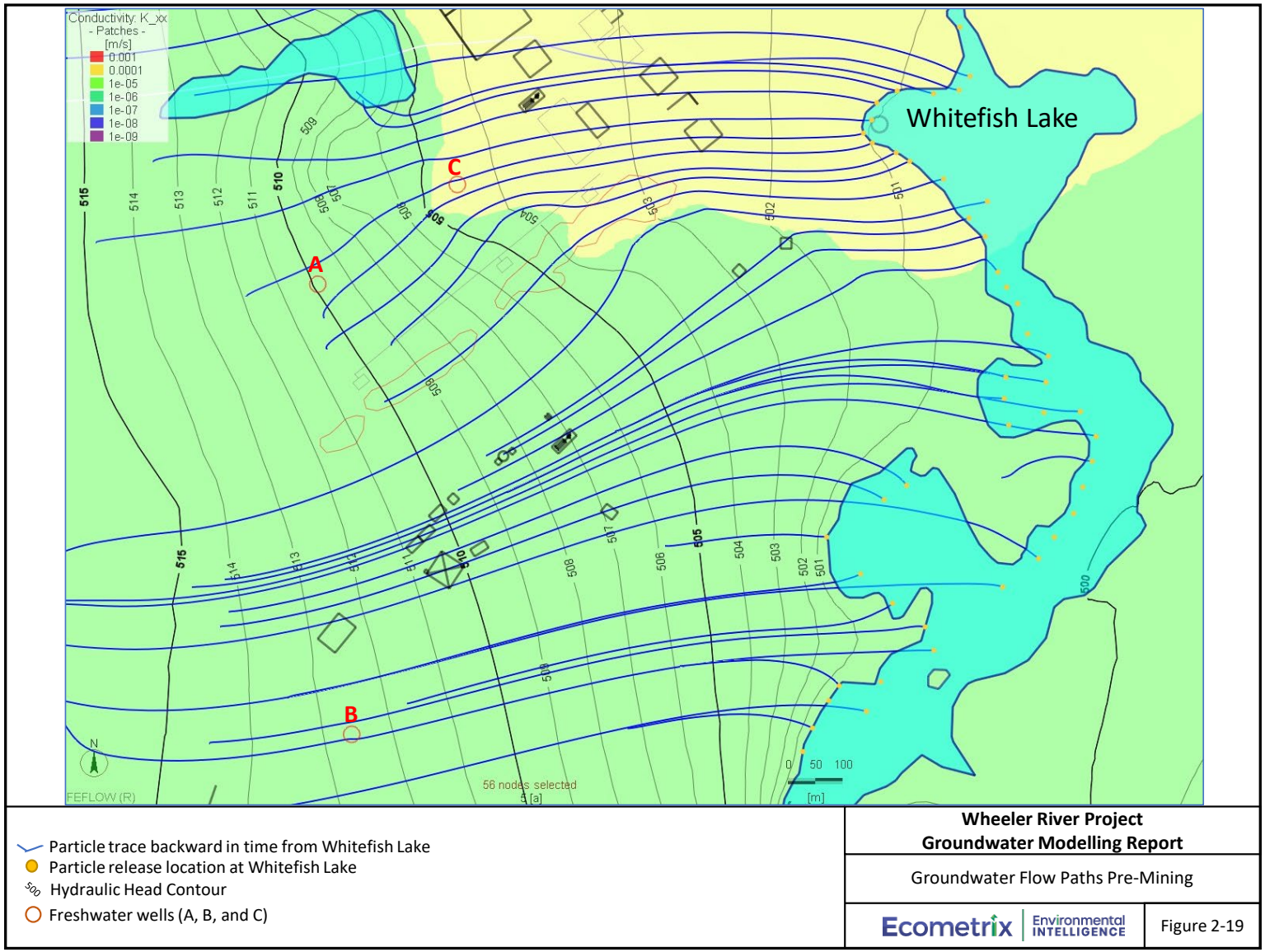

Figure 2-19: Groundwater Flow Paths Pre-Mining

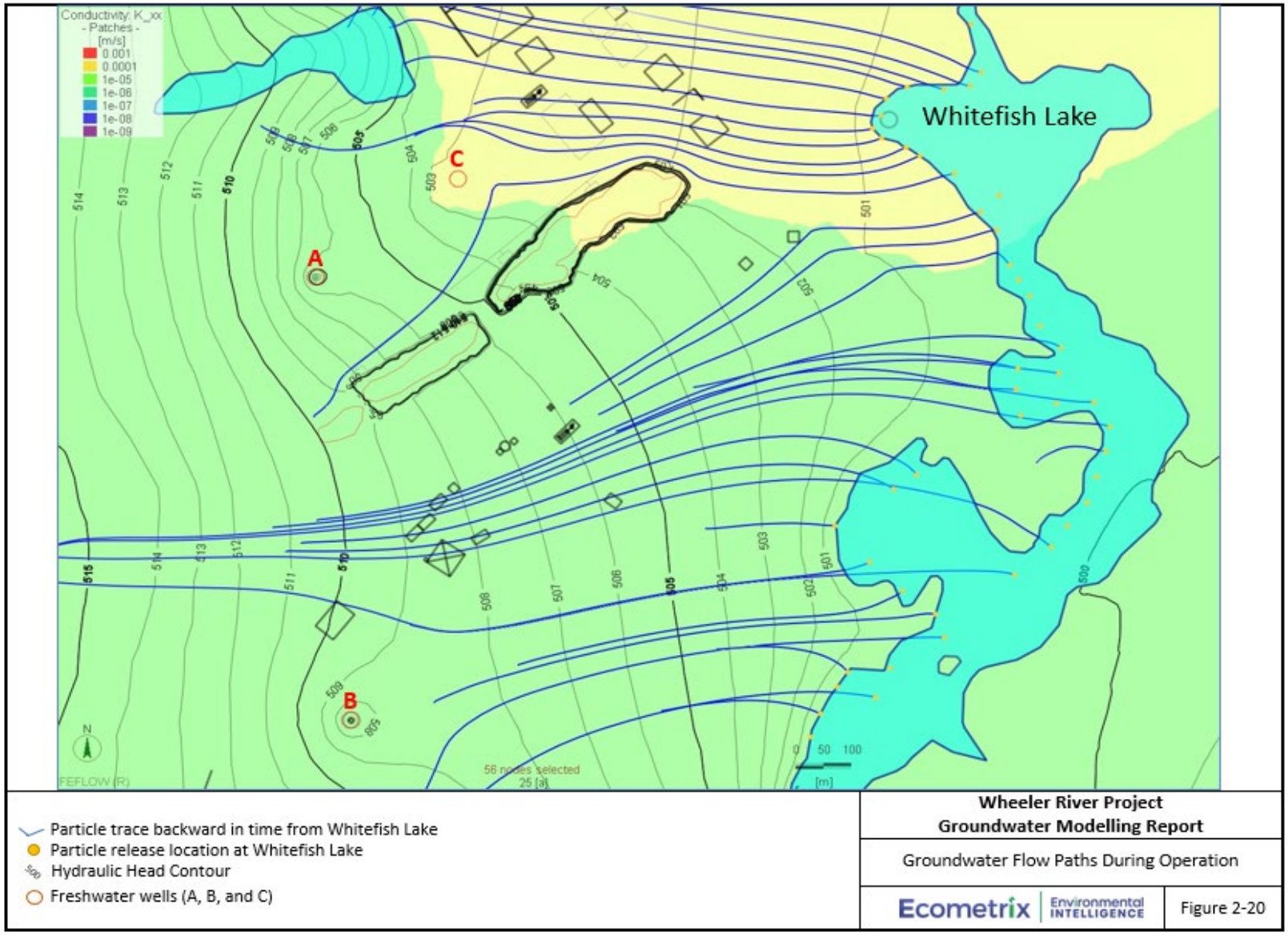

Figure 2-20: Groundwater Flow Paths During Operation

2.8 Parameter Uncertainty Assessment

Beyond the manual model calibration to groundwater flow conditions (Section 2.5), parameter estimation tools were employed to determine parameter combinations that yield an equivalent match to observed conditions. Such alternative, calibrated parameter sets are used to evaluate prediction uncertainty in subsequent simulations of post-decommissioning fate and transport.

2.8.1 Parameter Uncertainty within the 3D Model

All numerical models are approximations of the real-world environment and generalizations are necessary to take a complex hydrogeologic system and bring it into the numerical model.

The hydrostratigraphic characterization was conducted using all available data; however, additional heterogeneities within the aquifer and aquitard units may be present between or beyond available borehole data. The degree of scatter regarding the model calibration achieved is small (i.e., residuals are generally smaller than 0.81 m) however, the impact of such variability should be tested within prediction simulations.

Hydraulic conductivity values applied in the model were guided by aquifer test results which provided local estimates of parameters within the ore zone and Lower Sandstone Aquifers. Some hydraulic test data also exists beyond the ore zone. This data was used to assign parameter values throughout the model domain.

Recognizing these data and parameterization limitations, evaluation of alternative, calibrated parameter sets is important to understand the potential uncertainty regarding predictions of post-decommissioning scenarios.

2.8.2 Focus of Parameter Uncertainty Assessment

As described in Section 2.6.1, the primary flow pattern of interest is from the ore zone toward Whitefish Lake. This flow path presents the most conservative potential pathway for contaminants at depth to reach a sensitive environmental receptor. Recognizing this, the uncertainty regarding parameters along this flow path were the focus of the uncertainty analysis performed. Such parameter zones (i.e., groups of finite elements) included the following (Figure 2-21):

1) Lower Sandstone Aquifer immediately overlying the ore zone (subdivided into 3 zones);

2) Lower Sandstone Aquifer downgradient of the ore zone, extending northeast toward the area beneath Whitefish Lake, which is interpreted to contain desilicified sands;

3) Desilicified Zone extending through the Intermediate Sandstone Aquitard that overlies the ore zone;

4) Upper Sandstone Aquifer overlying the Desilicified Zone; and

5) Overburden Aquifer underlying Whitefish Lake.

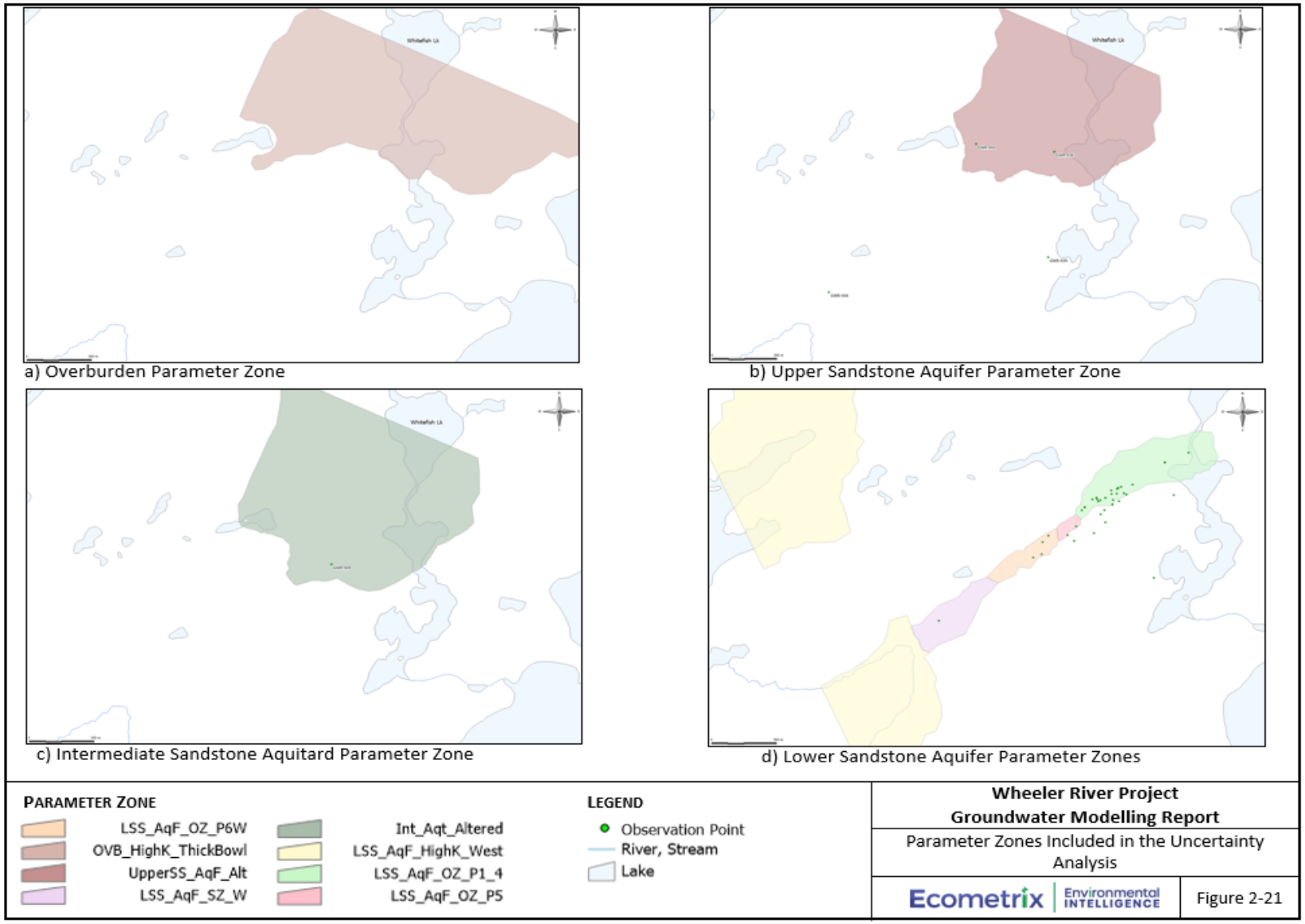

Figure 2-21: Parameter Zones Included in the Uncertainty Analysis

Each of the above zones lies along the predicted flow path between the ore zone and Whitefish Lake, and as such is important to defining the predicted fate and transport of contaminants along this flow path.

Parameter values for each of these zones were allowed to vary independently within a specified range to find combinations of parameter values that met statistical calibration criteria. By varying combinations of parameter values, increases in one parameter value were often offset by lowering other parameter values to maintain calibration. In this manner, 50 models (i.e., realizations) were generated that incorporate a range of parameter combinations that are consistent with the conceptual hydrogeologic model and available water level calibration data.

2.8.3 Parameter Uncertainty Assessment Approach and Results

To complete the parameter uncertainty assessment, a Parameter ESTimation utility, PEST++ IES (Doherty, 2015 and 2018; White, 2018 and 2020) was applied. PEST is a platform-independent utility that contains a suite of programs to support model parameter optimization and prediction uncertainty analysis. PEST embraces the fact that model calibration is non-unique and that a range of parameter combinations should be evaluated to understand potential environmental predictions.

The version of PEST++ employed used the Iterative Ensemble Smoother (IES) technique developed by White (2018) to produce a series of model parameter realizations, which each have different parameter values that produce a model that is as well calibrated as the original base case model. The group of model parameter realizations (i.e., model ensemble) are considered a representative sample of possible parameter sets, and the model predictions conducted using this ensemble can be considered a representative sample of possible predictions. The ensemble is created by randomizing the parameter values of the model within the probability distribution of parameter values. The group of model realizations are then calibrated using a sophisticated algorithm (modified Gauss-Levenberg-Marquardt algorithm) to produce a suite of realizations that all meet calibration target values (i.e., objective function).

Using this approach, fifty (50) calibrated realizations were generated for the Denison groundwater flow model. The range of hydraulic conductivity values applied for each parameter zone (Figure 2-22) indicates the potential variability of each parameter value that can be applied to maintain an equivalent degree of calibration to observed water levels. There is a relatively small range of acceptable parameter values along the primary flow path between the ore zone and Whitefish Lake (i.e., LSS_AqF_OZ_P1_4, Int_AqT_Altered, UpperSS_AqF_ Alt, and OVB_HighK_ThickBowl in Figure 2-21 and Figure 2-22). This indicates that the available water level calibration data is sufficient to constrain the values of these parameters. The hydraulic conductivity of the zone overlying Phase 5 of the proposed Phoenix mine was found to have the highest range of potential hydraulic conductivity values as there is less calibration data available to constrain that hydraulic conductivity.

Three (3) of the fifty (50) calibrated realizations were selected to represent the parameter value combinations (Figure 2-23) that would result in faster groundwater flow, and thus greater

transport of dissolved concentrations between the ore zone and Whitefish Lake. These realizations included:

a) Realization 3: higher hydraulic conductivity for the Lower Sandstone Aquifer (ore zone Phases 1-4, 5, and 6) as well as in the altered Desilicified Zone) within the Intermediate Sandstone Aquitard.

b) Realization 7: highest hydraulic conductivity for the combination of the Lower Sandstone Aquifer (ore zone Phase 5) and the Desilicified Zone within the Intermediate Sandstone Aquitard.

c) Realization 27: highest hydraulic conductivity for the Lower Sandstone Aquifer (ore zone Phase 5).

The statistical calibration (i.e., objective function value, phi; red asterisk in Figure 2-23) is similar for each realization, such that all realizations are considered well calibrated, and the model predictions are equally likely as the base case groundwater flow model.

The reactive transport simulations performed using these alternative parameter realizations are described within Section 4.6.

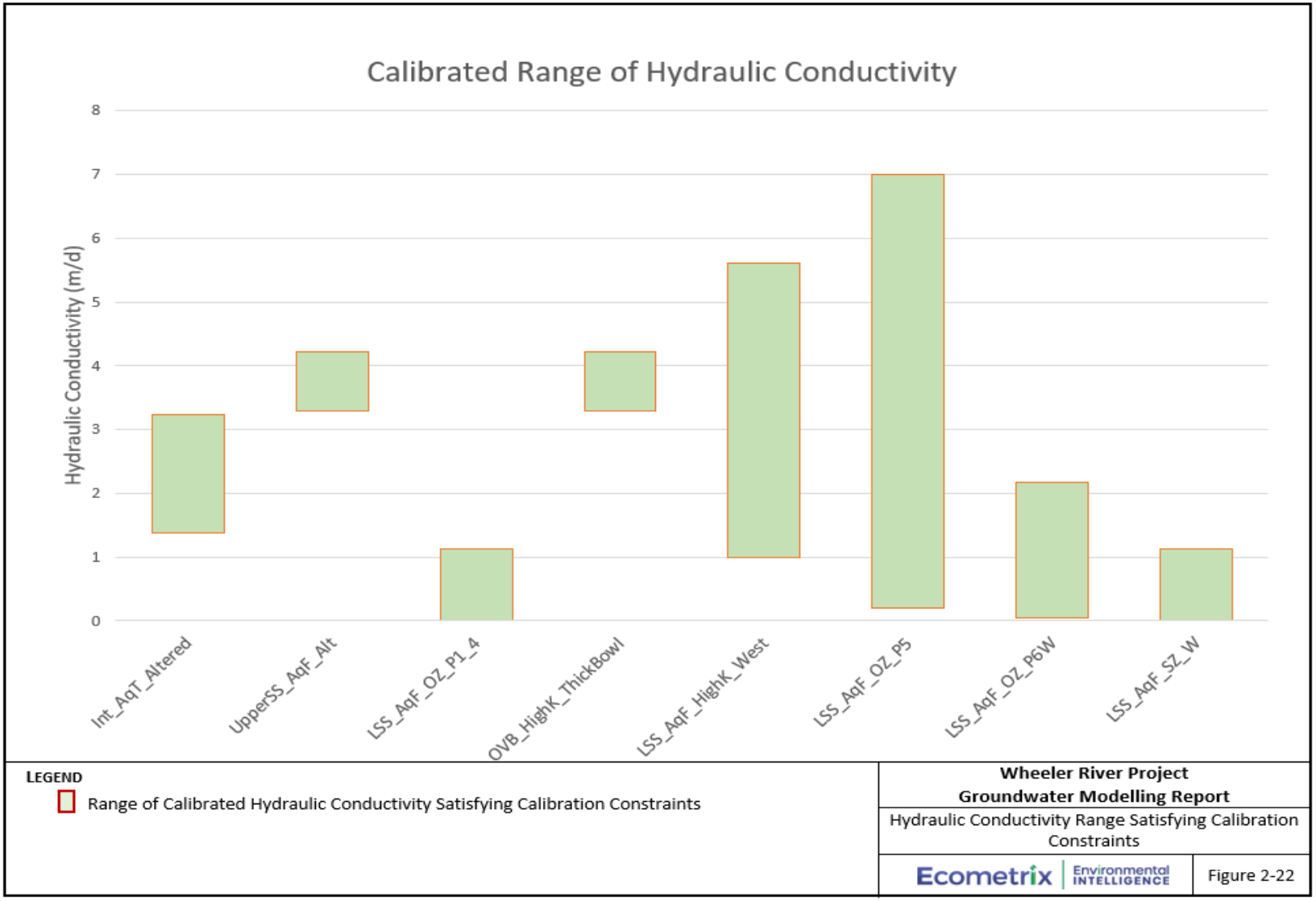

Figure 2-22: Hydraulic Conductivity Range Satisfying Calibration Constraints

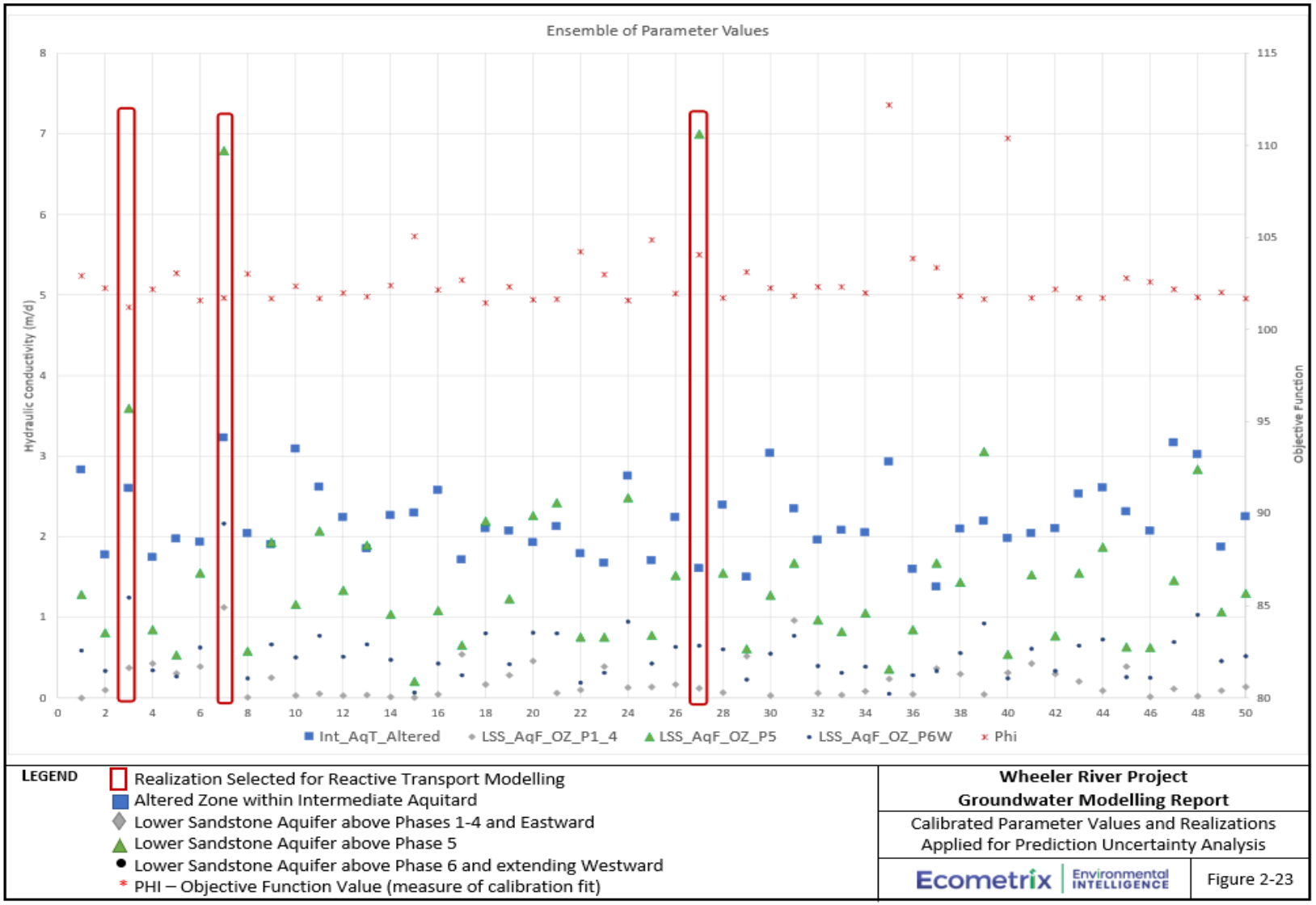

Figure 2-23: Calibrated Parameter Values and Realizations Applied for Prediction Uncertainty Analysis

3.0 Geochemical Reactions and Modelling

Together with understanding groundwater flow conditions, a robust characterization of subsurface geochemistry is the foundation for evaluating how the concentrations of chemical constituents in groundwater, and in the receiving surface water environment, may be affected by the Project. The subsurface geochemical conditions include the form and abundance/concentration of chemical constituents in the solid phase (the rock or sediment matrix), entrained particles (colloids or larger), and dissolved in groundwater. While constituents in groundwater can chemically interact with the solids along the groundwater pathway, only the dissolved constituents can migrate with the groundwater.

3.1 Important Concepts in Subsurface Assessment for ISR Projects

There are two aspects of primary importance for hydrogeological and geochemical assessments in support of ISR Projects. These are groundwater restoration or remediation post decommissioning and the assimilative capacity, including geochemical interactions in the groundwater system downflow from the mined ore zones.

3.1.1 Groundwater Remediation

During mining, mineralogical and hydrochemical conditions within the ore zone are altered, with the introduction of highly oxidizing solutions and the solubilization of uraninite and other ore minerals. When the mining of the ore zone is complete, remediation/restoration of groundwater quality within the ore zone begins. The objective of groundwater remediation is to achieve water quality within the leached mine chamber/area that does not pose a risk to receptors at a point of exposure.

The restoration phase of ISR projects globally have generally involved one or more approaches/phases, which are discussed in Davis and Curtis, 2007 (NUREG/CR-6870).

a) Groundwater Sweep: after injection of mining fluids is stopped, water continues to be pumped from the ore zone through both production and injection wells. This results in native groundwater being drawn into the ISR mining area to replace the solution being pumped out, and thus, flushing the remnant mining solution from the ore zone.

b) Groundwater Recirculation with or without amendment(s): after mining stops, groundwater is recirculated through the ore zone, with above-ground treatment of COPCs, as required. Amendments can be added to the recirculation stream to re-establish specific, designed geochemical conditions within the leaching zone. Examples of amending chemicals may be pH-neutralizing or buffering agents (alkaline solutions) or oxygen scavenger solutions, to establish reducing conditions.

Restoration is complete when remediation goals are achieved. For the Project, remediation will continue until groundwater quality in the mining area, which is defined spatially in Section 4.1

and shown in Figure 4-1, meets acceptable levels. These acceptable levels are considered to be the 'Decommissioning objectives' (the EIS, Section 2)

3.1.2 Assimilative Capacity

The assimilative capacity of the subsurface system downgradient of an ISR project is important to understand when developing restoration goals for groundwater quality after remediation. Natural geological/groundwater systems are characterized by a range in ability to sequester – and naturally attenuate uranium and other COPCs. Processes that contribute to this sequestration and natural attenuation are discussed in more detail in the sections below, but include advection, dispersion, matrix diffusion and chemical reactions of the constituents with other constituents in groundwater and with the solid phase (the rock and soil matrix). These natural processes that, on a spatial and temporal basis, act to (physically) spread the mass of constituents and transfer dissolved mass to the solids. The result is a permanent or temporary removal of dissolved constituents from groundwater and overall reductions in dissolved groundwater concentrations with increasing distance from the source location. Along with active remediation of groundwater, as described in Section 3.1.1, the assimilative capacity of the system acts to attenuate (i.e., reduce) concentrations of mining-associated constituents, with the potential to reduce concentrations to levels that do not pose a risk in the receiving environment. In general, the natural system surrounding the Phoenix deposit has been shown, based on baseline water quality, and is predicted to have high assimilative capacity into the future.

Conservative constituents in groundwater are those that undergo no or limited chemical reactions and whose velocity in the system reflects advection and dispersion only. Dissolved chloride is a good example of a constituent with conservative behaviour and, along with other conservative constituents, can be used better understand the groundwater flow system. Other constituents, such as uranium, can undergo chemical reactions such that that transport of uranium in the subsurface away from a source can be limited.

3.1.3 Geochemical Assessment Framework

The geochemical assessment is presented as follows:

- characterization of the mineral composition of the geologic materials in the groundwater flow system (Section 3.2.1);
- characterization of groundwater (hydro)chemistry within and surrounding the mineralized zone under pre-mining conditions (Section 3.2.2). Engineering design and mitigation measures (i.e., the freeze wall) will maintain groundwater quality outside of the mining zone at baseline conditions;
- identification of constituents of potential concern (COPCs) and ranges of concentrations associated with the remediated groundwater after mining (Section 3.3); and

- a conceptualization of the chemical reactions and physical processes that will occur and may affect the COPC concentrations in the remediated groundwater during migration along the groundwater flow pathways post-decommissioning (Section 3.4).

All of the above are the foundation for geochemical modelling that simulates COPC migration and identifies key chemical reactions (Section 3.5) that were included in the 3D geochemical reactive modelling (Section 4.0).

3.2 Pre-Mining Existing Conditions

3.2.1 Mineralogical Composition

Understanding the mineralogical composition of the geologic materials, including overburden and bedrock units in the LSA is important for understanding existing groundwater chemistry, and for conceptualizing the fate and transport of chemicals in groundwater post-decommissioning. The mineralogical compositions, including the chemical formulae for minerals, of the major lithologic units for the Project are summarized in Table 3-1. The mineralogical and groundwater quality discussion in this section and the next, respectively, do not address the competent basement aquitard. The influence of this unit on groundwater flow conditions and quality is considered very limited due to the low permeability and storage (Section 2.3.2), and any influence is accounted for in the description and discussion of conditions in the paleoweathered zone.

The mineralogical compositions presented in Table 3-1 summarize the extensive data set collected by Denison from core at the site using a number of analytical techniques: elemental analysis, infrared mineral analysis (i.e., PIMA), electron microscopy (i.e. QEMSCAN) and petrography. Composite samples were collected from core material every 5-20 m through the Athabasca Supergroup Sandstones and discrete samples collected every 0.5 m within and proximal to the ore zone. Clay mineralogy was determined from the bulk geochemical composition of the samples (elemental analysis) using a normative clay calculation, as described in the Baseline Report. Mineralogy was further evaluated in a subset of location and depth intervals by infrared mineral analysis (i.e., PIMA) and/or petrography.

The mineralogy of each unit is broken down into major – representing ≥ 2% w/w components – and minor components. Minor components represent < 2% (w/w), but also classified with "minor" components are those that were identified by petrography, and those with a small number of samples results resulting in greater uncertainty about their relative proportions. The ore zone has complex mineralogy, including sulfide, oxide, carbonate, clay minerals and quartz. The upper and lower clay units, and the paleoweathered zone are dominated by clay minerals and quartz. The Athabasca Supergroup sandstones are dominated by quartz (greater than 90%), with smaller proportions of iron and clay minerals. The mineralogy of the overburden has not been evaluated in detail and is not presented in Table 3-1. Grain size analysis on several overburden samples collected as part of a drilling program at the site in 2020 indicate that clay minerals make up from 1-9% by weight.

Clay, iron mineral, and CaO (as a proxy for calcite, $CaCO_3$) content of the Athabasca Supergroup sandstones and paleoweathered zone are shown in Table 3-2. The lithologic units of the Athabasca Supergroup sandstones are shown (i.e., Manitou Falls Group formations; MFa, MFb, MFc, and MFd), but results have also been tabulated for the Desilicified zone in the inferred downgradient direction from the mining area. The borehole locations included in the downgradient Desilicified zone are shown in Figure 3-1. The Desilicified zone was included as a hydrogeologic unit to reflect groundwater flow conditions, through the Desilicified Zone, to the receiving environment.

The calcite content of all the lithologic units is low (generally <0.2% CaO). The content of iron (as Fe_2O_3) varies by lithologic unit, and median values are in the range of 0.1-1%, except for the paleoweathered zone, where the median hematite (Fe_2O_3) content is approximately 2%. The clay content, reflecting the normative clay calculated from elemental concentrations, also varies by lithologic unit, with median concentrations ranging from approximately 2-6% in the Athabasca Supergroup sandstones and approximately 50% in the paleoweathered zone. Within the Athabasca Supergroup sandstones, the Bird Formation (MFb) is the richest in clay minerals. The distribution of total clay into mineral phase indicates that illite dominates the clay mineral content in the Athabasca Supergroup sandstones and, while illite is still present, chlorite dominates the clay mineral content in the paleoweathered zone. Understanding of changes to the mineralogy of the ore zone post-mining gained from metallurgical testing is discussed in Appendix F.

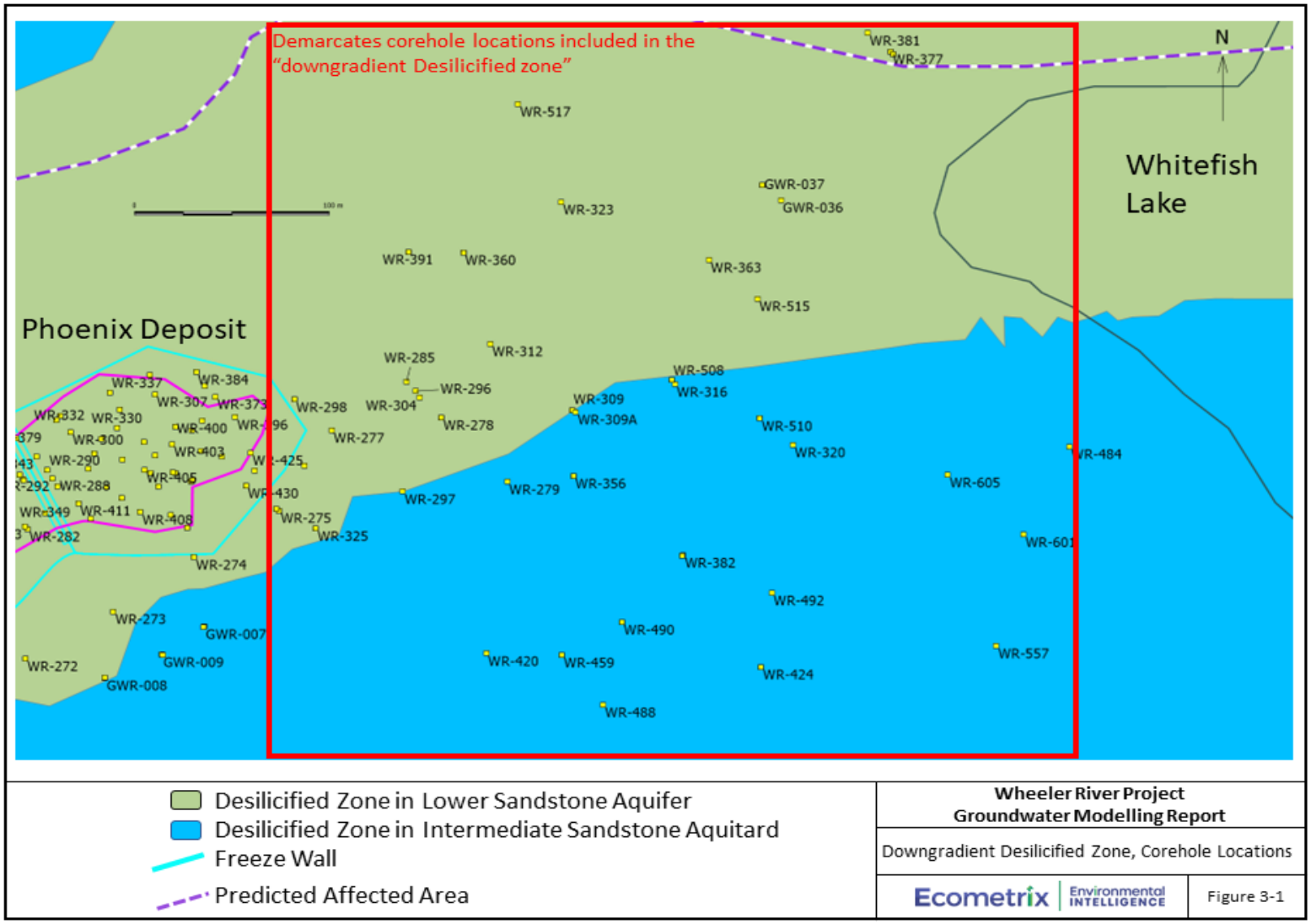

Figure 3-1: Downgradient Desilicified Zone, Corehole Locations

Table 3-1: Mineralogy by Unit

Unit	Mineral	Ideal Formula	Major (≥2% w/w)	Minor (< 2% w/w, or, shown to be present in Petrography or core logging)
Ore Zone	Pyrite	FeS2	X	
	Galena	PbS	X	
	Chalcopyrite	CuFeS2	X	
	Quartz	SiO2	X	
	Chlorite	(Fe,Mg)2(Al;Fe3+)3Si3AlO10(OH)8	X	
	Muscovite/Illite	KAl2(Si3Al)O10(OH;F)2	X	
	Kaolinite	Al2Si2O5(OH)4	X	
	Fe-oxy-hyroxides	FeO(OH)·nH2O	X	
	Uraninite	UO2	X	
	UO2.33	U3O7	X	
	UO2.25	U4O9	X	
	Schoepite	UO3:2H2O	X	
	Siderite	FeCO3	X	
	Fluorite	CaF2	X	
	Gersdorffite	NiAsS		X
	Nickeline	NiAs		X
	Dravite	NaMg3Al6(Si6O18)(BO3)3(OH)3(OH)		X
	Pyrrhotite	$Fe_{1-x}S$ (x=0-0.17)		X
	Sphalerite	(Zn,Fe)S		X
	Feldspar	KAlSi3O8		X
	Calcite	CaCO3		X
	Apatite	Ca5(PO4)3(F,Cl,OH)		X
	Corundum	Cr2O3		X
	APS Minerals	CaAl3(PO4)(PO3OH)(OH)6		X
Paleoweathered Basement	**Quartz**	SiO2	X	
	Chlorite	(Fe,Mg)2(Al;Fe3+)3Si3AlO10(OH)8	X	
	Illite	(K,H3O)(Al,Mg,Fe)2(Si,Al)4O10[(OH)2,(H2O)]	X	
	Kaolinite	Al2Si2O5(OH)4	X	
	Hematite	Fe2O3	X	
	Dravite	NaMg3Al6(Si6O18)(BO3)3(OH)3(OH)	X	
	Uraninite/Pitchblende	UO2		X
	Chalcopyrite	CuFeS2		X
	Pyrite	FeS2		X
	Galena	PbS		X
Upper and Lower Clay Zones	**Quartz**	SiO2	X	
	Chlorite	(Fe,Mg)2(Al;Fe3+)3Si3AlO10(OH)8	X	
	Illite	(K,H3O)(Al,Mg,Fe)2(Si,Al)4O10[(OH)2,(H2O)]	X	
	Kaolinite	Al2Si2O5(OH)4	X	
	Hematite	Fe2O3	X	
	Uraninite/Pitchblende	UO2	X	
	Dravite	NaMg3Al6(Si6O18)(BO3)3(OH)3(OH)		
	Uranophane	Ca(UO2)2(SiO3OH)2:5H2O		X
	Graphite	C		X
	Carbonates	various		X
	Chalcopyrite	CuFeS2		X
	Pyrite	FeS2		X
Athabasca Group sandstones	**Quartz**	SiO2	X	
	Hematite	Fe2O3	X	
	Chlorite[a]	(Fe,Mg)2(Al;Fe3+)3Si3AlO10(OH)8	X	X
	Illite[a]	(K,H3O)(Al,Mg,Fe)2(Si,Al)4O10[(OH)2,(H2O)]	X	X
	Kaolinite[a]	Al2Si2O5(OH)4	X	X
	Dravite	NaMg3Al6(Si6O18)(BO3)3(OH)3(OH)		X
	Pyrite/Sooty Pyrite	FeS2		X

Notes

Uraninite Indicates dominant minerals; can be present at values exceeding 40% w/w

Chlorite Indicates that the clay minerals bolded, combined, represent a dominant mineral group (i.e. > 40% w/w)

[a] In the Athabasca Group sandstones, the relative dominance of the clay minerals varies by HU. The individual and combined clay minerals do not always represent a major mineral group.

Table 3-2: CaO, Fe Oxide and Clay Content of the Athabasca Supergroup sandstones and Paleoweathered Zone

Lithologic Unit	Number of Samples (CaO and Fe2O3, %)	Number of Samples (Clay %)	Statistic	Elemental Analysis (wt % in sediment/rock)		Normative Clay (wt % in sediments/rock)[b]					PIMA (% of total clay content)[c]			
				CaO (%, Total)	Fe2O3 (%, Total)[a]	Clays (%)	Kaolinite (%)	Illite (%)	Dichlorite (%)	Dravite (%)	Illite (%)	Chlorite (%)	Kaolinite (%)	Dravite1 (%)
Overburden	8	84	Max	0.21	0.38	6.7	3.63	5.23	2.17	0.62	Data Not Collected			
			Min	0.005	0.03	0.20	0.00	0.06	0.00	0.01				
			Median	0.165	0.28	1.74	0.29	1.06	0.04	0.03				
			Average	0.14	0.26	1.94	0.47	1.22	0.25	0.08				
			Standard Deviation	0.063	0.10	1.23	0.52	0.94	0.47	0.11				
MFd	3077	3556	Max	0.71	1.7	39.6	17.2	24.4	15.2	8.03				
			Min	0.005	0.02	0.02	0.00	0.00	0.00	0.00				
			Median	0.005	0.05	2.05	0.32	1.45	0.00	0.28				
			Average	0.009	0.085	2.27	0.47	1.49	0.30	0.45				
			Standard Deviation	0.014	0.120	1.45	0.76	1.20	0.66	0.53				
MFc	8532	9065	Max	1.44	9.1	60.5	18.9	46.1	27.8	16.3				
			Min	0.005	0.02	0.03	0.00	0.00	0.00	0.00				
			Median	0.01	0.29	3.76	0.44	2.60	0.08	0.30				
			Average	0.02	0.52	4.08	0.84	2.73	0.49	0.66				
			Standard Deviation	0.02	0.60	2.50	1.23	1.96	1.17	0.99				
MFb	6086	7115	Max	2.48	7.23	64.3	32.61	31.95	52.59	21.60				
			Min	0.005	0.04	0.03	0.00	0.00	0.00	0.00				
			Median	0.02	0.89	5.85	0.95	4.17	0.00	0.17				
			Average	0.02	1.10	6.23	1.56	4.24	0.41	0.51				
			Standard Deviation	0.06	0.87	3.28	1.99	2.20	2.12	1.07				
MFa	10436	10817	Max	3.74	25.8	68.0	34.2	38.2	63.7	45.0				
			Min	0.005	0.01	0.03	0.00	0.00	0.00	0.00				
			Median	0.01	0.14	3.53	0.67	1.74	0.20	0.33				
			Average	0.021	0.52	4.76	1.16	2.67	0.93	1.00				
			Standard Deviation	0.056	1.08	4.73	1.94	2.95	2.79	2.03				
MFa in Downgradient DSZ	510	542	Max	0.28	5.77	41.3	28.8	17.0	20.9	9.22				
			Min	0.005	0.03	0.40	0.00	0.00	0.00	0.01				
			Median	0.02	0.09	2.62	0.51	0.42	1.18	0.15				
			Average	0.021	0.30	3.96	0.78	1.66	1.52	0.52				
			Standard Deviation	0.022	0.64	3.95	1.70	2.55	1.89	1.23				
Downgradient Desilicified Zone, All Units	1376	1459	Max	0.28	6.73	41.3	28.8	17.0	20.9	9.2				
			Min	0.005	0.03	0.30	0.00	0.00	0.00	0.01				
			Median	0.02	0.23	4.14	0.47	2.42	0.64	0.17				
			Average	0.019	0.58	4.63	0.79	2.94	0.90	0.47				
			Standard Deviation	0.017	0.78	3.05	1.28	2.60	1.36	0.89				
Paleoweathered Zone	109	109	Max	10.1	23.598	67.1	17.9	36.0	65.3	43.3	98.5	95.4	21.1	11.1
			Min	0.1	0	2.81	0.00	0.00	0.00	0.06	0	1.5	0	0
			Median	0.29	2.05	47.1	0.00	9.20	35.5	0.97	13.1	69.5	NC[d]	NC[e]
			Average	0.61	3.4	48.5	1.70	10.10	36.7	1.67	28.1	64.5	NC[d]	NC[e]
			Standard Deviation	1.51	4.2	10.4	3.60	7.60	12.60	4.10	33.2	30	NC[d]	NC[e]

Notes

[a] Iron oxide content for the paleoweathered zone is % Hematite (vs. total iron as Fe_2O_3)

[b] Normative clay values for predominantly basement-hosted paleoweathered zone may be erroneous due to variable host lithology chemistry

[c] The number of samples analyzed by PIMA for the paleoweathered zone was 9 (i.e., n= 9)

[d] Kaolinite was only detected in 3 samples in the paleoweathered zone using PIMA, and was "0" in all other samples. A. Median, average and standard deviation values were not calculated.

[e] Dravite was only detected in 1 sample in the paleoweathered zone using PIMA, and was "0" in all other samples. A. Median, average and standard deviation values were not calculated.

3.2.2 Hydrochemistry

Groundwater monitoring for the projects has occurred in a network of 21 discrete interval groundwater monitoring wells. The monitoring wells and the lithostratigraphy and hydrostratigraphic unit in which they are installed is summarized in Table 3-3. Groundwater quality collected to date in each well is provided in Appendix D.

Table 3-3: Existing Groundwater Monitoring Network for the Wheeler River Project

Well Name	Lithologic Unit	Hydrostratigraphic Unit
GWR-003	Overburden	Overburden Aquifer
GWR-005	Overburden	Overburden Aquifer
GWR-006	Overburden	Overburden Aquifer
GWR-008	MFa	Lower Sandstone Aquifer/Desilicified Zone
GWR-009	MFb	Intermediate Sandstone Aquitard/ Desilicified Zone
GWR-011	MFa	Lower Sandstone Aquifer/ Desilicified Zone
GWR-012	MFa	Lower Sandstone Aquifer/ Desilicified Zone
GWR-013	MFb	Intermediate Sandstone Aquitard/ Desilicified Zone
GWR-014	MFc	Intermediate Sandstone Aquitard/ Desilicified Zone
GWR-025	MFa	Lower Sandstone Aquifer
GWR-029	MFa	Lower Sandstone Aquifer
GWR-031	Ore and Barrier Zones	Paleoweathered Zone
GWR-032	MFa, Ore Zone, Barrier Zones, Basement Aquifer	Ore Zone
GWR-033	MFa	Lower Sandstone Aquifer
GWR-034	MFb	Intermediate Sandstone Aquitard
GWR-035	Overburden/MFd	Upper Sandstone Aquifer
GWR-036	Overburden	Overburden Aquifer
GWR-037	MFd	Upper Sandstone Aquifer/ Desilicified Zone
GWR-046	MFc	Intermediate Sandstone Aquitard
GWR-047	MFb	Lower Sandstone Aquifer/ Desilicified Zone
GWR-048	MFa	Lower Sandstone Aquifer

The GWR-series wells were installed in all lateral directions around the ore zone. The well network is shown in Figure 3-2. For the most part, the wells occur in clusters of three, with installations targeting the a) the Overburden and Upper Sandstone Aquifers (overburden, MFd, and upper MFc); b) the Intermediate Sandstone Aquitard (lower MFc and upper MFb), and c) the Lower Sandstone Aquifer (Lower MFb and MFa). Overlying the Phoenix deposit there are also five discrete interval monitoring wells that were sampled as part of the baseline program. These wells are GWR-011 (MFa) and GWR-013 (MFb), GWR-046 (MFc), GWR-047 (MFb), and GWR-048 (MFa). Groundwater quality within the mineralized zone is sampled in well GWR-032. The screened interval for GWR-031 straddles the paleoweathered zone, ore zone and the Basement Aquitards.

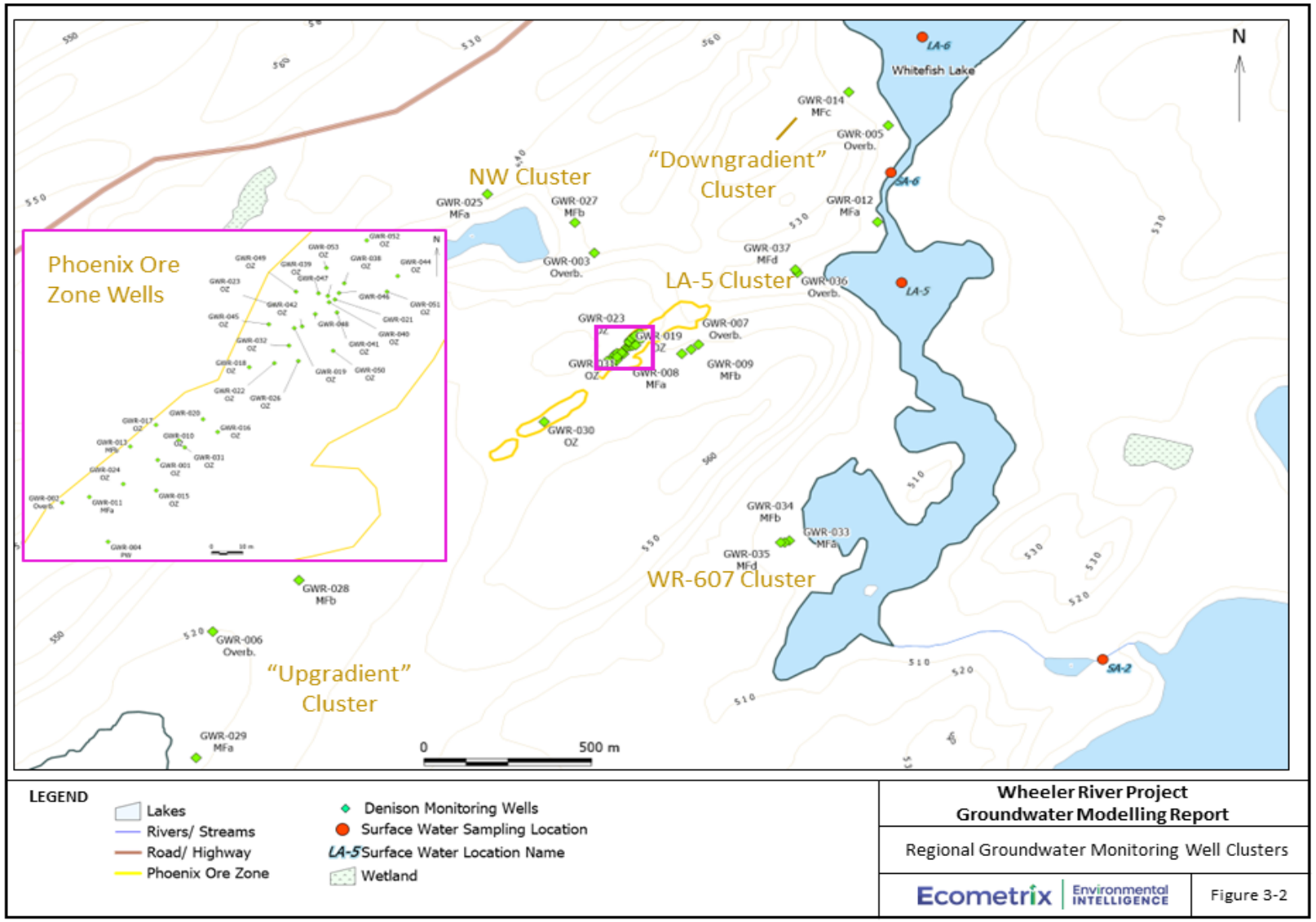

Figure 3-2: Regional Groundwater Monitoring Well Clusters

To evaluate the groundwater chemistry at the site, basic statistics were prepared and groundwater hydrochemical types were presented in the Baseline Report. Characterization of geochemical conditions in groundwater in the hydrostratigraphic units was further evaluated herein in support of geochemical modelling by examining pH and redox-dependent speciation of major constituents, using Pourbaix (pH-pe) diagrams.

Generally, groundwater associated with the Athabasca Supergroup sandstones and overburden is of circumneutral pH, with total dissolved solids (TDS) typically less than 250 mg/L, and alkalinity concentrations in the rang of 10 to126 mg/L (Appendix D). Groundwater in the ore zone is circumneutral, with TDS values greater than 500 mg/L and with, higher concentrations of radionuclides and some metals/trace elements than are measured in hydrostratigraphic units within the Athabasca Supergroup sandstones and overburden.

Summary statistics, including maximum, minimum and median concentrations in groundwater by hydrostratigraphic unit are provided as Table 3-4. In addition to the groundwater results, analytical results for surface water samples collected as part of the Wheeler River Project: Baseline Aquatic Environment Study (EcoMetrix, 2020) are also included, so that the quality of groundwater can be compared to that in surface water in the region surrounding the Phoenix deposit.

Table 3-4: Summary Statistics, Groundwater and Surface Water Quality, Wheeler River Project

Well Cluster	Units	Ore Zone (OZ)				Paleoweathered Zone (PWZ)				Lower Sandstone Aquifer (MFa)				Intermediate Sandstone Aquitard (MFb and MFc)[a]				Local Groundwater Flow System (OB and MFd)				Surface Water[b,c]				Constituent "Group"
		Number	Max	Min	Median	Number	Max	Min	Median	Number	Max	Min	Median	Number	Max	Min	Median	Number	Max	Min	Median	Number	Max	Min	Median	
Field Parameters																										
Field pH	pH units	2	6.83	6.79	6.81	2	7.21	7.03	7.12	13	8.70	6.08	7.02	5	10	6.4	7.4	12	7.5	5.9	6.5	-	-	-	-	(2) 3*
Field Temp.	°C	2	19	8.0	13	2	17	11.3	14	13	18	3.6	7.5	6	10	3.3	8.1	12	15	3.4	5.0	-	-	-	-	See note d
Field Conductivity	µS/cm	2	1486	737	1112	2	1162	588	875	13	1392.0	56.7	144.8	6	362	97	227	12	98	17	46	-	-	-	-	(2) 3*
ORP	mV	-	-	-	-	-	-	-	-	1	-57.5	-57.5	-	2	51	-85	-17	-	-	-	-	-	-	-	-	
Field SPC	µS/cm	2	1683	958	1321	2	1374	789	1082	13	2315	87.6	219	6	618	138	334	12	151	28	77	-	-	-	-	2
Field TDS	mg/L	2	1094	623	859	2	893	513	703	13	1505	0.11	142	6	402	0	218	12	98	18	53	-	-	-	-	2
Analytical Results																										
Bicarbonate	mg/L	3	174	118	155	2	167	160	164	13	112	29	51	6	188	75.20	85.7	12	35	12	24	32	20	2.0	8.1	2
Carbonate	mg/L	3	<1	<1	-	2	<1	<1	-	13	<1	<1	-	6	18	<1	-	12	<1	<1	-	32	<1	<1	-	2
Chloride	mg/L	3	234	202	220	2	151	145	148	13	319	2.7	7.4	6	8.6	<1	0.85	12	10	<0.1	0.90	32	0.80	0.10	0.37	2
Hydroxide	mg/L	3	<1	<1	-	2	<1	<1	-	13	<1	<1	-	6	<1	<1	-	12	<1	<1	-	32	<1.1	<1	-	See note e
P. alkalinity	mg/L	3	<1	<1	-	2	<1	<1	-	12	<1	<1	-	4	15	<1	-	12	<1	<1	-	32	<1.1	<1	-	See note e
pH	pH units	3	7.52	7.33	7.40	2	7.83	7.36	7.60	13	7.83	6.90	7.34	6	9.1	7.1	7.64	12	7.32	6.38	6.90	32	7.17	6.33	6.8	See note e
Specific conductivity	µS/cm	3	1000	860	965	2	810	686	748	13	1110	68	139	6	289	141	183	12	71	19	43	32	42	12	18	See note e
Sum of ions	mg/L	3	598	504	566	2	504	439	472	12	610	54	142	4	252	126	164	12	75	20	44	32	25	6.0	13	See note e
Total alkalinity	mg/L	3	143	97	127	2	137	131	134	13	92	24	42	6	154	62	81	12	29	10	20	31	16	2.0	6.9	See note e
Total hardness	mg/L	3	267	182	256	2	190	148	169	13	283	17	43	6	104	29	66	12	32	6.0	12	31	12	4.0	5.3	See note e
Ammonia as nitrogen	mg/L	2	1	0.31	0.5	2	0	0.05	0.2	13	0.35	<0.005	0.12	6	3.4	<0.005	0.05	12	0.17	<0.01	0.02	32	1.2	<0.01	-	2
N)	mg/L	3	0.04	<0.04	-	2	<0.04	<0.04	-	13	<0.04	<0.02	-	6	0.13	<0.02	-	12	0.49	<0.04	-	32	0.25	<0.04	-	1
Nitrite	mg/L	2	<0.03	<0.03		2	<0.03	<0.03	-	13	<0.03	<0.01	-	6	0.23	<0.01	-	12	0.05	<0.03	-	-	-	-	-	1
Nitrite+Nitrate as nitrogen	mg/L	2	0.01	<0.01	-	2	<0.01	<0.01	-	13	<0.01	<0.01	-	6	0.05	<0.01	-	12	0.11	<0.01	-	-	-	-	-	1
Ortho-phosphate as P	mg/L	2	0.01	<0.01	-	2	0.01	<0.01	-	12	0.16	<0.01	0.08	4	0	0.005	0.06	12	0.14	0.01	0.05	-	-	-	-	1
Organic carbon, dissolved	mg/L	2	36	6	21	2	68	6	37	13	16	1.0	2.0	6	35	2.0	13.5	12	3.9	0.40	1.2	32	8.40	1.50	2.4	2
Iron (II)		1	0.04	0.04	-	1	<0.02	<0.02	-	3	2.30	0.02	0.09	4	7.8	<0.02	-	4	0.07	<0.02	0.03					2
Fluoride	mg/L	3	0.23	0.19	0.22	2	0.42	0.32	0.37	13	0.24	0.01	0.14	6	0.2	0.06	0.08	12	0.14	0.01	0.04	32	0.06	0.01	0.02	2
Total dissolved solids	mg/L	3	639	599	628	2	536	393	465	13	653	59	122	6	264	132	169	12	199	45	65	32	35.00	11.00	23.17	See note e
Total suspended solids	mg/L	2	17	11.0	14	2	41	5.0	23	12	171	0.5	9.0	4	208	13.0	19	12	838	1.00	19	32	23.00	<1.5	-	1
Calcium	mg/L	3	84	55	78	2	58	43	51	13	84	4.7	13	6	33	8.2	23	12	5.2	1.2	2.8	32	3.50	1.00	1.39	2
Magnesium	mg/L	3	15	11.0	14	2	11	9.9	10	13	18	1.2	2.6	6	7.6	0.40	2.6	12	4.7	0.4	1.1	32	0.70	0.30	0.40	2
Potassium	mg/L	3	6	4.6	5.4	2	6	5.3	5.4	13	4.4	1.5	2.1	6	7	1.2	4	12	5.3	0.3	1.4	32	0.80	0.10	0.35	2
Sodium	mg/L	3	83	75	81	2	71	69	70	13	83	5.3	8.9	6	23	9.0	17	12	12	1.7	3.9	32	1.85	1.14	1.51	2
Sulfate	mg/L	3	30	8.0	13	2	40	6.6	23	13	67	0.70	5.9	6	10	2.3	4.7	12	8.0	0.90	3.8	32	8.30	0.30	0.68	2

Notes

	Shading is used to highlight median values
	Shading is used to indicate "Group 1" constituents - see text for details.
	Shading is used to indicate "Group 2" constituents - see text for details.
	Shading is used to indicate "Group 3" constituents - see text for details.
-	Indicates where median values were not calculated. Median values were only calculated when the frequency of detection for the constituent exceeded 50% of the samples from each group. Where values were below detection, the detection limit was used to calcualate median values.
	Blank Cells mean the constituent was not measured
a	Sample GWR-034 was not included in the summary statistics, as the groundwater was influenced by drilling fluids and additives and is not reflective of natural groundwater.
b	The surface water samples include all 32 lake and stream sample locations reported in Ecometrix, 2020 (Wheeler River Project: Baseline Aquatic Environment Study). Surface water quality at each location was measured on 1-6 occasions. Arithmetic mean values were reported in Ecometrix, 2020 at each location were used herein (i.e. the reported "max" value is the maximum arithmetic mean value, etc.,). This was considered acceptable for the comparison only purposes within this report.
c	Metal and trace element concentrations in the surface water samples are for Total concentrations, not disssolved.
d	Temperature and Dissolved oxygen are likely to be influenced to some extent by ambient conditions, and are thus not considered further in the interpretation of groundwater conditions at the Site.
e	These constituents are considered part of Group 2 but are not discussed further in the interpretation of groundwater conditions at the site because they are correlated to or represented by other parameters being carried forward (e.g. Fe^{2+} by Dissolved Iron; laboratory-measured TDS by field-measured TDS, etc.)
f	U-234 was calculated from U-238 assuming secular equilibrium. This assumption may not hold in the groundwater flow systems. This constittuent is not considered further in the interpretation of groundwater condtions at the Site.
g	Tritium concentrations were very low, with the exception of the ore zone and paleoweathered zone groundwater samples.

Table 3-4: Summary Statistics, Groundwater and Surface Water Quality, Wheeler River Project (continued)

Well Cluster	Units	Ore Zone				Paleoweathered Zone (PWZ)				Lower Sandstone Aquifer (MFa)				Intermediate Sandstone Aquitard (MFb and MFc)[a]				Local Groundwater Flow System (OB and MFd)				Surface Water[b,c]				Constituent "Group"
		Number	Max	Min	Median	Number	Max	Min	Median	Number	Max	Min	Median	Number	Max	Min	Median	Number	Max	Min	Median	Number	Max	Min	Median	
Aluminum, dissolved	mg/L	3	0.21	0.0006	0.01	2	0.0025	0.0005	-	13	0.05	<0.0005	0.002	6	0.8	0.003	0.02	12	0.48	<0.0005	0.01	32	0.028	0.001	0.005	(1) 3*
Antimony, dissolved	mg/L	3	0.00	<0.002	-	2	<0.002	<0.002	-	13	0.001	<0.0001	-	6	0.0007	<0.0001	-	12	<0.0002	<0.0002	-	32	0.00	<0.0002	-	1
Arsenic, dissolved	ug/L	3	3.40	0.2	0.3	2	1.20	1.00	1.1	13	4.1	<0.1	0.20	6	11	0.50	2.3	12	1.4	0.1	0.35	32	0.0003	<0.0001	-	(1) 3*
Barium, dissolved	mg/L	3	0.09	0.063	0.08	2	0.05	0.035	0.04	13	0.25	0.005	0.06	6	0.2	0.06	0.13	12	0.02	0.01	0.01	32	0.01	<0.00215	0.00	1
Beryllium, dissolved	mg/L	3	0.00	<0.0001	-	2	<0.001	<0.001	-	13	<0.0001	<0.00002	-	6	0.0002	<0.00002	-	12	0.0001	<0.0001	-	32	0.00	<0.0001	-	1
Bismuth, dissolved	mg/L	2	<0.002	<0.002	-	2	<0.002	<0.002	-	13	<0.0002	<0.00005	-	6	<0.0002	<0.00005	-	12	<0.0002	<0.0002	-	-	-	-	-	1
Boron, dissolved	mg/L	3	0.6	0.43	0.58	2	0.6	0.50	0.53	13	0.40	0.03	0.04	6	0.02	<0.01	0.02	12	0.03	<0.01	-	32	<0.01	<0.01	-	2
Bromine	µg/L	2	2300	2000	2150	2	1500	1100	1300	13	3600	34	100	6	34	<5	6.0	12	79	5.0	-	-	-	-	-	2
Cadmium, dissolved	mg/L	1	0.00001	<0.00001	-	2	<0.0001	<0.0001	-	13	<0.00001	<0.000005	-	6	0.00003	<0.000005	-	12	0.00005	<0.00001	0.00001	31	0.00	<0.00001	-	(1) 3*
Chromium, dissolved	mg/L	3	0.013	<0.0005	0.001	2	0.009	0.001	0.005	13	0.0007	<0.0005	-	6	0.0058	<0.0005	-	12	<0.0005	<0.0005	-	32	<0.0005	<0.0005	-	3
Cobalt, dissolved	mg/L	3	0.0007	<0.0001	0.00	2	0.0020	0.0002	0.00	13	0.0005	<0.0001	-	6	0.01	<0.0001	0.0002	12	0.001	<0.0001	0.0004	32	0.00	<0.0001	-	(1) 3*
Copper, dissolved	mg/L	3	<0.0002	<0.0002	-	2	<0.002	<0.002	-	13	0.002	<0.0002	-	6	0.01	<0.0002	0.0009	12	0.002	<0.0002	0.001	32	0.00	<0.0002	-	(1) 3*
Iron, dissolved	mg/L	3	6.4	3.83	4.2	2	3.6	0.09	1.8	13	16	0.01	2.8	6	15	0.01	3.05	12	4.8	0.01	0.41	32	9.50	0.01	0.10	(1) 3*
Lead, dissolved	mg/L	3	0.0005	<0.0001	0.0003	2	0.0010	<0.0001	-	13	0.0002	<0.00005	-	6	0.00157	<0.00005	-	12	0.0002	<0.0001	-	32	<0.00012	<0.0001	-	(1) 3*
Lithium, dissolved	µg/L	2	75	65	70	2	90	89	90	13	40	9.9	14	6	14	6.20	9.0	12	11	0.8	6.3	-	-	-	-	1
Manganese, dissolved	mg/L	3	0.2	0.20	0.2	2	0.2	0.13	0.2	13	2.6	0.085	0.4	6	3.9	0.0018	1.18	12	0.2	0.04	0.1	32	0.34	0.003	0.013	2
Molybdenum, dissolved	mg/L	3	0.08	0.004	0.01	2	0.06	0.01	0.04	13	0.03	<0.0001	0.001	6	0.01	0.0024	0.004	12	0.003	0.0001	0.0008	32	<0.00011	<0.0001	-	(1) 3*
Nickel, dissolved	mg/L	3	0.01	0.00	0.00	2	0.04	0.00	0.02	13	0.001	<0.0001	0.0002	6	0.05	0.0006	0.002	12	0.010	<0.0001	0.002	32	0.0003	<0.0001	-	(1) 3*
Selenium, dissolved	mg/L	3	0.0001	0.0001	0.0001	2	<0.001	<0.0001	-	13	0.0011	<0.00005	0.0001	6	0.0004	<0.0001	-	12	0.0008	<0.0001	-	32	<0.0001	<0.0001	-	(1) 3*
Silica, soluble, dissolved	mg/L	2	14	13.3	13	2	10	9.1	10	13	26	11	18	6	30	11.8	16	12	35	17	22	-	-	-	-	2
Silver, dissolved	mg/L	2	0.00005	<0.00005	-	2	<0.0005	<0.0001	-	13	<0.00005	<0.00001	-	6	0.00005	<0.00001	-	12	0.0001	<0.0001	-	32	<0.00005	<0.00005	-	1
Strontium, dissolved	mg/L	3	3	1.7	2.4	2	1	1.2	1.3	13	2.19	0.10	0.17	6	0.26	0.08	0.13	12	0.06	0.01	0.02	32	0.02	0.01	0.01	2
Sulfur	mg/L	2	4	2.7	4	2	13	2.2	8	13	22	0.2	2.0	6	8.7	0.80	1.6	12	2.7	0.30	1.3	-	-	-	-	See note e
Thallium, dissolved	mg/L	3	<0.002	<0.002	-	2	<0.002	<0.002	-	13	<0.0002	<0.00001	-	6	<0.0002	<0.00001	-	12	<0.0002	<0.0002	-	32	<0.0002	<0.0002	-	1
Tin, dissolved	mg/L	3	<0.0001	<0.0001	-	2	<0.001	<0.0001	-	13	<0.0001	<0.0001	-	6	0.0003	<0.0001	-	12	<0.0001	<0.0001	-	32	0.0007	<0.0001	-	1
Titanium, dissolved	mg/L	3	0.0003	<0.0002	-	2	<0.002	<0.0002	-	13	0.0004	<0.0002	-	6	0.009	<0.0002	-	11	0.005	<0.0002	-	32	0.0008	<0.0002	-	1
Vanadium, dissolved	mg/L	3	0.0074	<0.0001	0.0004	2	0.0005	<0.0001	-	13	<0.0005	<0.0001	-	6	0.002	<0.0005	-	12	0.0004	<0.0001	-	32	0.0005	<0.0001	-	3
Zinc, dissolved	mg/L	3	5	2.62	2.9	2	18	0.69	9.5	13	0.015	0.001	0.003	6	0.0	0.0007	0.001	12	0.010	0.001	0.004	32	0.0014	<0.0005	-	3
Phosphorus, dissolved	mg/L	2	<0.01	<0.01	-	2	<0.1	<0.01	-	13	0.29	<0.01	0.06	6	0	<0.05	0.06	12	0.06	<0.01	-	30	0.15	<0.01	-	1
Radionuclides																										
Uranium, dissolved	µg/L	3	299	5.7	11	2	50	17.0	34	13	9.0	0.10	0.70	6	55	0.30	11.60	12	5.8	<0.1	0.5	32	<0.0001	<0.0001	-	3
Uranium-234 calculated	Bq/L	2	2	0.21	0.95	2	11	0.46	5.58	12	0.36	0.001	0.01	4	11	0.02	0.2	12	0.1	0.001	0.0	-	-	-	-	See Note f
Uranium-238 calculated	Bq/L	2	2	0.21	0.95	2	11	0.46	5.58	12	0.36	0.001	0.01	4	11	0.02	0.2	12	0.1	0.001	0.01	32	<0.025	<0.02	-	3
Lead-210	Bq/L	3	3300	1200	2200	2	7300	1100	4200	13	0.66	0.01	0.1	6	8.0	0.08	1.0	12	0.60	<0.02	0.08	32	0.02	<0.005	-	3
Polonium-210	Bq/L	3	260	110	120	2	650	460	555	13	1.3	0.02	0.2	6	13	0.03	0.6	12	0.22	0.02	0.1	32	0.01	<0.005	-	3
Radium-226	Bq/L	3	400	180	300	2	120	76	98	13	1.6	0.07	0.3	6	17	0.06	0.3	12	0.36	0.02	0.1					3
Radon-222	Bq/L	3	3800000	400000	2700000	2	12000000	5900	6002950	13	620	<3	10	6	1800	<4	11	12	86	<5	20	28	<0.013	<0.01	-	3
Thorium-230	Bq/L	3	14	2.0	7.0	2	30	1.1	15.6	13	0.30	<0.01	0.01	6	4.70	<0.01	0.1	12	0.12	<0.01	-					3
Tritium	Bq/L	2	1800	950	1375	2	910	<15	-	13	0.5	0.1	-	6	19	0.1	1.0	12	1.1	0.10	-	-	-	-	-	See Note g

Notes

	Shading is used to highlight median values
	Shading is used to indicate "Group 1" constituents - see text for details.
	Shading is used to indicate "Group 2" constituents - see text for details.
	Shading is used to indicate "Group 3" constituents - see text for details.
(1) 3*	Indicates where a groundwater constituent was categorized as a Group 1 (or 2) constituent based on baseline groundwater quality, but was given a final categorization as a Group 3 constituent based on other information.
-	Indicates where median values were not calculated. Median values were only calculated when the frequency of detection for the constituent exceeded 50% of the samples from each group. Where values were below detection, the detection limit was used to calcualate median values.
	Blank Cells mean the constituent was not measured
a	Sample GWR-034 was not included in the summary statistics, as the groundwater was influenced by drilling fluids and additives and is not reflective of natural groundwater.
b	The surface water samples include all 32 lake and stream sample locations reported in Ecometrix, 2020 (Wheeler River Project: Baseline Aquatic Environment Study). Surface water quality at each location was measured on 1-6 occasions. Arithmetic mean values were reported in Ecometrix, 2020 at each location were used herein (i.e. the reported "max" value is the maximum arithmetic mean value, etc.,). This was considered acceptable for the comparison only purposes within this report.
c	Metal and trace element concentrations in the surface water samples are for Total concentrations, not disssolved.
d	Temperature and Dissolved oxygen are likely to be influenced to some extent by ambient conditions, and are thus not considered further in the interpretation of groundwater conditions at the Site.
e	These constituents are considered part of Group 2 but are not discussed further in the interpretation of groundwater conditions at the site because they are correlated to or represented by other parameters being carried forward (e.g. Fe^{2+} by Dissolved Iron; laboratory-measured TDS by field-measured TDS, etc.)
f	U-234 was calculated from U-238 assuming secular equilibrium. This assumption may not hold in the groundwater flow systems. This constittuent is not considered further in the interpretation of groundwater condtions at the Site.
g	Tritium concentrations were very low, with the exception of the ore zone and paleoweathered zone groundwater samples.

Examining the median values, three constituent "groups" emerged. These groupings are color coded in Table 3-4.

Group 1: This group, highlighted in pale green highlighting in Table 3-4, includes constituents for which concentrations in groundwater in all the hydrostratigraphic units and surface water did not vary significantly. This group generally included constituents present in low concentrations, often at or below analytical detection limits, and were not discussed further when interpreting baseline groundwater quality conditions for the Project in the Baseline Report.

Group 2: This group, highlighted by pale yellow shading in Table 3-4 includes general groundwater quality indicators, and select trace elements. Concentrations of this group of constituents informs the conceptualization of the groundwater flow systems at the Site.

Group 3: This group, highlighted in blue in Table 3-4, primarily includes radionuclides, but also some trace elements (Cr, V, and Zn). Median concentrations/activities of Group 3 constituents in the ore zone groundwater samples are generally more than two orders of magnitude higher than those in the Athabasca Supergroup sandstone and overburden hydrostratigraphic units. Elevated levels of these constituents are, like those of radionuclides, attributed to the mineralogy and geochemical conditions within the ore zone.

Median concentrations/activities of Group 3 constituents in the ore zone groundwater samples are generally more than two orders of magnitude higher than those in the Athabasca Sandstone Supergroup and overburden hydrostratigraphic units. The apparent attenuation of dissolved-phase constituents associated with the ore zone groundwater reflects the existing assimilative capacity and aquitard nature of the barrier zone, containing clay and sulphide minerals that cement the rock particles and which overlies and underlies the ore body. The resulting low flux of water and chemical constituents in groundwater from the ore zone to Semi-Regional and Shallow Flow systems, and ultimately to surface water is controlled by the clay barrier zone.

3.2.2.1 Hydrochemical Type, pH and Redox Conditions

The hydrochemical type for the groundwaters in the groundwater system are shown in Figure 3-3, and are interpreted to indicate:

1) Groundwaters in the Upper Sandstone Aquifer and overburden materials are of Ca-Na-HCO3 or Na-Ca-HCO3 type, and also contain Mg, K and sulphate. The groundwater chemistry reflects relatively fresh recharge water that becomes mineralized through the dissolution of quartz, feldspars, kaolinite and illite (AECL, 1994). Groundwater in the Intermediate Sandstone Aquitard and parts of the Lower Sandstone Aquifer also show these dominant hydrochemical types, reflecting the relatively uniform mineralogical composition in the MFa, MFb, MFc, MFd Formations. The low mineralization groundwater in the Lower Sandstone Aquifer is interpreted to be a result of fracture/fault conditions, such that some areas of the MFa are characterized by younger/recharge groundwaters.

2) There is a shift to higher mineralization and to a hydrochemical type more dominated by chloride (i.e., fall within the Ca/Mg-SO4-Cl quadrant of the Piper Diagram in Figure 3-3), areas of the Lower Sandstone aquifer, cross-gradient and downgradient of the uranium deposit. The higher chloride content occurs where the MFa has been interpreted to have been affected by hydrothermal alteration/desilicification. In this zone, prior work at Cigar Lake has attributed higher salinity groundwater in the MFa to the presence of remnant halides associated with the hydrothermal alteration (AECL, 1994).

3) Groundwater in the paleoweathered zone and ore zone also have higher chloride and sulphate concentrations relative to the fresher water in the Athabasca Supergroup sandstone units. This is interpreted as reflecting the different mineralogy in these zones, and the longer residence times and lower volumetric flow rates through these zones in comparison to the Athabasca rSupergoup sandstones.

Redox Conditions: Iron is a major constituent of the groundwater in the system, with concentrations reaching greater than10 mg/L in some of the monitoring wells. Dissolved Fe concentrations greater than 1 mg/L suggest that ferrous ion (Fe^{2+}) is present, and that the groundwater is anoxic or devoid of oxygen. Groundwater is anoxic and mildly reducing across the majority of the system, with moderately to strongly reducing conditions observed only in the ore zone; methanogenic bacteria were noted in the Cigar Lake study only in the ore zone (AECL, 1994). Measured oxidation-reduction potential (ORP) measurements are generally a qualitative indicator of redox conditions in groundwater and have been collected for a subset of groundwater samples for the project. ORP measurements collected in groundwater from the ore zone (data collected during preparations for a tracer test, Petrotek, 2022) are approximately -265 mV (Eh = -65 mV, pe = -1.3 at 7^0C, as shown in Table 3-5)

ORP measurements were collected in wells GWR-046 (MFc, Intermediate Sandstone Aquitard), GWR-047 (MFb, Intermediate Sandstone Aquitard, - Desilicified) and GWR-048 (MFa, Lower Sandstone Aquifer) in the Fall 2021 sampling event. Groundwater quality in those wells, as plotted on Pourbaix (Eh-pH) Diagrams (Figure 3-4), show that dissolved-phase Fe concentrations are primarily controlled in the Athabasca Supergroup sandstone units by the solubility of iron oxyhydroxides such as goethite (FeO_2H) and, potentially siderite ($FeCO_3$) and that ferrous iron (Fe^{2+}) is the stable form of iron in groundwater.

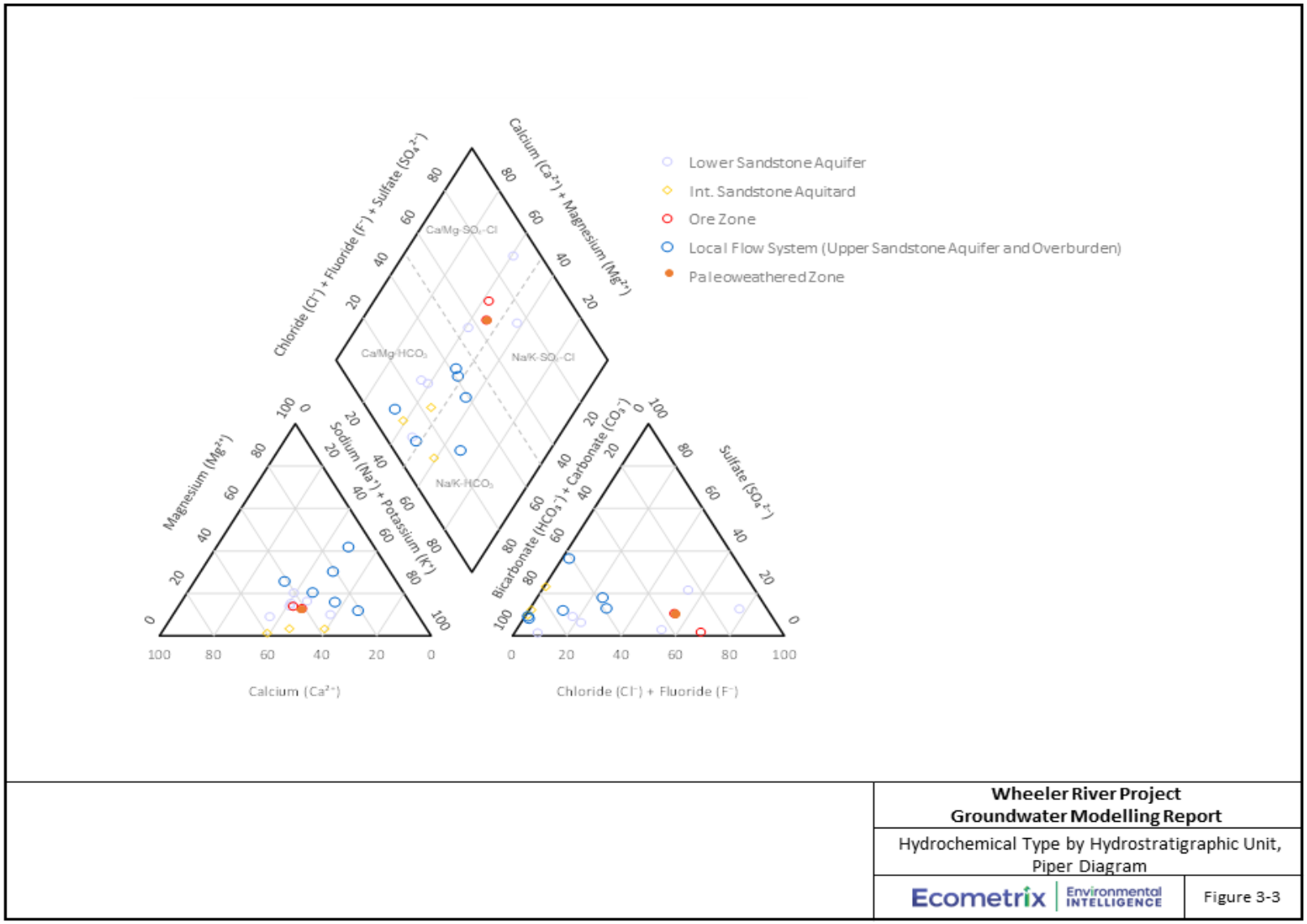

Figure 3-3: Hydrochemical Type by Hydrostratigraphic Unit, Piper Diagram

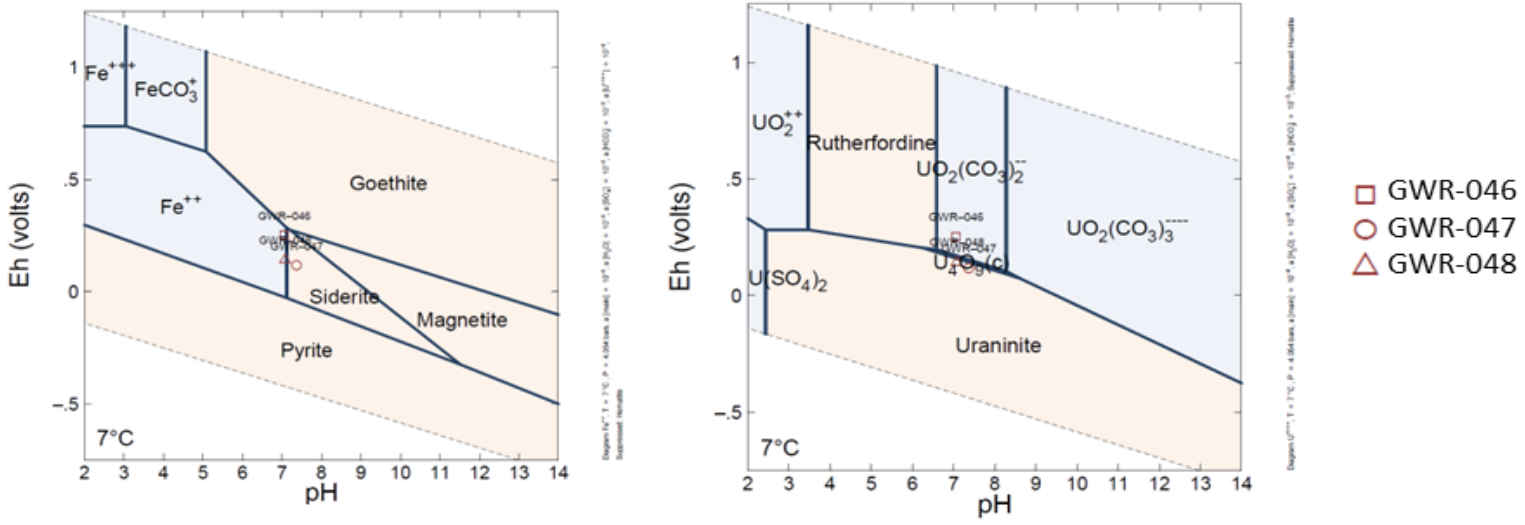

Pourbaix Diagrams were prepared in Geochemist's Workbench, Community Edition, version 15.0

	Wheeler River Project **Groundwater Modelling Report**
	Pourbaix Diagrams, Select Monitoring Wells
	Ecometrix Environmental INTELLIGENCE | Figure 3-4

Figure 3-4: Pourbaix Diagrams, Select Monitoring Wells

Dissolved-phase uranium concentrations are considered likely to reflect equilibrium with a number of uranium solid-phase associations, discussed in more detail in Section 3.5.6.2.1, but increasingly by uraninite, representing reduced uranium (U(IV)) minerals, with depth. Monitoring wells GWR-047 and GWR-048 are installed deeper in the subsurface than is GWR-046 and these two samples plot on/within the uraninite stability field in the Pourbaix diagram.

The data support the interpretation that redox conditions in the Athabasca Supergroup sandstones are lacking oxygen that, if present, would be represented by the top slanted line bordering the Goethite zone in the Eh-pH diagram, and not so reducing that methane (CH_4) is being produced as would be indicated by values in the lower regions of the pyrite or uraninite zones. This would suggest that the lower end of the redox zones are likely controlled by the reducing power of the sulphide mineral, pyrite and/or the reduced uranium mineral, uraninite.

3.3 Source Condition: Remediated Mining Area Water Quality

Metallurgical testing on the ore, including column tests, and core flooding tests, undertaken at the Saskatchewan Research Council, were completed to understand the anticipated evolution of groundwater hydrochemistry as the groundwater quality in the mineralized zone is remediated. Metallurgical testing for the Project is detailed in Appendix F. The constituents with concentrations that were outside of the range of values observed for baseline conditions in the leachate during metallurgical testing reflect the mineralogy of the ore zone (Table 3-1) and the mining fluids. The mining fluids are made up of sulfuric acid, ferric iron (Fe^{3+}) sulphate and hydrogen peroxide (the EIS, Section 2). Groundwater constituents identified as COPCs and carried forward for geochemical reactive transport modelling include: pH, sulphate, and dissolved Al, As, Cd, Co, Cu, Cr, Fe, Pb, Mo, Ni, Se, V, Zn and U and other radionuclides (discussed further in Section 3.5.6).

The chemical characteristics of the remediated groundwater used to conceptualize remediated groundwater quality for input into the reactive transport model were primarily from two coreflood tests: Coreflood#2B and Coreflood#3C. In the coreflood tests, core flushing was completed using groundwater and groundwater amended with sodium hydroxide (1.5 g/L; Coreflood #2B) or sodium bicarbonate (150-1500 mg/L $NaHCO_3$; Coreflood #3C). The coreflood tests simulated, in the lab, the rinsing of the ore zone that can be achieved in the field at the end of the mining operation. Results from these two tests were used primarily because they provided the most detailed information from which to understand remediated water quality at the time when the numerical model (presented herein) was being developed (2020-2021). As is detailed in Appendix F, more information from column and coreflood tests has become available that supports the use of results from Coreflood #2B and Coreflood 3C to conceptualize remediated groundwater quality.

"Restored Solution #1" and "Restored Solution #2" were developed to represent the bounding scenarios for groundwater quality evaluated in the reactive transport model, to assess the potential for environmental effects following remediation of the ore zone. The hydrochemistry of Restored Solutions #1 and #2 are shown in the Table 3-5. Included in Table 3-5 is the range in UBS constituent concentrations that represent the end of mining conditions (i.e., prior to

remediation) from the metallurgical testing, presented in Appendix F. Also, in Table 3-5 are groundwaters representative of baseline conditions in the hydrostratigraphic units in the LSA that are used as initial conditions in the numerical modelling. These are discussed in more detail in Section 3.5.4. Restored Solutions #1 and #2 generally are characterized by COPC concentrations outside of baseline conditions (i.e., uranium, radionuclide and metals/trace element concentrations are higher, and pH is lower) in the ore zone and in the overlying hydrostratigraphic units.

With the Wheeler River project, as with other ISR projects, it is anticipated that there will be a certain degree of outward migration (horizontal and vertical) of the oxidizing solution beyond the boundary of the operational well pattern/production area during the mining operation. This outward migration is a result of normal hydrodynamic behaviour, and the area affected outside of the well pattern is often referred to as the area affected by "flare" (IAEA, 2001). For the Wheeler River project, Denison has committed to containing flare through optimization of the well pattern and operational conditions and to limit the flare to 50 m vertically above the ore zone, through additional engineering means, as necessary. Laterally, any outward migration will be mitigated by the freeze wall.

Inclusion of flare in predictive numerical modelling has precedence in ISR projects, related both to ISR performance (e.g., Cameco, 2012) and fate and transport modelling downgradient of the ore zone (e.g., Johnson et al., 2016). For the numerical modelling of the mining area, herein, the flare was assumed to have a groundwater composition represented by 50% solution of the associated active mining area restored solution, diluted using typical groundwater chemistry from the Desilicified zone (Table 3-5). The resulting groundwater quality for the 50% solutions is summarized in Table 3-5. The assumptions made in the numerical model with respect to the groundwater quality at Decommissioning are described in more detail in Section 4.1.

Table 3-5: UBS Constituent Concentrations at end of mining, Restored Solutions and Representative Groundwater Composition by Hydrostratigraphic Unit

Parameter/ Groundwater or Restored Solution	Unit	Ore Zone (GWR-032)	PWZ (GWR-031 and Cigar Lake)	Lower Sandstone Aquifer and Decilisified Zone (GWR-011)	Intermediate Sandstone Aquitard (GWR-046)	Overburden and Upper Sandstone Aquifer (GWR-036, Primarily)	Range of Values of UBS constituent concentrations across Metallurgical tests from 2018-2021 representative of End of mining conditions		Restored Solution #1	50% Restored Solution #1	Restored Solution #2	50% Restored Solution #2
							Minimum	Maximum				
pH	unit	6.83	6.7	6.46	7.053	6.45	0.63	2.1	4.3	5.1	6.1	6.3
pe	unitless	-1.3	1.9	2.3	4.5	1.2	9.80	14.7	10	(set) 7	7.8	(set) 4
temp	^{0}C	7	7	7	7	7	7	7	7	7	7	7
Al	mg/L	6.00E-04	3.40E-02	5.20E-02	8.00E-01	3.70E-02	6.90E+01	4.61E+03	7.00E+00	3.53E+00	5.60E-01	3.06E-01
As	mg/L	2.00E-04	5.00E-02	1.30E-03	4.75E-06	3.00E-04	<0.1	2.12E+01	6.00E-02	3.07E-02	1.00E-01	5.07E-02
Ba	mg/L	6.30E-02	3.60E-02	5.40E-02	2.41E-01	5.70E-03	<0.05	<0.5	5.00E-02	5.20E-02	5.00E-02	5.20E-02
C(4)	mg/L	1.76E+02	1.54E+02	8.66E+01	1.01E+02	3.39E+01	-	-	5.80E+01	7.23E+01	1.05E+02	9.58E+01
Ca	mg/L	5.50E+01	6.76E+00	9.78E+00	1.07E+01	2.70E+00	5.80E+01	7.23E+02	1.10E+02	6.00E+01	1.00E+01	9.89E+00
Cd	mg/L	1.00E-05	1.00E-05	1.00E-05	3.36E-05	1.00E-05	1.80E-02	1.81E+00	1.50E-02	7.52E-03	4.00E-03	2.01E-03
Cl	mg/L	1.90E+02	8.65E+01	7.20E+00	8.63E+00	6.86E+00	<10	1.22E+03	2.00E+02	1.04E+02	5.00E+01	2.86E+01
Co	mg/L	1.00E-04	1.00E-02	1.00E-04	5.84E-03	4.00E-04	5.00E-01	1.49E+01	2.00E+00	1.00E+00	1.00E-02	5.05E-03
Cr	mg/L	5.00E-04	4.50E-03	5.00E-04	1.69E-03	5.00E-04	<0.1	9.14E+00	5.00E-02	2.53E-02	5.00E-02	2.53E-02
Cu	mg/L	2.00E-04	5.00E-03	1.80E-03	6.29E-03	6.00E-04	5.16E+00	9.64E+02	1.70E-01	8.60E-02	2.00E-02	1.09E-02
F	mg/L	2.30E-01	5.30E-01	1.80E-01	5.90E-02	6.00E-02	1.00E+00	3.40E+01	-	9.00E-02	8.00E-01	4.90E-01
Fe	mg/L	4.20E+00	4.90E-01	8.60E-01	6.03E+00	4.05E-01	8.20E+02	4.09E+03	1.00E+02	5.05E+01	4.70E+00	2.78E+00
K	mg/L	4.60E+00	5.60E+00	2.00E+00	6.77E+00	2.80E+00	6.20E+00	1.49E+02	9.00E+00	5.51E+00	3.50E+00	2.75E+00
Mg	mg/L	1.10E+01	3.09E+00	1.60E+00	3.91E+00	1.80E+00	<10	2.40E+02	6.00E+00	3.80E+00	3.00E+00	2.30E+00
Mn	mg/L	2.20E-01	7.00E-01	3.60E-01	3.91E+00	1.40E-01	2.70E+00	4.10E+01	3.40E+00	1.88E+00	4.80E-01	4.20E-01
Mo	mg/L	3.80E-03	1.28E-02	4.20E-03	3.89E-03	7.00E-04	1.65E+00	5.96E+01	1.00E-01	5.22E-02	1.30E-01	6.71E-02
Na	mg/L	8.10E+01	7.61E+01	6.10E+00	8.96E+00	2.90E+00	6.00E+00	1.23E+04	1.90E+02	9.82E+01	9.00E+01	4.81E+01
Ni	mg/L	1.00E-03	1.50E-02	1.00E-04	4.87E-02	1.80E-03	<1	2.68E+01	9.70E+00	4.86E+00	1.00E-02	5.05E-03
Pb	mg/L	1.00E-04	1.00E-04	1.00E-04	1.57E-03	1.00E-04	2.00E-01	1.95E+01	3.10E+00	1.55E+00	3.20E-01	1.60E-01
S(6)	mg/L	1.30E+01	4.55E+00	4.70E+00	1.01E+01	1.90E+00	5.21E+03	2.09E+05	7.03E+02	3.54E+02	1.36E+02	7.04E+01
S(-2)	mg/L	1.00E-08	1.00E-09	1.00E-09	1.00E-09	1.00E-09	-	-	1.00E-09	1.00E-09	1.00E-09	1.00E-09
Se	mg/L	1.00E-04	1.00E-04	1.00E-04	3.59E-04	8.00E-04	<0.025	2.64E+01	8.00E-02	4.01E-02	1.00E-02	5.05E-03
Si	mg/L	1.33E+01	9.18E+00	2.41E+01	1.31E+01	2.62E+01	3.07E+01	1.92E+02	4.00E+01	3.21E+01	4.00E+01	3.21E+01
Sr	mg/L	1.66E+00	1.17E+00	1.20E-01	1.15E-01	1.20E-02	6.00E-01	5.19E+00	4.40E+00	2.26E+00	2.40E+00	1.26E+00
Zn	mg/L	2.62E+00	4.25E-03	1.20E-02	1.25E-02	4.40E-03	2.30E+00	3.31E+02	1.40E+00	7.07E-01	5.00E-02	3.10E-02
P	mg/L	1.00E-02	1.00E-02	1.00E-01	5.00E-02	4.00E-02	2.20E+00	7.54E+01	4.00E+00	2.05E+00	4.00E+00	2.05E+00
U	mg/L	1.10E-02	1.24E-02	7.00E-04	2.26E-02	5.00E-04	7.70E+02	3.88E+04	1.00E+02	5.01E+01	3.00E+01	1.50E+01
V	mg/L	1.00E-04	1.00E-04	1.00E-04	1.20E-03	1.00E-04	6.16E+00	1.61E+02	5.10E-01	2.55E-01	1.60E-01	8.01E-02
^{226}Ra	mg/L	4.92E-06	5.47E-09	1.37E-08	2.54E-08	1.64E-09	6.29E-06	8.21E-05	5.47E-06	2.75E-06	1.01E-05	5.06E-06
^{230}Th	mg/L	9.17E-06	1.00E-06	1.31E-07	2.62E-07	2.62E-08	2.75E-02	2.88E-01	3.93E-06	2.02E-06	1.31E-06	7.14E-07

3.4 Expected Geochemical Reactions Along Flow Paths

Fate and transport mechanisms affecting the potential migration of COPCs from the remediated mining area, include the following:

- Advection: (physical) transport of dissolved mass along with groundwater flow.
- Dispersion: (physical) spreading of dissolved mass due to hydrodynamic mixing at the pore scale, and through the tortuosity of the fracture network within the fractured rock setting.
- Diffusion: (physical) spreading of mass due to concentration gradients. This is often associated with dispersion, however it is particularly important in fractured rock environments where diffusion into the rock matrix, where advection is minimal, further spreads the dissolved mass.
- Geochemical interactions, which may retard the velocity of COPCs in groundwater relative to that of groundwater and/or transfer constituents from groundwater to the host rock or soil structure (i.e., precipitation of mineral phases) such that further transport by groundwater is limited; and
- Decay: radioactive constituents will naturally decay.

In the LSA, geochemical reactions and radioactive decay will occur within the desilicified porous media, fracture spaces, as well as within the rock matrix. As such, the coupled effects of matrix diffusion and geochemical reactions compound the potential retardation and spreading effects. Key geochemical interactions in the fate and transport of uranium, other radionuclides, and trace elements are outlined in Table 3-6 (after US EPA 1999).

Table 3-6: Summary of Key Geochemical Processes for Transport of Uranium, other Radionuclides and Trace Elements (US EPA 1999)

Process	Mechanism	Effect on Constituent Mobility
Aqueous Complexation	Constituents in solution react with ligands to form dissolved-phase complexes	Can increase or decrease mobility
Redox Reactions	Some constituents, including U, can be present environmentally in a one or more redox states.	Redox state may enhance or reduce mobility
Adsorption (specific)	Dissolved constituents can form inner-sphere surface complexes on iron oxides, clay minerals, and quartz.	Retards constituent migration in groundwater; generally, a (fully) reversible process.
Ion Exchange (nonspecific adsorption)	Ions from the recovered solution replace other ions from soil or rock surfaces at exchange sites	Reduce mobility

Process	Mechanism	Effect on Constituent Mobility
Precipitation of solid phases	Concentrations of dissolved constituents may be such that the solubility of mineral phases is exceeded and may precipitate.	Reduce mobility
Subsurface colloids	Transport of colloidal precipitates in groundwater, that include (either through precipitation or sorption) constituents of the mining solution and/or uranium-bearing solution.	Enhances mobility

These key geochemical processes were explored in the geochemical modelling for the Project, as outlined in Section 3.5. The exception was subsurface colloids transport. U(VI) transport as colloids has been evaluated and considered at several sites and was concluded not to be an important transport mechanism (Colon et al., 2000). Average particle concentrations in the deep groundwater were found to be too low to have a significant effect on radionuclide migration (e.g., AECL, 1994). Based on the similarity of hydrochemical/geochemical conditions between the Wheeler River Project and those reported for Cigar Lake, it was considered reasonable to exclude colloidal transport of COPCs in this assessment. Further, complexation with dissolved organic matter was likewise not considered explicitly in this assessment; concentrations of dissolved organic carbon in the Athabasca Supergroup sandstones vary but are generally in the range of 2 mg/L. In the Cigar Lake studies (AECL, 1994), organic matter in groundwater was not predicted to have a significantly mobilizing effect on uranium (U(VI)) in groundwater.

3.5 Geochemical Modelling Approach

Geochemical modelling was used to simulate the behaviour of COPCs in groundwater migrating from the remediated mining area in Post-Decommissioning, when the freeze wall is thawed. A one-dimensional geochemical reactive transport model was developed as part of the overall numerical modelling approach for the Project. The goal of the one-dimensional (1D) model was to conceptualize and appropriately parameterize those reactions that will be important for the fate and transport away from the ore zone post-decommissioning, which were modelled ultimately in a 3D reactive transport model (Section 4.0). The 1D model and results of the assessment are the focus of the remainder of this section. The 1D and 3D models were used together iteratively to gain an understanding of COPC fate and transport in the groundwater system.

The 1D geochemical modelling supports an understanding of how and to what extent the key geochemical reactions may influence the migration of COPCs, and specifically, how these reactions will affect predictions of timelines and concentrations of COPCs in groundwater at the interface with the primary receiving body, Whitefish Lake.

3.5.1 Discussion of Solid Liquid Partition Coefficients (K_ds)

In groundwater modelling, sorption is often implemented using an equilibrium solid-liquid partition coefficient (K_d) to partition a constituent from the groundwater to the solid phase, and thus attenuate its concentrations in the aqueous phase relative that in the initial solution (source). This approach is often taken because it is a simple model and straightforward to include a K_d value into a 3-D groundwater fate and transport model to consider sorption effects. While the K_d model is simple, it is challenging to apply over a wide range of concentrations and other geochemical conditions such as pH. Recognizing the limitations of the K_d approach, analysis of reactive transport, herein, of COPCs away from the mining area employed more representative reactions, which more comprehensively address the multiple controls on the behaviour of metals, radionuclides, and trace elements in groundwater systems.

There is precedent for using geochemical codes, such as PHREEQC (Section 3.5.2) and other reactive transport computer codes, to predict and evaluate changes to groundwater quality associated with ISR projects as shown in the literature, including: Johnson et al., (2016); Lagneau et al., (2019); Reimus et al., (2019); de Boissezon et al., (2020). Driving the decision to move from a simpler K_d approach to using a geochemical model included the following:

- K_d values are derived for a specific set of conditions and are sensitive to pH values, and in this project, as in other ISR projects, pH values can vary considerably and need to be incorporated. This makes rationalizing a K_d value, or a set of K_d values difficult;

- The K_d model is reversible and assumes a linear relationship, meaning that the concentration in the water has a constant proportionality to that in the solid over a wide range of concentrations. However, the sorptive capacity of matrix materials/soils can decrease at higher aqueous concentrations, and the amount of sorbed mass that will desorb depends upon other geochemical conditions (e.g., pH, pE), which cannot be practically specified *a priori*. In practical terms, the K_d model is only linear over small ranges of concentrations in solution for most COPCs and application over wider ranges can result in over-estimation of sorption and underestimation of the aqueous concentrations. Alternatively, if the linear relationship for the high range of concentrations is applied to lower concentrations, the sorption will be biased high and concentrations in the water will be unrealistically overpredicted.

- Several COPCs will compete for sites at mineral surfaces. Thus, not accounting for this competition may over-estimate the amount of sorption. Further, aqueous species like carbonates are known to play an important role in the sorption of metals to solid surfaces. The interactions of metals with aqueous ligands are accounted for with site-specific sorption in the geochemical model, but not with a Kd approach.

Thus, in the geochemical model developed for the Project, rather than application of K_d values, ion exchange reactions and metal/trace element adsorption at solid surfaces by surface complexation was applied to evaluate sorption. The only exception to this was within the lake

bottom sediments. The application of the K_d values in the lake-bottom sediments is detailed in Section 3.5.6.2.4.

3.5.2 One-Dimensional Geochemical Evaluation

Fate and transport of COPCs in the remediated groundwater was explored in 1D with PHREEQC (Parkhurst and Appelo, 2013). PHREEQC (original acronym pH-REdox-EQuilibrium) is based on equilibrium chemistry of aqueous solutions interacting with minerals, gases, solid solutions, exchangers, and sorption surfaces.

The 1D transport model in PHREEQC includes a series of cells along a groundwater flow pathway. The advection of water from cell to cell is determined by the average linear groundwater velocity and size of the cells. Each cell also acts as a continuous stirred reactor in which the simulated geochemical reactions (e.g., sorption, redox, precipitation, etc.) occur. Only reactions that can plausibly be in thermodynamic equilibrium were considered in this assessment, including sorption-desorption and precipitation reactions. Dissolution reactions that are likely to be kinetically controlled were not included in this evaluation.

This approach provides the ability to simulate groundwater flow and mass transport along a single flow path parallel to the direction of groundwater flow, with the appropriate chemical reactions occurring in each cell along the flow path. The approach however also assumes no interaction with the volume surrounding the flow path, as would occur by diffusion and transverse dispersion in a real groundwater flow system and is thus considered a conservative assessment of potential transport and fate of constituents. A simplified schematic of a 1D transport simulation in PHREEQC is shown in Figure 3-5.

The conceptual geochemical site model is a simplified representation of the understanding of the real system. Two 1D models for the project were conceptualized and are shown in Figure Figures 3-6a and 3-6b. The first conceptualization was developed to examine sorption reactions primarily and included the ore zone, the Paleoweathered Zone, the Desilicified Zone and lake bottom sediments. The second conceptualization was streamlined, to focus on other key geochemical reactions and emphasized a groundwater pathway from the flare (zone of 50% restored solution above the ore zone; described in Section 4.1) through the Desilicified zone, (Figure 3-6b).

Development of the two conceptualizations followed from the early runs evaluating groundwater and geochemical reactive transport models in 3D, that demonstrated the following:

1) Multi-Zone Pathway: Groundwater from the ore zone and mined portion of the paleoweathered zone (i.e., zones of groundwater quality assumed to be 100% restored solutions) first flows primarily through the paleoweathered zone. This zone is rich in clay and is characterized by small groundwater velocities and long residence. Sorption of COPCs to clay is expected to be a key geochemical reaction in this hydrostratigraphic unit.

2) Desilicified Zone Pathway: The mass that first reaches Whitefish Lake from the remediated mining area is that of COPCs that behave conservatively (i.e., no geochemical interactions) and which originate in the flare and move along a flow path from the mining area to Whitefish Lake that is dominated by the Desilicified zone.

Geochemical modelling requires a number of detailed assumptions and checks on model simulations. These have been presented in the sections below, or, as appropriate, as part of the Supporting Information in Appendix E.

The length of the ore zone is approximately 700 m from the southwest to the northeast (see inset, Figure 2-6). Following from initial simulations in 3D that showed that groundwater followed more than one migration pathway, with not all mass migrating to Whitefish Lake (see Figure 4-6), the source length for the ore zone in the 1D model was assumed to be 450 m, which is the approximate length of the (longer) northeast portion of the ore deposit. The average linear groundwater velocity within the Desilicified zone was set at $8x10^{-8}$ m/s, derived from a hydraulic conductivity of $5x10^{-6}$ m/s (Table 2-2), a hydraulic gradient of 0.0032 m/m, and a porosity of 0.2 (Table 4-2). The same average linear velocity was assumed for the mining area (source zone), following from the discussion in Section 4.4.2, where the hydraulic conductivity value in this zone following mining was set to $5x10^{-6}$ m/s, and a porosity of 0.2 is assumed for the ore zone (Table 4-2). In the 1D model, the average linear velocity of the paleoweathered zone was conservatively set to $3x10^{-8}$ m/s to reflect the interpretation of a higher hydraulic conductivity values in the basement aquitard along the WS Shear due to this being an enhanced fracture zone (Section 4.7).

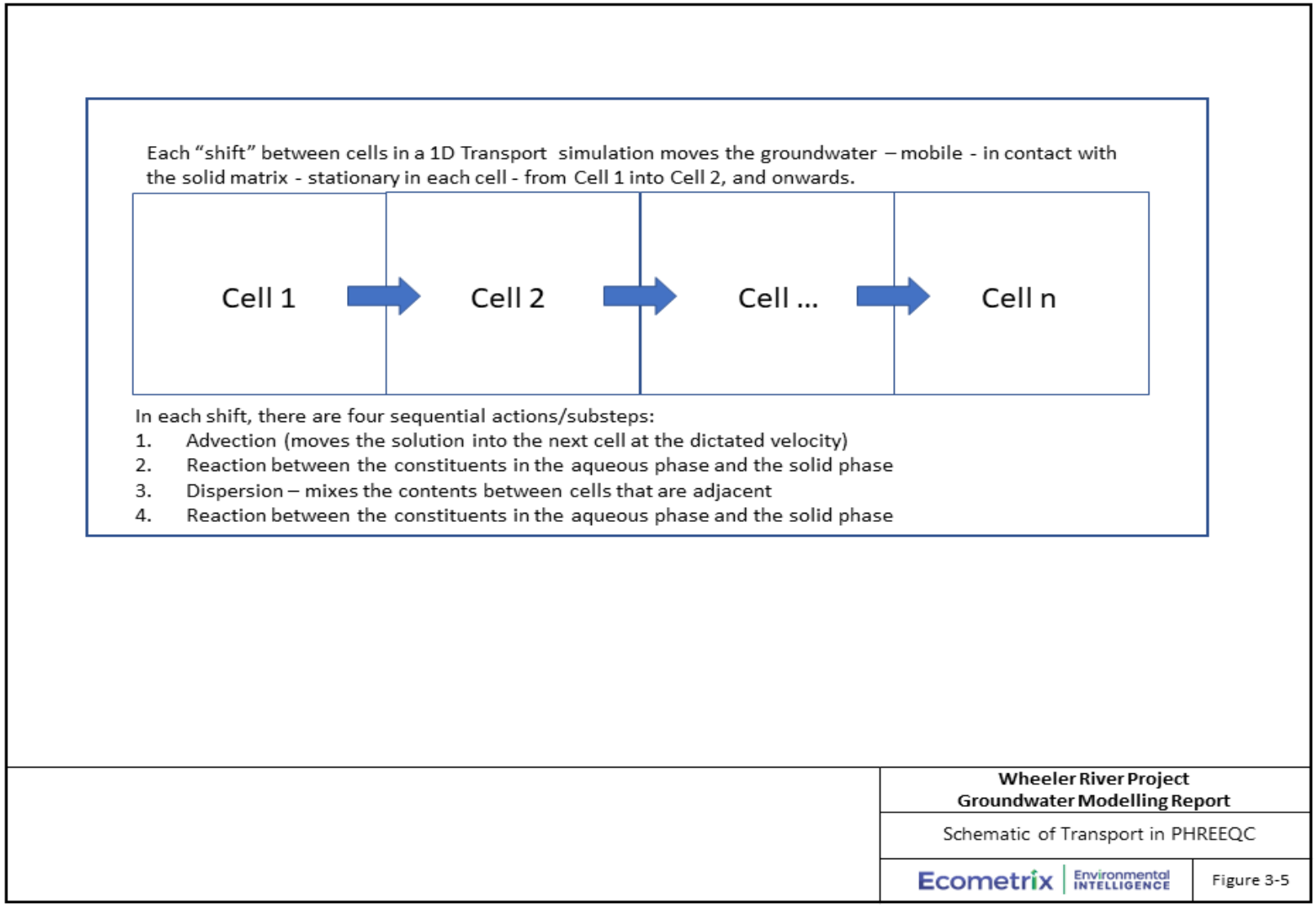

Figure 3-5: Schematic of Transport in PHREEQC

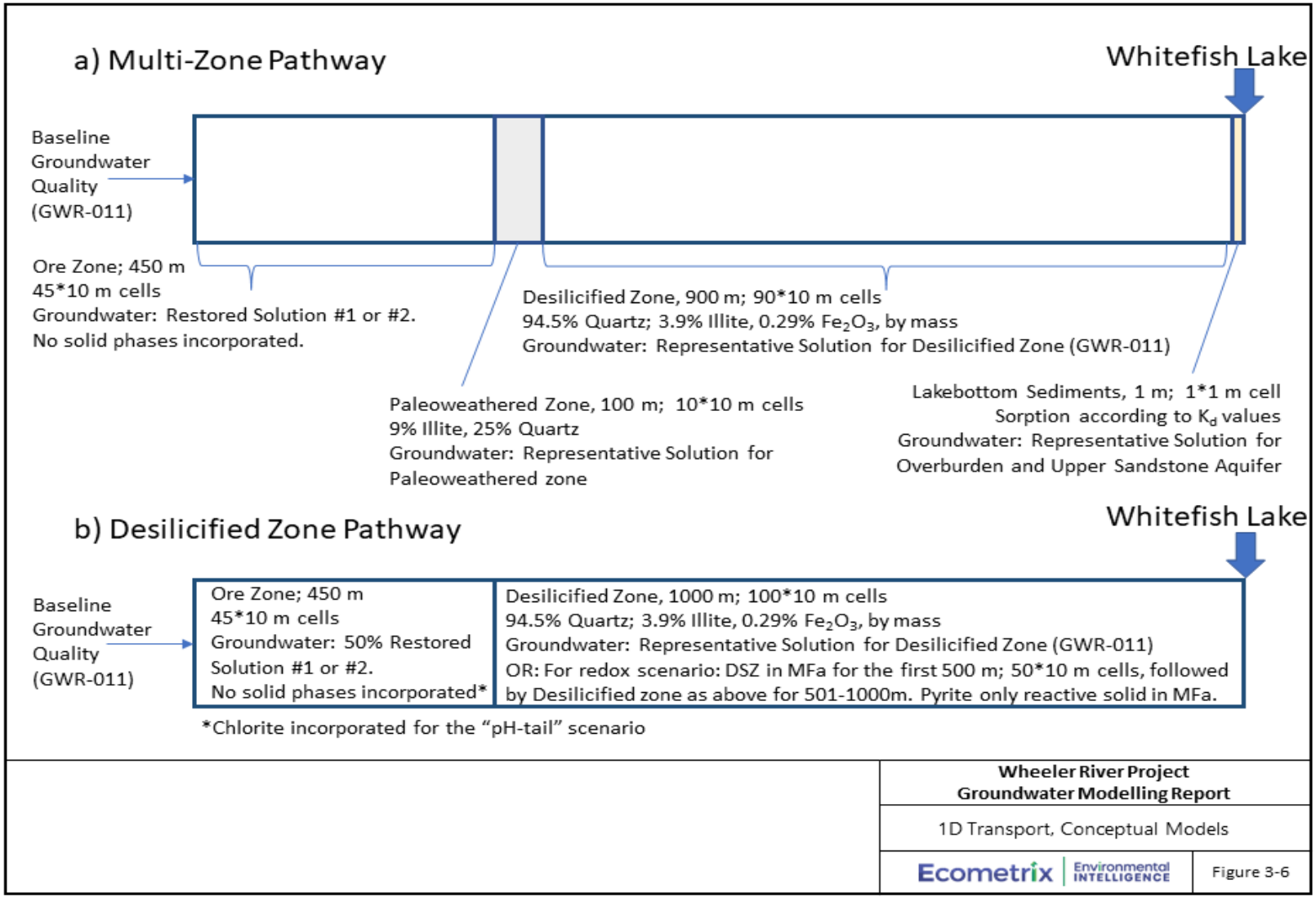

Figure 3-6: 1D Transport, Conceptual Models

3.5.3 Thermodynamic Database

The thermodynamic database used in PHREEQC was modified from/built on the minteq.v4 database that is available with the PHREEQC download. The database was updated with respect to current understanding of uranium complexation in solution with carbonate species (Guillaumont et al. 2003; Gorman-Lewis et al., 2008; Grenthe et al., 2020) and ternary complexes of uranium with calcium and magnesium and carbonates (Dong and Brooks, 2006). The database was also modified to contain aqueous speciation for radium and thorium and solid phases for uranium, radium and thorium, from the sit.dat database, also available with the PHREEQC download. Redox chemistry for Cr(III) (i.e., oxidation to Cr(VI)) was removed from the database as formation of Cr(VI) is not expected under the redox conditions in groundwater at the site.

The sources of binding constants for uranium, metals and radionuclides to sorbing mineral phases included in the database are discussed in more detail in Appendix E .

Note on ^{210}Po and ^{210}Pb

Thermodynamic data was not available for ^{210}Po. As such, this COPC was not evaluated directly in the numerical modelling. ^{210}Po is understood to be attenuated through adsorption in low to circumneutral water (Carvalho et al., 2017, Szabo et al., 2020). The distribution of ^{210}Po in the subsurface is strictly controlled by that of it's parent ^{210}Pb, and Pb behaviour is modelled.

3.5.4 Initial Solutions

For each hydrostratigraphic unit in the 1D model, an initial solution was required. The solutions used as input solutions in the model are presented in Table 3-5. The exception is for oxidation-reduction potential (as pe). For the reasons given below (Section 3.5.5), the redox conditions of the input solutions in the model were modified from those measured in the hydrostratigraphic units presented in Table 3-5.

Baseline groundwater quality for the ore zone (from GWR-032) was also presented in Table 3-5 but this solution was not used in the numerical modelling. As a result of ISR mining, groundwater conditions in the ore zone will change and the baseline water quality was included in Table 3-5 only for the purposes of comparison to the remediated groundwater quality, Post-Decommissioning. Groundwater quality in the mining area evaluated in the 1D models was represented by the remediated groundwater quality (Restored Solutions #1 and #2, and 50% restored solutions), as shown in Figure 3-6a and 3-6b, respectively.

For the other hydrostratigraphic units, the representative solutions were selected or developed as follows:

- Paleoweathered Zone: There is one well with water quality considered representative of the paleoweathered zone within the existing well network for the Wheeler River Project (GWR-031). As such, groundwater quality reported for a well installed in the paleoweathered zone at Cigar Lake (AECL, 1994; sampling location #199) was also

considered. The groundwater quality relied more heavily on that reported for Cigar Lake because of the cross-completion of well GWR-031 with other hydrostratigraphic units. Some constituent concentrations were adjusted to higher or lower values where there was discrepancy between groundwater quality between GWR-31 and the Cigar Lake sampling location.

- Desilicified Zone and Lower Sandstone Aquifer: GWR-011. This well is installed in desilicified sediments of the Lower Sandstone Aquifer. Concentrations/values of groundwater constituents in this well were close to the calculated median values for the Lower Sandstone Aquifer hydrostratigraphic unit, provided in Table 3-4.

- Intermediate Sandstone Aquitard: GWR-046. Groundwater quality was used for this hydrostratigraphic unit for the same reasons given above for the Desilicified Zone/Lower Sandstone Aquifer.

- Overburden and Upper Sandstone Aquifer: These two units make up the Local Groundwater flow system. Groundwater quality from well GWR-036 is close to median concentrations for this flow system. Concentrations of a small number of constituents were adjusted moderately to better reflect median values for the flow system.

The pe values shown in Table 3-5 reflect measured ORP values for the Project, discussed in Section 3.2.2.1, and, where not available, were supplemented with conditions reported for Cigar Lake (AECL, 1994) for the same hydrostratigraphic units. In alignment with the discussion of redox conditions above (Section 3.2.2.1), the lower pe values applied to the Athabasca Supergroup sandstones and paleoweathered zone are not understood to be so low as to reduce key chemical species, such as uranium and sulphate, that would cause precipitation or removal as reduced low solubility solid phases such as uraninite and pyrite (FeS_2), respectively. However, the pe in the deeper zones allowed ferrous iron to remain stable in solution rather than forcing oxidation to ferric iron and causing precipitation of ferric oxyhydroxide solid phases. The range of understood pe values also reflects any potential reduction and precipitation of key species that would not be expected in the absence of reducing substances such as organic matter, that current conditions indicate is not present at sufficiently high levels in the system (outside of the ore zone) to drive moderately to strongly reducing redox conditions.

Prior to use in the model, concentrations in groundwater samples were charge balanced and equilibrated to CO2(g) pressures in PHREEQC, at the depth of the well screened intervals. Each solution pH and total inorganic carbon concentration ("C(4)" in the model) was adjusted using the measured alkalinity – which is conserved at all pressures – and setting the partial pressure of CO2(g) based on sampling interval depth. Groundwater quality reported from the Cigar Lake studies, has already been corrected for CO2(g) partial pressures and was charge balanced (AECL, 1994). The representative solutions for each hydrostratigraphic unit presented in Table 3-5 have been charge balanced and pH corrected.

3.5.5 Subsurface Conditions Incorporated

The following subsurface conditions were assumed in the geochemical site conceptual models, (Figures 3-6a and 3-6b) except where indicated:

- The occurrence and extent of chemical reactions reflect thermodynamic equilibrium conditions. As such, sorbed COPCs can desorb to achieve thermodynamic equilibrium with the groundwater composition at each stage of modelling. This is a conservative assumption in the geochemical modelling because in natural systems, desorption is not always complete (i.e., does not always obey thermodynamic equilibrium; e.g. Allen et al., 2019). This is also a conservative assumption in evaluating COPC-containing mineral phases (precipitates) formed in the system. Often in natural systems, the chemical form/structure of the mineral phases changes over time, decreasing the solubility.

- although not an accurate reflection of (largely, anoxic) subsurface conditions, the solutions, once in the Paleoweathered Zone and Desilicified Zone, were equilibrated with atmospheric concentrations of oxygen. This is a modelling approach, that maintains U(VI), and other redox-reactive constituents, present in the oxidized form. This is conservative because the important redox-active constituents of concern are more mobile in their oxidized forms.

- the concentrations of iron in the remediated groundwater are elevated with respect to environmental concentrations (i.e., 100 mg/L in Restored Solution #1) and expected to occur as ferrous (Fe^{2+}) iron as a result of reduction by the residual uraninite and sulphide minerals such as pyrite (FeS_2) in the ore zone. Oxygenated conditions are not expected over most of the groundwater system and therefore ferrous iron will remain stable in the groundwater, with the potential exception of the upper portion of the Athabasca Supergroup sandstone units. Thus, the redox reaction resulting in oxidation of ferrous iron to ferric iron was supressed in the model, and it was conservatively assumed that ferrous iron (Fe^{2+}) would remain in solution with no solubility controls. This is supported by the presence of elevated dissolved iron concentrations at near neutral pH for existing conditions at the site (Appendix D). The formation of ferric iron solid phases from oxidation of ferrous iron can result in the production of hydronium ions that can lower the pH. The influence of iron oxidation and precipitation as ferric oxide/oxyhydroxide minerals on pH in the upper elevations of the flow system (where oxygenated conditions may be encountered) was also evaluated in the modelling scenarios (“Fe oxidation”).

- Conceptually, the paleoweathered zone mineral assemblage was made up of 9% clay by mass, as illite, and 25% quartz. The illite content was based on the normative clay composition determined from site-specific corehole elemental analysis (median illite by mass is 9.20%; Table 3-2). Portable infra-red mineral analysis supported the normative clay content in that chlorite is the dominant clay mineral (median 69.5% relative abundance) followed by illite (median 13.1% relative abundance; Table 3-2). The quartz content was based on a regional study by Macdonald (1980) evaluating the mineralogical composition of the weathered bedrock/saprolite regionally. The mineral composition of the

paleoweathered zone was conceptualized in this manner because the data set for the project with respect to clay minerals was for the sorptive properties of illite. Using the relatively smaller illite content of the paleoweathered zone compared to the more dominant chlorite content is conservative in that not all sorptive capacity of the clays is accounted for in the simulated paleoweathered zone.

- The conceptualization of the Desilicified Zone is based upon site-specific information from the extensive coring and is modelled as being made up of (by mass): 94.5% quartz, 3.9% illite and 0.29% Fe_2O_3 as goethite. This composition reflects the data from elemental analysis (including normative clay content) presented in Table 3-2. Illite was used to represent the total clay content, which varies from 1.74% to 5.85% by mass in the hydrostratigraphic units within the Athabasca Supergroup sandstones and Desilicified Zone.

- The remediated mining area is modelled as a finite source of COPCs and does not include any geochemically reactive surfaces/minerals, except in the "pH-tail" scenario that assumed that previously sorbed H^+ ions would be desorbed into groundwater flushing through and replacing the remediated ISR groundwater in the ore zone . The migration of dissolved constituents in porewater from the remediated mining area was simulated by the flushing by upstream groundwater. The residual reduced minerals, such as uraninite and pyrite were not considered to be a source of COPCs. This was considered appropriate because the upstream groundwater, passing through the mined zone, will not be oxidizing and groundwater conditions are expected to be similar to pre-mine conditions that indicated low and baseline concentrations of dissolved COPCs associated with the original mineralization.

- Carbonate minerals, which are important pH-buffering minerals and for the migration behaviour of some groundwater constituents (i.e., formation of gypsum following release of Ca from calcite dissolution), were, conservatively, not included in the numerical simulations. Calcite concentrations (calculated from median CaO wt % in Table 3-2) are less than 0.05 wt% over much of the groundwater flow path. is less than 0.05 %.

- The lowest pH solution initially in the ore zone was pH 4.3, representing Restored Solution #1 in Table 3-5. However, it was conservatively assumed that mineral dissolution to buffer pH does not occur. In the real system, it is expected that some minerals, such as gibbsite ($Al(OH)_3$), carbonates and some aluminosilicate minerals can dissolve to neutralize pH.

3.5.6 Evaluation of Geochemical Processes

There are several geochemical reactions that are expected to occur as the remediated groundwater (Restored Solution) migrates through the various regions along the groundwater flow path. The reactions were considered individually and tested to ensure that they were being applied properly with the appropriate input parameters and quality assurance reviews of the results were completed for each of the reactions. The simulations were also sequentially incorporated to evaluate the coupled affect of the reactions (e.g., redox and precipitation

reactions, along with limited sorption, or enhanced source conditions). The groundwater transport was first tested by assuming that there were no geochemical reactions, assuming all COPCs were chemically conservative. Reactions were then progressively incorporated in steps to illustrate the effects of each of the reactions. Some reactions were omitted in some runs to illustrate the sensitivity of the results to changes in reactions. The list of the simulations and the associated reactions that were considered in each simulation are summarized in Table 3-7.

Table 3-7: Progressive Geochemical Evaluation using the 1D Model

Simulation	Geochemical Interactions
Conservative	The system as a whole is assumed to be devoid of mineral phases that are reactive and all COPCs are considered to be chemically conservative.
Solubility Controls	Authigenic precipitation of uranyl mineral phases and other mineral phases was allowed to control or remove COPCs from the groundwater when thermodynamic conditions were appropriate
Base Case - Sorption	Dissolved constituents were allowed to adsorb and exchange at reactive sites associated with goethite, clay minerals, and quartz. Sorption was conservatively modeled as reversible for all constituents and reactions. Because minerals characterizing the subsurface – namely clays and iron oxyhydroxide minerals – are known to be important sorbing phases, sorption was considered to some extent in all model runs.
Sorption to fewer sites	The concentration of sorptive sites available for reaction with the solution phase was decreased from the total expected as a sensitivity scenario, to compare to the Base Case.
Redox - lower limits	The Redox scenario focused on the reactivity of uranium along the downgradient groundwater flow path, and the potential for U(VI) reduction to U(IV) to be a reaction that immobilizes uranium in the presence of a naturally occurring reductant, represented by pyrite (FeS_2), that is known to be present in the hydrothermally altered sediments of the lower Athabasca Supergroup sandstones.
Protons desorption from Clays ('proton tail')	Clay minerals in the ore zone were pre-equilibrated with protons at the pH of Restored Solution #1 to evaluate the effect of proton desorption on the pH of the downgradient plume, and potential effect on migration of other COPCs.

Radioactive Decay and Ingrowth: In the scenarios presented below, radioactive decay was not included in the geochemical processes for uranium isotopes because of the long half-lives of those isotopes and of the daughter product ^{230}Th. The radioactive decay of ^{230}Th and ingrowth of ^{226}Ra was evaluated along the groundwater flow path, as was decay of ^{226}Ra. Details are provided in Appendix E. In the numerical model scenarios presented below, radioactive decay was not included, because it was not shown to be a key process in the behaviour of those elements within the period modelled (maximum time on the order of 60,000 -100,000 years; see Section 4.7). The simulations are thus conservative with respect to concentrations of those

radionuclides in the subsurface. As introduce above, ^{210}Po could not be modelled, and contributions of ^{210}Pb from radioactive decay of ^{226}Ra to total Pb modelled was too small to be measurable, and ^{210}Pb produced will behave like Pb. Potential risks to ecological and human receptors associated with ^{210}Pb and ^{210}Po were evaluated through Environmental Risk Assessment (ERA) using the modelled mass flux of ^{226}Ra in groundwater at Whitefish Lake (Section 4.9, Ecometrix 2024b, and Denison, 2024a).

3.5.6.1 Solubility Controls

3.5.6.1.1 Mineral Saturation Indices

Some minerals, including COPCs, are naturally present within the geologic materials along the groundwater flow path and some minerals may also form within the system from direct precipitation from the dissolved phase. Minerals that are formed through direct precipitation from solution because equilibrium solubility of that mineral phase is reached (or, often, exceeded) in the dissolved phase are called authigenic minerals. Both authigenic minerals and existing minerals present already in a system can also dissolve when the solution composition changes and thermodynamic conditions are appropriate, adding COPC mass to the groundwater.

Previous studies have shown that precipitation of authigenic mineral phases resulting from higher trace metal/element concentrations in uranium mining-influenced groundwater can attenuate dissolved-phase concentrations over the period being examined. For example, Bain et al., 2001 found that precipitation of $Cr(OH)_3$ was an important control on the Cr(III) dissolved-phase concentrations in a sandstone aquifer receiving uranium mining-affected groundwater, but that $Ni(OH)_2$, for example, was not an important controlling phase for nickel for the conditions encountered.

Potentially important mineral phases were evaluated within the LSA by examining the saturation indices of the representative solutions and Restored Solutions. The saturation indices were calculated in PHREEQC for the solution conditions provided in Table 3-5. As a first step, the saturation indices for mineral phases were examined for existing/baseline conditions in the subsurface. The saturation index illustrates when a mineral phase is undersaturated with respect to dissolved concentrations in the water and therefore will be prone to dissolve if it is present in the solids and when it is supersaturated and will be prone, thermodynamically to precipitate from solution to re-establish equilibrium.

The concentrations of elements in association with the overburden and rock units in the LSA are well understood, and are provided in Appendix B. However, elemental concentrations were determined through total and partial digestion, and as such, do not provide information on the specific chemical speciation in which the elements are found, including mineral phases. Examining the saturation indices provides insight into mineral phases that may be controlling dissolved-phase concentrations of COPCs, through solubility control. Although, as introduced above, the baseline groundwater quality in the ore zone is not used as part of the numerical modelling, an examination of the saturation indices was undertaken as part of this assessment

to evaluate how the predicted mineral phase saturations aligns with the known mineral composition of the ore zone.

Mineral saturation indices were also examined in the Restored Solutions (and 50% restored solutions), as COPC concentrations were, generally, higher in the remediated groundwater in the mining area than are observed under baseline conditions. This was done to provide insight into the mineral phases to be considered for inclusion in the geochemical reaction model as important controls on solution-phase concentrations of COPCs.

Saturation indices for mineral phases examined are provided in Table 3-8. Noted is that reduced sulphur values (S(-2)) were not measured in groundwater (and thus, do not appear in Table 3-4 and Appendix D), but were added at a very low value in the groundwater composition of the representative samples for the inclusion of sulphide mineral phases in the PHREEQC speciation/output.

The saturation indices summarized in Table 3-8 indicate:

a. groundwater quality across the hydrostratigraphic units reflect, as expected based on the mineralogy, equilibrium with (primarily, ferric) iron mineral phases, quartz, clays, and potentially gibbsite (for aluminum);

b. groundwaters in the system are generally undersaturated with respect to carbonate minerals; groundwaters closest to saturation with respect to carbonate minerals occur in the ore zone and the intermediate sandstone aquitard, where the highest alkalinities in groundwater are observed (Appendix D; Table 3-4);

c. uranium concentrations in groundwater under existing conditions may reflect equilibrium with a reduced U(IV) oxide mineral phase (uraninite or other) at depth (i.e., within the Lower Sandstone Aquifer and Intermediate Sandstone Aquitard). The work done by Percival (1989) and discussed in detail below (Section 3.5.6.2.1) suggests that in the sandstones most closely overlying the ore zone, uraninite likely represents at least a portion of the uranium present and it's origin was the hydrothermal processes that formed the ore body (i.e., it is has been dissolved to a very limited extent over more than 1 billion years).

d. Uranyl (U(VI)) mineral phases are not predicted to be controlling dissolved-phase uranium concentrations under existing conditions; however, the restored solutions are supersaturated with respect to U(VI)-phosphate minerals (Uranyl Hydrogen Phosphate and Uranyl Orthophosphate), U(VI)-silicate minerals (Uranophane, Soddyite) and a U(VI)-vanadate mineral (Tyuyamunite). This suggests that the potential for those minerals could be important authigenic mineral phases to consider for uranium behaviour downgradient of the mining area.

e. Overall, the saturation indices suggest that under existing conditions in the paleoweathered zones, Athabasca Supergroup sandstones and overburden, the

dissolved phase concentrations of very few COPCs in groundwater are solubility controlled. Potential exceptions may be Mn (through equilibrium with rhodochrosite ($MnCO_3$)) and Cr(III) (through an oxide/hydroxide mineral phase). All solutions are supersaturated with respect to ThO_2 but this was not considered further as a mineral phase in the modelling for the reasons given below (Section 3.5.6.1.2).

There are important limitations to the above assessment because there may be other important mineral phases in an environment for which solubility constants are not known or are uncertain.

Table 3-8: Saturation Indices for Select Solid Phases in Groundwater Representative of Hydrostratigraphic Units

Mineral Groupings	Sample/Paramter	Ideal Formula	Ore Zone (GWR-032)	Paleoweatherd zone (GWR-031 and Cigar Lake Samples)	Lower Sandstone Aquifer/Desilicified Zone (GWR-011), high pe	Lower Sandstone Aquifer/Desilicified Zone (GWR-011), low pe	Intermediate Sandstone Aquitard (GWR-046), high pe	Intermediate Sandstone Aquitard (GWR-046), low pe	Overburden and Upper Sandstone Aquifer, single pe	Restoration Solution #1	50% Restoration Solution #1	Restoration Solution #2	50% Restoration Solution #2
	pH		6.79	6.71	6.36	6.36	7.03	7.05	6.46	4.24	5.07	6.20	6.31
	pe (calculated in PHREEQC)		-2.7	1.9	2.5	0.3	4.4	-3.0	1.2	10.0	7.0	7.6	4.0
	Partial Pressure CO2(g)		-1.8	-1.8	-1.8	-1.8	-2.2	-2.2	-2.2	-1.8	-1.8	-1.8	-1.8
Primary Host/Matrix Minerals	Goethite	FeOOH	-1.4	2.1	2.0	-0.2	6.3	-0.6	0.7	4.5	4.1	5.5	3.8
	Hematite	Fe2O3	-0.4	6.6	6.2	1.9	14.9	1.2	3.7	11.4	10.5	13.3	9.9
	Kaolinite	Al2Si2O5(OH)4	1.2	4.0	4.9	4.9	7.7	7.7	5.1	0.3	4.7	6.4	6.2
	Quartz	SiO2	0.6	0.4	0.9	0.9	0.6	0.6	0.9	1.1	1.0	1.1	1.0
Carbonate	Siderite	FeCO3	-0.7	-1.8	-2.2	-2.2	-0.9	-0.4	-2.8	-5.0	-3.2	-3.6	-1.9
	Calcite	CaCO3	-1.1	-2.1	-2.6	-2.6	-1.7	-1.6	-3.5	-6.1	-4.6	-3.1	-2.8
	CuCO3	CuCO3	-10.0	-3.7	-3.9	-5.8	-2.5	-7.6	-5.7	-6.0	-4.6	-2.9	-2.9
	Gypsum	CaSO4:2H2O	-2.5	-3.7	-3.5	-3.5	-3.1	-3.2	-4.4	-0.8	-1.2	-2.2	-2.4
	NiCO3	NiCO3	-8.1	-7.0	-9.8	-9.8	-6.2	-6.2	-8.8	-9.3	-7.9	-8.2	-8.3
	Otavite	CdCO3	-4.9	-4.9	-5.5	-5.5	-4.0	-4.0	-5.7	-6.9	-5.4	-3.3	-3.4
	Rhodochrosite	Mn(CO3)	-1.0	-0.6	-1.5	-1.5	0.4	0.5	-2.2	-5.1	-3.6	-1.8	-1.6
	Smithsonite	ZnCO3	-1.2	-4.1	-4.3	-4.3	-3.4	-3.4	-5.0	-6.8	-5.3	-4.1	-4.1
	Strontianite	SrCO3	-2.1	-2.4	-4.0	-4.0	-3.1	-3.1	-5.3	-7.0	-5.5	-3.1	-3.1
Oxides	Gibbsite	Al(OH)3	-0.56	0.98	1.02	1.02	2.68	2.68	1.09	-1.47	0.83	1.55	1.54
	Cd(OH)2	Cd(OH)2	-11.5	-11.5	-12.1	-12.1	-10.3	-10.3	-11.9	-13.6	-12.1	-10.0	-10.0
	Co(OH)2	Co(OH)2	-8.5	-6.6	-9.2	-9.2	-6.2	-6.1	-8.4	-9.5	-8.0	-7.7	-7.7
	Cr(OH)3(am)	Cr(OH)3	-0.9	0.0	-1.5	-1.5	0.0	0.1	-1.3	-4.6	-2.6	0.1	0.0
	Cr2O3	Cr2O3	-1.5	0.2	-2.8	-2.8	0.3	0.4	-2.4	-9.0	-5.0	0.5	0.3
	Cu(OH)2	Cu(OH)2	-10.7	-4.5	-4.7	-6.6	-2.8	-7.9	-5.9	-6.8	-5.3	-3.6	-3.7
	MoO2(s)	MoO2	2.0	-6.3	-6.5	-2.2	-13.2	1.5	-5.2	-12.2	-9.4	-14.8	-8.3
	Ni(OH)2	Ni(OH)2	-8.3	-7.2	-10.0	-10.0	-6.0	-6.0	-8.5	-9.5	-8.1	-8.4	-8.5
	Pb(OH)2	Pb(OH)2	-5.1	-5.2	-5.6	-5.6	-3.4	-3.4	-5.4	-5.7	-4.2	-2.6	-2.6
	Ra(OH)2(s)	Ra(OH)2	-29.9	-33.0	-33.2	-33.2	-31.7	-31.6	-33.9	-35.3	-33.9	-30.9	-30.9
	Sr(OH)2(s)	Sr(OH)2	-20.6	-20.8	-22.5	-22.5	-21.2	-21.1	-23.2	-25.4	-24.0	-21.6	-21.6
	ThO2(cr)	ThO2	3.3	2.4	1.8	1.8	2.0	2.0	1.5	-1.2	2.1	2.9	2.6
	V(OH)3	V(OH)3	-13.2	-13.2	-13.2	-13.2	-14.0	-12.1	-13.2	-15.0	-11.3	-15.8	-10.3
	V2O5	V2O5	-41.2	-23.1	-22.2	-30.8	-13.1	-38.9	-26.8	-4.2	-5.4	-7.3	-10.4
	VO(OH)2	VO(OH)2	-12.4	-7.9	-7.7	-9.8	-5.7	-11.3	-8.8	-4.1	-2.5	-5.2	-3.3
	Zn(OH)2	Zn(OH)2	-3.2	-6.1	-6.3	-6.3	-5.0	-4.9	-6.5	-8.8	-7.3	-6.1	-6.1

Table 3-8: Saturation Indices for Select Solid Phases in Groundwater Representative of Hydrostratigraphic Units, continued

Mineral Groupings	Sample/Paramter	Ideal Formula	**Ore Zone (GWR-032), high pe**	Ore Zone (GWR-032), low pe	Paleoweatherd zone (GWR-031 and Cigar Lake Samples)	Lower Sandstone Aquifer/Desilicified Zone (GWR-011), low pe	Intermediate Sandstone Aquitard (GWR-046), high pe	Overburden and Upper Sandstone Aquifer, single pe	Restoration Solution #1	50% Restoration Solution #1	Restoration Solution #2	50% Restoration Solution #2
Sulphate	Barite	BaSO4	-0.4	-0.4	-0.9	-0.6	0.3	-2.0	1.0	0.9	0.6	0.4
	Anglesite	PbSO4	-6.1	-6.1	-6.3	-6.0	-4.8	-6.3	0.0	-0.3	-1.3	-1.8
	Celestite	SrSO4	-2.4	-2.4	-2.8	-3.7	-3.4	-5.0	-0.5	-0.9	-1.1	-1.6
	CuSO4	CuSO4	-21.4	-22.9	-16.8	-18.1	-15.4	-18.1	-12.2	-12.6	-13.5	-14.0
	Ra(SO4)(s)	Ra(SO4)	-4.3	-4.3	-7.5	-7.0	-6.5	-8.3	-3.0	-3.3	-2.9	-3.4
Sulfides and Other Minerals in the Ore Body	Chalcopyrite	CuFeS2	-9.4	13.1	-54.6	-24.8	-98.3	-41.4	-136.7	-101.9	-134.8	-77.7
	Galena	PbS	-8.4	3.7	-32.9	-17.2	-54.4	-25.5	-71.6	-54.4	-69.8	-42.2
	Greenockite	CdS	-9.6	2.3	-34.1	-18.6	-56.2	-26.9	-74.5	-57.2	-72.2	-44.5
	MoS2	MoS2	-13.3	13.7	-67.6	-31.1	-121.0	-51.3	-150.0	-115.6	-155.2	-93.2
	NiAs(cr)	NiAs	-14.2	-6.7	-27.6	-20.6	-51.0	-24.9	-67.0	-51.3	-64.6	-40.4
	NiS(gamma)	NiS	-9.5	2.6	-32.8	-19.5	-55.0	-26.6	-73.4	-56.2	-73.6	-46.0
	Pyrite	FeS2	-16.2	4.8	-60.1	-32.0	-99.7	-47.3	-128.6	-99.7	-130.6	-80.5
	Sphalerite	ZnS	-7.1	4.9	-34.4	-18.4	-56.6	-27.3	-75.4	-58.1	-74.0	-46.2
Uanium Minerals	Coffinite	U(SiO4)	2.1	5.1	-2.8	0.8	-8.3	-0.8	-11.3	-5.9	-9.5	-2.8
	Metaschoepite	UO3:2H2O	-5.2	-5.2	-3.9	-4.6	-3.8	-4.1	-1.7	-0.7	-0.7	-0.9
	Rutherfordine	UO2CO3	-4.8	-4.8	-3.5	-4.2	-3.8	-4.3	-1.3	-0.3	-0.4	-0.6
	Schoepite	UO2(OH)2:H2O	-5.8	-5.8	-4.5	-5.2	-4.4	-4.8	-2.3	-1.3	-1.4	-1.6
	Soddyite	(UO2)2SiO4:2H2O	-7.9	-7.9	-5.5	-6.4	-5.1	-5.5	-0.4	1.5	1.4	0.9
	Sodium-compreignacite	Na2(UO2)6O4(OH)6:7H2O	-32.1	-32.1	-24.6	-31.5	-25.0	-29.4	-15.6	-8.4	-6.6	-8.2
	Tyuyamunite	Ca(UO2)2(VO4)2	-30.7	-36.7	-17.1	-26.6	-5.9	-22.0	2.3	4.6	4.1	0.9
	U2O7Na2(s)	U2O7Na2	-14.4	-14.4	-12.1	-16.3	-13.0	-15.9	-11.9	-8.7	-6.7	-7.4
	UO2.34(beta)	UO2.34	0.7	2.6	-2.1	-0.2	-5.7	-1.1	-7.3	-3.4	-5.9	-1.4
	Uraninite	UO2	2.6	5.6	-2.2	1.0	-7.8	-0.6	-11.3	-5.8	-9.5	-2.7
	Uranophane	Ca(UO2)2(SiO3OH)2:5H2O	-4.7	-4.7	-3.5	-4.5	-2.0	-3.9	-1.8	1.5	3.2	2.8
	Uranyl Hydrogen Phosphate	UO2HPO4:3H2O	-6.9	-6.9	-5.4	-4.6	-5.0	-4.7	1.5	1.5	0.9	0.3
	Uranyl Orthophosphate	(UO2)3(PO4)2:4H2O	-10.5	-10.5	-6.4	-5.5	-5.4	-5.2	9.6	10.7	9.4	8.0
Other	Cumetal	Cu	1.1	2.6	-0.2	1.6	-4.3	0.2	-13.8	-7.9	-9.9	-2.9
	Fluorite	CaF2	-2.4	-2.4	-2.5	-3.3	-4.2	-4.7	NA	-7.5	-3.1	-3.0
	Plumbgummite	PbAl3(PO4)2(OH)5:H2O	-3.8	-3.8	1.1	3.7	8.5	3.2	2.6	9.0	11.8	10.9
	Semetal(am)	Se	2.6	-0.4	2.1	5.3	-9.2	6.9	-15.2	-7.5	-16.4	-2.8

Notes

1.0	Groundwater is saturated with respect to this mineral (calculated saturation index>0)
-3.0	Groundwater is unsaturated with respect to this mineral (calculated saturation index<-2)

3.5.6.1.2 Incorporation of Mineral Phases in the Geochemical Model

Model simulations were also completed to evaluate the potential importance of solid-phase solubility on the behaviour of COPCs along the groundwater flow path from the mining area to Whitefish Lake.

In the discussion below, as with discussion of results throughout the remainder of Section 3.0, results are focused on uranium and other key COPCs, including Radium-226 and pH. Results for all COPCs are discussed in more detail for the results of the 3-D numerical modelling (Section 4.0).

Uranium

The uranyl mineral phases included above in Table 3-8 were included in model simulations involving the Desilicified Zone conceptual model (Figure 3-6b). Uranium concentrations in porewater were first simulated in the absence of any chemical reactions along the groundwater flow path. Because this is a 1D plug flow model, incorporating modest to low longitudinal dispersivity, the uranium concentrations at breakthrough (i.e., at the point of discharge) are largely unchanged from the concentrations in the mining area (50% Restored Solution #1). Travel time to Whitefish Lake, for all COPCs that were considered as chemically conservative, is approximately 300-500 years.

Authigenic uranyl (U(IV)) minerals Soddyite, Tyuyamunite, Uranophane and Uranyl Orthophosphate were predicted to precipitate. In the absence of other geochemical reactions, precipitation of authigenic uranyl minerals resulted in a order of magnitude decrease in peak uranium concentrations in groundwater adjacent to Whitefish Lake compared to the simulation with no geochemical reactions (Figure 3-7). Both sorption and authigenic mineral formation were then explored by adding in the sorption processes described below (Section 3.5.6.2). Figure 3-7 shows the predicted uranium concentrations when “full solids”, based in the understood LSA mineralogy, were included. Concentrations of uranium in groundwater discharging to Whitefish Lake in the 4000 years following Decommissioning were not substantively different if precipitation of authigenic mineral phases and sorption were included in the model versus sorption alone.

The sensitivity to the density of reactive sorption sites on mineral surfaces was evaluated by decreasing the number of sorption sites in the Desilificified Zone by a factor of 10. The rationale for this sensitivity evaluation is discussed further is Section 3.5.6.2. Simulated uranium concentrations were higher when authigenic minerals were not included in the model run. In both the full sorption and 10% sorption scenarios, authigenic uranyl precipitation was predicted to occur only within approximately 100 m of the remediated mining area, where uranium and other constituents were initially present in highest concentrations post closure.

There is some evidence that authigenic uranyl minerals are present with the Athabasca Supergroup sandstones because of groundwater re-work of localized U(IV) mineralization (Kermeen, 1955), and for other environments where uranium in the dissolved form has been

released from the shallow subsurface (e.g., Arai et al., 2007; Bond et al, 2007). However, the specific potential for precipitation of authigenic uranyl minerals in the LSA is currently unknown. As such, it was considered conservative to assume no precipitation of uranyl minerals and that sorption, which is a well documented controlling reaction for uranium downgradient of ISR mining areas, will be the dominant controlling reaction for uranium (Colon et al., 2000; Johnson et al., 2016; de Boissezon et al., 2020).

^{226}Radium

All of the solutions examined are undersaturated with respect to $Ra(SO_4)(s)$. However, a number of studies have demonstrated that a solid solution of radium sulphate ($RaSO_4$) and barite ($BaSO_4$) is an important phase for ^{226}Ra migration downgradient of ISR mining areas (e.g., Intera, 2013; de Boissezon et al., 2020). This solid solution was evaluated in the 1D model simulations.

The influence of the precipitation of barium-radium sulphate ($(Ba,Ra)SO_4$) as a solid solution with barite ($BaSO_4$) on predicted ^{226}Ra concentrations in porewater was evaluated and results are shown in Figure 3-8. Sulphate from the mining area behaves conservatively and with no geochemical reactions exhibits peak concentrations at about 500 years after decommissioning. When formation of the solid solution is considered alone, ^{226}Ra concentrations first decrease reflecting the formation of the solid solution under conditions of maximum sulphate concentrations in the system interacting with background radium (and barium) concentrations. However, as the sulphate decreases with continuing groundwater flow, the solid solution is rapidly re-dissolved when groundwater with much lower sulphate concentrations flow into the system. This results in a peak ^{226}Ra concentration that arrives later than that when no precipitation and dissolution of the barium-radium sulphate solid occurs.

When sorption is considered (both 'full solids' and '1 in 10 solids', see Section 3.5.6.2), the solid solution continues to be formed and re-dissolved in the system, but the processes work together to attenuate peak ^{226}Ra concentrations. Because both sorption and formation of the solid solution are understood to be important in ISR mining activities (e.g. de Boissezon et al., 2020), both processes are incorporated in 3D modelling.

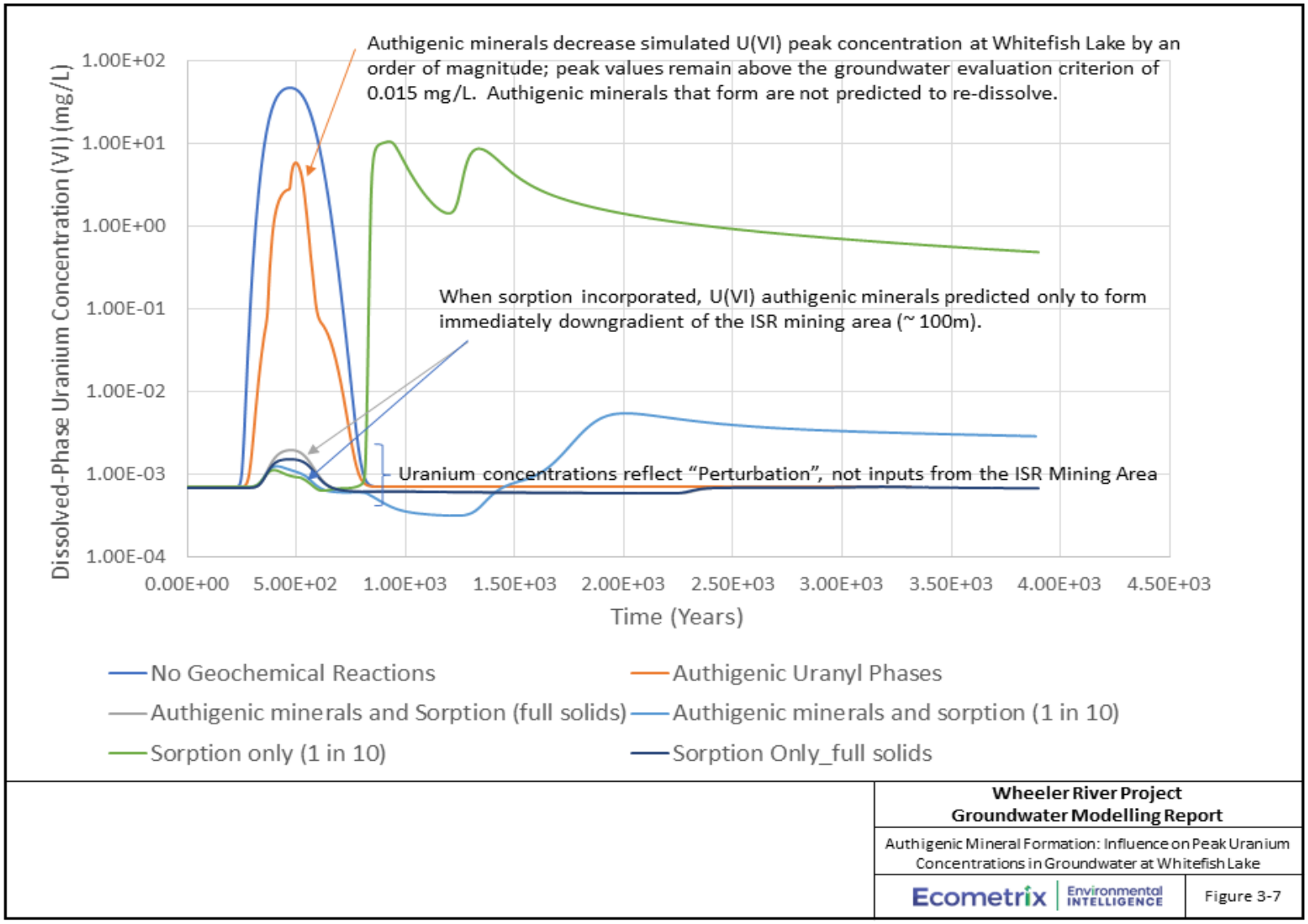

Figure 3-7: Authigenic Mineral Formation: Influence on Peak Uranium Concentrations in Groundwater at Whitefish Lake

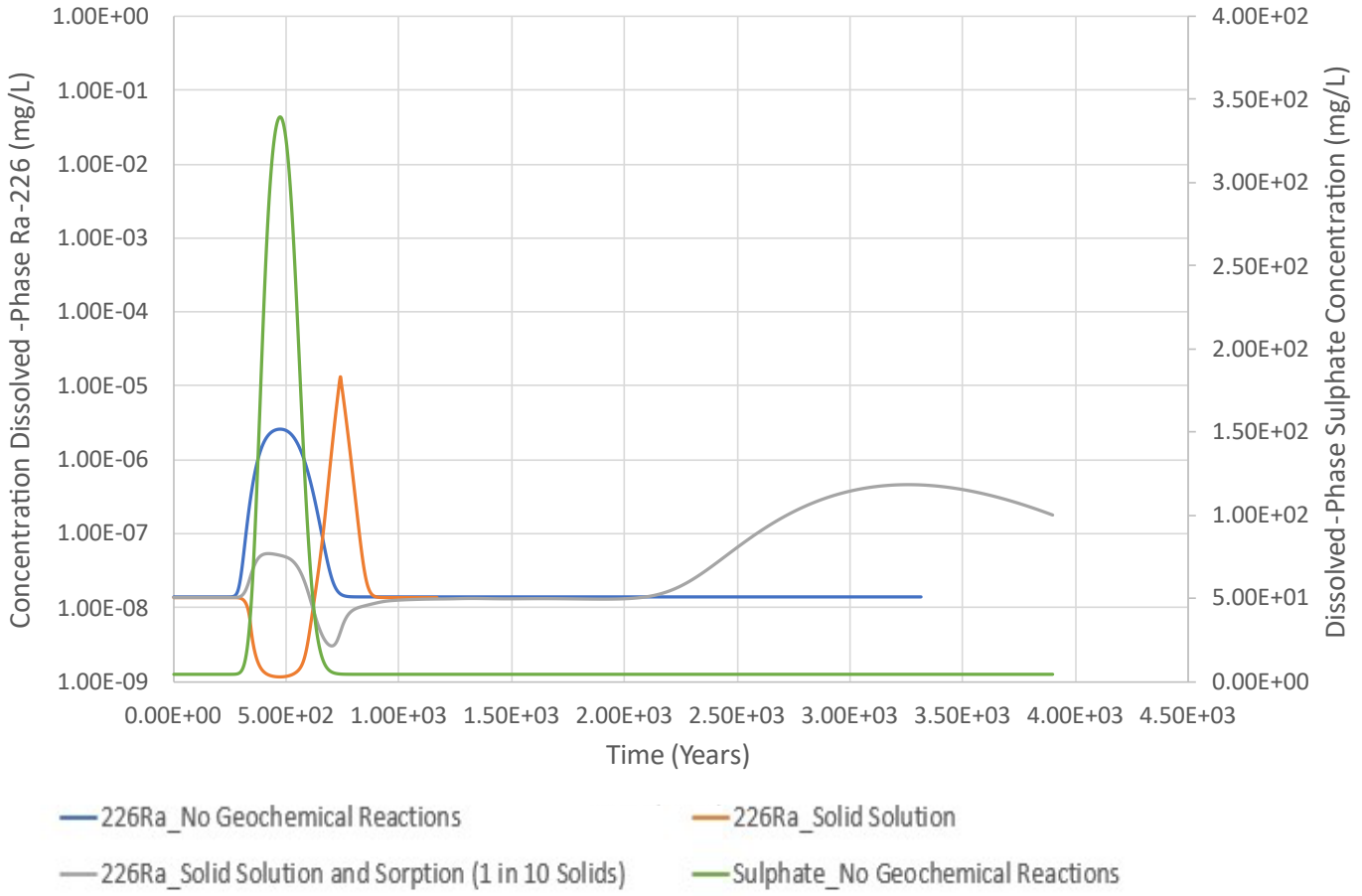

	Wheeler River Project **Groundwater Modelling Report**
	Authigenic Mineral Formation: Influence on Peak ^{226}Radium Concentrations in Groundwater at Whitefish Lake
	Ecometrix Environmental INTELLIGENCE — Figure 3-8

Figure 3-8: Authigenic Mineral Formation: Influence on Peak ^{226}Radium Concentrations in Groundwater at Whitefish Lake

Other Minerals

ThO_2 was not evaluated as a mineral phase in the model because:

- Th is known to be present not as ThO_2 but as part of the solid solution series of the crandellite group (aluminophosphate minerals; Mwenifumbo and Bernius, 2007) in the Athabasca Supergroup sandstones and particularly the Bird Formation. This is likely the reason that all baseline groundwaters are supersaturated with respect to ThO2 – it is not the correct solid phase to reflect the existing Th solid-phase speciation.

- Multiple studies have demonstrated that Th (IV) has a high sorptive affinity for mineral phases such as those present in the LSA (iron oxides/oxyhydroxides and clay minerals; e.g. Laflamme and Muray, 1987; Iida et al., 2016). A study by Melson (2011) shows that dissolved-phase Th concentrations solubility-controlled by ThO2 and those expected from sorption at mineral surfaces (iron oxides and clays) are comparable over the pH range being examined in this study. Thus, it was considered appropriate and conservative to evaluate sorption as the primary geochemical reaction for Th in the model.

The precipitation of $Cr(OH)_3$ was evaluated and was not found to substantively change the concentrations of Cr(III) along the groundwater flow path. As such, this mineral phase was not included as a solid phase. Aluminum concentrations in the system were controlled through solubility with gibbsite ($Al(OH)_3$). Controls on dissolved-phase iron concentrations are discussed in more detail in Section 3.5.6.5.

3.5.6.2 Incorporation of Sorption Processes

As introduced above (Table 3-7), sorption – including both ion exchange and adsorption at solid surfaces – was considered to some extent in all the model simulations for COPC geochemical reactive transport. Incorporation of sorption is supported by reviewed literature, which has demonstrated that sorption of uranium and other metals/trace elements occurs on the surfaces of quartz, iron oxides and clays (e.g., Dzombak and Morel, 1991), and assemblages of those mineral phases (e.g., Dong and Wan, 2014). Sorption was implemented using geochemical reactions rather than using a simplified partitioning coefficient approach, as described below.

3.5.6.2.1 Information Supporting Incorporation of Sorption

To the best of our knowledge, there is very little information published about the solid-phase speciation of uranium and other constituents associated with ore bodies and the overlying and underlying rocks in the Athabasca basin. Information on solid-phase speciation, meaning, how uranium and other elements occur in the subsurface can provide supporting information for model simulations.

One study was identified of core samples at Cigar Lake (Percival, 1989), wherein solid-phase uranium speciation in core samples from a) the sandstones closest to the clay barrier material, b) the unconformity, and c) the "altered basement" were examined using sequential extraction. The

objective of that study was to identify if uranium associated with these units resulted form primary ore-formation or because of secondary alteration/hydromorphic dispersion – meaning remobilization and movement of uranium after primary mineralization. Five extraction solutions were used in the sequential extraction, and the results are summarized in Table 3-9.

Table 3-9: Solid Phase Speciation of Uranium, Existing Conditions (after Percival, 1989)

Unit	Extraction	% of Total U (range, and median value)[a]	Interpretation of uranium speciation (Percival, 1989)
Clay-Rich Sandstones Overlying the Unconformity (n = 11, < 2 µm fraction)	Carbonate Associated and Exchangeable	2-16%, 9%	Generally low, probably the most mobile form of uranium
	Uraninite, Sulfide and Organic Bound	13-73%, 35%	No visible reaction on addition of reagent, unlikely that an organic-bound form of U is present. Uraninite is assumed to be the main digestible fraction by this treatment.
	Amorphous Fe-bound	1-14%, 3%	Relatively low contribution reflects the overall low concentrations of these mineral phases in the subsurface
	Crystalline Fe-bound	6-54%,18%	Associated with noeformed (during the period of hydrothermal alteration) iron oxides
	Residual	10-46%, 33%	Associated with noeformed (during the period of hydrothermal alteration) clay minerals, and strong relationship with illite.
Paleoweathered Zone (n=1, < 2µm fraction)	Carbonate Associated and Exchangeable	13%	Same interpretations as above.
	Uraninite, Sulfide and Organic Bound	31%	
	Amorphous Fe-bound	4%	
	Crystalline Fe-bound	10%	
	Residual	42%	

Notes

Fraction representing the greatest percentage of the total uranium in the sample

a Values presented for the Paleoweathered Zone reflect only a single sample analyzed

Percival (1989) concluded that uranium present outside of the ore zone is primarily related to ore-forming processes, and that there has been very limited secondary mobilization of uranium. This was concluded on the basis that uranium concentrations in the overlying sandstones remain low, and most of the uranium is associated with uraninite, crystalline iron oxides, and the residual phase. The uranium in the residual phase was interpreted to be associated with silicate minerals, including clay minerals (illite, sudoite, and kaolinite), quartz, tourmaline, and zircon. Uranium, dispersed because of the hydrothermal alteration, was interpreted to have been incorporated into neoformed clay minerals and iron oxides.

The results of Percival (1989) inform the modelling evaluation herein in that they indicate uranium is present in a number of chemical forms (species) in the subsurface, and that there is evidence for reactivity of clay minerals and iron oxides (amorphous and crystalline) for uranium. Specifically, the reactivity of illite is suggested by observation that samples with higher illite content and furthest from the unconformity had higher proportion of uranium associated with the residual/silicate fraction. Further, the redox conditions in the subsurface have allowed for

uranium to remain stable and largely immobilized, meaning, even outside of the ore zone, some portion of the uranium naturally in the samples is likely present as uraninite.

3.5.6.2.2 Ion Exchange and Surface Complexation

Partitioning of metals or trace elements can also occur because of chemical or electrostatic interactions between the solution species and reactive sites associated with a solid phase. When the interaction occurs at the surface of a solid particle, the term "surface complexation" is used to describe the interaction.

Surface complexation reactions included in the geochemical model described herein are generally those in which a chemical bond is formed between a reactive site at the surface and the species from solution, a process referred to as "adsorption". Surface complexation reactions involve a known (input), including the total number of, typically, diprotic reactive sites at the mineral surface. The number of sites and the constants driving adsorption of protons, metals and other species are specific to individual mineral phases and are based on experimental derivation. Because there are a finite number of diprotic sites, surface complexation modelling inherently considers the competition between protons and other elements/species for the same sites, and thus, provides a means of understanding how adsorption of elements/species changes with pH. Further, the finite number of sites means that competition amongst metals/species is accounted for, and the sites can become saturated, such that no further adsorption to the solid is allowed.

Adsorbing mineral surfaces were included in the geochemical model for the paleoweathered zone, Desilicified Zone, and in the Lake Bottom Sediments (described in more detail in Section 3.5.6.2.4). The nature of the adsorbing surfaces is detailed in Table 3-10. Illite was selected as the clay mineral phase because this was reported to be the dominant clay mineral (i.e., of illite, kaolinite and dichlorite) in the Athabasca Supergroup sandstones, and paleoweathered lithologic unit (Table 3-2 and Denison, 2022b).

Because there are multiple COPCs and other groundwater constituents being considered in the modelling simulations, it was important to ensure, as much as possible, that surface complexation reactions and associated surface complexation (binding) constants for COPCs were related to the same mineral. For this reason, a substantive literature review was undertaken to identify and compile appropriate surface complexation constants for COPCs to illite and quartz. The metals for which surface complexation constants were applied in the model and the sources of the constants are outlined in Table 3-10 and further explained in Appendix E. Metal/species adsorption to goethite was used as a proxy for sorption to hematite and other ferric oxyhydroxides (limonite) present in the system. Surface complexation constants for trace elements and radionuclides with goethite were, for the most part, taken from Mathur and Dzombak (2006), with exceptions outlined in Appendix E.

Table 3-10: Properties of Adsorbing Mineral Phases

Sorbent Phase	Site Density (mol/kg)	Specific Area (m2/g)	Reference
Goethite (FeOOH)	0.203	60	Mathur and Dzombak, 2006
Quartz (SiO_2)	0.00118	0.31	Prikryl et al., 2001
Illite	Strong Sites: 0.002 (metals and protons sorb); Weak Sites; 0.04 (protons only sorb)	97	Bradbury and Baeyans, 2009

Sorption to a mineral phase can also include electrostatic-driven interactions. Ion exchange reactions were included in the geochemical model for clay minerals. For exchangeable cations, the cation exchange capacity (CEC) for illite of 225 meq/kg was taken from Bradbury and Baeyans (2009). The exchanger was defined (as Y-) and reactions of cations and protons with the exchange site were written as half reactions. For example, the reaction of exchange sites on illite, saturated with Na and then exchanged with Ca is:

Ca^{2+} + 2Y- = CaY2

K = 11; log K = 1.04 (Thermodynamic constant from Bradbury and Baeyans, 2009).

3.5.6.2.3 Model Check – Baseline Conditions

An important step in developing the model was a check that the sorptive capacity of the mineral surfaces for COPCs applied in the model using literature values for the mineral properties (i.e. surface area, site density) and surface complexation constants under initial/baseline conditions, did not exceed the existing/baseline solid phase concentrations of those COPCs. In PHREEQC, the solids are "pre-loaded" (pre-equilibrated) with COPCs to bring the solid phase concentrations into equilibrium with the dissolved phase concentrations before the transport simulation is started. For example, for a given dissolved concentration of uranium, the solid phases in each zone (e.g., desilicified zone) are pre-loaded with uranium on the reactive sorption sites. The pre-loading continues in accordance with the surface complexation constants for uranium with those minerals, until equilibrium is reached between uranium in the dissolved phase (set in the initial solution) and uranium sorbed on the solids (calculated in PHREEQC).

Shown in Table 3-11 are the solid-phase concentrations of COPCs calculated in the manner described above in PHREEQC. Also shown are "apparent K_d" values (with units of L/kg). These values express the dissolved concentration of the COPC (mg/L) to the total sorbed concentration of the COPC (mg/kg); the total sorbed concentration is the total concentration of COPC on all sorbing phases (quartz and/or illite and/or goethite depending on availability of surface complexation constants; see Appendix E). For the majority of the COPCs and for both the Desilicified and paleoweathered zones, the modelled solid phase concentrations and apparent K_d values were below those measured, and calculated from measured values, respectively. This indicates that the model is not overpredicting solid-phase concentrations based on sorption, nor are the apparent K_d values exceeding those reported in the literature.

Noted is that these represent existing/pre-restoration solid phase concentrations and K_d values; the solid phase concentration and K_d value will change during the reactive transport of the plume, reflecting binding of COCPs and the saturation level of the reactive sites on the mineral surfaces.

Work done to verify that the adsorption of COPCs was aligned with the adsorption behaviour of those constituents in the literature is provided in Appendix E. In Appendix E are a series of figures that plot the adsorption behaviour using the solid properties and thermodynamic database developed for this project, and where relevant, it is compared to adsorption behaviour in the literature.

Table 3-11: Solid-Phase Concentrations and Partitioning Constants for COPCs, measured and simulated

Desilicified Zone													
	Units	As (Partial)	Cd	Co	Cr	Cu	Mo	Ni	Pb	Se (Partial)	U	V	Zn
Solid Phase Concentration - Maximum	mg/kg	8.46E+00	7.00E-01	2.25E+01	1.09E+02	1.09E+02	4.51E+00	1.58E+02	7.33E+01	4.00E-01	2.13E+02	3.71E+02	9.30E+01
Solid Phase Concentration - Minimum	mg/kg	9.00E-02	5.00E-02	1.20E-01	2.00E+00	2.00E-01	4.00E-02	1.00E+00	7.80E-01	1.00E-01	5.00E-01	1.40E+00	5.00E-01
Solid Phase Concentration - Median	mg/kg	5.60E-01	1.00E-01	4.90E-01	8.00E+00	2.00E+00	1.70E-01	6.00E+00	2.95E+00	1.00E-01	1.77E+00	7.70E+00	3.00E+00
Concentration in Representative Groundwater	mg/L	1.30E-03	1.00E-05	1.00E-04	5.00E-04	1.80E-03	4.20E-03	1.00E-04	1.00E-04	1.00E-04	7.00E-04	1.00E-04	1.20E-02
K_d - maximum value	L/kg	6.51E+03	7.00E+04	2.25E+05	2.18E+05	6.06E+04	1.07E+03	1.58E+06	7.33E+05	4.00E+03	3.04E+05	3.71E+06	7.75E+03
K_d - minimum value	L/kg	6.92E+01	5.00E+03	1.20E+03	4.00E+03	1.11E+02	9.52E+00	1.00E+04	7.80E+03	1.00E+03	7.14E+02	1.40E+04	4.17E+01
K_d - median value	L/kg	4.30E+02	1.00E+04	4.90E+03	1.60E+04	1.11E+03	4.05E+01	6.00E+03	2.95E+04	1.00E+03	2.53E+03	7.70E+04	2.50E+02
Modelled Solids Concentration **Base Case**	mg/kg	7.70E-03	1.11E-04	5.62E-03	1.90E+00	3.57E+00	5.51E-07	1.30E-02	8.68E-02	6.60E-06	7.25E-02	3.90E-07	1.37E+00
Apparent K_d value in the **Base Case** model	(L/kg)	5.92E+00	1.11E+01	5.62E+01	3.81E+03	1.98E+03	1.31E-04	1.30E+02	8.68E+02	6.60E-02	1.04E+02	3.90E-03	1.14E+02
Apparent K_d value in the model; **1/10 reactive sites**	(L/kg)	5.92E-01	1.11E+00	5.62E+00	3.81E+02	1.98E+02	1.31E-05	1.30E+01	8.68E+01	6.60E-03	1.04E+01	3.90E-04	1.14E+01
Paleoweathered Zone													
	Units	As (Partial)	Cd	Co	Cr	Cu	Mo	Ni	Pb	Se (Partial)	U	V	Zn
Solid Phase Concentration - Maximum	mg/kg	5.66E+02	8.00E+00	4.23E+02	4.41E+02	5.24E+04	3.93E+03	5.88E+02	5.15E+03	2.00E+02	5.56E+04	6.05E+03	1.58E+03
Solid Phase Concentration - Minimum	mg/kg	5.00E-01	1.00E-01	6.00E+00	6.00E+00	5.00E+00	5.00E-01	4.40E+01	1.00E+00	5.00E-01	9.00E+00	2.20E+01	7.00E+00
Solid Phase Concentration - Median	mg/kg	2.40E+01	1.00E+00	2.80E+01	1.55E+02	2.28E+02	5.00E+00	1.67E+02	4.60E+01	1.00E+00	4.03E+02	3.10E+02	3.10E+01
Concentration in Representative Groundwater	mg/L	5.00E-02	1.00E-05	1.00E-02	4.50E-03	5.00E-03	1.28E-02	1.50E-02	1.00E-04	1.00E-04	1.24E-02	1.00E-04	4.25E-03
K_d - maximum value	L/kg	1.13E+04	8.00E+05	4.23E+04	9.80E+04	1.05E+07	3.07E+05	3.92E+04	5.92E+07	2.00E+06	4.49E+06	6.05E+07	3.72E+05
K_d - minimum value	L/kg	1.00E+01	1.00E+04	6.00E+02	1.33E+03	1.00E+03	3.91E+01	2.93E+03	7.00E+04	5.00E+03	7.26E+02	2.20E+05	1.65E+03
K_d - median value	L/kg	4.80E+02	1.00E+05	2.80E+03	3.44E+04	4.56E+04	3.91E+02	1.11E+04	8.30E+05	1.00E+04	3.25E+04	3.10E+06	7.29E+03
Modelled Solids Concentration **Base Case**	mg/kg	1.87E-01	9.80E-05	4.69E-01	0.00E+00	5.30E+00	0.00E+00	2.34E+00	6.34E-02	2.87E-06	3.63E-01	0.00E+00	4.41E-01
Apparent K_d value in the **Base Case** model	(L/kg)	3.74E+00	9.80E+00	4.69E+01	0.00E+00	1.06E+03	0.00E+00	1.56E+02	6.34E+02	2.87E-02	2.93E+01	0.00E+00	1.04E+02
Apparent K_d value in the model; **1/10 reactive sites**	(L/kg)	3.74E-01	9.80E-01	4.69E+00	0.00E+00	1.06E+02	0.00E+00	1.56E+01	6.34E+01	2.87E-03	2.93E+00	0.00E+00	1.04E+01
Literature K_d values (mean value and range)[a,b]	L/kg	550 (25-3000)	15 (2.0-250)	$1.9x10^3$ (29-99,000)	18 (1.0-1600)	530 (760-2700)	40 (7-130)	58 (7.0-1100)	2000 (25-130,000)	56 (4-1600)	740 (2.6 - $6.2x10^4$)	1.1-2.7	$1.6x10^3$ (6.2-30,000)

Notes

[a] Literature K_d values are for pH values ranging from 5-8 from IAEA, 2010. These values show mean values (and range). Value for Cd is for soils with pH < 6.5. Where pH dependent K_d values were not available, the mineral soil texture values were obtained. Where a K_d was not available for mineral soil, the value for "All soil" texture or "Sand" was used.

[b] Literature range of K_d values for Vanadium taken from US EPA, 2005

[c] Literature value of maximum K_d for pH values ranging from 5-7 from IAEA, 2010.

3.5.6.2.4 Lake Bottom Sediments

A 1 m layer of lake-bottom sediments was simulated for Whitefish Lake. Reversible sorption of chemical constituents in groundwater to the lake-bottom sediments was simulated by applying the water-to-sediment partition coefficients (K_d) applied in the Wheeler River IMPACT Model (Ecometrix, 2024b). The K_d values (Table 3-12) consist of regional published values that have been calibrated on similar sites in northern Saskatchewan and have been checked against Wheeler River measurement data (Ecometrix 2024b; ERA Report).

Table 3-12: Distribution Coefficients (Coefficients (K_d) Used in the IMPACT Model

COPC	Distribution Coefficient L/kg (dw)
Arsenic	9.64E+04
Cadmium	1.50E+04
Chromium	1.16E+04
Cobalt	2.50E+03
Copper	3.00E+03
Molybdenum	3.17E+03
Selenium	2.00E+04
Uranium	2.00E+04
Vanadium	9.10E+04
Zinc	1.50E+04
Radium-226	1.20E+04
Thorium-230	2.30E+03

Water quality in the porewater of the lake bottom sediments was not available. Initial porewater quality in the model was assumed to be that of groundwater in the Upper Sandstone Aquifer/obverburden (Table 3-5).

3.5.6.2.5 Sensitivity Analysis, Fewer Sorption Sites

A sensitivity analysis was run assuming that only 10% of the total sites on the adsorbing solids are reactive ("Sorption to fewer sites" in Table 3-8). This order of magnitude decrease was based on the understanding that the number of reactive sites is very sensitive to surface area and that the available surface area of mineral phases in situ in the LSA may be different from those assumed based on literature sources. In addition, the decision to decrease sites by an order of magnitude was made after evaluation of the apparent K_d values presented in Table 3-11 Generally, the apparent K_d values were comparable to or lower than the K_d values from the literature. For Cr, Cu and Ni, the apparent K_d values in the Desilicified zone and paleoweathered zones were better aligned with the literature values when the number of reactive sites assumed was 10% of those in the base case (full solids).

3.5.6.2.6 Results from Sorption Assessment

3.5.6.2.6.1 Dissovled Uranium, and "Perturbation" Effects

Uranium concentrations in groundwater at Whitefish Lake are predicted to change only marginally from existing baseline conditions in the more than 100,000 years following Decommissioning in the base case scenario (Figure 3-10). When there is a lower concentration

of reactive sorption sites assumed, the simulation results indicate the potential for uranium in groundwater to be elevated with respect to baseline conditions. The results for uranium migration between the base case and the lower sorption site density scenario, shown in Figure 3-10, and in Figure 3-7, point to the need to further evaluate the sensitivity of the modelling results in 3D to the concentrations of reactive surface sites.

Noted in Figure 3-7 is a marginal increase in dissolved uranium concentrations in groundwater at Whitefish Lake between approximately 300 and 500 years. This is referred to herein as uranium concentrations that result from system 'perturbation'.

Many groundwater constituents behave conservatively with respect to migration. The plume of conservative constituents and pH results in a "perturbation" to the existing system with respect to the binding of metals like uranium. What this means is that aqueous concentrations of species like sulphate, and carbonate change, and bring about an associated shift in the speciation of U(VI) in solution. This, in turn, affects the equilibrium between aqueous U(VI) and the pre-mine naturally occurring sorbed U(VI) in solids along the groundwater flow path. Thus, the increase in dissolved uranium concentrations is a result of the chemical conditions in the groundwater affected and does not reflect dissolved uranium arriving at Whitefish Lake from the mining area in that period.

3.5.6.2.6.2 Other COPCs

Results for the 1D modelling have not been shown for all constituents. The sorption assessment indicates the following general behaviour for COPCs and other constituents (e.g., chloride):

- sulphate, arsenic, selenium, ferrous iron, molybdenum, vanadium and chloride behave conservatively, meaning they do not interact appreciably with the solid phase, and thus, they are transported at the average linear groundwater velocity from the mineralized zone to the lake.
- Hydronium ions do interact with the solid phases, and thus, pH changes occur somewhat later than changes in concentrations for conservative constituents.
- Constituents that do not behave conservatively, meaning they interact to various degrees with the solid phase include Al, Cd, Co, Cr, Cu, Ni, Pb, U(VI), Zn, ^{226}Ra, and ^{230}Th.

3.5.6.3 Redox Scenario

Uraninite is known to be present in the native Athabasca Supergroup sandstones, which could act as a secondary source of uranium, however, there are no known oxidants downgradient of the restored solution capable of oxidizing the uranium and mobilizing it as the oxidized U(VI) form in solution. Pyrite is known to be present from hydrothermal alteration of the Athabasca Supergroup Sandstones (i.e., associated with the Desilicified zone), which, through reactions with the uranyl ion could lead to reduction of U(VI) and re-precipitation as U(IV)/uraninite, similar to the process that resulted in the formation of the ore body. The latter reaction was explored through geochemical modelling.

The model set-up for the Redox scenario was a modification of the Desilicified Zone Pathway conceptual model shown in Figure 3-6b. A small amount of reactive pyrite was assumed for the first 500 m of transport away from the ore zone in the model, primarily in the desilicified sediments of the Lower Sandstone Aquifer, and deeper portion of the Intermediate Sandstone Aquitard. Support for the presence of pyrite in hydrothermally altered materials came from the core logging by Denison personnel, and specifically, from coreholes advanced in the locations shown in Figure 3-1. Alterations with the potential to affect (decrease) matrix permeability were logged, including the occurrence and strength (weak, moderate, high) of the alteration for mineral phases including diagenetic hematite, hydrothermal hematite, pyrite, sooty pyrite and limonite. Related to the latter, the occurrence Liesgang bands were also reported.

The presence of pyrite was reported between an approximate depth interval of 240-390 mbgs. There were two exceptions to this where pyrite was noted at two shallower depth intervals (less than 150 m bgs). Generally, the pyrite was observed within fractures, or as 'fractured hosted-stringers'. Sooty pyrite often occurred pervasively over intervals upwards of 50 m in depth within the larger depth interval indicated above. Hydrothermal hematite also, typically, present over the same depth range, as bands or irregular beds. The median iron oxide (Fe_2O_3) content of the MFa is 0.14 wt%. The core logging and elemental analysis do not provide the means to apportion the iron content further between oxidized and reduced forms.

In the modelling simulations, pyrite was allowed to come to equilibrium with the groundwater/restored solution plume. As a result of this equilibrium, dissolved U(VI) was reduced to U(IV) and precipitated as uraninite. Groundwater conditions over the long term (i.e., baseline groundwater quality in the Desilicified zone, including pe conditions) are such that the uraninite is stable and is not predicted to re-dissolve. Following the 500m reactive zone with pyrite, the plume was allowed to react with adsorbing phases as it travelled upwards through the Desilicified zone toward Whitefish Lake. No sorbing phases were included in the first 500 m of the groundwater pathway (where pyrite was present).

The exact solid that will be formed through the reaction of dissolved U(VI) with pyrite in the subsurface is not known; experimental work has suggested a mixed U(VI)/U(IV) solid ($U_3O_8/U_4O_9/U_3O_7$) (e.g., Yang et al., 2014) is formed. Thus, the solid formed through reaction of U(VI) with pyrite in the subsurface was assumed to be U_3O_7 (as $UO_{2.24}$(beta)) in the thermodynamic database). The model simulations demonstrated that a small fraction (<1%) of the total concentration of solid-phase Fe in this zone would have to be present as reactive pyrite (FeS_2) to react with dissolved uranium (U(VI)) in the remediate groundwater from the mining area and immobilize it as a reduced solid phase. Through the reduction and precipitation reactions of U(VI), concentration of dissolved uranium in groundwater at a distance of 500 m downgradient of the mining area, are consistent with measured baseline conditions.

3.5.6.4 Proton Desorption from Clay; 'pH Tail'

Other ISR projects have indicated that sorption of protons on clays in the ore zone as a result of the mining process result in long-term desorption of the protons with an associated depression

in pH compared to background (e.g., de Boissezon et al., 2020). This was evaluated herein by pre-equilibrating clay surfaces in the ore zone with the Restored Solution #1, for the multi-zone pathway conceptual model (Figure 3-6a).

The dominant clay in the ore zone is chlorite. It is possible that the mining process itself will affect the structure/mineralogy of the chlorite; however, it was assumed that chlorite will remain the dominant phase. The amount of chlorite in the ore zone was assumed to be 7.5% based on information provided by Denison (Denison, 2022c).

The sorptive properties of chlorite for protons was taken from Zazzi et al., 2012, and Zazzi, 2009. Proton sorption occurred on surface sites as several studies have shown that chlorite has a small cation exchange capacity (less than 5 meq/100 g) so protons exchanged at the surface were not included in the modelling simulations.

Table 3-13: Sorbent Properties of Chlorite

Sorbent Phase	Site Density (mol/kg)	Specific Area (m2/g)	Reference
Chlorite	0.00168	0.5	Zazzi et al., 2012

Results for the pH Tail scenario are shown in Figures 3-10 and 3-11. Sorption of protons to the clay mineral chlorite within the mining area is predicted to influence pH at the point of discharge over a longer period. Minimum pH values were approximately 6 under baseline conditions (Table 3-4 and Appendix D). The proton tail scenario is predicted to depress pH to some extent versus baseline conditions. Concentrations of uranium in groundwater at Whitefish Lake remain low with the changes in pH predicted.

3.5.6.5 Iron oxidation

The coreflood information shows that soluble iron concentrations remain high with flushing. Residual ferric iron is not expected within the Restored solution, as it will be consumed with reactions with uraninite and sulphide minerals, mainly pyrite (FeS_2), while conditions remain adequately oxidizing. In Restored Solution #1, with a pH of 4.3, the 100 mg/L of iron is expected to be present as dissolved ferrous iron.

However, there is evidence in the core logging (introduced in Section 3.5.6.3) of limonite in the shallow bedrock of the Athabasca Supergroup sandstones, suggesting oxidation of ferrous iron in that zone. Thus, ferrous iron was allowed to be oxidized by dissolved oxygen and to precipitate as ferrihydrite within the last 100 m of the flow path in order to evaluate the potential effects on pH if oxidation of the ferrous iron occurred along the groundwater flow path. The influence on pH is shown in Figure 3-9. The pH is depressed slightly by the oxidation of ferrous iron and precipitation of ferrihydrite, but the pH is not predicted to fall outside of minimum pH conditions (~ 6) under baseline conditions (Table 3-4 and Appendix D).

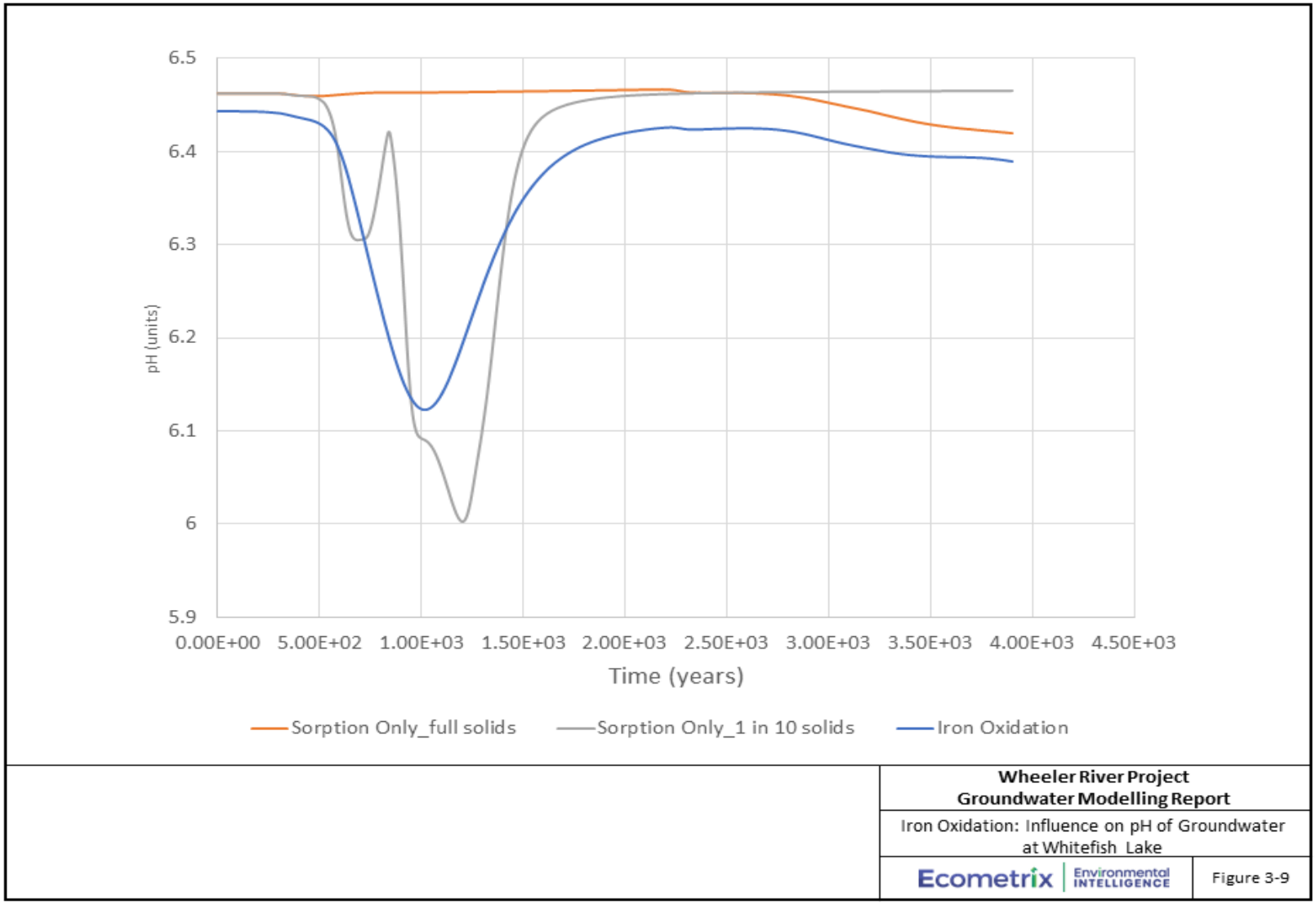

Figure 3-9: Iron Oxidation: Influence on pH of Groundwater at Whitefish Lake

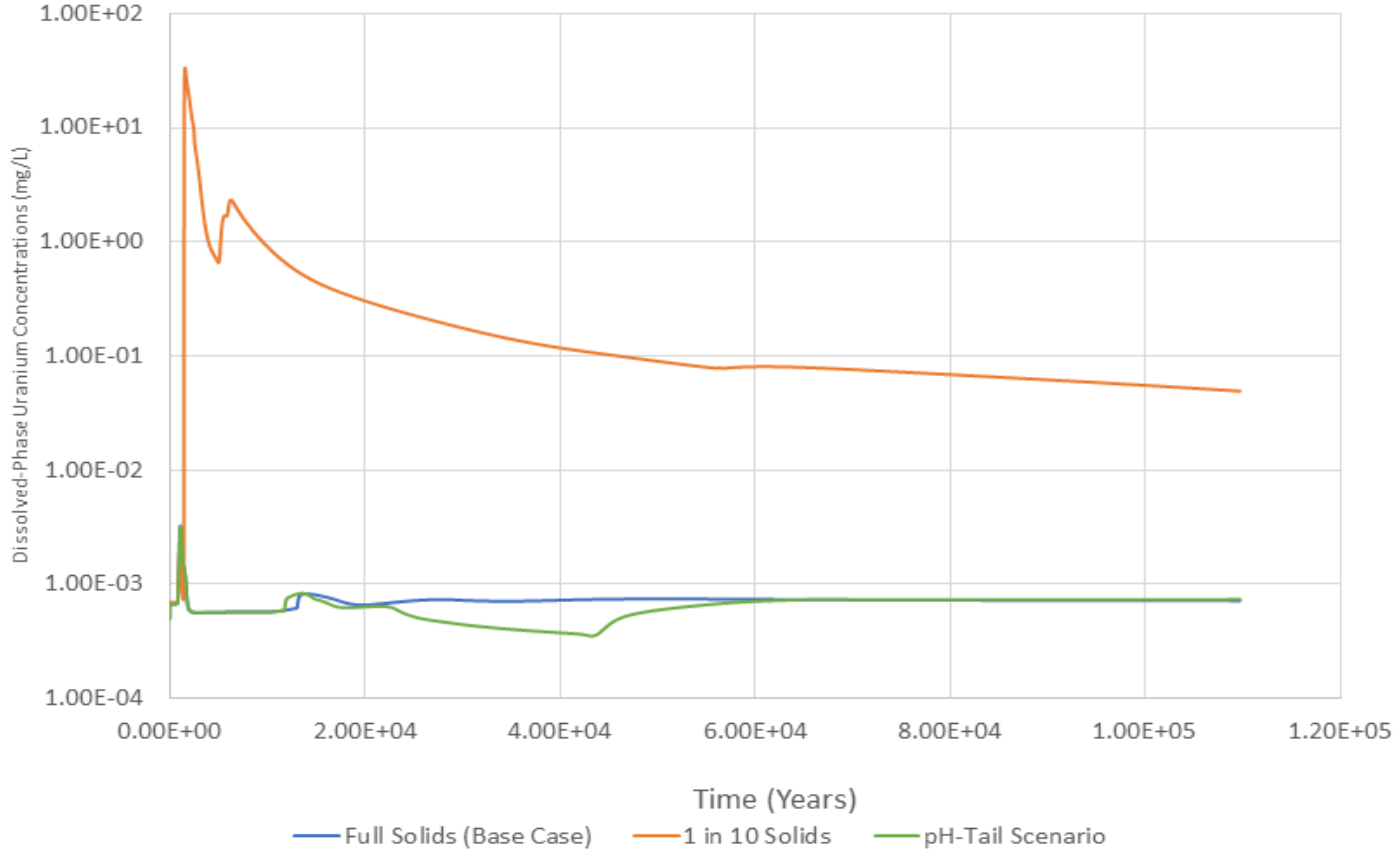

Wheeler River Project
Groundwater Modelling Report

Sorption and pH-tail: Influence on Peak Uranium Concentrations in Groundwater at Whitefish Lake

Ecometrix Environmental INTELLIGENCE | Figure 3-10

Figure 3-10: Sorption and pH-tail: Influence on Peak Uranium Concentrations in Groundwater at Whitefish Lake

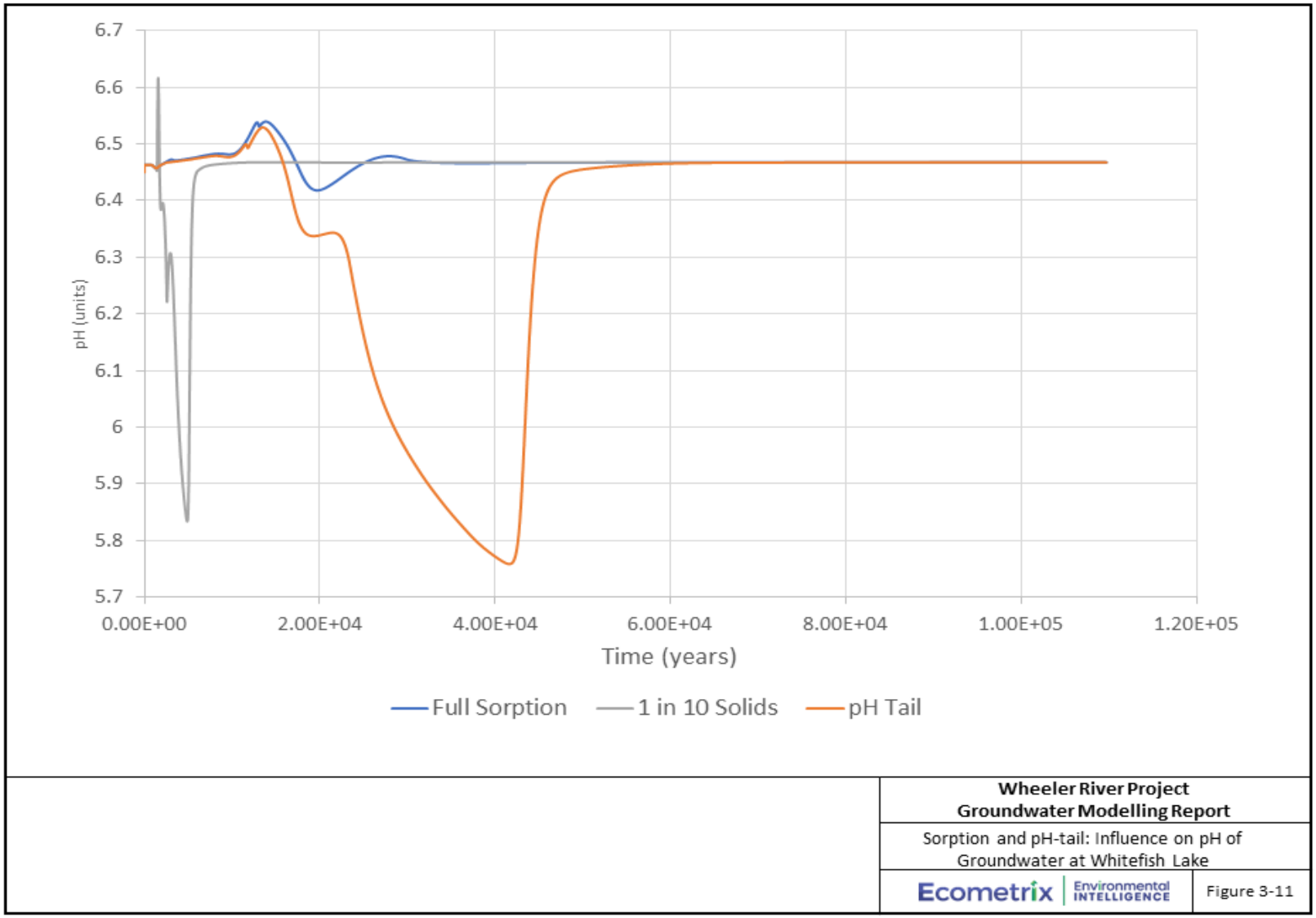

Figure 3-11: Sorption and pH-tail: Influence on pH of Groundwater at Whitefish Lake

3.6 Understanding Gained through 1D Geochemical Modelling

Key understanding gained through the 1D geochemical reactive transport modelling includes:

- Concentrations of uranium and several other COPCs arriving at Whitefish Lake are sensitive to the sorptive capacity assumed for the system. Some COPCs and other groundwater constituents, including sulphate, arsenic, selenium, ferrous iron, molybdenum, chloride, and vanadium behave conservatively, meaning they do not interact appreciably with the solid phase, and thus, they are transported at the average linear groundwater velocity from the mineralized zone to the lake.

- The base case (sorption) scenario, based on very well understood mineralogical conditions at the site, shows very strong attenuation of uranium and other COPCs in the subsurface. Reducing the density or number of reactive sites available in association with mineral surfaces results in less sequestration of uranium in the subsurface. For this reason, modelling in 3-D conservatively focused on the base case and simulations with fewer reactive sites associated with the mineralogical assemblages.

- The precipitation of authigenic mineral phases was not considered a key geochemical process controlling the behaviour of dissolved-phase U(VI) precipitation and was not carried forward as geochemical reaction in the 3D numerical modelling. Precipitation of uranyl solid phases was simulated, and when no adsorption was assumed, the concentration of uranium is attenuated to some extent. However, assuming the formation of secondary uranyl mineral phases in the absence of sorption along the entire subsurface pathway is not realistic.

- Solubility control/precipitation of authigenic mineral phases was evaluated and was carried forward into 3D numerical modelling as key geochemical reactions for dissolved aluminum (dissolved-phase concentrations controlled by formation of gibbsite ($Al(OH)_3$)), and dissolved 226Ra (through the formation of a solid solution of $RaSO_4$ and $BaSO_4$).

- In zones of hydrothermal alteration where pyrite has been observed, the effective immobilization of dissolved U(VI) was demonstrated to be possible through reduction of U(VI) dissolved in solution and formation of a solid phase - uraninite (UO_2) or mixed U(IV) and U(VI) oxide phase. This is aligned with the redox buffering by pyrite present in the ore zone and surrounding clay barrier zones considered important for maintaining uranium in the reduced form and solid form in the Athabasca basin unconformity ore deposits, since their formation (AECL, 1994).

- pH is a COPC and an important control on the extent of sorption of COPCs in the subsurface. Thus, the potential for pH to be depressed outside of baseline conditions through desorption of protons from clays in the mining area after remediation and for ferrous iron oxidation in the downgradient portion (Upper Sandstone Aquifer) of the groundwater flow path was evaluated further in the 3D numerical modelling.

3.7 Control Files for Three-Dimensional Modelling Analysis

Using the knowledge developed through the 1D PHREEQC modelling, input files for the 3D reactive transport modelling were developed. The input files generated control the following:

- initial groundwater constituent concentrations within each hydrostratigraphic unit (corresponding to the representative solutions given in Table 3-5).
- reactions conceptualized as key geochemical reactions through the 1D modelling for each hydrostratigraphic unit (e.g., redox conditions, pH, authigenic mineral formation, etc.,);
- available sorption reaction sites, calculated for each hydrostratigraphic unit based on the interpreted effective porosity; and
- concentrations for water quality at boundary conditions in the model at depth and within the shallow system, again corresponding to representative water quality in the hydrostratigraphic units presented in Table 3-5.

More details regarding the input files utilized within the 3D reactive transport model are contained in Sections 4.2, 4.5 and 4.6.

4.0 Post-Decommissioning Reactive Transport Modelling

The focus of the geochemical reactive transport modelling is post-decommissioning conditions. As documented in the EIS, decommissioning (i.e., remediation) of the ore zone and surrounding area within the freeze wall will be initiated once mine operation is completed and will continue until dissolved concentrations reach an acceptable decommissioning level (i.e., where natural attenuation processes can be relied upon to effectively mitigate risk to potential receptors). The following steps are planned to complete decommissioning in the mining area (the EIS; Section 2):

- Water will be injected into the mining area via injection wells and then recovered through the recovery wells, the same way mining was conducted during operations.
- Produced water will be processed through the processing plant until non-economic uranium concentrations are observed. Non-economic produced waters will be treated and mixed with fresh water for continued circulation in the mining area. Circulation through the mining area will continue until recovered water reaches acceptable groundwater quality decommissioning objectives.
- During groundwater restoration, reagents such as sodium bicarbonate and sodium hydroxide may be added to the injected water to accelerate groundwater quality recovery.
- After remediation has been completed, the freeze wall will be turned off and allowed to thaw. This will allow the eventual re-establishment of the pre-construction groundwater flow regime in the Phoenix area.

Metallurgical testing, including batch reactions, column tests, and core flooding tests have been undertaken at the Saskatchewan Research Council, to understand the anticipated evolution of groundwater hydrochemistry as the groundwater quality in the mining area is remediated. "Restored Solution #1" and "Restored Solution #2" (Table 3-5) were developed to represent the bounding scenarios for groundwater quality considered in the reactive transport model to evaluate the potential for environmental effects following remediation of the mining area. As Restored Solution #1 (RS1) contains the higher remaining concentrations, and lower pH (i.e., differs more from baseline conditions in the ore zone), this solution was primarily applied within the geochemical reactive transport modelling to evaluate environmental effects.

4.1 Post Decommissioning Source Zones

During mine operation and decommissioning, Denison has committed to actively manage any excursions within the zone immediately surrounding the ore zone (the EIS, Section 2). As such modelling of conditions during mine operation was not undertaken. During mine operation, the planned freeze walls will limit the potential lateral extent of any excursions, while active pumping will be used to create hydraulic controls that will limit vertical migration to a zone that lies within 50 m above the ore zone (the EIS, Section 2). Below the ore zone, the underlying basement rock has very low hydraulic conductivity (Section 2.3) that will act to limit the

downward vertical migration. Despite this limit to downward migration, the solubility enhancing fluids used during mine operation, which will have a density and specific gravity greater than sea water, has the potential to migrate downward to the base of the Paleoweathered Basement Aquitard. Details regarding the planned mine operation and decommissioning are contained within the EIS (Section 2).

Given these hydraulic and hydrogeologic controls, the expected distribution of restored solutions (Table 3-5) includes the following attributes:

- The mining area, which is simulated to contain two zones.
- Zone containing restored solution at 100% strength, and including the:
    - The active mining area (ore zone),
    - 15 m above the ore zone,
    - Paleoweathered Basement underlying the ore zone,
    - Each of the above zones extend laterally to the freeze wall location.
- Zone containing restored solution at 50% strength will be limited to:
    - Zone above the ore zone from 15 m to a maximum of 50 m above the ore zone,
    - Extending laterally to the freeze wall location.

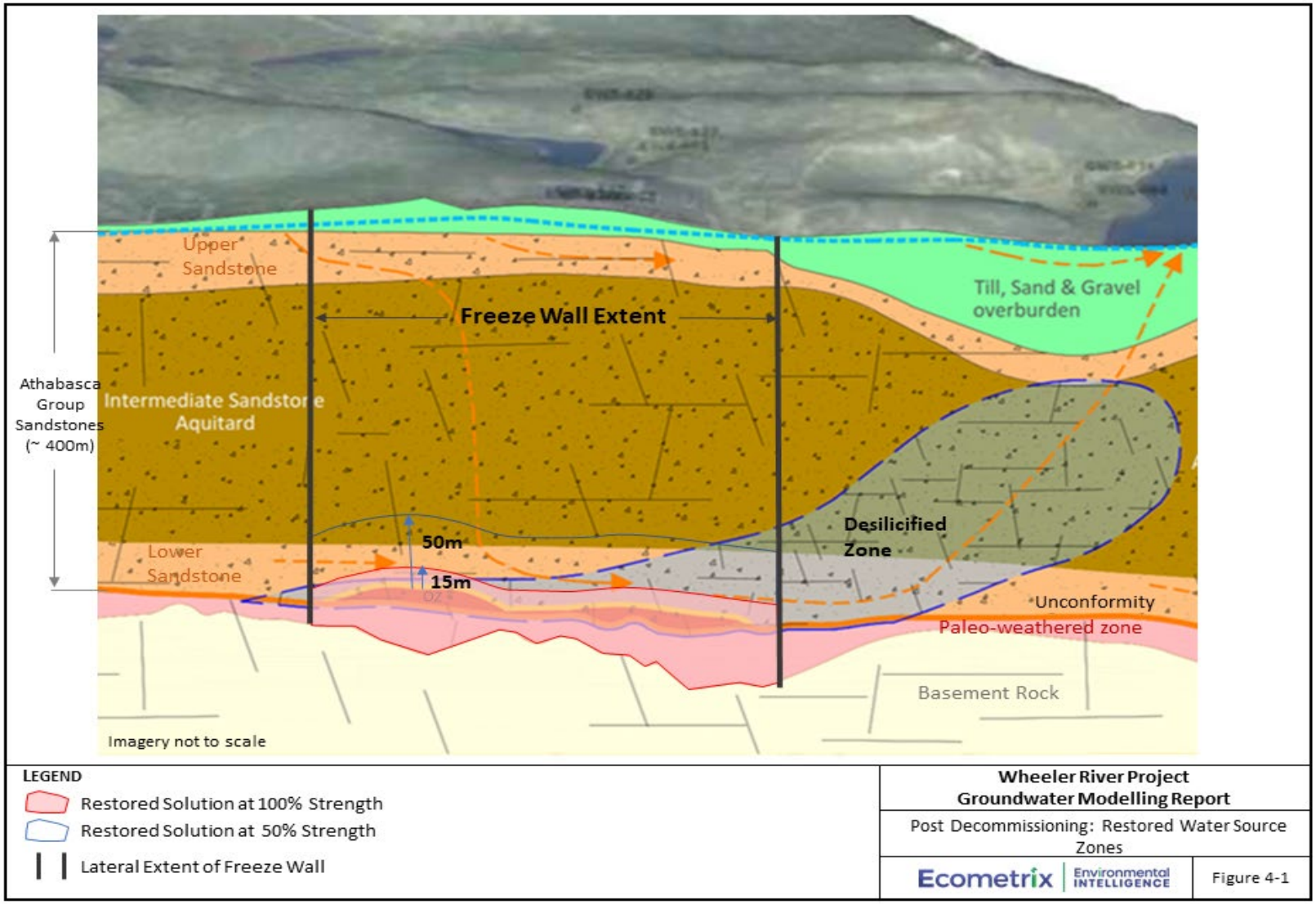

Figure 4-1: Post Decommissioning: Restored Water Source Zones

These zones describe above are illustrated in Figure 4-1. The zone containing restored solution at 50% strength is referred to as the operational flare (i.e., flare zone), which is considered to be a conservative estimation of the zone that could receive vertical migration of solutions during ISR operation and decommissioning. Testing to date suggests that the maximum upward migration of mining fluids will be approximately 11 to 13 m, so the extension of the source zone to 50 m above ore zone is considered to represent a conservative source condition.

These two defined zones are used as the source zones for the geochemical reactive transport model; migration from these source zones results in fate and transport of dissolved chemical constituents in groundwater following the cessation of the freeze wall (i.e., post-decommissioning). Given the active hydraulic controls planned by Denison for conditions during mine operation, the estimated source zones described above are considered conservatively large but appropriate for the environmental impact assessment.

Geochemical reactive transport modelling was undertaken to support Denison in developing restoration water quality targets, defined as residual concentrations of constituents in the restored groundwater that would not pose an adverse effect on the receiving water body. The focus of geochemical reactive transport modelling is evaluation of the COPC fate and transport from the defined source zones to the potential receiving water body, Whitefish Lake.

4.2 Simulated COPCs in 3D Reactive Transport Model

The COPCs simulated within the 3D geochemical reactive transport model are those documented in Section 3.5. As noted in Section 3.7, PHREEQC control files were established for model node groups to define the initial concentrations associated within each geochemical zone (Table 3-5). Each node within the model was assigned to belonged to one group, such that initial concentrations were specified for every simulation node. To simplify, uniform initial concentrations were applied withing each node group; this led to discontinuity of initial concentrations at geochemical zone boundaries, which are smoothed as the simulation progresses.

The initial groundwater quality within the mining area is described above (Section 4.1). Beyond the active mining area and flare zones, initial concentrations were specified based on representative water quality samples within each geochemical zone (Section 3.5.4). Initial concentrations are further discussed within section 4.4.

4.3 Groundwater Quality Screening Criteria

Denison's commitment in the EIS is to protect the receiving surface water environment. As such, groundwater quality screening criteria were compiled from available generic guidelines protective of aquatic life and were used, at a screening level, to evaluate the quality of groundwater at the interface with Whitefish Lake. The groundwater evaluation criteria and sources of the criteria are provided in Table 3-7.

Table 4-1: Groundwater Quality Screening Criteria

Constituent	Unit	CCME Protection of Aquatic Life (1)		Federal Environmental Quality Guideline		Saskatchewan Environmental Quality Guidelines (SEQG Online) (2)		Other		Selected Groundwater Quality Screening Criteria	Source
		Long Term	Note	Long Term	Note	Long Term	Note	Long Term	Note		
Aluminum, dissolved	mg/L	1.0E-01	(3)	-	-	1.0E-01	-	5.0E-02	(4)	5.0E-02	BC MOE
Arsenic, dissolved	mg/L	5.0E-03	-	-	-	5.0E-03	-	-	-	5.0E-03	SEQG/CCME
Barium, dissolved	mg/L	-	-	-	-		-	-	-	-	
Boron, dissolved	mg/L	1.5E-03	(5)	-	-	1.5E-03	-	-	-	1.5E-03	SEQG/CCME
Cadmium, dissolved	mg/L	4.0E-05		-	-	4.0E-05	-	-	-	4.0E-05	SEQG/CCME
Chromium, dissolved	mg/L	8.9E-03	(6)	-	-	8.9E-03	-	-	-	8.9E-03	SEQG/CCME
Cobalt, dissolved	mg/L	-	-	7.8E-04	(7)		-	-	-	7.8E-04	FEQG
Copper, dissolved	mg/L	2.0E-03	(8)	-	-	2.0E-03	(8)	-	-	2.0E-03	SEQG/CCME
Iron, dissolved	mg/L	3.0E-01		-	-			-	-	3.0E-01	CCME
Lead, dissolved	mg/L	1.0E-03	(8)	-	-	1.0E-03	(8)	-	-	1.0E-03	SEQG/CCME
Manganese, dissolved	mg/L	2.3E-01	(9)	-	-	-		-	-	2.3E-01	CCME
Molybdenum, dissolved	mg/L	7.3E-02	-	-	-	3.1E+01	-	-	-	3.1E+01	SEQG
Nickel, dissolved	mg/L	2.5E-02	(8)	-	-	2.5E-02	(8)	-	-	2.5E-02	SEQG/CCME
Selenium, dissolved	mg/L	1.0E-03				1.0E-03		2.0E-03	(10)	2.0E-03	BC MOE
Strontium, dissolved	mg/L	-	-	2.5E+00	(11)	-	-	-	-	2.5E+00	FEQG
Uranium, dissolved	mg/L	1.5E-02	-	-	-	1.5E-02	-	-	-	1.5E-02	SEQG/CCME
Vanadium, dissolved	mg/L	-	-	1.2E-01	(12)	-	-	-	-	1.2E-01	FEQG
Zinc, dissolved	mg/L	1.1E-02	(13)	-	-	3.0E-02	-	-	-	1.1E-02	CCME
Ammonia as nitrogen	mg/L	5.7E+00	(14)	-	-	5.7E+00	(14)	-	-	5.7E+00	SEQG/CCME
Chloride	mg/L	1.2E+02		-	-	1.2E+02	-	-	-	1.2E+02	SEQG/CCME
Sulphate	mg/L	-	-	-	-	-	-	1.28E+02	(15)	1.28E+02	BC MOE
Radium-226	Bq/L	-	-	-	-	1.1E-01		-	-	-	-
Radium-226 (converted)	mg/L	-	-	-	-	3.0E-09	-	-	-	3.0E-09	SEQG
Lead-210	Bq/L	-	-	-	-	-	-	2.2E+01	(16)	-	-
Lead-210 (converted)	mg/L	-	-	-	-	-	-	7.8E-09	-	7.8E-09	US DOE
Polonium-210	Bq/L	-	-	-	-	-	-	1.4E+01	(16)	-	-
Polonium-210 (converted)	mg/L	-	-	-	-	-	-	8.1E-11	-	8.1E-11	US DOE
Thorium-230	Bq/L	-	-	-	-	-	-	9.5E+01	(16)	-	
Thorium-230 (converted)	mg/L	-	-	-	-	-	-	1.24E-04	-	1.24E-04	US DOE
pH	units	6.5 -9		6.5-9		6.5-9		<6.5 and 6.5-9	(17)	6.5-9	SEQG/CCME

Notes:

(1) CCME, 2008. Canadian Water Quality Guidelines.

(2) Saskatchewan Water Quality Objectives, SEQG on-line (https://envrbrportal.crmp.saskatchewan.ca/seqg-search/) for groundwater.

(3) Guideline is for total Al. Based on a median pH in suface waters of 6.8 (i.e. pH of >6.5).

(4) British Columbia Ministry of Environment (BC MOE). 2001. Water Quality Criteria for Aluminum: Overview Report. Water Protection and Sustainability Branch, Environmental Sustainability and Strategic Policy Division. August 7, 2001. Victoria, B.C. Guideline is for dissolved Al. Based on a median pH in suface waters of 6.8 (i.e. pH of >6.5).

(5) CCME, 2009. Canadian Water Quality Guidelines for the Protection of Aquatic Life, Boron.

(6) Value for inorganic chromium (Cr(III)) is an interim guideline.

(7) Environment Canada 2017. Federal Environmental Quality Guidelines, Cobalt, May. Value adopted is for a hardness of 52 mg/L, as extrapolation of the equation for hardness-dependence

(8) Hardness dependent WQOs. Median hardness in surface water samples (Table) is 5.3 mg/L; Cu guideline reflects hardness >0 to <82 mg/L; Ni and Pb guidelines reflect hardness > 0 to ≤

(9) Scientific Criteria Document for the Development of the Canadian Water Quality Guidelines for the Protection of Aquatic Life - Manganese, Appendix B - Canadian Water Quality Guidelines Calculator (pH = 6.8, hardness = 10 mg/L). Guideline is based on dissolved manganese.

(10) BC MOE, 2014. Companion Document to: Ambient Water Quality Guidelines for Selenium Update.

(11) Environmenta and Climate Change Canada (ECCC). 2020. Federal Environmental Quality Guidelines Strontium. July.

(12) Environment Canada 2016. Federal Environmental Quality Guidelines, Vanadium. May.

(13) Based on a hardness of 23.4 mg/L (bottom of recommended range), and site-specific pH of 6.8 and DOC of 2.4 mg/L. pH and DOC reflect median values for baseline surface water

(14) Total ammonia-N calculated from the total ammonia guideline for a temperature of 15°C and a pH of 7.0.

(15) British Columbia Ministry of Environment & Climate Change Strategy Water Protection & Sustainability Branch (BC MECCS). 2021. British Columbia Approved Water Quality Guidelines: Aquatic Life, Wildlife & Agriculture. https://www2.gov.bc.ca/assets/gov/environment/air-land-water/water/waterquality/water-quality-guidelines/approved-wqgs/wqg_summary_aquaticlife_wildlife_agri.pdf

(16) US DOE 2019. A Graded Approach for Evaluating Radiation Doses to Aquatic and Terrestrial Biota

(17) (BC MECCS) British Columbia Ministry of Environment and Climate Change Strategy. 2021. British Columbia Approved Water Quality Guidelines: Aquatic Life, Wildlife & Agriculture - Guideline Summary. Water Quality Guideline Series, WQG-20. Prov.B.C., Victoria B.C. Unrestricted changed permitted within the range of 6.5-9.0. At pH levels <6.5, the requirement is to show no statistically significant decrease in pH value from background.

4.4 3D Sub-Domain Model Development

The computational requirements of a 3D geochemical reactive transport model with multiple constituents exceeded what was practically achievable within the regional-scale 3D model. To facilitate the efficient simulation of fate and transport, a sub-domain model was developed (Figure 4-2). The sub-domain model was designed to encompass flow and transport pathways simulated using the regional-scale 3D model described in Section 2, allowing for a buffer of approximately 200 m beyond the simulated transport pathways. Hydrogeologic units, parameter values, boundary conditions, and calibration data were taken from the 3D regional-scale model to efficiently construct the sub-domain model. In this manner, the sub-domain model is founded on the calibrated, regional-scale model.

4.4.1 Sub-Domain Model Area and Mesh

While the sub-domain model mesh was redesigned from the regional-scale model, the model area was designed based on flow conditions within the regional-scale model, as follows:

- Western boundary of the sub-domain model follows a simulated equipotential from the regional-scale 3D model
- North and south boundaries of the sub-domain model follow simulated flow lines, and
- Eastern boundary of the sub-domain model follows a shallow groundwater divide.

The sub-domain model is approximately 1 km in width (i.e., north to south), and 2.1 km long, extending 250 to 300 m upgradient of the source and downgradient beyond Whitefish Lake (Figure 4-2). The sub-domain model also extends from ground surface to the basement rock (Figure 4-3).

The sub-domain model was discretized into 91,179 nodes to achieve element lengths of 20 m within the plume trajectory indicated through particle tracking (Figure 4-2); element sizes were designed to be relatively uniform to maintain appropriate Peclet and Courant criteria for reactive transport simulations. The number of nodes in the sub-domain model is a significant reduction from the 804,000 nodes required within the 3D regional-scale model, making the sub-domain model much more efficient for the 3D geochemical reactive transport modelling.

4.4.2 Sub-Domain Model Hydrogeologic Parameters

The property zones calibrated within the regional model were directly mapped onto the sub-domain model mesh (Figure 4-3), to ensure the sub-domain model parameters were consistent with those calibrated within the regional model. An additional layer of elements was added 1 m below ground surface within the sub-domain model to permit simulation of lake bottom sediments (see insert on Figure 4-3). Additional layers of elements were also inserted within hydrostratigraphic layers to create relatively uniform vertical layer thicknesses.

One key difference between the sub-domain model input parameters and those assigned in the 3D Regional Model were in the assignment of the properties associated with the Upper Barrier Aquitard Zone, the ore zone, and the Lower Barrier Aquitard Zones. As there is uranium mineralization contained within the Upper and Lower Barrier Zones, the hydraulic conductivity of those zones is expected to be enhanced during ISR mine operation and as such, the hydraulic conductivity values representing these units were replaced with elevated hydraulic conductivity values relative to those assigned in the regional scale model. Specifically, a hydraulic conductivity value of $5x10^{-6}$ m/s was assigned to represent the mining horizon post-decommissioning. This value ($5x10^{-6}$ m/s) is a factor of 5 greater than (i.e., 5x) the value assumed for the ore zone in the 3D regional-scale model and conservatively simulates that the Upper and Lower Barrier Zones no longer result in effective barriers for mineral transport from the ore zone.

4.4.3 Sub-Domain Model Flow Boundary Conditions

Boundary conditions applied to the sub-domain model were also made to be consistent with the regional model as follows:

- Groundwater recharge zones were mapped to the sub-domain mesh and the same recharge rates applied,
- The mesh was designed to conform to surface water boundary locations and the same hydraulic heads were applied,
- Equivalent lateral flow through the sub-domain was achieved by specifying hydraulic head values, sourced from the regional-scale model, around the perimeter of the sub-domain model domain.

4.4.4 Sub-Domain Model Transport Boundary Conditions

Transport boundaries were added to the sub-domain model perimeter to allow inflowing water to enter with constituent concentrations consistent with background geochemistry (Figure 4-4). Inflowing water via groundwater recharge and lateral inflow within the Upper Sandstone were specified to have inflow concentrations consistent with the local groundwater flow system (Table 3.4). Water inflow to the Lower Sandstone Aquifer was specified to have concentrations consistent with that unit (Table 3.4).

As described in Section 4.2, restored water quality was specified within the ore zone and surrounding area (Section 4.1) using initial conditions. Similarly, a 50% strength restored water quality solution was specified as the initial concentration in the flare zone, overlying the mining horizon. Initial conditions throughout the remainder of the model were specified to represent interpreted background geochemistry, which were based on field-measured parameters (see Section 3.2 and Appendix D).

Transport parameters were specified for diffusion ($1x10^{-9}$ m^2/s), longitudinal dispersivity (10 m along the plume trajectory), and transverse dispersivity (5 m). A literature value was applied for diffusion as migration to Whitefish Lake is advection-dominated such that diffusion along the

flow path would not appreciably enhance transport timing. The longitudinal dispersivity value is consistent with the expected dispersivity within a sandstone unit for a plume of 0.9 to 1.7 km (Gelhar et al, 1992; Schulze-Makuch, 2005; Chapman et al., 2014; Martin, 2019). Alternative literature (e.g., Neuman, 1995) suggests an even larger value. Elements of transverse dispersivity (i.e., horizontal and vertical), which are typically differentiated due to anisotropic hydraulic conductivity settings, are uniformly applied for this site as a reflection of the interpreted isotropic conditions within desilicified hydrogeologic units.

Neither decay, nor matrix diffusion processes were simulated to produce conservative predictions of fate and transport; adsorption, ion exchange and precipitation reactions were simulated using PHREEQC (Parkhurst and Wissmeier, 2015), as discussed in Section 4.5.

4.4.5 Sub-Domain Model Calibration Check

Prior to applying the sub-domain model for geochemical reactive transport simulations, the model calibration was checked to ensure that it was consistent with that achieved in the regional-scale model. This calibration check provided confidence that the sub-domain model was able to represent the 3D groundwater flow system to an equivalent degree as the 3D regional-scale model. The calibration checks included comparison of both the calibration statistics, as well as the advective flow path and rates.

Observation wells from the 3D regional model were carried forward into the sub-domain model and used to confirm that a statistically equivalent local calibration was maintained (see table in Figure 4-4).

Flow paths and flow rates were checked by comparing particle track trajectory and timing to verify the representation of conditions simulated within the 3D regional-scale model were replicated in the sub-domain model. The simulated groundwater flow paths from the ore zone and flare within the sub-domain model (Figure 4-4) follow the same trajectory as those within the regional-scale model (Figure 2-16). Note that the image in Figure 4-4 contains a vertical exaggeration factor of 2, which exaggerates the horizontal to vertical transition in the flow paths. Figure 4-4 also contains a table summarizing the flow path lengths and advective travel times to Whitefish Lake from the flare and ore zones. Travel times within the sub-domain model are comparable to those simulated using the regional-scale model.

As noted in Figure 4-4, flow path lengths from the ore zone and flare to Whitefish Lake range from 900 to greater than 1700 m. Advective travel time was simulated to range from less than 400 to almost 1200 years, depending on the distance along the travel pathways, and the hydraulic conductivities experienced along each pathway. The average velocity of particles was simulated to range from 1.4 to 2.3 m/annum (i.e., m/a), reflecting the relatively slow groundwater flow rates through the groundwater system. The range of travel distances, timing, and velocities simulated using particle tracking indicate that significant spreading of COPCs transported from the mining horizon will naturally occur; this observation further supports the need for 3D analysis of geochemical reactive transport (i.e., plug flow conditions assumed for a 1D model are not able to represent the entire plume).

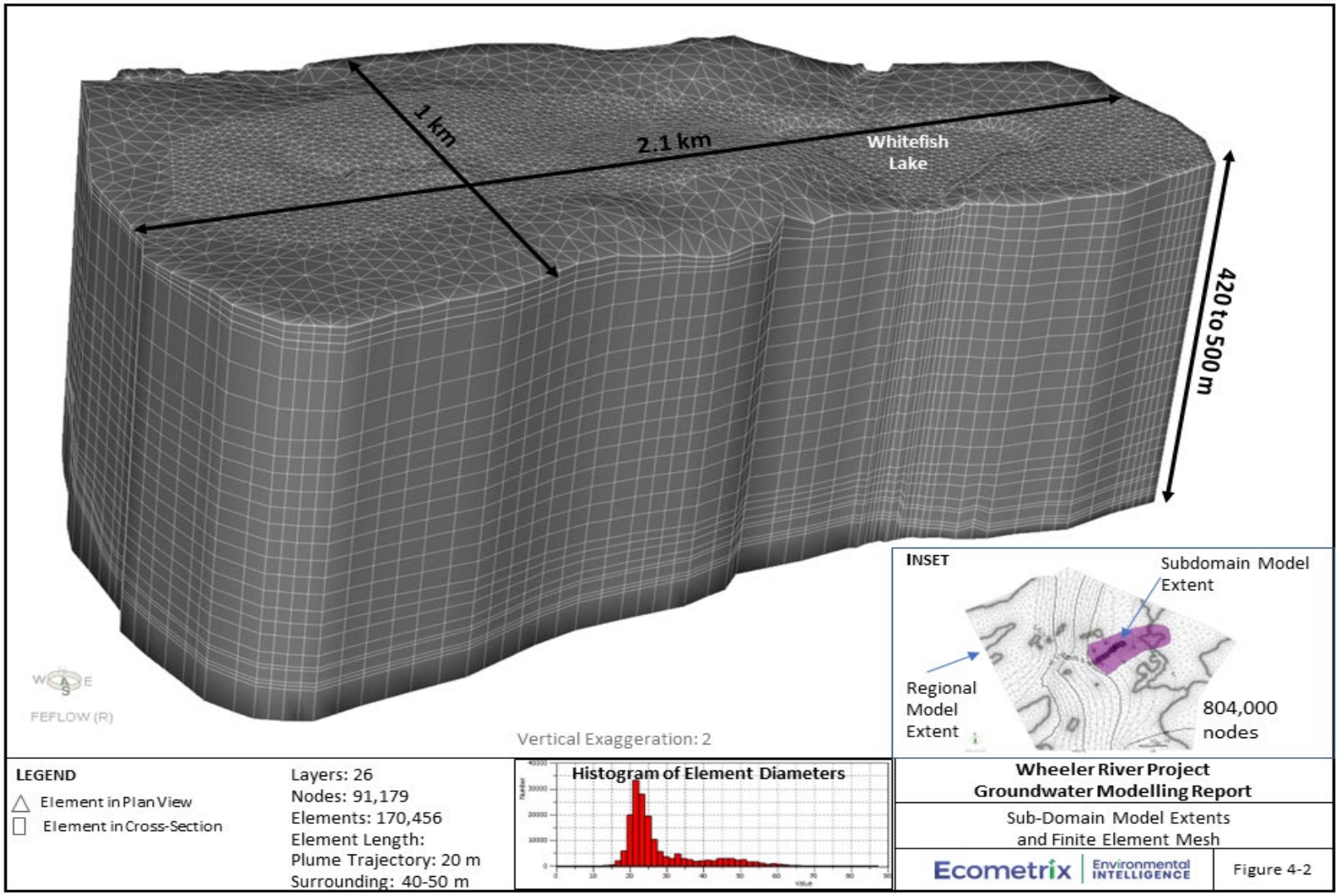

Figure 4-2: Sub-Domain Model Extents and Finite Element Mesh

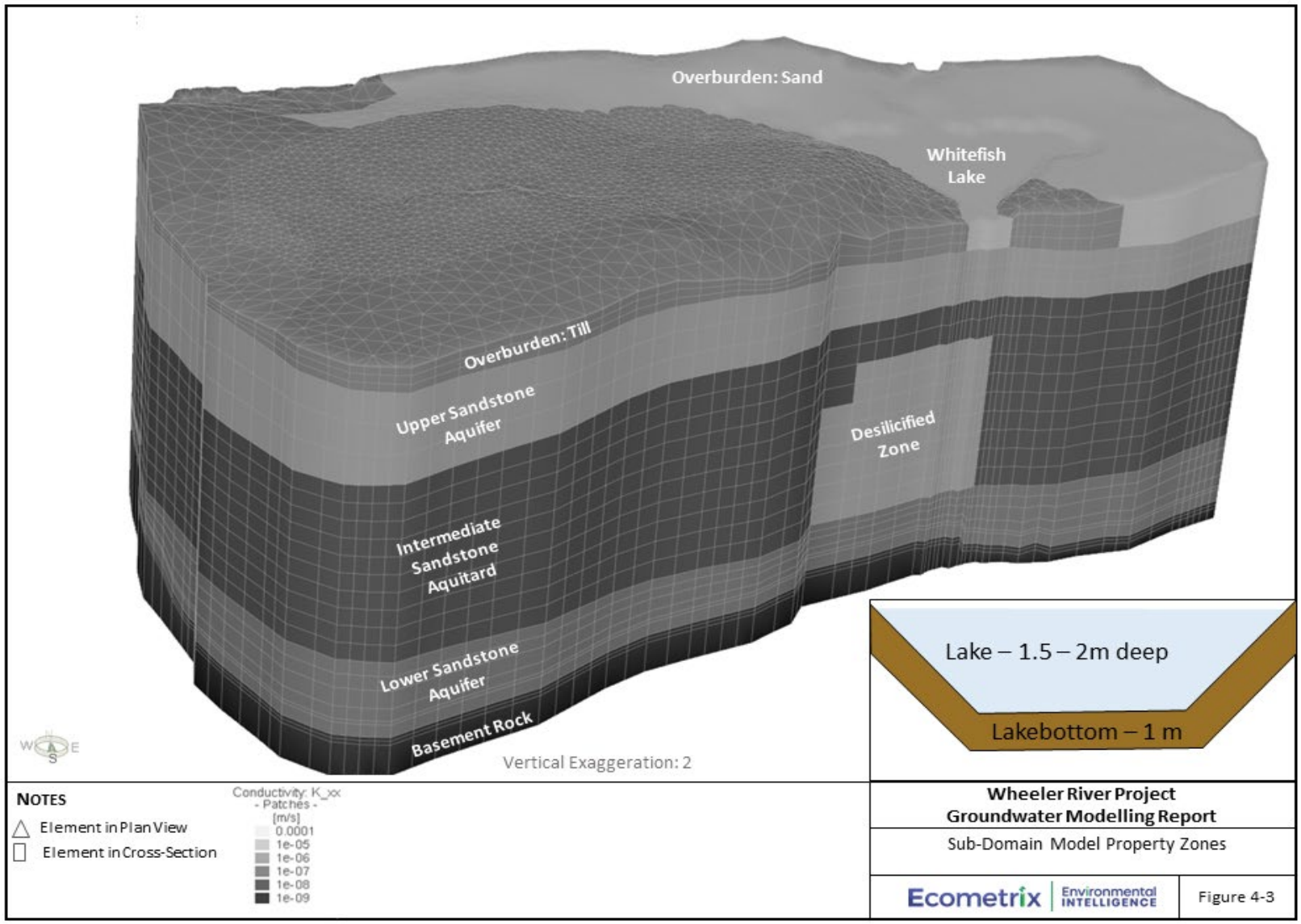

Figure 4-3: Sub-Domain Model Property Zones

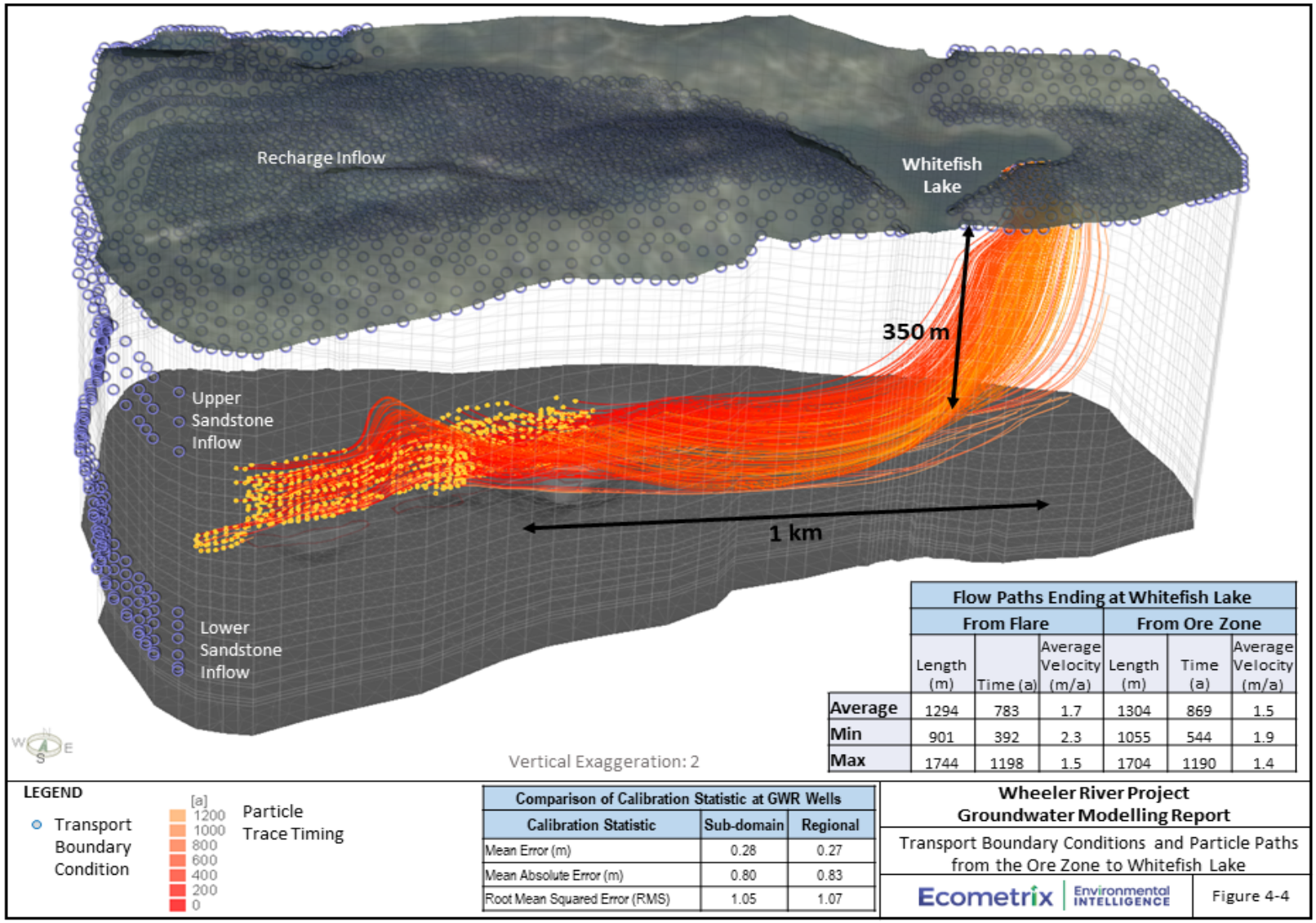

Flow Paths Ending at Whitefish Lake						
	From Flare			From Ore Zone		
	Length (m)	Time (a)	Average Velocity (m/a)	Length (m)	Time (a)	Average Velocity (m/a)
Average	1294	783	1.7	1304	869	1.5
Min	901	392	2.3	1055	544	1.9
Max	1744	1198	1.5	1704	1190	1.4

Comparison of Calibration Statistic at GWR Wells		
Calibration Statistic	Sub-domain	Regional
Mean Error (m)	0.28	0.27
Mean Absolute Error (m)	0.80	0.83
Root Mean Squared Error (RMS)	1.05	1.07

Wheeler River Project
Groundwater Modelling Report

Transport Boundary Conditions and Particle Paths from the Ore Zone to Whitefish Lake

Ecometrix Environmental INTELLIGENCE | Figure 4-4

Figure 4-4: Transport Boundary Conditions and Particle Paths from the Ore Zone to Whitefish Lake

4.5 3D Geochemical Reactive Transport Simulation: PiChem

Geochemical reactive transport modelling required integrating multi-component, time-varying flow and transport simulations using FEFLOW's simulator with the chemical processes that affect the migration of COPCs along the groundwater flow path. 3D geochemical reactive transport modelling was accomplished using the piChem "plug-in" option available with the FEFLOW software. PiChem (Wissmeier, 2016) facilitates the linkage of multi-component, time-varying flow and transport simulations using FEFLOW's simulator with geochemical reactions simulated using PHREEQC (Parkhurst and Wissmeier, 2015). FEFLOWs multi-component transport capabilities permit simultaneous simulation of multiple, interactive constituents. Reactive transport is simulated using an operator splitting technique, wherein solute transport and geochemical reactions are decoupled into sequential calculation steps.

The piChem reaction module takes multiple component concentrations from each model node, runs geochemical reactions using the capabilities of PHREEQC, and returns updated component concentrations to each node (Parkhurst and Wissmeier, 2015). The split operator technique is applied in piChem using a sequential, non-iterative, approach at every model timestep. The ion constituent composition is reconstructed from the transported element assembly and charge balanced before it is speciated with the available solid phases.

As described in Section 3.0, the PHREEQC model reactions were first evaluated and confirmed to be appropriate using the 1D model before implementing the simulations in 3D. To enable piChem, PHREEQC control files are required for each of the following:

1) Reaction database specifying the solution master species, appropriate stochiometric equations, exchange species, surface master species, etc.

2) Transport boundary conditions where inflowing water is simulated. Control files specify the constituents and dissolved background concentrations within the influent water.

3) Initial conditions / geochemical reactions / reactants for groups of elements within the model domain (IC files).

Independent transport boundary conditions were established for water entering the shallow units (Overburden and Upper Sandstone Aquifers), and deep units (Lower Sandstone Aquifer). The water type entering the Upper Sandstone Aquifer through lateral inflow is interpreted to be of similar quality as water recharging the overburden units, as the overburden units are derived from the underlying sandstones (see Figure 4-4 for locations of boundary conditions where inflow concentrations are specified).

To represent the geochemical heterogeneity throughout the 3D model domain, independent initial condition (IC) files were generated for each of the node groups listed in Table 4-2. These zones conform to hydraulic conductivity and effective porosity zones defined in the model and utilized during model calibration. Independent initial conditions and reactions were designed to replicate the variability observed in field samples; reactions were adjusted from one zone to

another based on understanding of geochemical conditions (e.g., redox conditions and sorption potential).

A forced gradient tracer test undertaken by Petrotek (2022) which was designed to evaluate the degree of capture that could be achieved using injection and extraction wells oriented in a star pattern within a relatively small (i.e., 5 to 10 m radius surrounding GWR-040) portion of the ore zone. The tracer test was performed after permeability enhancement efforts (e.g., MaxPerf, Gas Gun and Kraken tools) which are designed to enhance the effective porosity beyond the natural state. Effective porosity values were derived from the peak arrival time of the injected potassium chlorate solution at extraction wells, utilizing the recorded distance and hydraulic conductivity values estimated from pumping tests performed after permeability enhancement efforts. Effective porosity values ranged from 1% (GWR-038) to 7% (GWR-041). The lower value (i.e., 1%) supports the effective porosity assigned within the deep sandstone units (e.g., Lower Sandstone Aquifer) as it is interpreted to reflect areas where permeability enhancement was unsuccessful. The higher value (i.e., 7%) provides a lower bound on the effective porosity for the ore zone post-mining; higher values are expected within the ore zone post-mining which will result in increased travel times.

Table 4-2: Geochemical Zones in 3D Reactive Transport Model

Node Group	Porosity	Description
Lake Bottom Sediments	0.25	Silt/clay rich sediments, which promote adsorption
Overburden	0.18	Lower porosity zone representing sand-till regions.
	0.22	Moderate porosity zone representing transition between sand-till and sand-rich regions.
	0.25	High porosity zone representing sandy regions.
Upper Sandstone Aquifer	0.02	Fractured Sandstone
Lower and Intermediate Sandstone outside of the Desilicified Zone	0.01	Fractured Sandstone
Desilicified Zone (Lower and intermediate sandstone)	0.20	Loose sand with minor clay and mineral content.
Ore Zone and Immediate Surroundings (to 15 m above the Ore Zone)	0.20	Contains restored solution at full strength initially. After initial time, solution disperses, diffuses, and reacts throughout the simulation. Porosity reflects post-decommissioning conditions.
Flare above ore zone (to 50 m above the ore zone)	0.20	Contains restored solution at 50% strength. After initial time, solution disperses, diffuses, and reacts throughout the simulation. Porosity reflects post-decommissioning conditions.
Paleoweathered Basement Aquitard	0.10	Fractured basement rock with higher mineral content. Total porosity specified to simulate matrix diffusion effects.

While the variable initial conditions files allowed for specification of heterogeneous geochemical parameter and reaction zones throughout the model domain, differences in these specified

conditions lead to initial disequilibrium where differing initial condition zones meet (e.g., boundary between the Upper Sandstone and Desilicified Zone, or at the margins of the restored solution source zone). Such differences led to some numerical instability at early time (e.g., the first 10-years of simulation), which reduced as the simulation progressed and spatial transitions were smoothed.

4.6 3D Sub-Domain Model: Base Case Scenario Predictions

The base case scenario within the 3D sub-domain model incorporated the following features:

- Restored mining horizon with a pH of 4.1, and enhanced concentration of dissolved minerals that reflect the post-decommissioning, restored-groundwater conditions (Section 3.3). As noted above, the restored solution extended laterally to the freeze walls, to 15 m above the ore zone, and below the ore zone to the base of the Paleoweathered Basement Aquitard.

- Flare zone that extended from 15 to 50 m above the ore zone. The flare zone is conservatively estimated to have enhanced dissolved mineral contents at 50% of the restored mining horizon. As noted above, the extension to 50 m above the ore zone is considered conservative as testing and analysis to date suggests this flare zone will be limited to 11 to 13 m.

- Paleoweathered Basement Aquitard with high mineral and clay content to promote adsorption, and a relatively high effective porosity that reflects matrix diffusion processes.

- Desilicified Zone with a relatively low mineral content, and modest clay content (moderate adsorption potential).

- Remaining sandstone units (Lower Sandstone Aquifer, Upper Sandstone Aquifer, and Intermediate Sandstone Aquitard) with low porosity and moderate adsorption potential.

- Overburden sands with relatively high porosity but moderate adsorption potential.

- Lake bottom sediments (estimated as 1 m thick) with high porosity, higher silt and clay content, and a higher adsorption potential.

4.6.1 Advective Transport of Dissolved Constituents

Figure 4-4 illustrates particle tracking (advective transport without dispersion, adsorption, or any other reactions) from the ore zone and overlying flare (i.e., the source) to Whitefish Lake. As illustrated, the general groundwater flow path extends horizontally through the Lower Sandstone Aquifer from the source for approximately 1 km before migrating vertically upward through the Desilicified Zone toward Whitefish Lake (note that the image in Figure 4-4 contains a vertical exaggeration factor of 2, which exaggerates the horizontal to vertical transition in the flow paths). Upward migration through the Desilicified Zone is the dominant flow path due to its higher hydraulic conductivity relative to the non-desilicified Intermediate Sandstone

Aquitard. Path lengths and travel times from the ore zone and flare to Whitefish Lake are documented on Figure 4-4, indicating a minimum path length of 900 m and a minimum travel time of just under 400 years; this path length and timing represents particles emanating from the eastern edge of the source. Maximum travel times can reach 1,200 years, and a length of 1,700 m (almost double the shortest paths) for particles that migrate from the western-most portion of the ore zone and flare, and/ or for particles that travel through lower hydraulic conductivity zones. Average linear groundwater velocities calculated for minimum and maximum path lengths, range from 1.4 to 2.3 m/annum, respectively.

This broad spread of particle travel times, travel lengths, and average groundwater velocities indicates that the restored solution transport post-decommissioning:

- Timing: will take centuries to reach Whitefish Lake.
- Duration: will continue seep into Whitefish Lake over many centuries.
- Change: will cause a gradual change from background conditions over a long time-period.

4.6.2 Advection and Dispersion of Dissolved Constituents

To better understand fate and transport conditions occurring along these path lines, mass transport conditions were simulated. While all simulations are completed in 3D, for ease of interpretation, transport results on figures within this and subsequent report sections are illustrated along a vertical cross-section that transects the model domain from west to east. The cross-section bends to extend through the ore zone and follow the trajectory of the flow paths from the ore zone to Whitefish Lake (Figure 4-5).

As an example of transport patterns, conditions for a chemically conservative or non-reactive constituent, chloride, are presented. Figure 4-6 illustrates a time-series of plume snapshots from 50 to 800 years post-decommissioning. This figure illustrates that as the dissolved constituents migrate toward Whitefish Lake through the Desilicified Zone, the concentration decreases. The result is that the concentration reaching Whitefish Lake is less than 10 mg/L, whereas the concentration in the initial restored solution (Table 3-5) is 200 mg/L. The reduction in concentration along the flow path for this non-reactive constituent is caused by hydrodynamic dispersion (i.e., dispersion due to mechanical mixing, and diffusion due to concentration gradients). Dissolved chloride is transported along with groundwater along the flow paths illustrated in Figure 4-4; however, hydrodynamic dispersion tends to spread the concentrations throughout the advective migration period. Hydrodynamic dispersion results from both concentration gradients (transport from areas of higher to lower concentrations) and mechanical mixing as the water travels through the tortuous pathways along interconnected fractures (fractured sandstone and basement rocks), or through variably-sized pore spaces between soil grains (i.e., within the Desilicified Zone and overburden). Note that the high concentrations persist within the Paleoweathered Basement Aquitard for much longer than within the Lower Sandstone Aquifer due to the relatively low hydraulic conductivity ($5x10^{-9}$ m/s) simulated within

the Paleoweathered Basement. As noted earlier, this low hydraulic conductivity is supported by both site-specific testing as well as the geochemical nature of the water found within this unit.

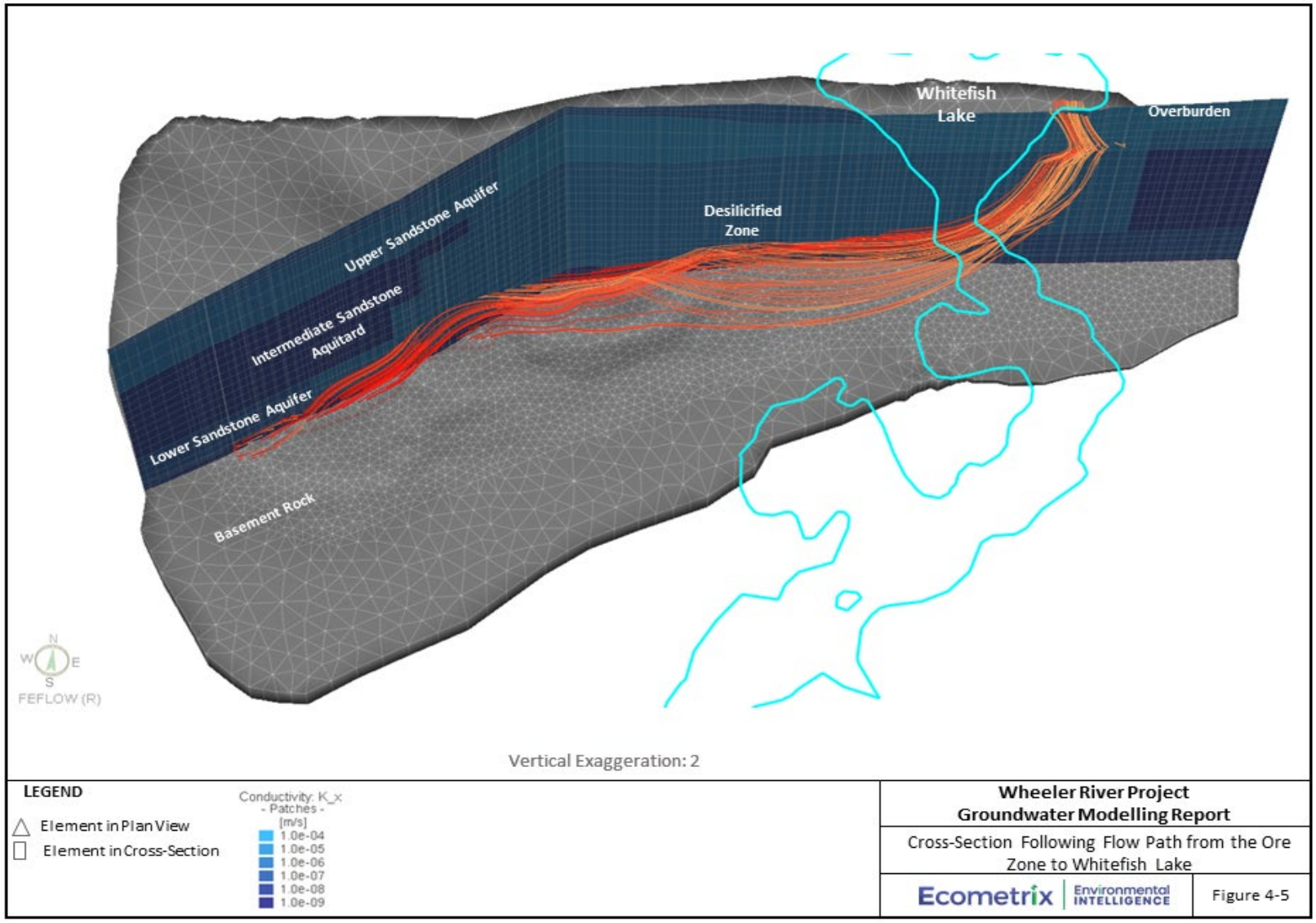

Figure 4-5: Cross-Section Following Flow Path from the Ore Zone to Whitefish Lake

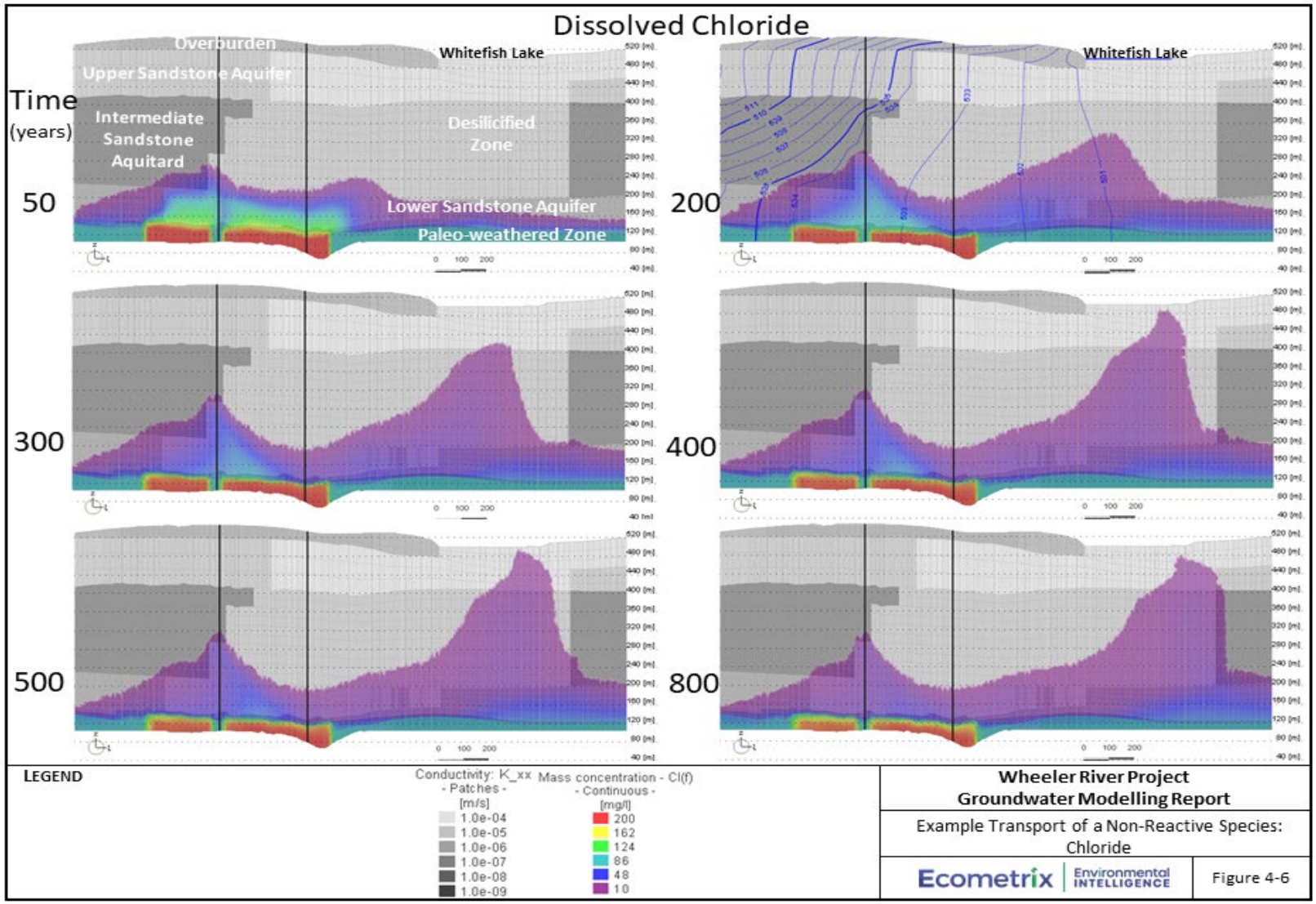

Figure 4-6: Example Transport of a Non-Reactive Species: Chloride

4.6.3 Advection, Dispersion, and Geochemical Reactions

There are several types of chemical reactions that can affect the concentrations of COPCs along the groundwater flow path. Chemical reactions that can act to retard the velocity of groundwater plumes relative to the average linear velocity of groundwater (i.e., advection) and/or attenuate COPC concentrations in groundwater include precipitation as a mineral phase, sorption, and redox transformation (and subsequent precipitation and/or sorption). Other processes, like radioactive decay and ingrowth can affect concentrations of radiological constituents along the groundwater flow path but were not included in the simulations.

Many of the geochemical constituents simulated as part of the restored solution (Table 3-5) experience geochemical reactions along the travel pathway in addition to advection and dispersion. Geochemical reactions have the effect of reducing the mass of a constituent within the dissolved phase and distributing a portion of that mass onto sorbed or solid phases. Sorbed or solid phases of the constituent becomes immobile until conditions change, and desorption or re-dissolution occur. When concentrations within the dissolved phase significantly reduce, desorption or re-dissolution can occur, re-mobilizing the sorbed mass. The rate of sorption and desorption depends upon the affinity of the constituent to be in solution verses sorbed in the conditions being simulated at a point in space and time within the sub-surface. The ratio of sorbed to dissolved mass depends on the overall composition of the water, including the ionic strength, pH, redox conditions, competing ions, ligands in solution, and the availability of sorption sites.

At all times, an equilibrium between the dissolved mass and the sorbed mass was maintained. The slow advection rate facilitates ample time for water-rock interactions to occur. The availability of sorption sites was calculated from mineral analyses completed for extracted core samples, as described in Section 3.5.6.2. Sorption was simulated to occur to clay, quartz, and goethite minerals. The percentage of available sorption sites were varied in the simulations to reflect the potential that in situ mineral surface conditions (i.e., number of reactive sites; particle size, available surface area) may differ from those assumed from available literature sources.

As an example of the effect of sorption reactions taking place throughout the simulation, Figure 4-7a and 4.7b illustrate the transport of dissolved selenium (left column) and its partitioning onto clay minerals contained within the host rock (right column). The image sequence illustrates the changes in dissolved and sorbed concentration distribution over time as the dissolved phase migrates from the source location. At early time (i.e., 50-years post-decommissioning), the mineral phase initially forms at the up- and down-gradient edges of the source zone (see Figure 4-1 for location). As the dissolved plume migrates into areas where there are additional available sorption sites (note: only sorption to clay minerals is shown in Figure 4-7a) mass in solution is sorbed onto the sorption site, reducing the concentrations in the dissolved phase. This slows the velocity of the dissolved plume relative to the average linear groundwater velocity (i.e., advection); this process is referred to as plume retardation. As time progresses, in areas where the concentration within the dissolved phase decreases, the mass of selenium sorbed onto the clay surfaces is reduced as it desorbs back into solution. Selenium shows a low affinity for the

solid phase and thus migration to Whitefish Lake is retarded to a limited extent in comparison to chloride, which is a conservative constituent.

In addition to the sorption of mass and retardation of the dissolved plume, dispersion processes around the perimeter of the dissolved plume reduce the concentrations below the plotted threshold; in this case, the threshold illustrated is the groundwater evaluation criterion for selenium. The combination of sorption and dispersion processes act to limit the plume migration distance from the source. This concept is known as reaching a steady-state plume (Cherry, personal conversation) which is a term used to illustrate that the limits of a plume, at a concentration above a threshold, will not migrate as far as the associated groundwater. As noted with chloride, the plume source persists within the paleoweathered Basement Aquitard due to the low hydraulic conductivity of that unit.

Figures 4-8a and 4-8b illustrate similar trends in the dissolved and sorbed mass for cadmium, but over a much longer period of time (50,000 years) than for selenium (2,500 years). Similar to that observed with selenium, dispersion and sorption processes act to restrict the migration of dissolved cadmium, at concentrations above the groundwater quality screening criteria (GQSC). Most of the dissolved constituents experience similar transport conditions that act to limit the migration toward Whitefish Lake.

4.6.3.1 Uranium Fate and Transport

Figures 4-9a and 4.9b illustrate the dissolved and sorbed uranium mass over a 50,000-year time-period. Uranium is very strongly sorbed to the mineral phases present within the Athabasca Supergroup sandstone units and underlying paleoweathered bedrock. Because of this, migration is very strongly retarded and uranium in the dissolved phase is not predicted to reach Whitefish Lake in 50,000 years or beyond. Like cadmium, the distance that the uranium plume (i.e., concentrations above the GQSC) migrates is limited by the sorption reactions and dispersion. The uranium plume is simulated to grow modestly over the first 5,000 years of the simulation, but then start to retract (i.e., shrink) for later times as the source concentrations are depleted. Depletion of the source concentration occurs as background water carrying lower constituent concentrations flows through the source area. Concentrations above the GQSC remain longest within the paleoweathered zone due to the lower hydraulic conductivity of, and the lower flow rates through, that unit.

Figure 4-10 illustrates the distribution of uranium mass within the model between the dissolved and various sorbed phases (i.e., sorbed to clay, goethite, quartz, and lake-bottom sediments). As illustrated, the dissolved uranium is simulated to decrease as time progresses. Dissolved mass is transferred to available sorption sites on clay, quartz, and goethite minerals; mass sorbed to clay is approximately one order of magnitude greater than that sorbed to quartz or goethite. The mass adsorbed to clay is the dominant form and is the majority of all uranium mass in the model (i.e., total uranium mass).

Figure 4-11 illustrates the 3D extent of uranium plume 5,000 years post-decommissioning. The plume iso-surface illustrated is for the GQSC of 0.015 mg/L. These figures illustrate that the

uranium mass above the GQSC is simulated to remain at depth in the area surrounding, and down-gradient of the ore zone. Lateral spreading is predicted to be limited as well due to the relatively low groundwater velocities.

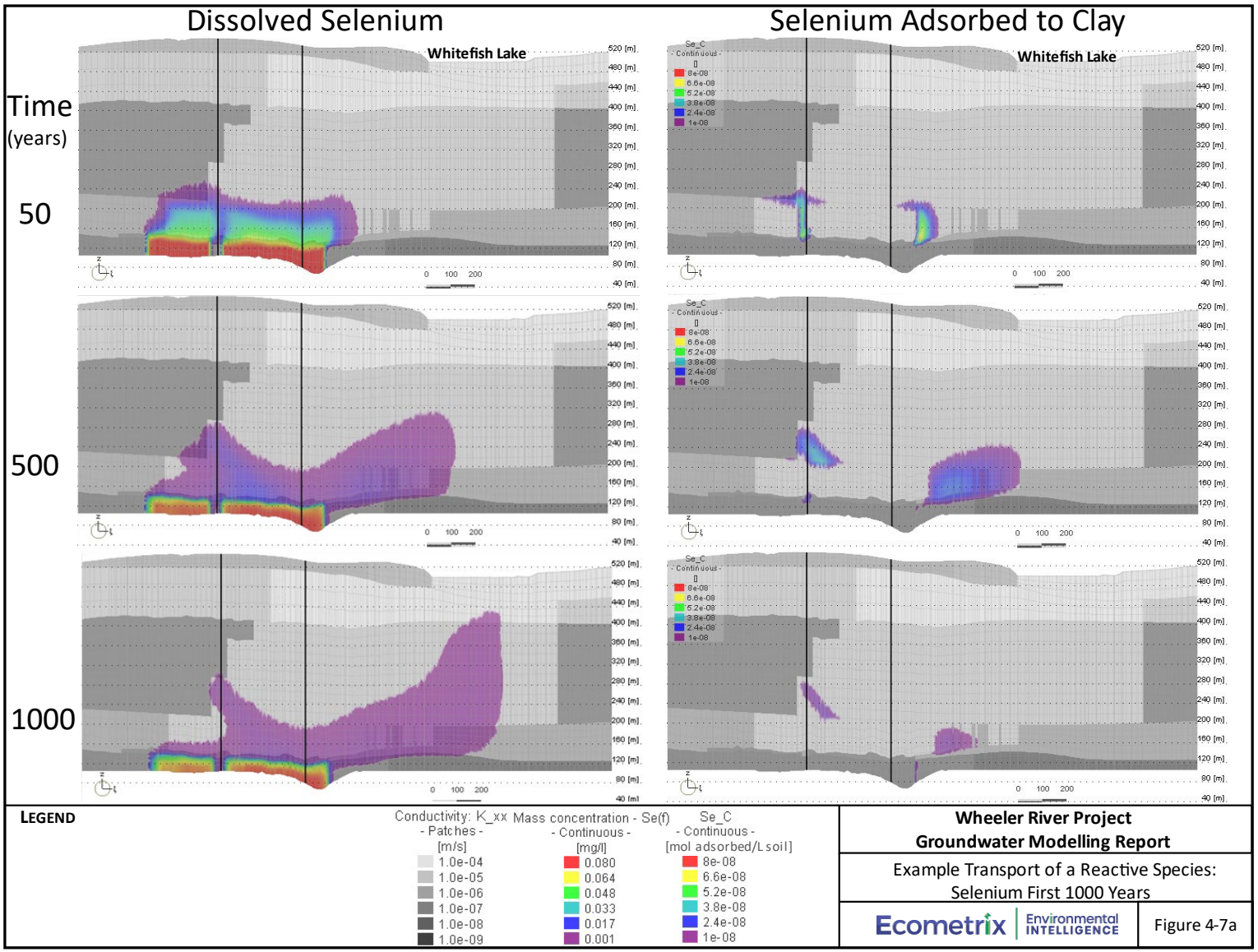

Figure 4-7a: Example Transport of a Reactive Species: Selenium First 1000 Years

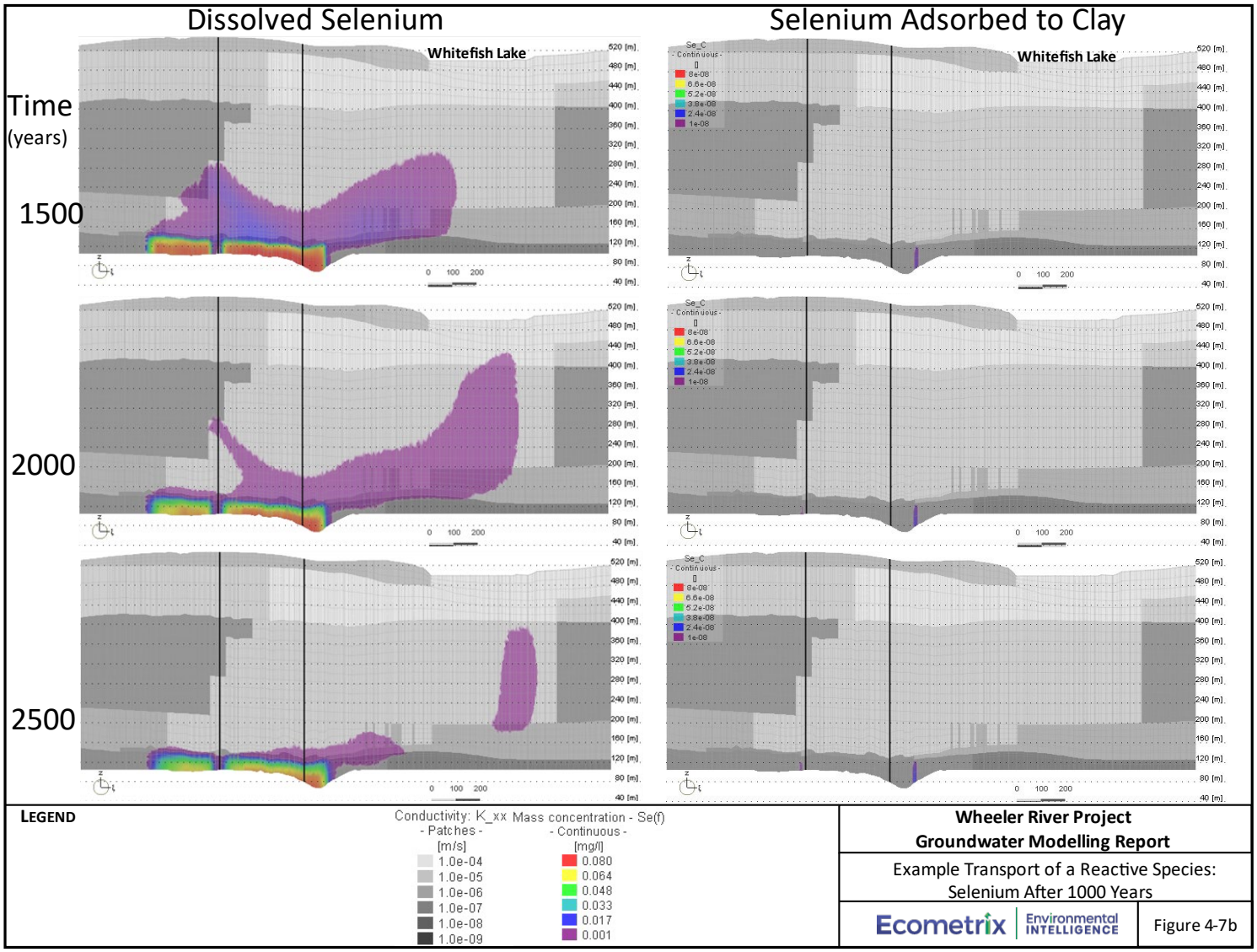

Figure 4-7b: Example Transport of a Reactive Species: Selenium After 1000 Years

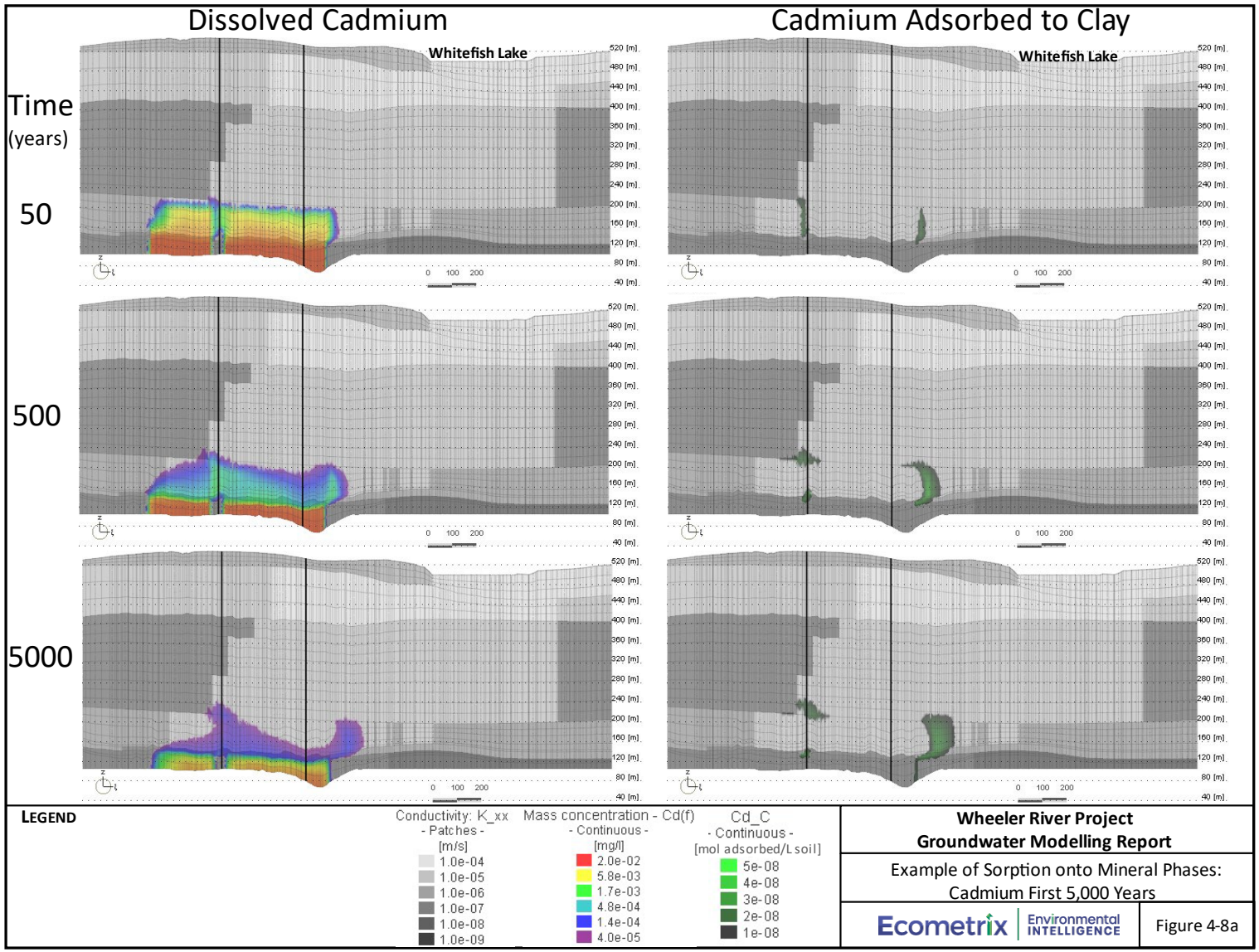

Figure 4-8a: Example of Sorption onto Mineral Phases: Cadmium First 5,000 Years

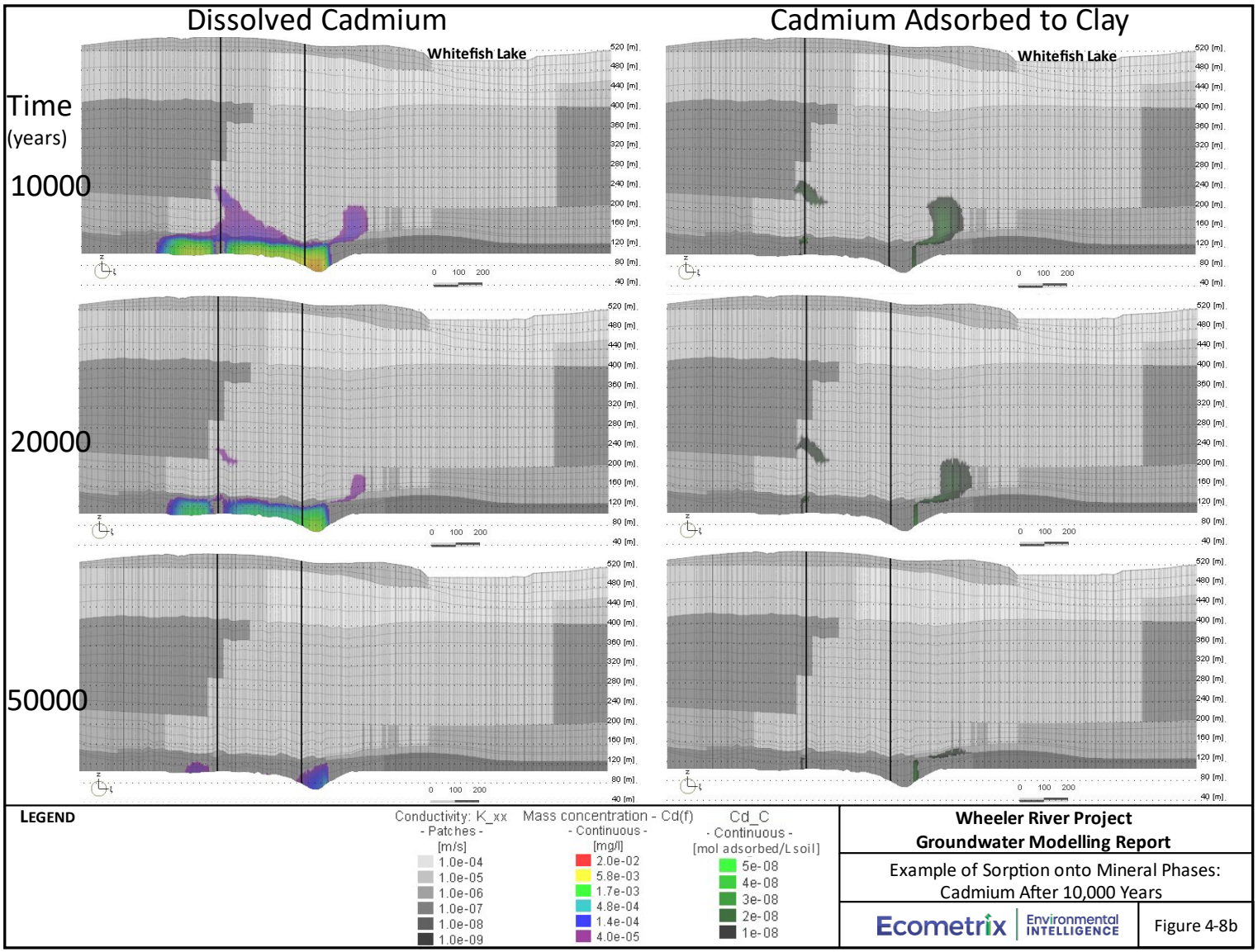

Figure 4-8b: Example of Sorption onto Mineral Phases: Cadmium After 10,000 Years

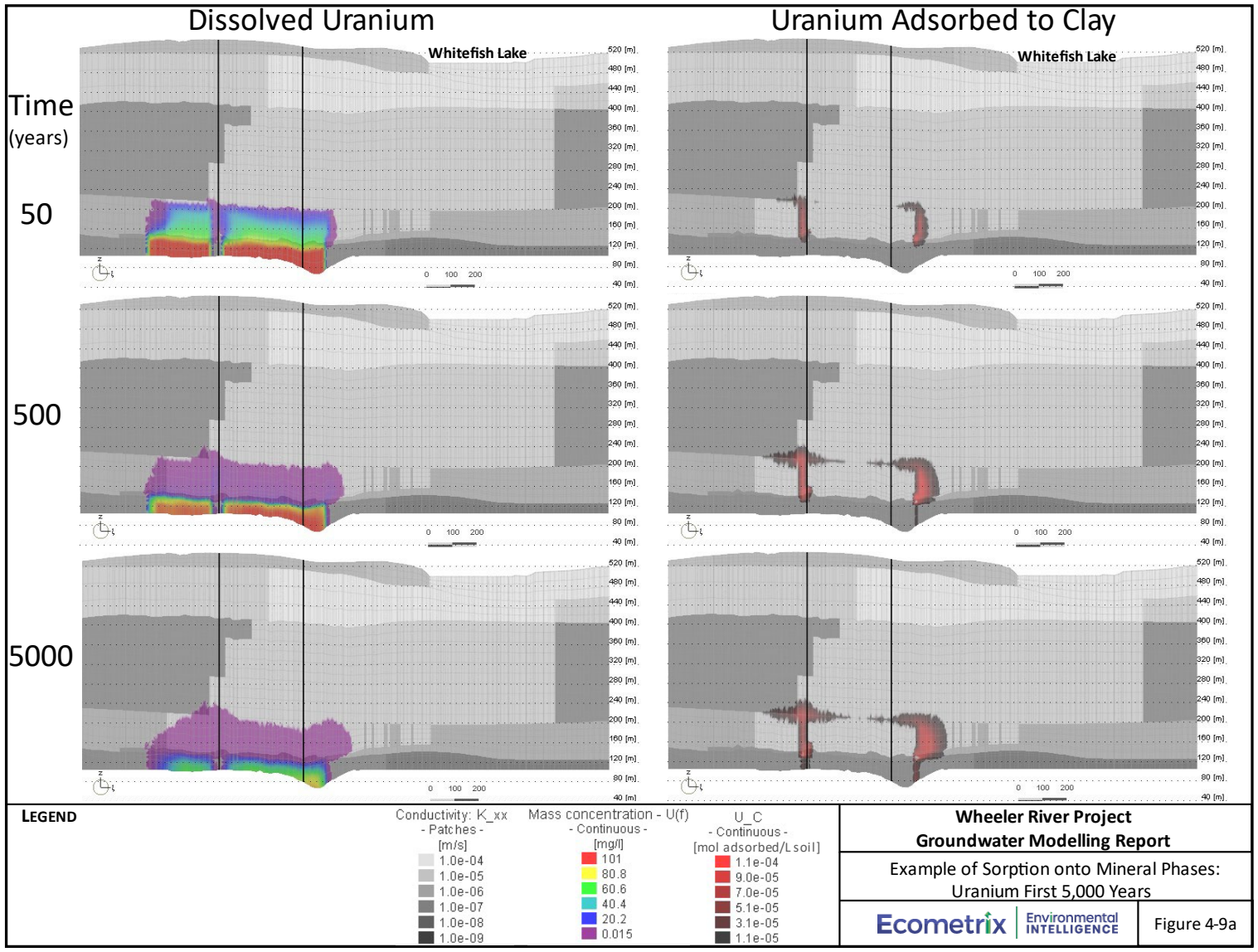

Figure 4-9a: Example of Sorption onto Mineral Phases: Uranium First 5,000 Years

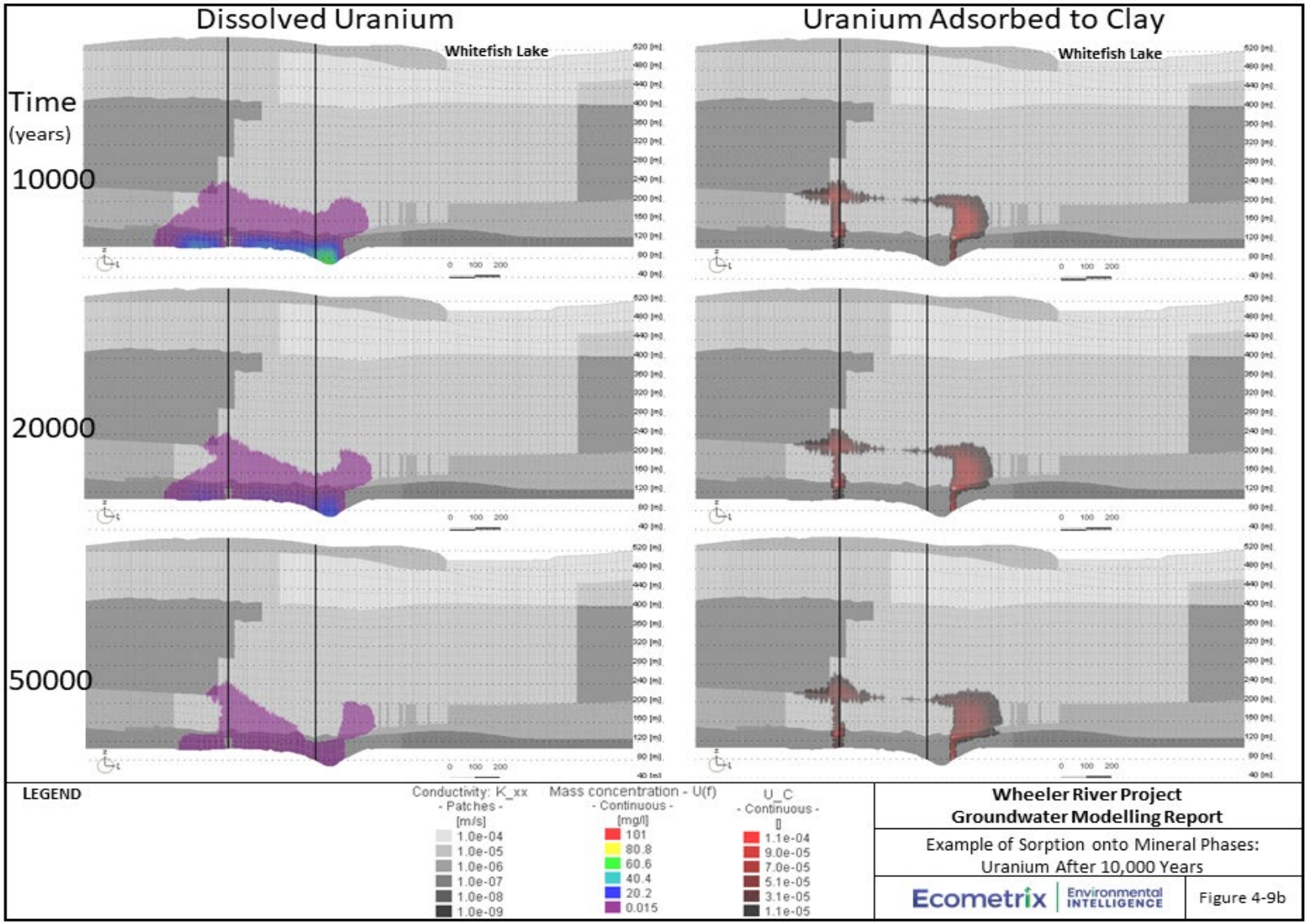

Figure 4-9b: Example of Sorption onto Mineral Phases: Uranium First 10,000 Years

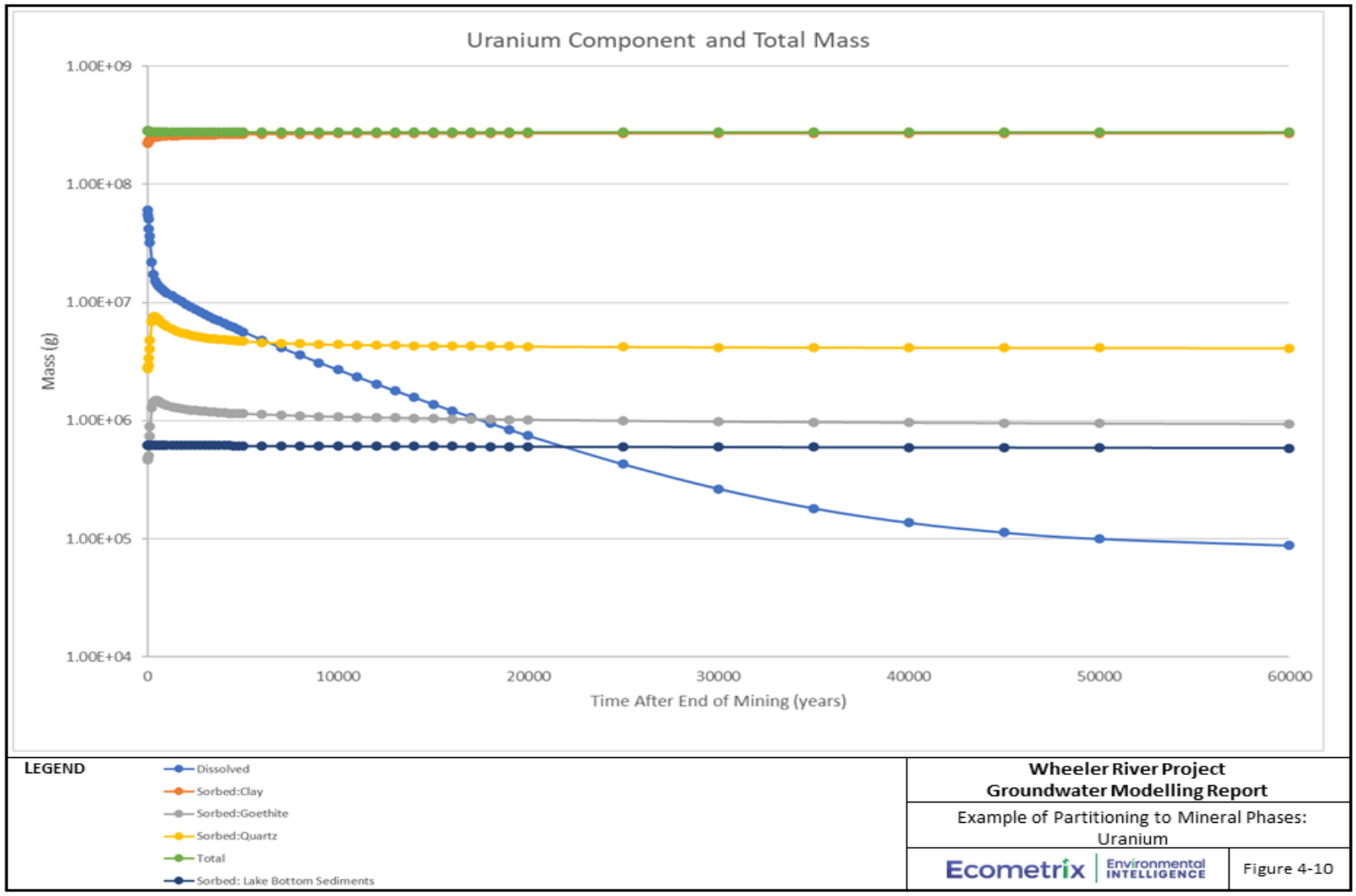

Figure 4-10: Example of Partitioning to Mineral Phases: Uranium

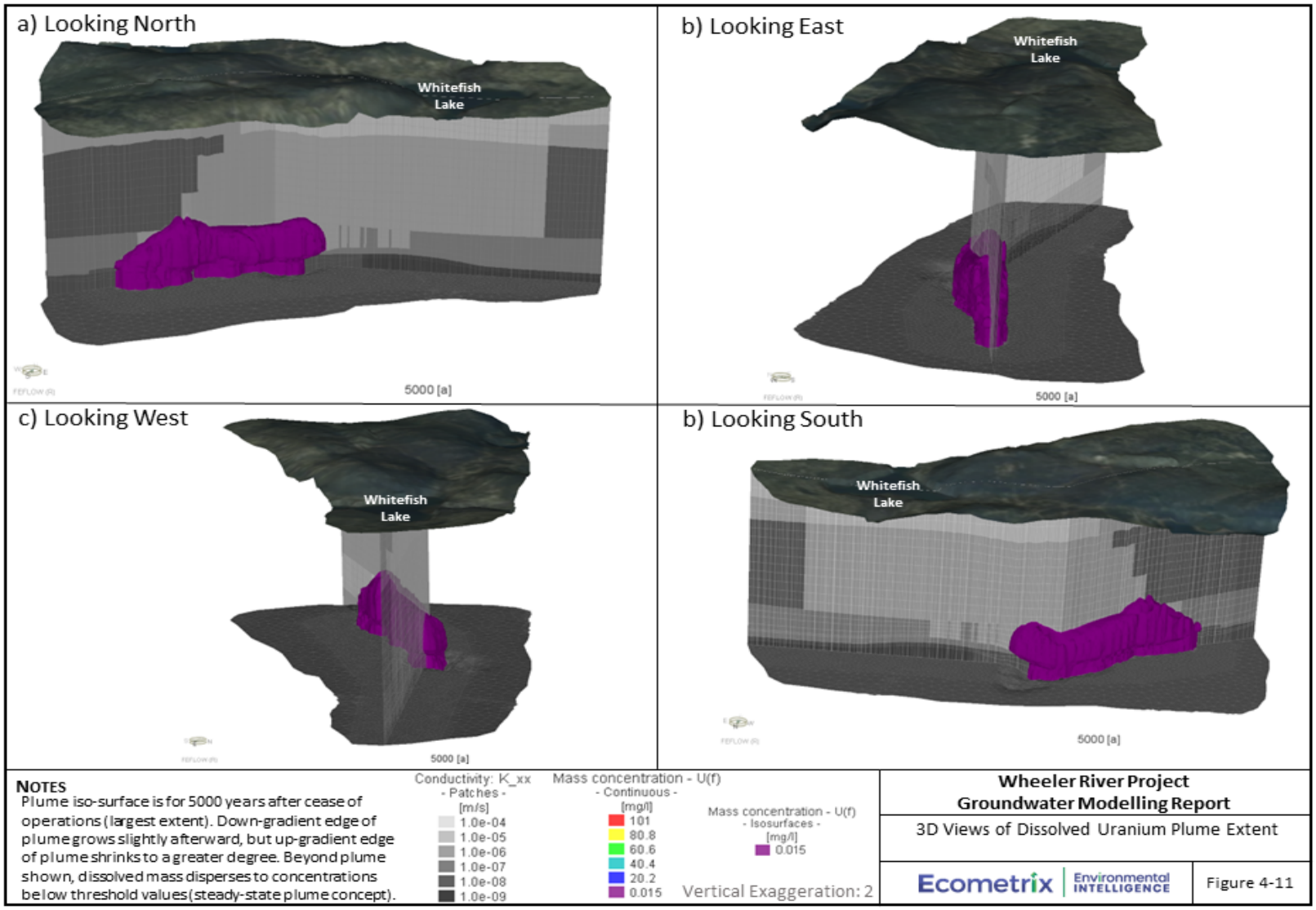

Figure 4-11: 3D Views of Dissolved Uranium Plume Extent

4.6.4 Matrix Diffusion

An additional process that is expected to occur in the natural system, but is not simulated in the results presented, is matrix diffusion. Matrix diffusion is expected to occur within the fractured rock portions of the sub-surface and will act to further retard the migration of dissolved-phase constituents. It is interpreted to be most prevalent within the Paleoweathered Basement Aquitard, but it can also likely occur within fractured media surrounding and within the ore zone. Without matrix diffusion, which is a physical process, the model is conservatively overpredicting the migration of all constituents.

4.6.5 Constituents Reaching Whitefish Lake

The groundwater model simulates the potential flow of groundwater and transport of constituents toward multiple downstream surface water bodies, including Whitefish Lake, McGowan Lake, LA-2, and Russell Lake. Whitefish Lake was found to be the most likely receiving water body based on proximity to the Phoenix ore zone, and observed water level data, and model simulation results further support that Whitefish Lake is the primary receiving water body. Other receptors located further away, including Russell Lake, are predicted to experience no measurable effects as a result of their increased distance from the Phoenix site, and additional dispersion that would occur along the potential transport pathways. Consequently, the groundwater quality reaching the base of Whitefish Lake is the focus of the discussion in the following sections. Figures 4-12 and 4-13 illustrate results from the base simulation.

Figure 4-12 illustrates concentrations of select COPCs reaching Whitefish Lake over the first 2,000 years post-decommissioning (i.e., future centuries). Primary and secondary vertical axes are used to plot constituents with higher and smaller mass flux on the same figure. Note that COPCs and other constituents that did not have a measurable change in concentration throughout the first 2000 years of the simulation are not included in this figure. As shown on Figure 4-12, concentrations for contaminants of potential concern are simulated to not vary appreciably from initial, baseline, conditions; changes are gradual and will result in an evolution of the groundwater quality reaching Whitefish Lake. Of note are the elongated peaks for vanadium and selenium; these peaks are stretched due to storage of mass within the lake bottom sediments.

The maximum concentrations for COPCs, over the entire 60,000-year period simulated, are also presented in Table 4-2. The constituent concentrations are for groundwater seeping into the base of the lake and do not reflect the mixing that will occur within the lake. Beyond these groundwater simulations, environmental effects within Whitefish Lake were also assessed, as described in Section 4.9. All constituents, with exception of iron (Fe), manganese (Mn) and pH, were simulated to have concentrations that remain below the GQSC throughout the period of simulation (60,000 years post-decommissioning). Both iron and manganese are naturally observed to have elevated concentrations in groundwater, with background iron concentrations observed to be above the GQSC (See Table 3-4). The simulated pH is very marginally below the lower value of the GQSC (pH 6.5), and all simulated pH values were within the range of natural groundwater pH values in the Local Groundwater System (overburden and Upper Sandstone

Aquifer). Background conditions are also discussed in detail in the Baseline Report (Ecometrix, 2024a).

As evident on Figure 4-12 (and documented on Table 4-3), more conservative constituents (chloride, iron, sulphate) are simulated to reach their peak concentrations in groundwater at the lake in approximately 400-years; this is consistent with the early arrival particle traces illustrated on Figure 4-4. Other constituents that react to a greater degree with the mineral surfaces (e.g., selenium) reach their peak concentrations much later, and highly reactive constituents (e.g., arsenic, uranium) reach their peak concentration after tens-of-thousands of years, or never reach the Lake at noticeable concentration levels. Conservative transport was experienced for strontium (Sr), chloride (Cl), iron III (Fe), sulphate ($S0_4$), and vanadium (V) with peak concentrations occurring within 400-500 years. Other constituents experienced very little change during the first 2000-years of post-decommissioning (e.g., uranium, cobalt, cadmium, Thorium-230 and Radium-226); these are interpreted to remain at background concentrations throughout this period. Minor fluctuations in all concentrations were simulated at early time (e.g., less than 100 years) as the model approached a continuous, smooth equilibrium from the piece-wise constant node groups used to apply initial concentrations.

Table 4-3 documents the mass flux of constituents reaching Whitefish Lake, while Figure 4-13 illustrates this mass flux over the first 2000 years (i.e., future centuries). This evaluation of mass flux over time provides an indication of how much conditions will change within Whitefish Lake over the future centuries period post-decommissioning. Primary and secondary vertical axes are used to plot constituents with higher and smaller mass flux on the same figure. As Figure 4-13 illustrates, the simulated change in mass flux for all constituents is relatively small. Sulphate is shown to experience the largest change in mass flux (14%), however most of the constituent's experience less than 5% change in mass flux. The predictions of mass flux to Whitefish Lake, summarized in Table 4-4, are further used within a subsequent effects assessment (Section 4.9), to understand the implication of changes in COPC mass flux to Whitefish Lake.

The 60,000-year simulation time was chosen because by that time the source concentration for uranium is reduced to 1/100th the initial conditions, and as such, the potential for a plume from the source is all but eliminated as conditions have returned to background.

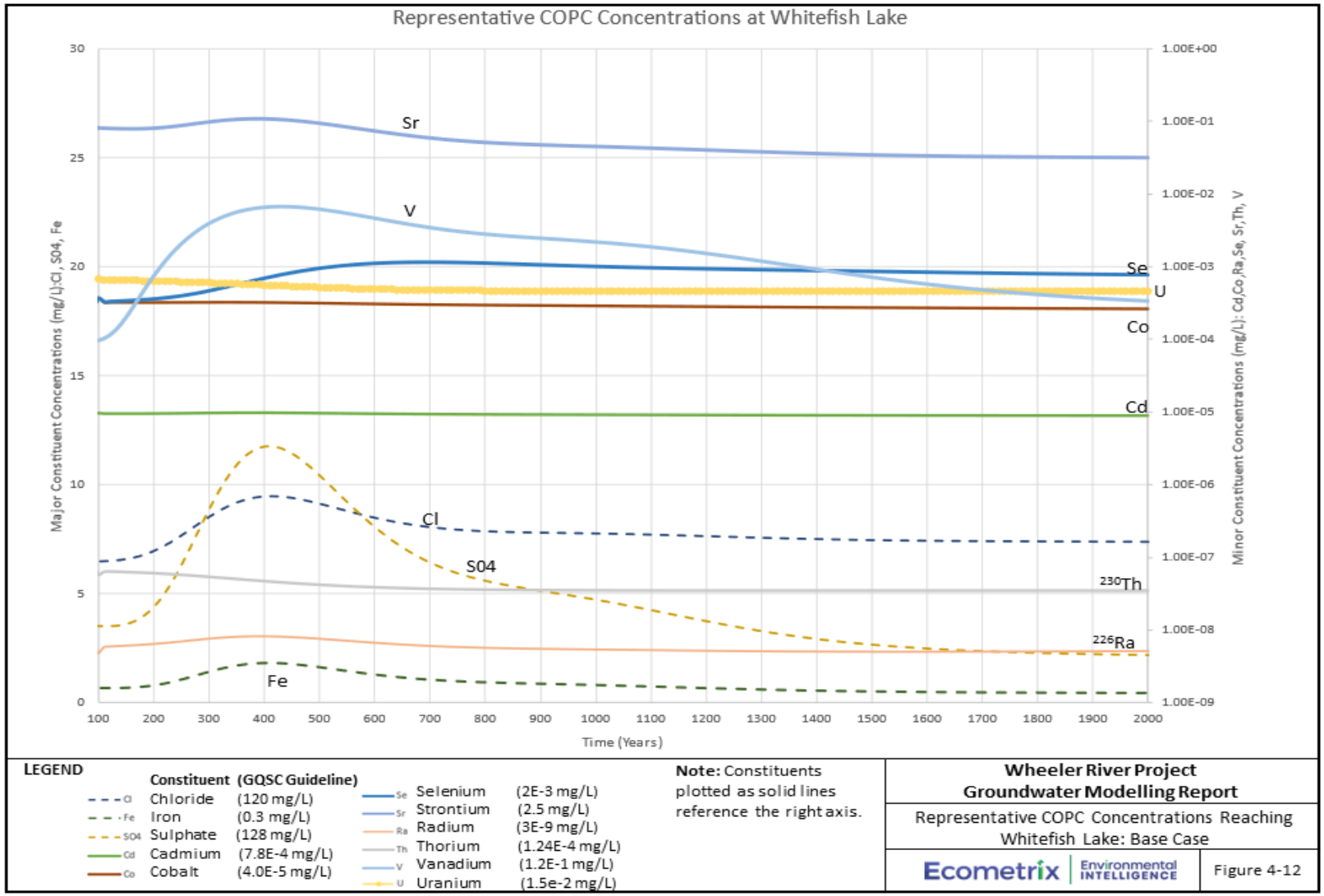

Figure 4-12: Representative COPC Concentrations Reaching Whitefish Lake: Base Case

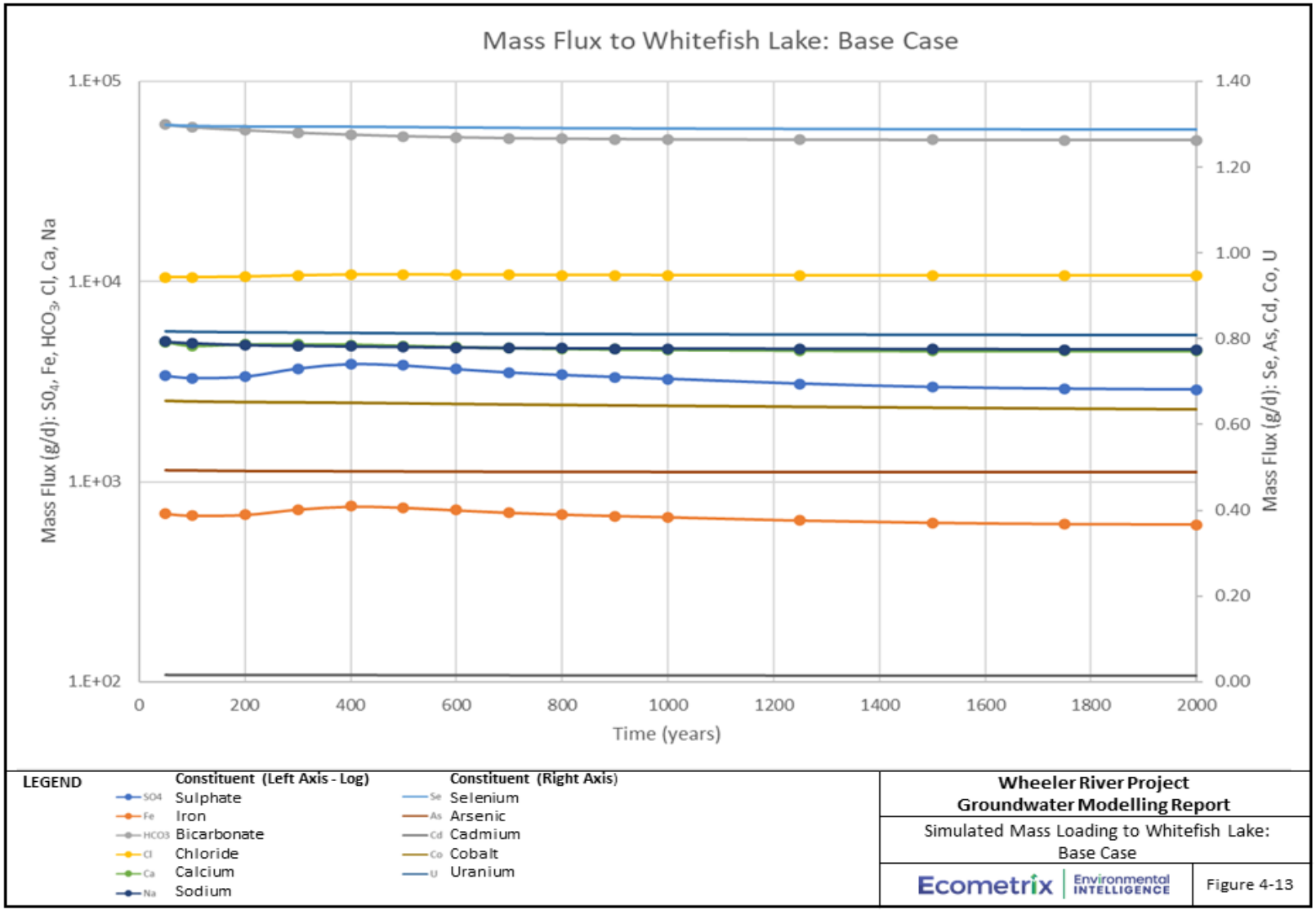

Figure 4-13: Simulated Mass Loading To Whitefish Lake: Base Case

Table 4-3: Peak Concentrations in Groundwater Reaching Whitefish Lake Base Case

Element	Groundwater Quality Screening Criteria	Concentration (mg/L)	Peak Time (Yr)	Comment
Al	0.05	0.040	9000	Background, naturally near threshold
As	0.005	$8x10^{-4}$	47075	Background
Ba*	--	0.039	50	Background
Ca	--	7.01	370	Conservative transport from Ore Zone
Cd	$4.0x10^{-5}$	$1.1x10^{-5}$	510	Background
Cl	120	10.0	420	Conservative transport
Co	$7.8x10^{-4}$	$4.2x10^{-4}$	400	Background
Cr*	$8.9x10^{-3}$	$5.3x10^{-4}$	400	Background
Cu*	$2.0x10^{-3}$	$7.0x10^{-4}$	100	Background
F*	--	0.06	8720	Background
Fe	0.3	**1.94**	410	Conservative transport, naturally above threshold
K	--	3.05	20	Background
Mg	--	2.76	75	Background
Mn*	0.23	**0.28**	500	Conservative transport, naturally near threshold
Mo*	31	$3.1x10^{-3}$	400	Background
Na	--	5.1	380	Conservative transport
Ni	$2.5x10^{-2}$	$1.9x10^{-3}$	400	Conservative transport
P*	--	0.074	1250	Background
Pb	$1.0x10^{-3}$	$1.2x10^{-4}$	50	Background
pH	6.5-9	6.45	400	Reactive transport, naturally below threshold
SO_4	128	12.6	410	Conservative transport
Se	$2.0x10^{-3}$	$8.3x10^{-4}$	700	Reactive transport
Sr*	2.5	0.12	400	Conservative transport
Ra*	$3.0x10^{-9}$	$2.3x10^{-9}$	8720	Reactive transport
Th*	$1.24x10^{-4}$	$3.2x10^{-8}$	8720	Reactive transport
U	0.015	$5.5x10^{-4}$	60000	Reactive transport
V*	0.12	$6.6x10^{-3}$	430	Conservative transport
Zn*	0.011	$4.7x10^{-3}$	8720	Reactive transport

* Simulation limited to 8720 years for full suite of constituents. **BOLD = Exceedance**

Table 4-4: Mass Flux to Whitefish Lake: Base Case

	Mass Flux to Whitefish Lake (g/d)																												
Time	Al	As	Ba	C	Ca	Cd	Cl	Co	Cr	Cu	F	Fe	K	Mg	Mn	Mo	Na	Ni	P	Pb	Ra	S	Se	Si	Sr	Th	U	V	Zn
50	4.79E+1	4.95E-1	1.85E+1	1.25E+4	5.23E+3	1.63E-2	1.09E+4	6.52E-1	8.18E-1	1.00E+0	7.52E+1	7.27E+2	4.36E+3	3.00E+3	2.47E+2	1.15E+0	5.23E+3	2.95E+0	6.77E+1	1.68E-1	2.69E-6	1.18E+3	1.31E+0	1.91E+4	4.03E+1	4.24E-5	8.19E-1	1.64E-1	7.18E+0
75	4.80E+1	4.95E-1	1.78E+1	1.24E+4	5.07E+3	1.63E-2	1.09E+4	6.51E-1	8.18E-1	9.99E-1	8.03E+1	7.20E+2	4.36E+3	3.03E+3	2.45E+2	1.15E+0	5.20E+3	2.95E+0	6.64E+1	1.68E-1	2.69E-6	1.17E+3	1.31E+0	1.91E+4	3.86E+1	4.25E-5	8.18E-1	1.64E-1	7.18E+0
100	4.81E+1	4.95E-1	1.72E+1	1.23E+4	5.04E+3	1.63E-2	1.09E+4	6.51E-1	8.17E-1	9.98E-1	8.27E+1	7.15E+2	4.33E+3	3.00E+3	2.47E+2	1.15E+0	5.17E+3	2.95E+0	6.71E+1	1.67E-1	2.69E-6	1.16E+3	1.31E+0	1.91E+4	3.73E+1	4.25E-5	8.18E-1	1.63E-1	7.17E+0
200	4.82E+1	4.95E-1	1.53E+1	1.19E+4	5.10E+3	1.63E-2	1.09E+4	6.49E-1	8.17E-1	9.93E-1	8.62E+1	7.21E+2	4.22E+3	2.89E+3	2.57E+2	1.16E+0	5.08E+3	2.94E+0	7.07E+1	1.66E-1	2.70E-6	1.18E+3	1.31E+0	1.92E+4	3.45E+1	4.26E-5	8.19E-1	1.63E-1	7.17E+0
300	4.82E+1	4.95E-1	1.37E+1	1.16E+4	5.10E+3	1.63E-2	1.11E+4	6.48E-1	8.16E-1	9.91E-1	8.82E+1	7.67E+2	4.20E+3	2.86E+3	2.58E+2	1.16E+0	5.04E+3	2.94E+0	7.15E+1	1.66E-1	2.70E-6	1.29E+3	1.31E+0	1.92E+4	3.42E+1	4.28E-5	8.18E-1	1.64E-1	7.17E+0
400	4.83E+1	4.95E-1	1.25E+1	1.13E+4	5.09E+3	1.63E-2	1.12E+4	6.47E-1	8.16E-1	9.88E-1	8.98E+1	7.92E+2	4.18E+3	2.84E+3	2.59E+2	1.16E+0	5.01E+3	2.94E+0	7.20E+1	1.65E-1	2.70E-6	1.35E+3	1.31E+0	1.92E+4	3.37E+1	4.29E-5	8.18E-1	1.64E-1	7.17E+0
500	4.83E+1	4.95E-1	1.17E+1	1.11E+4	5.03E+3	1.63E-2	1.12E+4	6.46E-1	8.15E-1	9.86E-1	9.09E+1	7.83E+2	4.16E+3	2.81E+3	2.59E+2	1.17E+0	4.98E+3	2.94E+0	7.23E+1	1.65E-1	2.71E-6	1.33E+3	1.31E+0	1.92E+4	3.21E+1	4.29E-5	8.17E-1	1.64E-1	7.17E+0
600	4.83E+1	4.95E-1	1.11E+1	1.10E+4	4.96E+3	1.63E-2	1.11E+4	6.44E-1	8.14E-1	9.84E-1	9.18E+1	7.60E+2	4.15E+3	2.77E+3	2.58E+2	1.17E+0	4.95E+3	2.93E+0	7.25E+1	1.64E-1	2.71E-6	1.28E+3	1.31E+0	1.92E+4	3.01E+1	4.30E-5	8.17E-1	1.65E-1	7.16E+0
700	4.83E+1	4.95E-1	1.07E+1	1.09E+4	4.91E+3	1.63E-2	1.11E+4	6.43E-1	8.14E-1	9.83E-1	9.24E+1	7.39E+2	4.14E+3	2.74E+3	2.57E+2	1.17E+0	4.93E+3	2.93E+0	7.26E+1	1.64E-1	2.71E-6	1.23E+3	1.31E+0	1.92E+4	2.85E+1	4.30E-5	8.17E-1	1.65E-1	7.16E+0
800	4.83E+1	4.95E-1	1.04E+1	1.08E+4	4.87E+3	1.63E-2	1.11E+4	6.42E-1	8.13E-1	9.82E-1	9.28E+1	7.25E+2	4.13E+3	2.72E+3	2.56E+2	1.17E+0	4.92E+3	2.93E+0	7.27E+1	1.64E-1	2.71E-6	1.20E+3	1.31E+0	1.92E+4	2.73E+1	4.30E-5	8.16E-1	1.65E-1	7.15E+0
900	4.83E+1	4.95E-1	1.01E+1	1.08E+4	4.84E+3	1.63E-2	1.11E+4	6.40E-1	8.12E-1	9.81E-1	9.31E+1	7.13E+2	4.13E+3	2.70E+3	2.56E+2	1.17E+0	4.91E+3	2.92E+0	7.27E+1	1.64E-1	2.71E-6	1.17E+3	1.31E+0	1.93E+4	2.64E+1	4.31E-5	8.16E-1	1.65E-1	7.15E+0
1000	4.83E+1	4.96E-1	9.96E+0	1.07E+4	4.82E+3	1.63E-2	1.11E+4	6.39E-1	8.12E-1	9.81E-1	9.33E+1	7.03E+2	4.13E+3	2.69E+3	2.55E+2	1.17E+0	4.90E+3	2.92E+0	7.27E+1	1.64E-1	2.71E-6	1.15E+3	1.31E+0	1.93E+4	2.58E+1	4.31E-5	8.16E-1	1.66E-1	7.15E+0
1250	4.83E+1	4.96E-1	9.74E+0	1.07E+4	4.78E+3	1.63E-2	1.11E+4	6.37E-1	8.11E-1	9.81E-1	9.37E+1	6.78E+2	4.14E+3	2.67E+3	2.53E+2	1.17E+0	4.89E+3	2.92E+0	7.26E+1	1.63E-1	2.72E-6	1.09E+3	1.30E+0	1.93E+4	2.46E+1	4.31E-5	8.16E-1	1.66E-1	7.15E+0
1500	4.83E+1	4.96E-1	9.65E+0	1.07E+4	4.76E+3	1.63E-2	1.10E+4	6.34E-1	8.09E-1	9.80E-1	9.40E+1	6.61E+2	4.14E+3	2.65E+3	2.52E+2	1.17E+0	4.87E+3	2.91E+0	7.25E+1	1.63E-1	2.72E-6	1.05E+3	1.30E+0	1.93E+4	2.38E+1	4.32E-5	8.16E-1	1.66E-1	7.15E+0
1750	4.83E+1	4.96E-1	9.58E+0	1.07E+4	4.75E+3	1.63E-2	1.10E+4	6.32E-1	8.08E-1	9.81E-1	9.43E+1	6.52E+2	4.15E+3	2.64E+3	2.50E+2	1.17E+0	4.86E+3	2.91E+0	7.23E+1	1.63E-1	2.73E-6	1.03E+3	1.30E+0	1.93E+4	2.33E+1	4.32E-5	8.15E-1	1.66E-1	7.15E+0
2000	4.83E+1	4.96E-1	9.50E+0	1.07E+4	4.75E+3	1.63E-2	1.10E+4	6.30E-1	8.08E-1	9.81E-1	9.44E+1	6.48E+2	4.16E+3	2.63E+3	2.49E+2	1.17E+0	4.85E+3	2.91E+0	7.21E+1	1.63E-1	2.73E-6	1.02E+3	1.30E+0	1.93E+4	2.31E+1	4.32E-5	8.15E-1	1.66E-1	7.15E+0
2250	4.83E+1	4.96E-1	9.43E+0	1.06E+4	4.75E+3	1.63E-2	1.10E+4	6.28E-1	8.07E-1	9.81E-1	9.45E+1	6.46E+2	4.16E+3	2.63E+3	2.48E+2	1.17E+0	4.84E+3	2.90E+0	7.19E+1	1.63E-1	2.74E-6	1.02E+3	1.30E+0	1.93E+4	2.30E+1	4.32E-5	8.15E-1	1.66E-1	7.15E+0
2500	4.83E+1	4.97E-1	9.39E+0	1.06E+4	4.75E+3	1.63E-2	1.10E+4	6.26E-1	8.06E-1	9.81E-1	9.46E+1	6.45E+2	4.17E+3	2.63E+3	2.47E+2	1.17E+0	4.83E+3	2.90E+0	7.17E+1	1.63E-1	2.74E-6	1.02E+3	1.30E+0	1.93E+4	2.29E+1	4.33E-5	8.15E-1	1.66E-1	7.16E+0
2750	4.83E+1	4.97E-1	9.36E+0	1.06E+4	4.75E+3	1.63E-2	1.10E+4	6.24E-1	8.05E-1	9.82E-1	9.47E+1	6.44E+2	4.18E+3	2.62E+3	2.46E+2	1.17E+0	4.83E+3	2.90E+0	7.15E+1	1.63E-1	2.75E-6	1.02E+3	1.30E+0	1.93E+4	2.28E+1	4.33E-5	8.15E-1	1.66E-1	7.16E+0
3000	4.83E+1	4.97E-1	9.34E+0	1.06E+4	4.75E+3	1.62E-2	1.10E+4	6.22E-1	8.04E-1	9.82E-1	9.47E+1	6.44E+2	4.18E+3	2.62E+3	2.44E+2	1.17E+0	4.82E+3	2.90E+0	7.13E+1	1.63E-1	2.76E-6	1.01E+3	1.30E+0	1.93E+4	2.26E+1	4.33E-5	8.14E-1	1.66E-1	7.16E+0
3250	4.83E+1	4.97E-1	9.33E+0	1.06E+4	4.75E+3	1.62E-2	1.10E+4	6.21E-1	8.03E-1	9.82E-1	9.48E+1	6.44E+2	4.19E+3	2.62E+3	2.43E+2	1.17E+0	4.81E+3	2.89E+0	7.11E+1	1.63E-1	2.76E-6	1.01E+3	1.30E+0	1.93E+4	2.25E+1	4.33E-5	8.14E-1	1.66E-1	7.16E+0
3500	4.83E+1	4.97E-1	9.32E+0	1.06E+4	4.75E+3	1.62E-2	1.10E+4	6.19E-1	8.02E-1	9.82E-1	9.48E+1	6.43E+2	4.19E+3	2.61E+3	2.42E+2	1.17E+0	4.81E+3	2.89E+0	7.10E+1	1.63E-1	2.77E-6	1.01E+3	1.30E+0	1.93E+4	2.24E+1	4.34E-5	8.14E-1	1.66E-1	7.17E+0
3750	4.83E+1	4.97E-1	9.31E+0	1.06E+4	4.74E+3	1.62E-2	1.10E+4	6.17E-1	8.01E-1	9.83E-1	9.48E+1	6.43E+2	4.19E+3	2.61E+3	2.41E+2	1.17E+0	4.80E+3	2.89E+0	7.08E+1	1.63E-1	2.77E-6	1.01E+3	1.30E+0	1.93E+4	2.22E+1	4.34E-5	8.14E-1	1.66E-1	7.17E+0
4000	4.83E+1	4.97E-1	9.31E+0	1.06E+4	4.74E+3	1.62E-2	1.10E+4	6.15E-1	8.00E-1	9.83E-1	9.49E+1	6.43E+2	4.20E+3	2.61E+3	2.40E+2	1.17E+0	4.80E+3	2.89E+0	7.06E+1	1.63E-1	2.78E-6	1.01E+3	1.30E+0	1.93E+4	2.21E+1	4.34E-5	8.14E-1	1.66E-1	7.17E+0
4250	4.83E+1	4.98E-1	9.30E+0	1.06E+4	4.74E+3	1.62E-2	1.10E+4	6.14E-1	7.99E-1	9.83E-1	9.49E+1	6.43E+2	4.20E+3	2.61E+3	2.39E+2	1.17E+0	4.79E+3	2.88E+0	7.04E+1	1.63E-1	2.78E-6	1.01E+3	1.30E+0	1.93E+4	2.20E+1	4.34E-5	8.13E-1	1.66E-1	7.18E+0
4500	4.83E+1	4.98E-1	9.30E+0	1.06E+4	4.73E+3	1.62E-2	1.10E+4	6.12E-1	7.99E-1	9.83E-1	9.49E+1	6.43E+2	4.21E+3	2.61E+3	2.38E+2	1.17E+0	4.79E+3	2.88E+0	7.02E+1	1.63E-1	2.79E-6	1.01E+3	1.30E+0	1.93E+4	2.19E+1	4.34E-5	8.13E-1	1.66E-1	7.18E+0
4750	4.83E+1	4.98E-1	9.30E+0	1.06E+4	4.73E+3	1.62E-2	1.10E+4	6.10E-1	7.98E-1	9.84E-1	9.49E+1	6.43E+2	4.21E+3	2.61E+3	2.37E+2	1.17E+0	4.79E+3	2.88E+0	7.01E+1	1.63E-1	2.79E-6	1.01E+3	1.30E+0	1.93E+4	2.18E+1	4.34E-5	8.13E-1	1.66E-1	7.18E+0
5000	4.83E+1	4.98E-1	9.30E+0	1.06E+4	4.73E+3	1.62E-2	1.10E+4	6.09E-1	7.97E-1	9.84E-1	9.49E+1	6.43E+2	4.21E+3	2.61E+3	2.36E+2	1.17E+0	4.78E+3	2.88E+0	6.99E+1	1.63E-1	2.80E-6	1.01E+3	1.30E+0	1.93E+4	2.17E+1	4.35E-5	8.13E-1	1.66E-1	7.18E+0
6000	4.82E+1	4.98E-1	9.29E+0	1.06E+4	4.71E+3	1.62E-2	1.09E+4	6.03E-1	7.93E-1	9.85E-1	9.50E+1	6.42E+2	4.23E+3	2.60E+3	2.33E+2	1.16E+0	4.77E+3	2.86E+0	6.92E+1	1.63E-1	2.82E-6	1.01E+3	1.30E+0	1.93E+4	2.13E+1	4.35E-5	8.12E-1	1.66E-1	7.20E+0
7000	4.82E+1	4.99E-1	9.29E+0	1.06E+4	4.70E+3	1.62E-2	1.09E+4	5.97E-1	7.90E-1	9.85E-1	9.51E+1	6.42E+2	4.24E+3	2.60E+3	2.31E+2	1.16E+0	4.76E+3	2.85E+0	6.86E+1	1.63E-1	2.83E-6	1.01E+3	1.30E+0	1.93E+4	2.11E+1	4.36E-5	8.11E-1	1.66E-1	7.21E+0
8000	4.82E+1	4.99E-1	9.29E+0	1.06E+4	4.69E+3	1.62E-2	1.09E+4	5.93E-1	7.87E-1	9.86E-1	9.51E+1	6.42E+2	4.25E+3	2.60E+3	2.29E+2	1.16E+0	4.76E+3	2.84E+0	6.81E+1	1.63E-1	2.85E-6	1.01E+3	1.30E+0	1.93E+4	2.08E+1	4.36E-5	8.10E-1	1.66E-1	7.22E+0

4.6.6 Summary of Base Case Transport Analysis

The base-case simulations indicated that post-decommissioning conditions would not generate any exceedances at Whitefish Lake for the future centuries period, apart from those that reflect natural conditions. The only exceedances noted in the base case simulation were iron, manganese and pH, but concentrations/values of these parameters are naturally above or near the guideline criteria for freshwater aquatic life.

Simulations illustrate that the geochemical reactive transport conditions interpreted for the site would sorb and retain most of the restored groundwater concentrations in the vicinity of the ore zone (Figures 4-9 to 4-10), such that only minor changes from background would occur at Whitefish Lake throughout the future centuries period. Simulation of key constituents such as uranium, indicate that the mass will be removed from the dissolved solution and sorbed onto available sorption sites of clay, iron, and goethite contained throughout the Athabasca Supergroup sandstone units. This process, coupled with dispersion in three-dimensions, acts to limit the maximum extent of the dissolved plume at concentrations above the groundwater quality screening criteria.

The simulations presented are considered conservative, as they do not consider all potential attenuating processes. Matrix diffusion is expected to further constrain transport of dissolved constituents, particularly based on the long travel times.

4.7 Prediction Uncertainty Analysis

The understanding of the geochemistry and important processes evolved throughout the geochemical simulation progress. Initial simulations were performed using a subset of constituents (19 constituents solved using multi-species transport). Results were reviewed and parameters, or geochemical conditions were varied to test hypotheses and uncertainties in parameter assumptions. Areas of simulation evolution and testing regarding parameter uncertainty included the following:

- suite of COPC necessary to be simulated,
- characteristics of the paleoweathered zone,
- characteristics of lake-bottom sediments and their capacity for sorption and attenuation,
- importance of incorporating spatially variable porosity in computing solids fractions,
- variability in clay content within and surrounding the ore zone related to post-decommissioning migration and reactive transport,
- availability of iron within different hydrostratigraphic units, and
- availability of potential sorption sites along the transport pathway.

As part of the uncertainty scenarios, the period of simulation was varied. The 3D geochemical reactive transport model simulations were run for thousands, to tens-of-thousands of years after thawing of the freeze wall (i.e., post-decommissioning and beyond). Simulations of up to 100,000 years were performed to ensure that desorption, ion exchange and other processes had reached a stable equilibrium and would not yield additional mass available for transport. However, through the base case simulation, the following key time periods were observed:

- the dissolved uranium mass was reduced by 90% within the first 5,000 years,
- a steady-state uranium plume was achieved within the first 10,000 years,
- by 25,000 years, the dissolved uranium mass was reduced to 1% of the decommissioning restored solution mass with the majority of the dissolved mass remaining within the low conductivity paleoweathered bedrock.
- By 60,000 years, maximum dissolved concentrations for uranium were reduced to 1% the initial conditions with the highest concentrations persistent within the low conductivity paleoweathered bedrock.
- Beyond 60,000 years when peak concentrations are predicted to be 1% of the source concentrations, the potential for a continued groundwater plume from the ISR mining area is all but eliminated and conditions have returned to baseline conditions.

Through these findings, the most important period for simulation was considered to be the first 10,000 years; this period is generally considered sufficient time to understand geochemical processes. Simulation of conditions beyond 50,000 to 60,000 years was generally found to produce very little change from background conditions.

Table 4-5 outlines a suite of additional simulations that were performed to explore uncertainty regarding the source condition, hydrogeologic parameters, and the geochemical transport processes that can affect predicted concentrations reaching Whitefish Lake. The scenarios were designed to evaluate the potential uncertainties associated with peak concentrations that may reach Whitefish Lake. Each scenario provide insight into the potential changes in predictions if the model parameters differ from those applied in the base case model simulations.

Uncertainties with respect to the source conditions included a) the suite of constituents within the source zone and transported to Whitefish Lake (Base+ scenario), b) the spatial extent of the source zone, and c) the temporal extent of the source zone. The Base+ scenario evaluates the fate and transport of the full suite of characterized COPCs, including Barium, Chromium, Copper, Floride, Potassium, Magnesium, Manganese, Molybdenum, Phosphorous, Radium, Strontium, Thorium, Vanadium, and Zinc. In addition to the Base+ scenario, uncertainty scenarios (Table 4-5) are further described as follows:

1. Scenario 1: To evaluate the spatial extent, the flare zone overlying the restored solution (Figure 4-1) was considered to have the same solution strength as the area immediately surrounding the ore zone. This extends the source zone vertically; the lateral extent is physically constrained by the freeze walls. This scenario effectively simulates an increase in the dissolved mass of the source.

2. Scenario 2: To evaluate the temporal extent of the source, clay content and proton sorption to clays within the source zone were tested. Simulation of proton desorption from clay can result in a plume of lower pH for a longer period. This lower pH plume can affect the sorption behaviour of COPCs.

Uncertainty with respect to transport conditions between the ore zone and Whitefish Lake was evaluated by extending the simulated time period for transport, varying hydraulic conductivity

of materials along the flow path (6 scenarios), reducing the number of available reaction sites along the flow path (3 scenarios), reducing the dispersion that tends to reduce concentrations in three dimensions in groundwater, enhancing the iron oxidation and ferric iron precipitation such that lower pH conditions may be present within the shallower zones, and evaluating the effect of dissolved U(VI) with pyrite in the desilicified sediments (Redox scenario, Section 3.5.6.3). In Scenarios 3, 4 and 5, the values for increased hydraulic conductivities in the Lower Sandstone Aquifer and Desilicified Zone of the Intermediate Sandstone Aquitard were developed using a robust uncertainty analysis (Section 2.8). This approach was used in recognition that model calibration is non-unique and that a range of parameter combinations should be evaluated to understand potential environmental predictions.

These scenarios are further described as follows:

3. Scenario 3: The transport simulation time was extended to 100,000 years following cessation of mining to evaluate the potential that desorption, ion exchange and other processes could yield additional mass available for transport.

4. Scenario 4: A set of higher hydraulic conductivity values selected from the groundwater flow uncertainty assessment (Section 2.8.3). Realization 3, from the parameter uncertainty assessment, contains a higher hydraulic conductivity for the Lower Sandstone Aquifer (above Phoenix mining phases 1-4, 5, and 6) as well as within the altered (desilicified) portion of the Intermediate Sandstone Aquitard (Figure 2-23).

5. Scenario 5: A set of higher hydraulic conductivity values selected from the groundwater flow uncertainty assessment (Section 2.8.3). Realization 7, from the parameter uncertainty assessment, contains the highest hydraulic conductivity for the combination of the Lower Sandstone Aquifer (above Phoenix phase 5) as well as within the altered (desilicified) portion of the Intermediate Sandstone Aquitard (Figure 2-23).

6. Scenario 6: A set of higher hydraulic conductivity values selected from the groundwater flow uncertainty assessment (Section 2.8.3). Realization 27, from the parameter uncertainty assessment, contains the highest hydraulic conductivity for the Lower Sandstone Aquifer (above Phoenix phase 5) of any of the 50 calibrated realizations (Figure 2-23).

7. Scenario 7: Higher hydraulic conductivity within the ore zone, representing the potential that the ore zone may have enhanced flow through rate, and thus create a greater mass flux leaving the ore zone.

8. Scenario 8: Higher hydraulic conductivity along the WS Shear, within the paleo-weathered zone. The WS Shear is interpreted to have an enhanced fracture zone (damaged zone) surrounding the fault plane, with the frequency and apertures of fractures decreasing exponentially away from the fault plane (i.e., typical interpretation for fracturing surrounding a fault). The enhanced fracturing along the WS shear is only

expected to be relevant within the paleoweathered portion of the sub-surface as the overlying sediments have been desilicified, and thus are expected to behave more like porous media than fractured media.

9. Scenario 9: The hydraulic conductivity was enhanced along exploration coreholes where grout was only placed in the 15 m above the ore zone. The overlying coreholes were simulated to have enhanced hydraulic conductivity through the Intermediate Sandstone Aquitard (Figure 2-6).

10. Scenario 10: The number of available reaction sites at mineral surfaces was reduced to 10% ('1 in 10 solids') assumed in the base case to reflect the potential that site densities and other mineral properties (e.g., surface area) from the literature may not accurately reflect those found in situ. This was evaluated in the 1D model in Section 3.5.6.2.5. Consequently, the potential for dissolved mass to adsorb (and thus have transport retarded) was reduced.

11. Scenario 11: The number of available reaction sites at the mineral surfaces was reduced 10% (as above, #10), but with the full suite of constituents.

12. Scenario 12: Reduction in the number of available reaction sites within the Lower Sandstone Aquifer. The Lower Sandstone Aquifer naturally has relatively low clay and iron concentrations. These minerals were removed altogether from this zone to evaluate the influence on the COPC migration.

13. Scenario 13: The longitudinal and transverse dispersivity were reduced by a factor of 2 to reduce the potential dispersion of the plume along the flow path to values of 5 m and 2.5 m respectively. This has the effect of increasing the maximum concentrations along the dominant flow paths.

14. Scenario 14: Oxygenated conditions may be encountered in the upper flow zone. Oxidation of ferrous iron from the mining area to ferric iron and subsequent precipitation of the ferric hydroxide to goethite was simulated, and the effect on pH and COPC behaviour evaluated.

15. Scenario 15: Alternative REDOX conditions were considered for the transformation of uranium and other COPCs. The groundwater is largely anoxic and pyrite is present in the zone of thermal alteration in the Lower Sandstone Aquifer. The potential for U(VI) reduction to (U(IV) linked to pyrite oxidation was explored. In this scenario, no sorption was assumed in the Lower Sandstone Aquifer for U(VI) or other COPCs.

Each of these uncertainty scenarios provides a means to evaluate the variation in the predicted outcomes (i.e., concentrations) reaching Whitefish Lake.

Table 4-5: Predictive Uncertainty Simulations

#	Description	Key Changes			
		Number of Constituents	Source	Transport	Objective
Base	Base Case	19	RS1	Reactive along entire flow path	Best estimate of expected transport including geochemical reactions.
Base+	Base Case with Additional Constituents	31	RS1++	Base	Potential for other constituents to reach Whitefish Lake.
1	Expanded Source into Overlying Flare	19	Flare @ 100% Restored Solution	Base	Conservative source extent and total mass
2	Elongated Source due to Slow Release of sorbed Constituents	19	RS1+sorbed mass	Base	Conservative source timing and total mass
3	Extended Transport time	19	RS1	Base	Potential for any longer-range changes
4	Higher hydraulic conductivity (Realization 3)	19	RS1	Base Transport Processes, but with enhanced hydraulic conductivity	Potential for earlier breakthrough of constituents and less time for constituents to react along the flow path.
5	Higher hydraulic conductivity (Realization 7)	19	RS1		
6	Higher hydraulic conductivity (Realization 27)	19	RS1		
7	Higher hydraulic conductivity in ore zone	19	RS1		Ore zone does not collapse, leaving higher conductivity in source area
8	Higher hydraulic conductivity along the WS Shear within the paleo-weathered zone	19	RS1		Potential for enhanced fracturing along WS Shear
9	Higher hydraulic conductivity along exploration coreholes	19	RS1		Potential for exploration coreholes to be preferential transport pathways
10	Fewer Reaction Sites	19	RS1	Reaction sites limited to 1 in 10 of base case	Conservative number of reaction sites
11	Fewer Reaction Sites, full suite of constituents	31	RS1	Reaction sites limited to 1 in 10 of base case	Conservative number of reaction sites, full suite of constituents
12	Minimal Sorption within Lower Sandstone Aquifer	31	RS1	Iron sorption sites omitted within the Lower Sandstone Aquifer	Lower potential for sorption, potentially higher peak breakthrough
13	Lower Dispersivity	19	RS1	Less dispersion	Potential for less dispersion
14	Iron Oxidation Causing low pH	19	RS1	Reduced pH due to iron oxidation	Lower potential for sorption
15	Alternative REDOX conditions	31	RS1	Reduced potential transformation of uranium	Less potential for uranium transport to be retarded due to REDOX transformations.

*Effects assessment completed using the results from the Base+ scenario, which contained the complete set of constituents.

4.7.1 Prediction Uncertainty Results

Table 4-5 presents a summary of the predicted concentrations reaching Whitefish Lake under each of the evaluated uncertainty scenarios. The constituent concentrations are for groundwater seeping into the base of the lake and do not reflect the mixing that will occur within the lake. Exceedances of the groundwater quality screening criteria (GQSC) are shown as using a bold, red font.

Exceendances of the GQSC for iron (Fe^{3+}), manganese (Mn) and pH were found in most simulations. Exceedances of for iron are not surprising as initial conditions for iron were observed to be above criteria throughout the Athabasca Supergroup sandstone units and even in surface water samples (Table 3-4). Similarly, exceedances of the GQSC for manganese were anticipated as Mn was observed to have concentrations above the GQSC in the Lower Sandstone Aquifer, the Intermediate Sandstone Aquitard, as well as surface water (Table 3-4). These GQSC exceedances are not caused by mining activities, rather they are naturally occurring within the Athabasca Supergroup sandstone units. pH values were also marginally lower than the GQSC but varied to a very limited extent and were within the range of pH values measured in the overburden and Upper Sandstone Aquifer (Table 3-4 and Appendix D).

Modest exceedances of the GQSC for cobalt (Co) and selenium (Se) were also simulated for the scenario where a lower dispersivity value was applied; exceedances were a factor of 1.2 and 1.1 times the GQSC for these two elements, respectively. Figure 4-14 illustrates that a minor portion area of the groundwater below the lake would be subjected to concentrations greater than the GQSC for selenium, while Figure 4-15 illustrates a similar occurrence for cobalt. The timing of the exceedance is dependent upon the reactive nature of each constituent, and so the exceedance for cobalt is not predicted to occur until 30,000 years post-decommissioning, while the exceedance for selenium is predicted to occur 500 years post-decommissioning. The area of the lake experiencing concentrations above the GQSC in the underlying groundwater is small, and the mass flux entering the lake would not change appreciably. The predicted concentrations in the groundwater entering the base of Whitefish Lake would be further readily reduced during mixing within the lake, as evaluated through the Effects Assessment (Section 4.9).

The uncertainty scenario that yielded the most change was the reduction of the longitudinal dispersivity value from 10 to 5 m (Scenario 13). Over the length of the plume (i.e., 1 km), and recognizing the potential tortuosity associated with flow paths through fractured rock horizons, the 10 m dispersivity value (i.e., base case) is considered the most appropriate value, while the uncertainty value (i.e., longitudinal dispersivity of 5 m; transverse dispersivity of 2.5 m) is considered conservative.

These uncertainty scenarios provide a measure of the potential range of concentrations that may be observed in groundwater beneath Whitefish Lake via groundwater transport. The consistency of the scenario results illustrates the ability of the natural conditions to attenuate restored mining solutions such that elevated concentrations will remain at depth, and concentrations that reach Whitefish Lake will be similar to existing, background conditions. In

addition, the consistency of the uncertainty results with the base case affirms that the base case simulation is appropriate for decision-making.

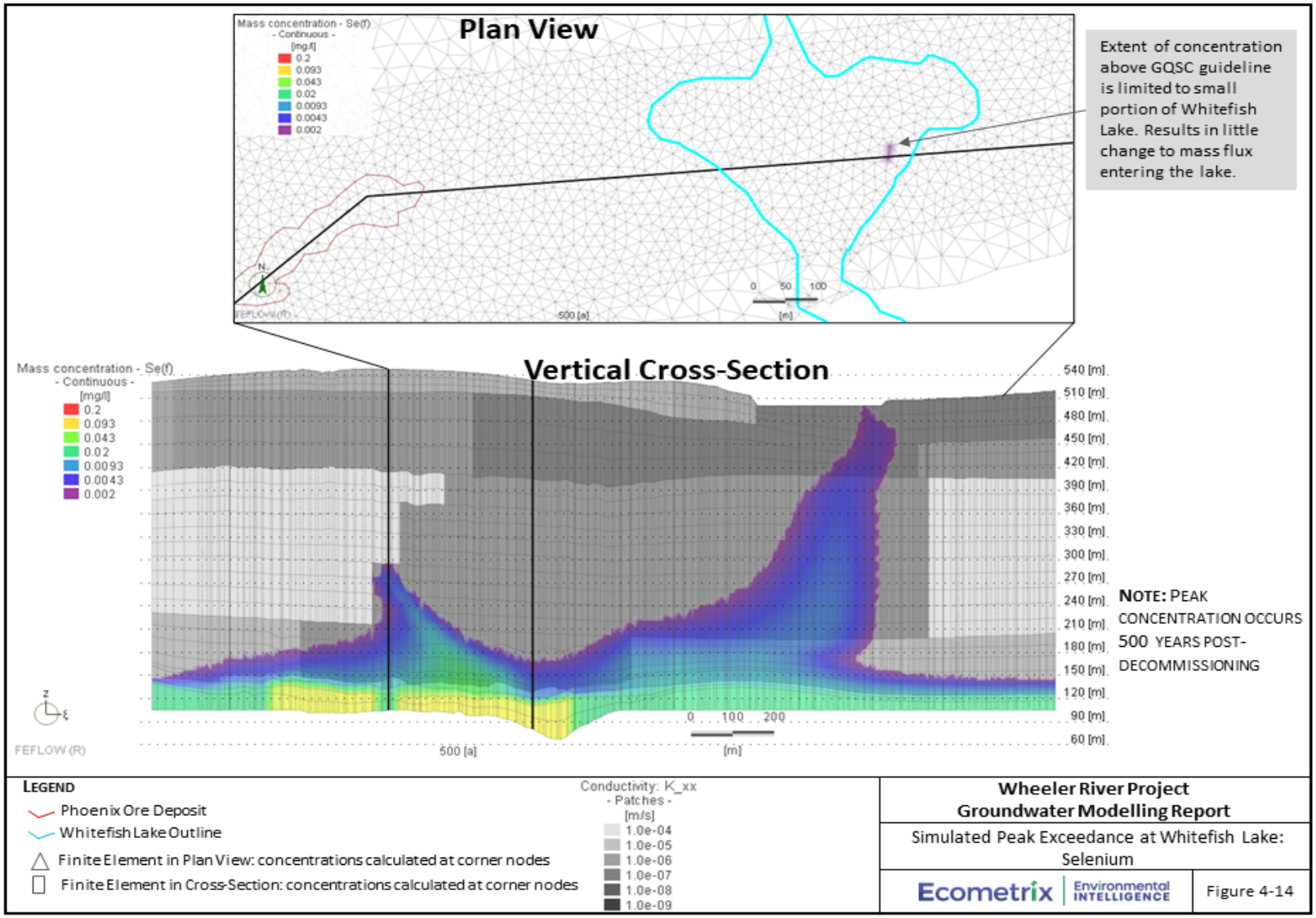

Figure 4-14: Simulated Peak Exceedance at Whitefish Lake: Selenium

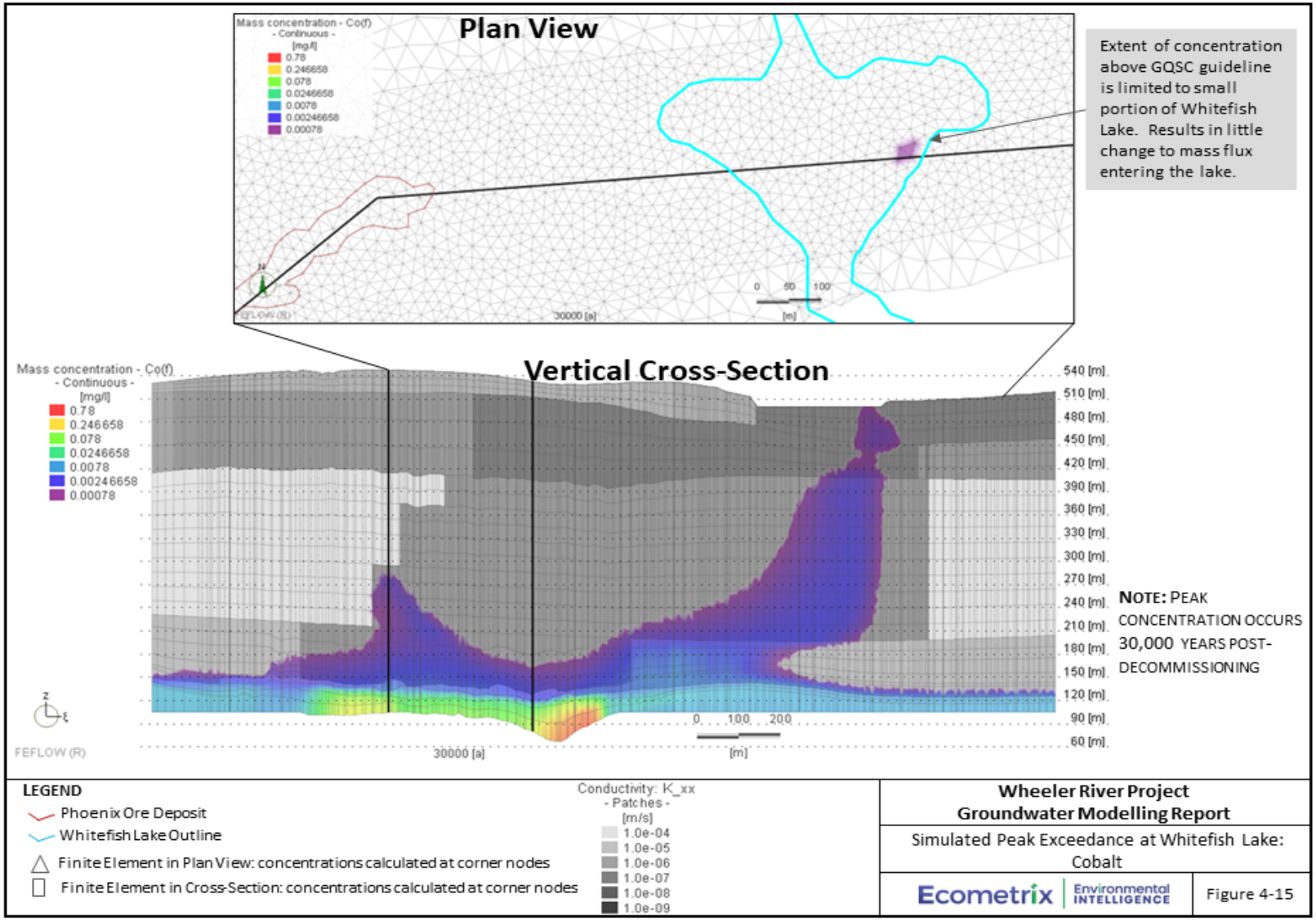

Figure 4-15: Simulated Peak Exceedance at Whitefish Lake: Cobalt

Table 4-6: Uncertainty Results: Groundwater Concentrations at Whitefish Lake

Scenario	MaxTime	pH	Al	As	C	Ca	Cd	Cl	Co	Fe	K	Mg	Na	Ni	Pb	SO_4	Se	Si	U	Ba	Cr	Cu	F	Mn	Mo	P	Ra	Sr	Th	V	Zn
Base	**60000**	6.45	**4.00E-2**	**7.82E-4**	**1.34E+1**	**7.01E+0**	**1.07E-5**	**9.98E+0**	**4.23E-4**	1.94E+0	**3.05E+0**	**2.76E+0**	**5.12E+0**	**1.92E-3**	**1.18E-4**	**1.26E+1**	**8.35E-4**	**1.22E+1**	**5.50E-4**											
Base+*	8720	6.47	2.98E-2	3.22E-4	1.34E+1	7.02E+0	1.07E-5	9.88E+0	4.22E-4	**1.95E+0**	3.05E+0	2.78E+0	5.13E+0	1.92E-3	1.19E-4	**1.27E+1**	8.36E-4	1.22E+1	5.45E-4	3.94E-2	5.25E-4	7.00E-4	6.14E-2	2.79E-1	3.09E-3	7.43E-2	2.28E-9	1.19E-1	3.16E-8	6.64E-3	4.71E-3
1	50000	6.43	4.01E-2	4.19E-4	1.34E+1	8.36E+0	1.10E-5	1.17E+1	4.33E-4	2.85E+0	3.05E+0	2.87E+0	5.58E+0	1.96E-3	1.18E-4	**1.89E+1**	8.48E-4	1.22E+1	5.50E-4											
2	50870	6.42	4.20E-2	4.11E-4	1.34E+1	7.06E+0	1.07E-5	1.00E+1	4.24E-4	1.95E+0	3.05E+0	2.78E+0	5.14E+0	1.92E-3	1.18E-4	**1.26E+1**	8.35E-4	1.22E+1	5.51E-4											
3	100000	6.45	3.98E-2	1.40E-3	1.34E+1	5.83E+0	1.43E-5	1.03E+1	4.85E-4	2.10E+0	3.42E+0	3.08E+0	6.17E+0	1.90E-3	1.17E-4	**1.37E+1**	1.37E-3	1.22E+1	8.71E-4											
4	35000	6.45	4.01E-2	1.03E-3	1.47E+1	5.03E+0	1.30E-5	1.05E+1	4.19E-4	8.55E-1	3.26E+0	3.20E+0	5.87E+0	1.91E-3	1.21E-4	**5.03E+0**	1.38E-3	1.22E+1	1.70E-3											
5	25450	6.45	4.02E-2	9.82E-4	1.47E+1	5.01E+0	1.42E-5	9.87E+0	4.19E-4	8.13E-1	3.23E+0	3.19E+0	5.47E+0	1.91E-3	1.21E-4	**4.74E+0**	1.28E-3	1.22E+1	1.54E-3											
6	25075	6.45	4.01E-2	1.10E-3	1.46E+1	5.02E+0	1.38E-5	1.10E+1	4.19E-4	1.06E+0	3.28E+0	3.18E+0	6.32E+0	1.91E-3	1.21E-4	**6.46E+0**	1.44E-3	1.22E+1	1.81E-3											
7	10000	6.44	4.02E-2	1.58E-3	1.34E+1	6.10E+0	2.27E-5	1.00E+1	4.16E-4	1.95E+0	3.17E+0	2.94E+0	6.59E+0	1.89E-3	1.18E-4	**1.27E+1**	1.47E-3	1.22E+1	7.69E-4											
8	10000	6.44	4.02E-2	2.00E-3	1.34E+1	6.18E+0	2.59E-5	1.05E+1	4.16E-4	2.02E+0	3.17E+0	2.95E+0	6.92E+0	1.89E-3	1.18E-4	**1.31E+1**	1.57E-3	1.22E+1	7.69E-4											
9	10000	6.45	4.00E-2	3.21E-4	1.34E+1	7.01E+0	1.07E-5	9.95E+0	4.23E-4	1.94E+0	3.05E+0	2.76E+0	5.12E+0	1.92E-3	1.18E-4	**1.26E+1**	8.35E-4	1.22E+1	5.50E-4											
10	50000	6.44	4.02E-2	4.68E-4	1.34E+1	6.61E+0	1.14E-5	9.95E+0	6.33E-4	1.95E+0	2.95E+0	2.71E+0	6.98E+0	1.92E-3	1.18E-4	**1.26E+1**	8.35E-4	1.22E+1	1.40E-3											
11	11175	6.46	4.69E-2	3.33E-4	1.34E+1	6.68E+0	1.18E-5	9.86E+0	4.48E-4	1.95E+0	2.95E+0	2.72E+0	6.66E+0	1.92E-3	1.19E-4	**1.27E+1**	8.36E-4	1.22E+1	1.37E-3	3.93E-2	5.27E-4	7.86E-4	6.17E-2	2.82E-1	9.14E-4	9.41E-2	2.52E-9	1.20E-1	3.80E-8	1.30E-4	4.93E-3
12	8540	6.47	2.98E-2	3.25E-4	1.34E+1	6.95E+0	1.07E-5	9.89E+0	4.22E-4	1.95E+0	3.05E+0	2.78E+0	5.29E+0	1.92E-3	1.19E-4	**1.27E+1**	8.36E-4	1.22E+1	5.45E-4	3.94E-2	5.25E-4	6.99E-4	6.14E-2	2.79E-1	9.12E-4	7.46E-2	2.26E-9	1.20E-1	3.15E-8	1.30E-4	4.70E-3
13	35000	6.43	4.15E-2	1.93E-3	1.49E+1	7.48E+0	3.96E-5	1.20E+1	9.10E-4	2.91E+0	3.27E+0	3.21E+0	8.38E+0	1.92E-3	1.21E-4	**1.93E+1**	2.19E-3	1.22E+1	9.58E-3											
14	50000	6.38	4.21E-2	1.49E-3	1.34E+1	6.14E+0	2.22E-5	1.00E+1	6.62E-4	6.48E-3	3.17E+0	2.94E+0	6.62E+0	1.90E-3	1.17E-4	**1.26E+1**	1.40E-3	1.22E+1	3.15E-3											
15	15000	6.39	3.83E-2	6.97E-4	1.34E+1	6.96E+0	1.07E-5	9.89E+0	4.22E-4	2.00E+0	3.05E+0	2.78E+0	5.30E+0	1.91E-3	1.18E-4	**1.26E+1**	8.34E-4	1.22E+1	5.34E-4	3.94E-2	5.14E-4		6.17E-2	2.89E-1	9.12E-4	7.74E-2	2.61E-9	1.20E-1	3.41E-8	1.30E-4	5.00E-3
Groundwater Quality Screening Criteria		6.5-9	5.00E-2	5.00E-3			4.00E-5	1.20E+2	7.80E-4	3.00E-1				2.50E-2	1.00E-3	1.28E+2	2.00E-3		1.50E-2		8.90E-3	2.00E-3		2.30E-1	3.10E+1		3.00E-9	2.50E+0	1.24E-4	1.20E-1	1.10E-2

Notes:
* Base+ Scenario used to evaluate effects within Whitefish Lake in the l
Exceedances of Groundwater Quality Screening Criteria are shown in red

4.8 Summary of Reactive Transport Results

Transport of dissolved constituents was simulated using a 3D groundwater flow modelling approach with coupled geochemical reactive transport wherein the chemical reactions were computed using PHREEQC and the transport was computed using FEFLOW. In this manner, dissolved constituents were allowed to interact with the geologic media through which they are migrating, allowing realistic sorption reactions to be incorporated into the transport calculations. Simulations extended post-decommissioning for thousands of years to evaluate potential effects throughout the future-centuries period.

Transport of dissolved constituents generally follows the predicted flow paths (Figure 4-4), with additional spreading and mixing related to dispersion. Dispersion reduces the concentrations as time progresses and the dissolved plume migrates (Figure 4-6), and results in much lower concentrations reaching Whitefish Lake than those that are simulated post-decommissioning within the mining area (see Section 4.1 for source conditions). In addition to the dispersion, constituent's experience geochemical reactions along the flow path including sorption reactions. Dissolved groundwater constituents sorb to available reaction sites on minerals within the host material (i.e., quartz, and/or goethite, and/or clay) as the dissolved constituents reach these sites. Sorption and precipitation reactions have the effect of taking mass out of the dissolved phase and making it stationary in the sub-surface until conditions are appropriate for desorption or re-dissolution. These reactions effectively retard the dissolved mass available to be transported toward Whitefish Lake (Figures 4-7 a, b to 4-9 a, b). The transformation of mass from the dissolved to a sorbed state is illustrated in Figure 4-10 for uranium. Similar mass distributions occurs for all reactive constituents. Sorption occurs to different extents for each constituent, and there can be competition for sorption sites by multiple constituents in solution. All constituents are, therefore, simultaneously transported and allowed to react within the simulations to appropriately evaluate the transport and fate of the suite of constituents.

By accounting for the reactions included in the model, the simulated plumes of dissolved COPCs migrating from the mining area are found to reach a maximum extent within the Lower Sandstone Aquifer and the deeper part of the Desilicified Zone (Figure 4-11) after about 5,000 to 10,000 years, depending on the constituent. Consequently, the conditions at Whitefish Lake are predicted to experience modest variations from background/baseline conditions. For example, a maximum change of 14% for the mass flux of sulphate, a chemically conservative constituent in the groundwater was predicted from background conditions, as shown in Figures 4-12 and Figure 4-13). Under the base case scenario, there are only minor exceedances of GQSC for constituents (e.g., iron, manganese) which are naturally found at elevated levels within the Athabasca Supergroup sandstones, and pH is marginally below the GWSC but within baseline range. Consequently, these GQSC exceedances are attributed to natural processes, not the mine post-decommissioning.

Assessment of parameter and geochemical uncertainty suggested there may be a low probability for modest GQSC exceedances for cobalt and selenium in groundwater below the lake. The portion of Whitefish Lake predicted to experience such potential exceedances is relatively small (see Figure 4-14 and 4-15) such that the mass flux to Whitefish Lake is not expected to be

appreciably altered. Similarly, the concentrations within Whitefish Lake, which will be subject to considerable mixing (see Section 2.6.4), are not expected to be measurably altered.

4.9 Output for Effects Assessment at Whitefish Lake

Predictions of mass flux to Whitefish Lake (Section 4.6.5) were further incorporated within a subsequent effects assessment, to understand the implication of such changes in mass flux to Whitefish Lake. Such effects are documented under separate cover (Ecometrix, 2024b) with a summary contained within the EIS (Section 10).

To evaluate the effect of predicted dissolved concentrations seeping into the base of Whitefish Lake, predicted concentration and mass flux changes from the 3D groundwater flow and reactive transport model were further assessed using the IMPACT model (Ecometrix, 2024b). IMPACT is used to assess the potential risks to in the environment, including humans, from exposure to COPCs.

Concentration data (Table 4-3) and mass flux data (Table 4-4; Figure 4-13), from the Base+ scenario were used within IMPACT; the Base+ was used as that scenario represents the best estimate of concentrations and mass loading to Whitefish Lake, for the full suite of constituents.

5.0 Summary and Conclusions

Groundwater flow and reactive transport modelling tools were constructed to simulate conditions in the Phoenix area. The models reflects over 16 years of data collection and interpretation by Denison and the hydrogeologic site conceptual model detailed in Ecometrix, 2024a.

The groundwater flow model was calibrated to observed water level and stream baseflow data. The calibrated groundwater flow patterns were also found to be consistent with natural geochemical trends in groundwater chemistry in the region associated with the Phoenix ore deposit. Groundwater flow within the calibrated groundwater model is dominated by lateral flow within the overburden and Upper Sandstone aquifers, but also includes some flow through the deeper, Lower Sandstone Aquifer. Deep groundwater flow travels eastward within the Lower Sandstone Aquifer before moving upward through the remaining Athabasca Supergroup Sandstone and overburden deposits toward Whitefish Lake. This flow path is largely influenced by the interpreted Desilicified Zone, which is better described as a porous media rather than a fractured rock and that facilitates the connection between the Upper Sandstone Aquifer and Lower Sandstone Aquifer flow systems. From a water budget perspective, the calibrated groundwater flow model was used to identify that groundwater discharge to Whitefish Lake is primarily through the local groundwater flow system (i.e., Overburden and Upper Sandstone Aquifer), with a lesser component flowing from the Lower Sandstone Aquifer, through the Desilicified Zone, into the base of Whitefish Lake near its eastern shore.

Transport of dissolved constituents was simulated for post-decommissioning using a 3D geochemical reactive transport approach wherein the chemical reactions were computed using PHREEQC and the transport was computed using FEFLOW. In this manner, dissolved constituents were allowed to interact with the geologic media through which they are migrating, allowing physically-based adsorption, precipitation, redox and ion exchange reactions to be incorporated into the transport calculations. Transport of dissolved constituents generally followed predicted groundwater flow paths, with additional spreading of chemical concentrations from the plume centre-line due to dispersion. Dispersion acts to attenuate dissolved constituent concentrations in groundwater as time progresses and the dissolved plume migrates. In addition to the dispersion, geochemical reactions (e.g., sorption to reaction sites on minerals such as quartz, goethite, and clay) act to retard and further attenuate dissolved constituent concentrations in groundwater.

By accounting for these transport and fate processes, the simulated plumes of dissolved constituents sourced in the mining area were assessed throughout the future centuries period; they were found to reach maximum spatial extents within the Lower Sandstone Aquifer unit and the deeper part of the Desilicified Zone within 5,000 to 10,000 years, with elevated concentrations of COPCs generally remaining within these deep hydrogeologic units. Consequently, the conditions at Whitefish Lake are simulated to represent modest variations from the background conditions.

A suite of parameter and process uncertainty scenarios were performed to evaluate the potential for COPC concentrations in groundwater to reach Whitefish Lake at levels above/outside of GQSC. Fifteen additional scenarios are presented; all scenarios indicated that concentrations of most constituents would not exceed GQSC in groundwater at the lake. The exceptions include:

- constituents consistently simulated to be outside of GQSC because they are naturally elevated (iron and manganese) or are naturally below the GQSC range (pH); and
- A scenario with conservative dispersivity values wherein selenium and cobalt concentrations were simulated to exceed the GQSC to a moderate extent (1.1 and 1.2 times their GQSCs, respectively) and over a very localized area of the lake.

The 3D geochemical reactive transport model is considered conservative as not all potential attenuating processes are simulated, such as matrix diffusion. The geochemical reactions are site-specific and are well-founded on available literature and site-specific data. Transport analysis incorporates background conditions that were derived from groundwater quality observations throughout the site, geochemical reactions sites based on solid phase constituent concentrations and mineralogical assemblages from core analyses, and source conditions consistent with those observed during lab core leaching and flushing experiments.

5.1.1 Understanding of Post-Decommissioning Fate and Transport

Based on the detailed numerical modelling completed, the restored solution remaining within and surrounding the mining area following remediation in Decommissioning was predicted to result in no adverse conditions to the surface environment over the 'future centuries' period. Constituents dissolved and mobilized as part of the mining process are interpreted and simulated to react with, and sorb to mineral (quartz, clay, goethite) surfaces as they are transported away from the mining area.

Less reactive constituents such as chloride, sulphate and selenium are simulated to exhibit small increases in concentrations in groundwater reaching Whitefish Lake. Concentrations of all COPCs, with are simulated to remain below GQSC with the exceptions of iron, manganese and pH. For these parameters, concentrations/values in groundwater are outside of the GQSC under baseline conditions.

The validity of the simulation results was tested by performing a suite of over 16 process and parameter uncertainty scenarios. All scenarios produced similar results, providing enhanced confidence that the future predicted conditions at Whitefish Lake under the base case scenario represent the likely outcome. The consistency of the scenario results illustrates the capacity of the natural setting to attenuate COPC concentrations associated with restored mining solutions such that elevated concentrations will remain at depth, and concentrations that reach Whitefish Lake will be similar to existing, background conditions.

5.2 Limitations

5.2.1 Simplifications

As with any numerical model, the groundwater flow model developed for Denison's Phoenix deposit is a simplification of the real hydrogeologic setting. The development of the model follows Occam's Razor which can be paraphrased as "the simplest solution is most likely the right one" and is similar to Einstein's teachings that hypotheses "should be made as simple as it can be [to explain observed conditions], but not simpler." With respect to numerical modelling of groundwater flow and transport, the adoption of these principles infers that the model should only incorporate conceptual features, boundary conditions and parameter heterogeneity that are important to explain primary variations in observed data; where practical, generalized parameter distributions should be applied. In the context of groundwater modelling this is referred to as applying the "principle of parsimony" (Hill and Tiedeman, 2007).

Following this approach, simplifications contained within the calibrated numerical model include:

- Structure of the model layers is generalized to the interpreted hydrostratigraphic units for the Phoenix site.

- Hydrogeologic property values are applied uniformly for:

  - Sandy and till regions of the overburden,
  - Upper Sandstone Aquifer,
  - Intermediate Sandstone Aquitard, outside of the Desilicified Zone,
  - Desilicified Zone;
  - Lower Sandstone Aquifer beyond the immediate area of desilicified materials,
  - Paleoweathered bedrock zone, and
  - Basement aquitard

- Boundary conditions were applied only where surface water was mapped, or to allow regional groundwater inflow and outflow, where such flow was evident. No specified head or concentration boundary conditions exist within the numerical model footprint; they are only located at the model perimeter.

- Groundwater recharge was applied in two generalized zones, representing upland recharge (tills) and lowland recharge (sandy zones).

While natural variability of parameters is expected, the level of generalization applied replicates the observed groundwater flow conditions and produces an acceptable degree of calibration. As such, additional heterogeneity and complexity was not warranted.

In addition to the groundwater flow conceptualization, simplifications were also incorporated within the transport simulation approach applied as follows:

- Parameters such as dispersivity, and diffusion were applied uniformly throughout the model.

- Transport properties were assigned uniformly within hydrostratigraphic units that have the same effective porosity values.

- Reactive transport boundary conditions were applied uniformly within the shallow aquifer zones, and deep aquifer zones to represent average "background conditions" for areas of inflowing water.

- Reactive transport initial conditions were assigned uniformly within hydrostratigraphic units with the same effective porosity values.

- Geochemical reactions were assigned uniformly within hydrostratigraphic units with the same effective porosity values.

5.2.2 Assumptions

Assumptions that are inherent in the simulation results presented are outlined in the following section. These assumptions are consistent with the conceptual understanding, and would equally impact each scenario, so would not affect the comparison of results in each scenario.

- The regional groundwater system is assumed to have groundwater levels and gradients that are stationary and reflect a groundwater flow system that is in equilibrium. Observed water levels from monitoring wells are assumed to represent long-term average conditions. Thus, a steady-state groundwater flow simulation approach is appropriate.

- Groundwater recharge, pumping, and other hydraulic conditions were simulated to remain constant during the simulation period (i.e., 100,000 years into the future).

- Hydraulic conductivities values measured and interpreted through on-site fieldwork investigations are representative of conditions throughout the model footprint.

- Exploration coreholes that lie within the Desilicified Zone are interpreted to have collapsed and thus are interpreted to not act as preferential pathways.

- Surface water boundary conditions are assumed to be constant elevations in time, which allows groundwater discharge to be naturally simulated.

- The Desilicified Zone was delineated based on available geotechnical parameters collected within exploration coreholes including fracture frequency, friability, RQD, and similar data.

- Adsorption reactions occur throughout the model domain. Reaction sites are assumed to be uniformly available throughout the sub-surface parameter zones.

- Mineral distribution, and associated reaction sites are assumed to be uniformly distributed throughout each hydrogeologic unit. Samples collected by Denison are assumed to provide representative information regarding mineral content and availability.

At the time of this report, all these assumptions are believed to be reasonable and appropriate. In many cases (e.g., reaction site availability) even more conservative assumptions are applied in the prediction uncertainty assessment (Section 4.7).

5.2.3 Limitations

This report has been prepared for the exclusive use of Denison. Information, interpretations, and summary comments contained herein are provided for the purpose stated in the scope of modelling (Section 1.0). Under no circumstance may this information be used for purposes other than those specified unless formal authorization is provided.

This report must be read in its entirety as some sections could be falsely interpreted when taken individually or out-of-context. Further, the contents and findings of this document reference and rely on the contents of the baseline hydrogeology report (EcoMetrix, 2024a) and should not be interpreted independently. The final version of this report and its content supersedes any other text, opinion or preliminary version produced by EcoMetrix Incorporated.

Groundwater systems are naturally complex at a level that cannot be explicitly replicated, and conditions must be interpolated between observation and measurement points; as such, groundwater models are a simplification of nature. The validity and accuracy of the model depends on the amount and quality of data available for characterization and model calibration relative to the degree of complexity of the geologic setting, as well as the complexity of the groundwater flow and transport processes. For this assessment, the breadth of data collected provides confidence in the characterization as well as the numerical model calibration.

The groundwater modelling described in this report was conducted in a manner exceeding the level of care and skill typically exercised by engineering and science professionals currently practising under similar conditions. The developed model was used to refine understanding of the conceptualization by determining conceptual hypotheses that can successfully replicate observed conditions, and conversely those that cannot (i.e., model calibration). Typically, more than one conceptualization can replicate observed conditions and prediction uncertainty analyses were completed which incorporate multiple levels of conservatism.

The groundwater flow and reactive transport assessment provided in this report presents the understanding gained through completing the detailed model development, calibration, and predictive uncertainty assessments, and as such this work follows recognized professional approaches for numerical modelling (e.g., Anderson et al., 2015).

Despite the level of care employed, no warranty, express or implied, is made regarding individual modelling predictions. The insights gained through the breadth of modelling scenarios evaluated, in which multiple levels of conservatism were explored, should be used to guide decisions; decision confidence is strengthened because of the detailed approach followed and the bracketed outcome analysis provided.

6.0 References

AECL (Atomic Energy of Canada Ltd.), 1994. Final Report for the AECL/ SKB Cigar Lake Analog Study. Report No. AECL-10851. July.

Allen, N., Dai, C., Hu, Y., Kubicki, J.D., and Kabengi, N. 2019. Adsorption Study of Al3+, Cr3+, and Mn2+ onto Quartz and Corundum using Flow Microcalorimetry, Quartz Crystal Microbalance, and Density Functional Theory. ACS Earth and Space Chemistry. 3, 3. **https://doi.org/10.1021/acsearthspacechem.8b00148**.

Anderson, M.P. and W.W. Woessner. 2002. Applied Groundwater Modeling: Simulation of Flow and Advective Transport. Academic Press, San Diego, CA.

Anderson M.P., W.W. Woessner and R. J. Hunt. 2015. Applied Groundwater Modelling. Second Edition. Copyright Elsevier Inc.

Appelo, C.A.J, and A. Dimier. 2004. Geochemistry, Groundwater and Pollution: Learning by Modelling. U.S. Federal Agency Workshop. April, 2004.

Arai Y, Marcus MA, Tamura N, Davis JA, Zachara JM. 2007. Spectroscopic Evidence for Uranium Bearing Precipitates in Vadose Zone Sediments at the Hanford 300-area Site. Environ Sci Technol. 2007 Jul 1;41(13):4633-9. doi: 10.1021/es062196u. PMID: 17695908.

Bain, J.G., K. U. Mayer, D. W. Blowes, E.O. Frind, J.W.H. Molson, R. Kahnt, U. Jenk. 2001. Modelling the Closure-Related Geochemical Evolution of Groundwater at A Former Uranium Mine. Journal of Contaminant Hydrology 52 2001 109–135.

BC MOE (British Columbia Ministry of Environment), 2001. Water Quality Criteria for Aluminum: Overview Report. Water Protection and Sustainability Branch, Environmental Sustainability and Strategic Policy Division. August 7, 2001. Victoria, B.C.

BC MOE (British Columbia Ministry of Environment), 2014. Ambient Water Quality Guidelines for Selenium Technical Report Update., Water Protection and Sustainability Branch.

BC MECCS (British Columbia Ministry of Environment & Climate Change Strategy). 2021. British Columbia Approved Water Quality Guidelines: Aquatic Life, Wildlife & Agriculture. Water Protection & Sustainability Branch.

Bea, S.A., H. Wainwright, N. Spycher, B. Faybishenko, S. Hubbard. M. Denham. 2013. Identifying Key Controls on The Behavior of an Acidic-U(VI) Plume in The Savannah River Site Using Reactive Transport Modeling. Journal of Contaminant Hydrology 151 (2013) 34–54.

Bond, D.L.; Davis, J.A., and Zachara, J.M. 2007. Uranium(VI) Release from Contaminated Vadose Zone Sediments: Estimation of Potential Contributions from Dissolution and Desorption. US Department of Energy Publications. 198. **https://digitalcommons.unl.edu/usdoepub/198**

Bradbury M.H., Baeyens B., 2009. Sorption Modelling on Illite Part I: Titration Measurements and the Sorption of Ni, Co, Eu and Sn. Geochimica et Cosmochimica Acta.; 73:990–1003. doi: 10.1016/j.gca.2008.11.017

Cameco Corporation (Cameco). 2012. *Cameco Resources Smith Ranch Project Technical Report*. Nuclear Regulatory Commission Source Material License No. SUA-1548. License Renewal Application Technical Report.

Carvalho, F., Fernandes, S., Fesenko, S, Holm, E., Howard, B., et al., 2017. The Environmental Behaviour of Polonium. International Atomic Energy Agency, Vienna. Technical reports series No. 484.

CCME (Canadian Council of Ministers of the Environment), 1999. Canadian Water Quality Guidelines for the Protection of Aquatic Life: Chromium — Hexavalent Chromium and Trivalent Chromium., Canadian Environmental Quality Guidelines.

CCME (Canadian Council of Ministers of the Environment), 2008. Canadian Water Quality Guidelines.

CCME (Canadian Council of Ministers of the Environment), 2009. Canadian Water Quality Guidelines for the Protection of Aquatic Life: Boron., Canadian Environmental Quality Guidelines.

CCME (Canadian Council of Ministers of the Environment), 2010. Canadian Water Quality Guidelines for the Protection of Aquatic Life: Ammonia., Canadian Environmental Quality Guidelines.

CCME (Canadian Council of Ministers of the Environment), 2019. Canadian Water Quality Guidelines for the Protection of Aquatic Life: Manganese., Canadian Environmental Quality Guidelines.

Chapman, S.W., B. Parker, J. Cherry, P. Martin, D. Abbey, S.D. McDonald. 2014. Combined EPM-DFN Modelling Approach for Plume in Sedimentary Bedrock Aquifers. DFNE 2014-236.

Colon, C.F.J., Brady, P.V., Siegel, M.D., and Lindgren, E.R. 2000. Historical Case Analysis of Uranium Plume Attenuation. Prepared for U.S. Nuclear Regulatory Commission. SAND2000-2557J.

de Boissezon, H., L. Levy, C. Jakymiw, M. Distinguin, F. Guerin, M. Descostes, 2020. Modelling Uranium and 226Ra Mobility during and after Acidic In Situ Recovery Test (Dulaan Uul, Mongolia). Journal of Contaminant Hydrology, 235:103711.

Denison (Denison Mines), 2024a. Wheeler River Project. Environmental Impact Statement. February 2024.

Denison (Denison Mines), 2022b. Wheeler River Project, 3D Modelling of Hydrogeologic Units, Phoenix Deposit. Unpublished report by M. Tetland and S. Donmez, February 2022.

Denison (Denison Mines), 2022c. Pheonix – Clay Zones and Clay Speciation. Internal Memorandum from Mikkel Tetland to Chad Sorba. May 03, 2022.

Diersch, H., 2014. FEFLOW Finite Element Modeling of Flow, Mass and Heat Transport in Porous and Fractured Media. Springer, New York.

Doherty, J., 2015. Calibration and Uncertainty Analysis for Complex Environmental Models. Watermark Numerical Computing, Brisbane, Australia. ISBN: 978-0-9943786-0-6.

Doherty, J. 2018. PEST: Model-Independent Parameter Estimation User Manual, 7th ed. Brisbane, Queensland, Australia: Watermark Numerical Computing.

Dong, W., Brooks, S.C., 2006. Determination of the Formation Constants of Ternary Complexes of Uranyl and Carbonate with Alkaline Earth Metals (Mg2+, Ca2+, Sr2+, and Ba2+) Using Anion Exchange Method. Environmental Science & Technology 40, 4689–4695. **https://doi.org/10.1021/es0606327**

Dong, W., Wan, J., 2014. Additive Surface Complexation Modeling of Uranium (VI) Adsorption onto Quartz-Sand Dominated Sediments. Environmental Science & Technology 48, 6569–6577. **https://doi.org/10.1021/es0606327**

Dzombak, D.A., Morel, F.M.M., 1991. Surface Complexation Modeling: Hydrous Ferric Oxide. Wiley.

EC (Environment Canada), 2017. Federal Environmental Quality Guidelines: Cobalt., Canadian Environmental Protection Act, 1999. May.

ECCC (Environment and Climate Change Canada), 2016. Federal Environmental Quality Guidelines: Vanadium. Canadian Environmental Protection Act, 1999. May.

ECCC (Environmental and Climate Change Canada), 2020. Federal Environmental Quality Guidelines: Strontium. July.

Ecometrix (Ecometrix Incorporated), 2020. Wheeler River Project: Baseline Aquatic Environment Study. Report prepared for Denison Mines Corp., March 2020.

Ecometrix (Ecometrix Incorporated), 2024a. Wheeler River Project Baseline Geology and Hydrology. Report prepared for Denison Mines Corp., February 2024.

Ecometrix (Ecometrix Incorporated), 2024b. Appendix 12-A: Environmental Risk Assessment for Wheeler River. Report prepared for Denison Mines Corp., February 2024.

Freeze, R.A., and Cherry, J.A., 1979, Groundwater: Englewood Cliffs, NJ, Prentice-Hall, 604 p.

Gelhar, L.W., Welty, C., & Rehfeldt, K.R. (1992). A critical review of data on field-scale dispersion in aquifers. Water Resources Research 28, no. 7, 1955-1974.

Gorman-Lewis D., Burns P.C., Fein J.B., 2008. Review of Uranyl Mineral Solubility Measurements. J. Chem. Thermodynamics, 40:335–352. doi: 10.1016/j.jct.2007.12.004

Government of Saskatchewan, 2021. Saskatchewan Environmental Quality Guidelines. Last Accessed, December 22, 2021. **https://envrbrportal.crm.saskatchewan.ca/seqg/**.

Grenthe, I., Gaona, X., Plyasunov, A. V., Linfeng, R., Runde, W. H., Grambow, B., Konings, R. J., Smith, A. L., and Moore, E. E., 2020. Second Update on the Chemical Thermodynamics of Uranium, Neptunium, Plutonium, Americium and Technetium, vol 14, OECD Publications, Paris, France, 2020.

Guillaumont, R., Fanghanel, T., Neck, V., Fuger, J., Palmer, D.A., Grenthe, I., Rand, M.H., 2003. Update on the Chemical Thermodynamics of Uranium, Neptunium, Plutonium, Americium and Technetium. Elsevier.

Hill, M.R. and C.R. Tiedeman. 2007. Effective Groundwater Model Calibration: With Analysis of Data, Sensitivities, Predictions, and Uncertainty. John Wiley & Sons.

IAEA (International Atomic Energy Agency), 2001. M*anual of Acid in Site Leach Uranium Mining Technology*. IAEA-TECDOC-1239. Vienna. 283 p.

IAEA (International Atomic Energy Agency), 2010. Handbook of Parameter Values for the Prediction of Radionuclide Transfer in Terrestrial and Freshwater Environments. Report No. STI/DOC/010/472, Technical Reports Series No.472.

Iida, Y., Barr, L., Yamaguchi, T., Hemmi, K. 2016. Sorption Behavior of Thorium onto Montmorillonite and Illite. Journal of Nuclear Fuel Cycle and Environment, 23(1): 3-8.

Intera, 2013. Appendix A, Cameco Geochemical Modeling Report. Prepared for: Cameco Resources (USA). May 13, 2013.

Johnson, R.H., Grover, B.P.C., and Tutu, H. 2016. Prediction of Uranium Transport in an Aquifer at a Proposed Uranium In Situ Recovery Site: Geochemical Modeling as a Decision-Making Tool. In: Management of Hazardous Wastes. Eds: El-Din, H., Saleh, M., and Rahman, A. 53-67. 10.5772/61668

Kermeen, J.S., 1955. A Study of Some Uranium Mineralization in Athabasca Sandstone, Near Stony Rapids, Northern Saskatchewan, Canada. Master's Thesis, University of Saskatchewan, **http://hdl.handle.net/10388/etd-08082012-134529**

LaFlamme, B.D., Murray, J.W., 1987. Solid / solution interaction: The Effect of Carbonate Alkalinity on Adsorbed Thorium. Geochimica et Cosmochimica Acta 51, 243–250. February. **https://doi.org/10.1016/0016-7037(87)90235-3**

Lagneau, V., Regnault, O., and Descotes, M. 2019. Industrial Development of Reactive Transport: An Application to Uranium in situ Recovery. Reviews in Mineralogy and Geochemistry, 85, 499-528.

Melson, N.H., 2011. Sorption of Th onto Subsurface Geomedia. M.Sc. Thesis, Auburn University, Alabama. December 12, 2011. 62 pp.

Macdonald, C.C., 1980. Mineralogy and geochemistry of a precambrian regolith in the Athabasca Basin. Mastrers Thesis Submitted to the University of Saskatchewan.

Martin, P.J., B. Parker, S. Chapman, and K. Walton. 2019. Utilizing the DFN-M Framework to Inform Transport Modelling. Presentation at the American Geophysical Union (AGU).

Mathur, S.S. and Dzombak, D.A. 2006. Surface Complexation: Goethite. In, Surface Complexation Modelling, J. Lutzenkirchen (editor). Elsevier. p443.

Miller, N. C., 1993. Predicting Flow Characteristics of a Lixiviant in a Fractured Crystalline Rock Mass. United States Department of the Interior. Bureau of Mines: Report of Investigations 9457.

Moore, K. 2020. Numerical Reactive Transport Modeling of Soluble Mineral and Fluid Interactions in the Subsurface and Application to Sedimentary Geothermal Systems. Ph.D. Thesis Submitted to The University of Manitoba.

Mwenifumbo, C.J.; Bernius, G.R., 2007. Crandallite-group Minerals: Host of Thorium Enrichment in the Eastern Athabasca Basin, Saskatchewan. EXTECH IV: Geology and Uranium EXploration TECHnology of the Proterozoic Athabasca Basin, Saskatchewan and Alberta; by Jefferson, C W (ed.); Delaney, G (ed.); Geological Survey of Canada, Bulletin no. 588, 2007 p. 521-532; 1 CD-ROM, **https://doi.org/10.4095/223795**

Neuman, S.P. 1995. On advective dispersion in fractal velocity and permeability fields. Water Resources Research 31, no. 6: 1455–1460.

Newmans Geotechnique Inc. (2020). Wheeler River In-Situ Leach Surface Freezing Option Pre-Feasibility. Report to Denison Mines Ltd. August 2020.

Nicholai, J. 2015. 3D Reactive Transport Modeling of Wellfields for In-Situ Leaching Using the FEFLOW Plug-in piChem. Umwelt- und Ingenieurtechnik GmbH Dresden (UIT), Germany.

Parkhurst, D.L., Appelo, C.A.J., 2013. Description of Input and Examples for PHREEQC Version 3 - A Computer Program for Speciation, Batch-Reaction, One-Dimensional Transport, and Inverse Geochemical Calculations. U.S. Geological Survey Techniques and Methods Section A, Groundwater Book 6, Modeling Techniques, Denver, Colorado, pp. 497.

Parkhurst, D.L., Wissmeier, L., 2015. PhreeqcRM: A Reaction Module for Transport Simulators Based on the Geochemical Model PHREEQC. Adv Water Resour 83: 176–189.

Percival, J.B.M., 1989. Clay Mineralogy, Geochemistry, and Partitioning of Uranium within the Alteration Halo of the Cigar Lake Uranium Deposit, Sasketchewan, Canada. Ph.D. Submission. Carleton University, Ottawa, Ontario. November.

Petrotek, 2020. Interim Hydrogeologic Report - Wheeler River Project Phoenix Deposit. Unpublished report prepared for Denison Mines. March 2020.

Petrotek. 2022. Hydrologic Report, Summary of Findings, 2019-2021, Wheeler River Project. Unpublished report prepared for Denison Mines. January 2022. Prikryl, J.D., Jain, A., Turner, D.R., Pabalan, R.T., 2001. Uranium VI Sorption Behavior on Silicate Mineral Mixtures. Journal of Contaminant Hydrology, 47, 241–253.

Reimus, P.W., Dangelmayr, M.A., Clay, J.T., and Chamberlain, K.R. 2019. Uranium Natural Attenuation Downgradient of an In-Situ Recovery Mine Inferred from a Cross-Hole Field Test. Environmental Science and Technology, 53, 13, 7483–7493.

Schulze-Makuch, D. 2005. Longitudinal Dispersivity Data and Implications for Scaling Behavior. GROUND WATER 43, no. 3: 443–456.

Scibek, 2019. Hydrogeological Investigations of Test Area 1 & 2 Phoenix Deposit, Wheeler River Project, Saskatchewan. Matrix and Bulk Permeability, Porosity, Density Distribution and Description of Hydrogeologic Units. November.

Spitz, K., and J. Moreno, 1996. A Practical Guide to Groundwater and Solute Transport Modelling, John Wiley & Sons, Inc., New York, New York

Szabo, Z., Stackelberg, P.E., and Cravotta, C.A., III. 2020. Occurrence and Geochemistry of Lead-210 and Polonium-210 Radionuclides in Public-Drinking-Water Supplies from Principal Aquifers of the United States. Environmental Science & Technology. 2020, 54(12), 7236-724. DOI: 10.1021/acs.est.0c00192.

U.S. DOE (United States Department of Energy), 2019. A Graded Approach for Evaluating Radiation Doses to Aquatic and Terrestrial Biota. Report No. DOE-STD-1153-2019. February.

U.S. EPA (United States Environmental Protection Agency), 1999. Understanding Variation in Partition Coefficient, Kd, Values; Volume 1: The Kd model, Methods of Measurement, and Application of Chemical Reaction Codes. EPA 402-R-99-004A. August 1999.

U.S. EPA (United States Environmental Protection Agency), 2005. Partition Coefficients for Metals in Surface Water, Soil, and Waste. Report No. EPA/600/R-05/074. July.

U.S. EPA (United States Environmental Protection Agency), 2012. Ground Water Modeling Studies at In Situ Leaching Facilities and Evaluation of Doses and Risks To Off-Site Receptors from Contaminated Ground Water. Revision 2. December 2012.

White, J.T., Hunt, R.J., Fienen, M.N., and Doherty, J.E., 2020, Approaches to Highly Parameterized Inversion: PEST++ Version 5, a Software Suite for Parameter Estimation, Uncertainty Analysis, Management Optimization and Sensitivity Analysis: U.S. Geological Survey Techniques and Methods 7C26, 51 p., **https://doi.org/10.3133/tm7C26**.

White, J.T., 2018, A Model-Independent Iterative Ensemble Smoother for Efficient History-Matching and Uncertainty Quantification in very High Dimensions: Environmental Modelling & Software, v. 109, p. 191–201.

Wissmeier, L., 2016. piChem - A FEFLOW Plugin for Advanced Geochemical Reactions. MIKE powered by DHI, Hørsholm, Denmark, pp. 28.

Wissmeier, L., Barry, D.A., 2008. Reactive Transport in Unsaturated Soil: Comprehensive Modelling of the Dynamic Spatial and Temporal Mass Balance of Water and Chemical Components. Advances in Water Resources, 31(5): 858-875.

Yang Z, Kang M, Ma B, et al. Inhibition of U(VI) reduction by synthetic and natural pyrite. Environmental Science & Technology. 2014 Sep;48(18):10716-10724. DOI: 10.1021/es502181x. PMID: 25148405.

Zazzi, A. 2009. Chlorite: Geochemical properties, Dissolution kinetics and Ni(II) sorption. Doctoral Thesis in Chemistry KTH Chemical Science and Engineering Stockholm, Sweden, 2009

Zazzi, A., Jakobsson, A-M., Wold, S. 2012 Ni(II) sorption on natural chlorite. Applied Geochemistry, 27, 6, 1189-1193.

Appendix A Creation of Numerical Model Surfaces

Hydrostratigraphic Model Layers
The following sections outline the methodology and data sets used to create the hydrostratigraphic model layers represented in the regional scale groundwater flow model. The layers are discussed stratigraphically from ground surface to the bottom of the competent basement rock.

Ground Surface / Top of Overburden
The ground surface represented in the FEFLOW model is illustrated on Figure B1. The surface was provided by Denison at the onset of the project and was derived by stitching together two digital elevation model surfaces that joined on a west-east line at the Phoenix deposit. Some ground surface anomalies were noted at the interface between the two surface and these anomalies were smoothed in the FEFLOW model.

As illustrated on Figure B1 the ground surface elevation is highest on the drumlin ridges and lowest along the surface water features including Whitefish Lake (approximately 500 m asl) and McGowan Lake (494 m asl).

Top of Upper Sandstone Aquifer/ Bottom of Overburden
The surface representing the top of the Upper Sandstone Aquifer unit was the bottom of overburden surface that was created and provided by Denison in April 2020 ("overburden_Wheeler_bottom.grd").

The top surface of the unit is highest (510 m asl) in the southwest and declines in a northeasterly direction towards the western portion of Whitefish Lake where there is an interpreted deepening of the bedrock surface in an interpreted glacially scoured bedrock trough that is incised approximately 50 m into the surrounding topographic surface (Figure B2). The bedrock the centre of this trough has an elevation of approximately 400 m asl.

Top of Intermediate Sandstone Aquitard / Bottom of Upper Sandstone Aquifer
The surface representing the top of the Intermediate Sandstone Aquitard was created by the Ecometrix team by generating and interpreting cross-sections using normative clay values reported at each exploration borehole in the study area. The contact between the two was identified at the interface between the Upper Sandstone Aquifer that has normative clay content generally less than 4%, and the underlying Intermediate Sandstone Aquitard that has normative clay content greater than 4 to 6%. The contact was picked at each borehole where data was available and the elevations at the points were interpolated in FEFLOW to generate the continuous surface.

The top surface of the intermediate sandstone aquitard is highest (430 m asl) in the area southeast of the Phoenix deposit and declines to an elevation of approximately (390 m asl) in the area west of Phoenix near the Gryphon deposit (Figure B3).

Top of Lower Sandstone Aquifer / Bottom of Intermediate Sandstone Aquitard

Like the overlying surface, the top of the Lower Sandstone Aquifer was created by the Ecometrix project team by interpreting cross-sections using normative clay values reported at each exploration borehole in the study area. The contact between these two units in each borehole was picked at the elevation where normative clay was higher than 4% in the overlying aquifer, and less normative clay values in the underlying aquifer unit.

The top surface of the Lower Sandstone Aquifer varies from a high of 320 m asl at the highest point on the quartzite ridge (where the unit is absent) to a low of approximately 120 m asl in the western reaches of the study area near Kratchkowsky Lake (Figure B4).

Top of Clay Cap/ Bottom of Lower Sandstone Aquifer
The exact position of the clay cap overlying the ore zone was not defined by Petrotek or Denison, so was assumed to have a uniform thickness of 2 m overlying the ore zone. This surface was continuous only along the ore zone itself so the surface representing the unconformity was assigned in the areas of the model that lie outside the ore zone ("Unconformity_Detailed_Explicit_10m" provided in Feb 2021). As noted in the modelling report, the hydraulic conductivity values of the units above were assigned where the paleoweathered portion of the basement is interpreted to be absent, and the layer is minimally thin.

Top of Ore Zone / Bottom of Upper and Lower Barrier Zones
The surface representing the top of the ore was provided by Denison in April 2020 ("Mineralization_Phoenix_top"). This surface was continuous only along the ore zone itself so the surface representing the unconformity (minus one metre) was assigned in the areas of the model that lie outside the ore zone ("Unconformity_Detailed_Explicit_10m" provided in Feb 2021). As noted in the modelling report, the hydraulic conductivity values of the units above were assigned where the weathered basement aquitard is interpreted to be absent, and the layer has a minimal thickness.

Top of Paleoweathered Basement Aquitard / Bottom of Ore Zone
The surface representing the top of the weathered basement aquitard and the base of the ore zone was provided by Denison in April 2020 ("Mineralization_Phoenix_Bottom"). This surface was continuous only along the ore zone itself so the surface representing the unconformity (minus three metres) was assigned in the areas of the model that lie outside the ore zone ("Unconformity_Detailed_Explicit_10m" provided in Feb 2021). As noted in the modelling report, the hydraulic conductivity values of the units above were assigned where the basement aquifer is interpreted to be absent, and the layer has a minimal thickness.

Top of Competent Basement Aquitard/ Bottom of Weathered Basement
The surface representing the top of the Competent Basement Aquitard (and the base of the Weathered Basement Aquitard) was developed by Denison and provided to the Ecometrix team in February 2021("Baseofpaleoweatheredzone").

Bottom of Model
The bottom of the model was arbitrarily set at sea level

Appendix B Calibrated Hydraulic Conductivity Distributions by Model Layer

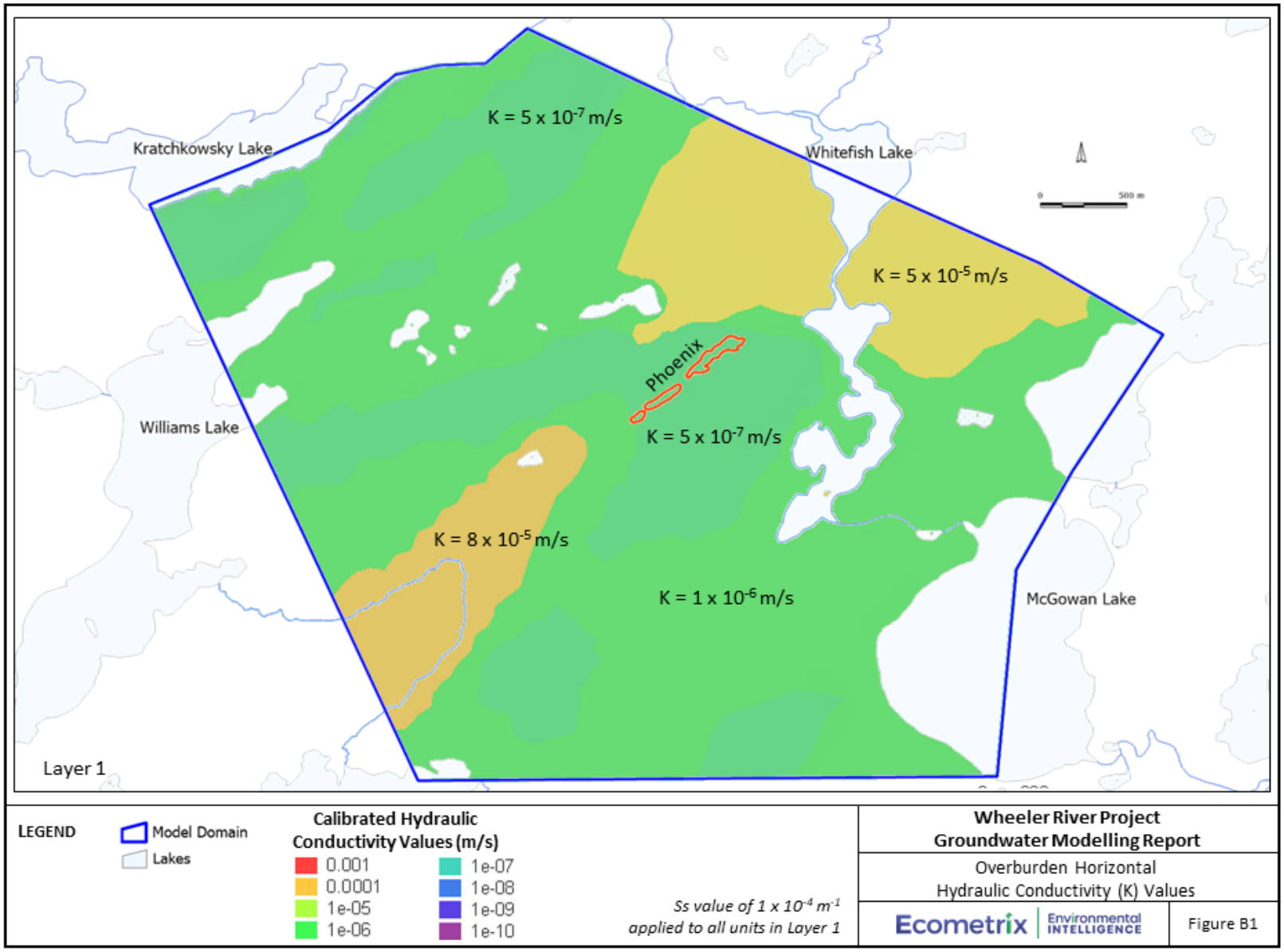
K = 5 x 10-7 m/s
Kratchkowsky Lake
Whitefish Lake
K = 5 x 10-5 m/s
Phoenix
Williams Lake
K = 5 x 10-7 m/s
K = 8 x 10-5 m/s
K = 1 x 10-6 m/s
McGowan Lake
Layer 1
LEGEND
Model Domain
Lakes
Calibrated Hydraulic Conductivity Values (m/s)
0.001
0.0001
1e-05
1e-06
1e-07
1e-08
1e-09
1e-10
Ss value of 1 x 10-4 m-1 applied to all units in Layer 1
Wheeler River Project
Groundwater Modelling Report
Overburden Horizontal Hydraulic Conductivity (K) Values
Ecometrix Environmental INTELLIGENCE
Figure B1

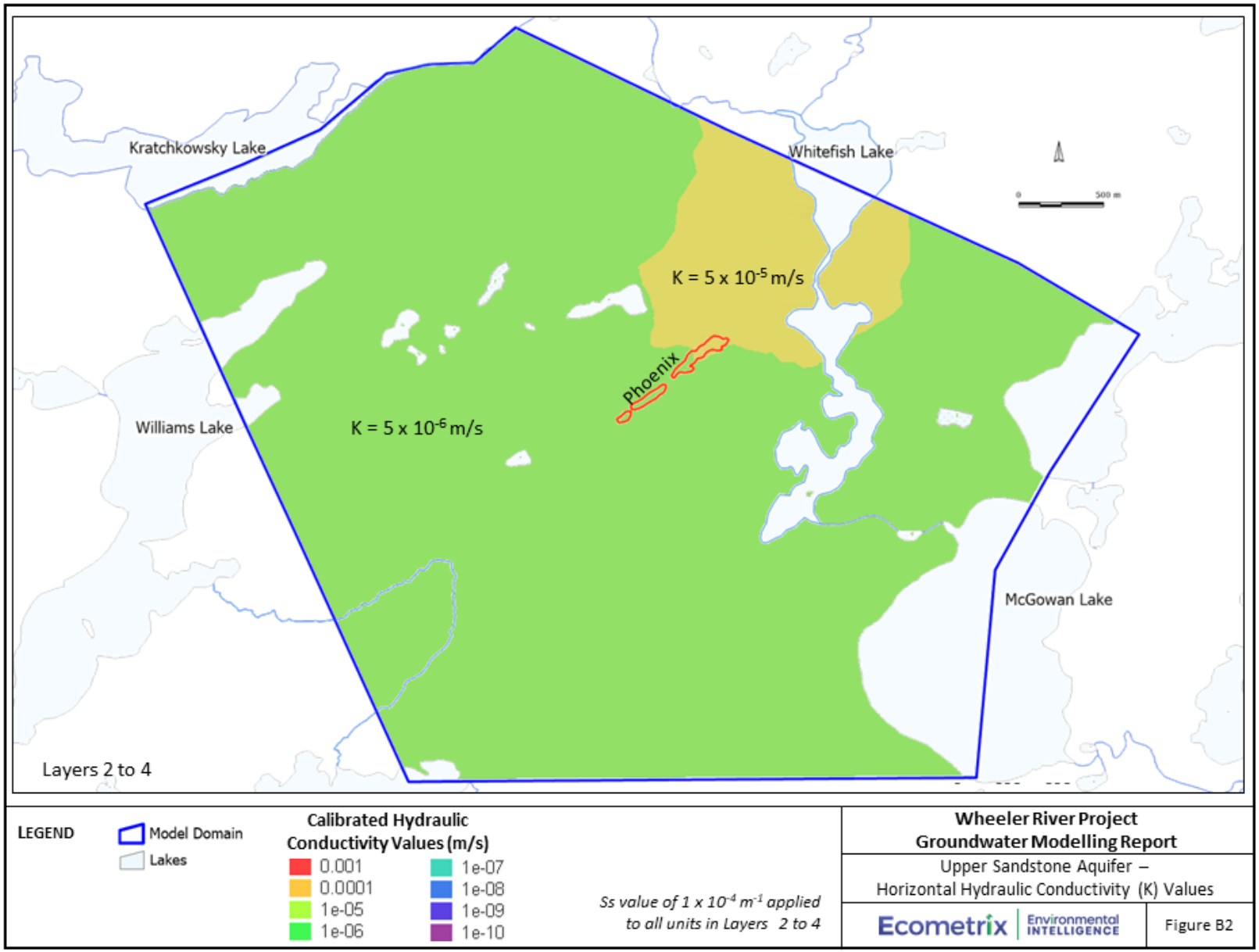
Kratchkowsky Lake
Whitefish Lake
K = 5 x 10-5 m/s
Phoenix
Williams Lake
K = 5 x 10-6 m/s
McGowan Lake
Layers 2 to 4
LEGEND
Model Domain
Lakes
Calibrated Hydraulic Conductivity Values (m/s)
0.001
0.0001
1e-05
1e-06
1e-07
1e-08
1e-09
1e-10
Ss value of 1 x 10-4 m-1 applied to all units in Layers 2 to 4
Wheeler River Project
Groundwater Modelling Report
Upper Sandstone Aquifer –
Horizontal Hydraulic Conductivity (K) Values
Ecometrix Environmental INTELLIGENCE
Figure B2

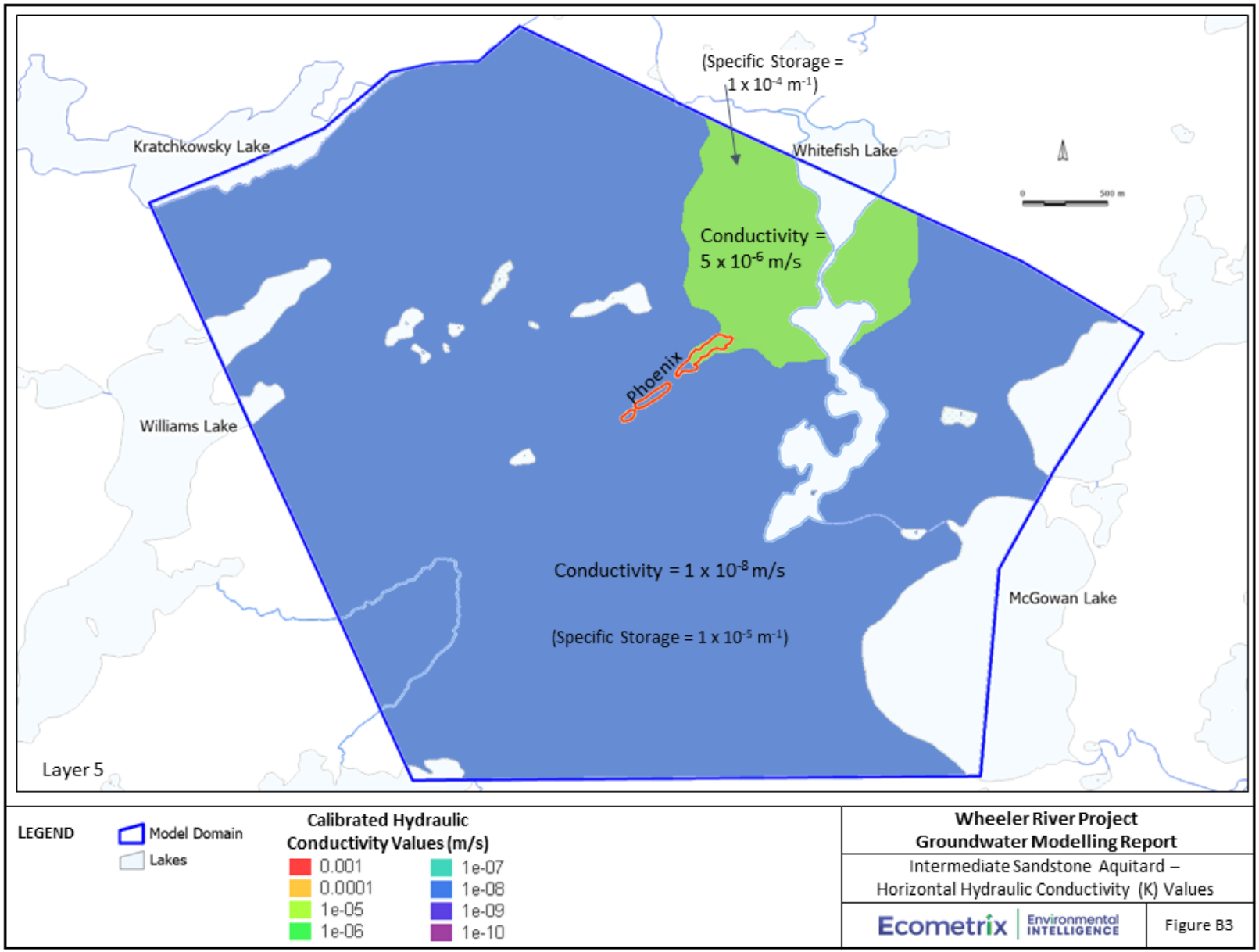
(Specific Storage = 1 x 10-4 m-1)
Kratchkowsky Lake
Whitefish Lake
Conductivity = 5 x 10-6 m/s
Phoenix
Williams Lake
Conductivity = 1 x 10-8 m/s
(Specific Storage = 1 x 10-5 m-1)
McGowan Lake
Layer 5
LEGEND
Model Domain
Lakes
Calibrated Hydraulic Conductivity Values (m/s)
0.001
0.0001
1e-05
1e-06
1e-07
1e-08
1e-09
1e-10
Wheeler River Project
Groundwater Modelling Report
Intermediate Sandstone Aquitard – Horizontal Hydraulic Conductivity (K) Values
Ecometrix Environmental INTELLIGENCE
Figure B3

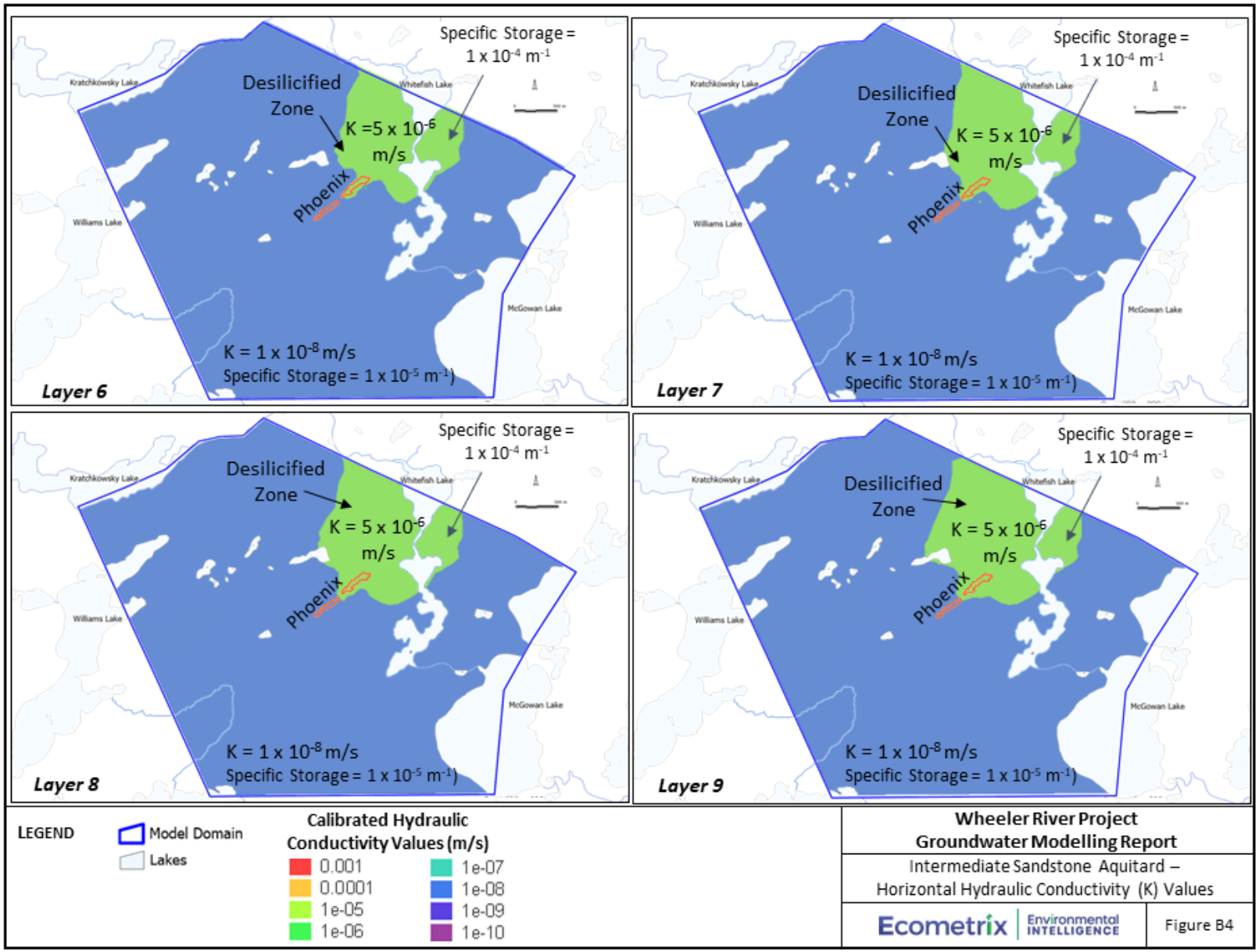
Specific Storage = 1 x 10-4 m-1
Desilicified Zone
K =5 x 10-6 m/s
Phoenix
Kratchkowsky Lake
Whitefish Lake
Williams Lake
McGowan Lake
K = 1 x 10-8 m/s
Specific Storage = 1 x 10-5 m-1)
Layer 6
Specific Storage = 1 x 10-4 m-1
Desilicified Zone
K = 5 x 10-6 m/s
Phoenix
K = 1 x 10-8 m/s
Specific Storage = 1 x 10-5 m-1)
Layer 7
Specific Storage = 1 x 10-4 m-1
Desilicified Zone
K = 5 x 10-6 m/s
Phoenix
K = 1 x 10-8 m/s
Specific Storage = 1 x 10-5 m-1)
Layer 8
Specific Storage = 1 x 10-4 m-1
Desilicified Zone
K = 5 x 10-6 m/s
Phoenix
K = 1 x 10-8 m/s
Specific Storage = 1 x 10-5 m-1)
Layer 9
LEGEND
Model Domain
Lakes
Calibrated Hydraulic Conductivity Values (m/s)
0.001
0.0001
1e-05
1e-06
1e-07
1e-08
1e-09
1e-10
Wheeler River Project
Groundwater Modelling Report
Intermediate Sandstone Aquitard –
Horizontal Hydraulic Conductivity (K) Values
Ecometrix Environmental INTELLIGENCE
Figure B4

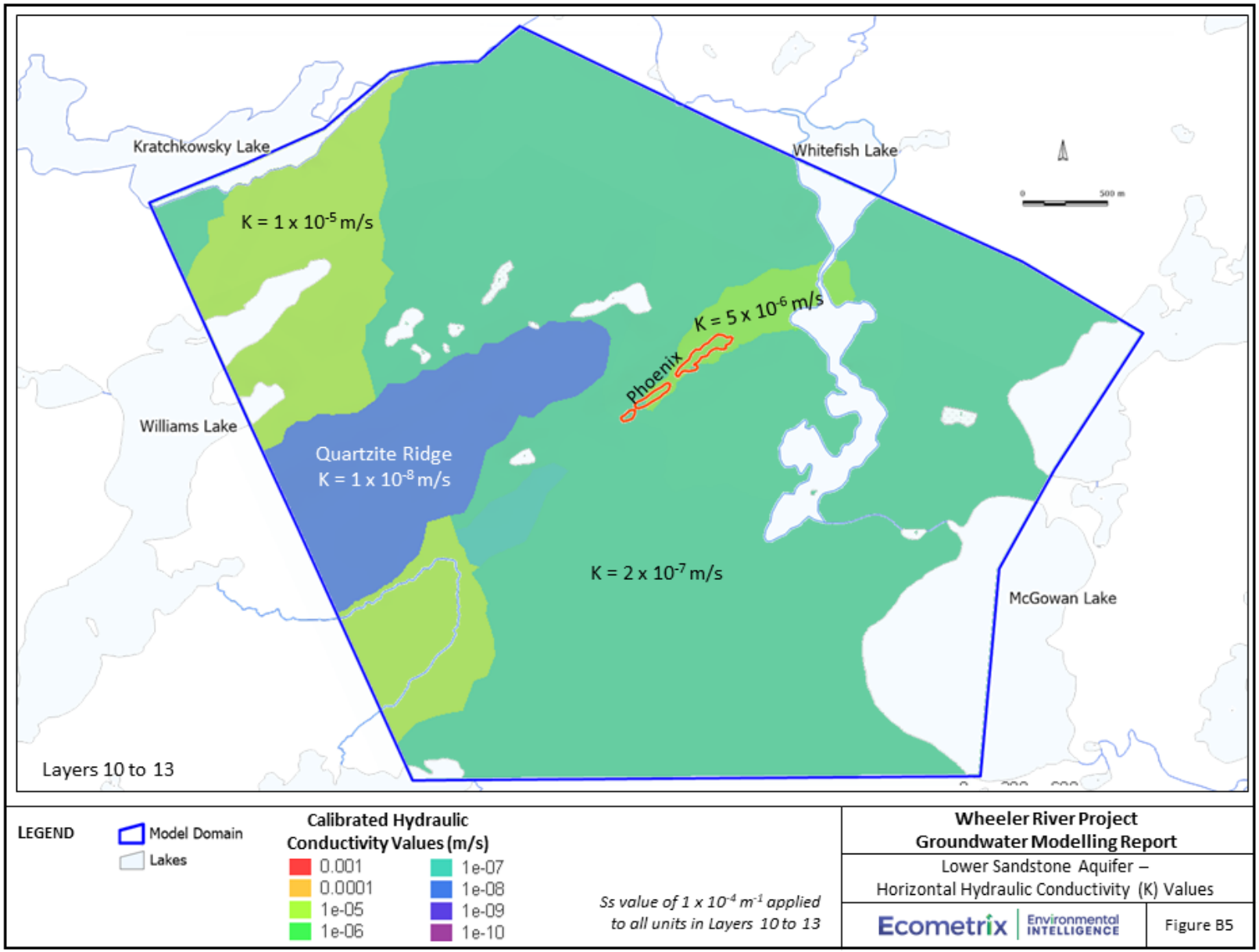
Kratchkowsky Lake
Whitefish Lake
K = 1 x 10-5 m/s
K = 5 x 10-6 m/s
Phoenix
Williams Lake
Quartzite Ridge
K = 1 x 10-8 m/s
K = 2 x 10-7 m/s
McGowan Lake
Layers 10 to 13
LEGEND
Model Domain
Lakes
Calibrated Hydraulic Conductivity Values (m/s)
0.001
0.0001
1e-05
1e-06
1e-07
1e-08
1e-09
1e-10
Ss value of 1 x 10-4 m-1 applied to all units in Layers 10 to 13
Wheeler River Project
Groundwater Modelling Report
Lower Sandstone Aquifer –
Horizontal Hydraulic Conductivity (K) Values
Ecometrix Environmental INTELLIGENCE
Figure B5

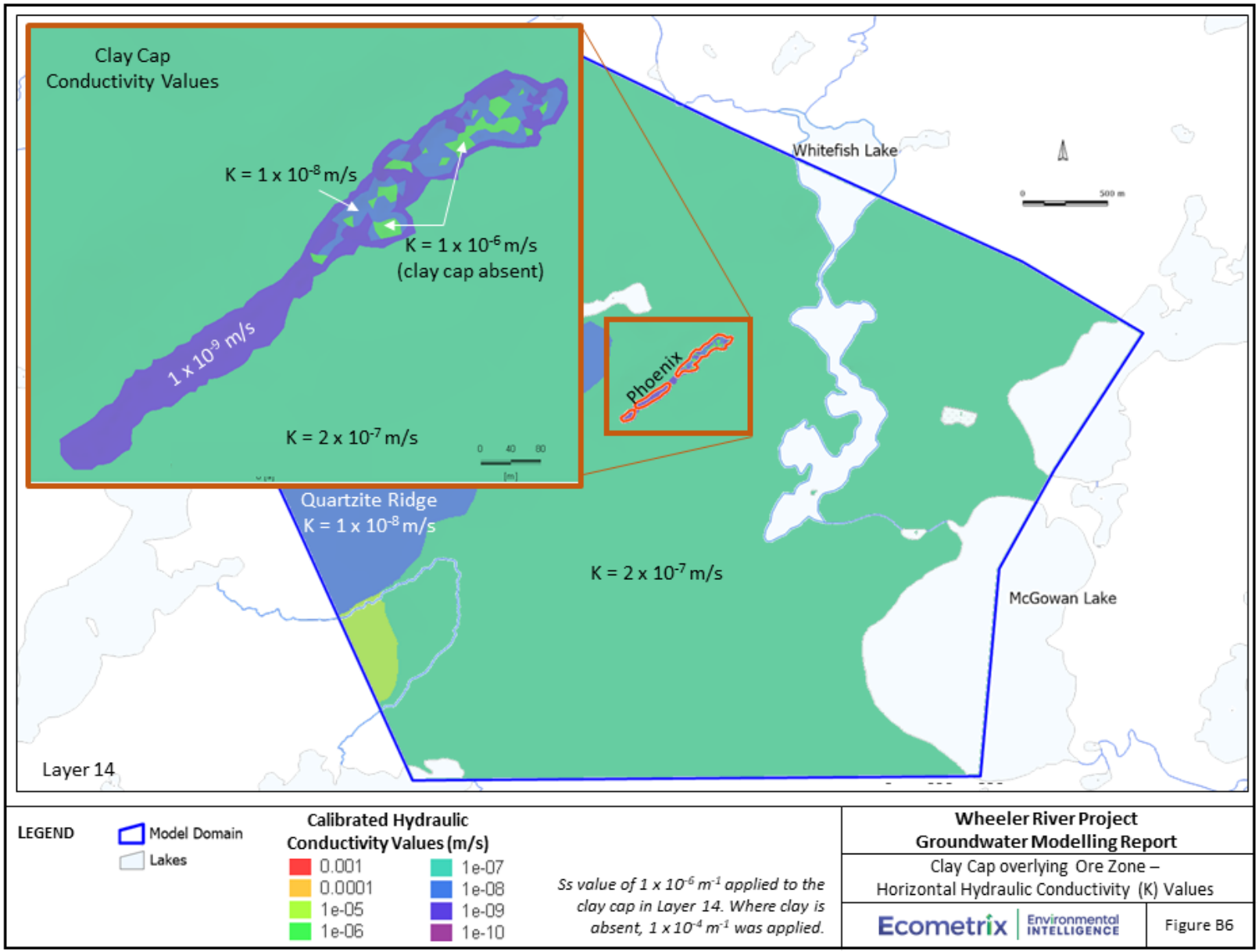
Clay Cap
Conductivity Values
K = 1 x 10-8 m/s
K = 1 x 10-6 m/s
(clay cap absent)
1 x 10-9 m/s
K = 2 x 10-7 m/s
Phoenix
Whitefish Lake
Quartzite Ridge
K = 1 x 10-8 m/s
K = 2 x 10-7 m/s
McGowan Lake
Layer 14
LEGEND
Model Domain
Lakes
Calibrated Hydraulic Conductivity Values (m/s)
0.001
0.0001
1e-05
1e-06
1e-07
1e-08
1e-09
1e-10
Ss value of 1 x 10-6 m-1 applied to the clay cap in Layer 14. Where clay is absent, 1 x 10-4 m-1 was applied.
Wheeler River Project
Groundwater Modelling Report
Clay Cap overlying Ore Zone –
Horizontal Hydraulic Conductivity (K) Values
Ecometrix Environmental INTELLIGENCE
Figure B6

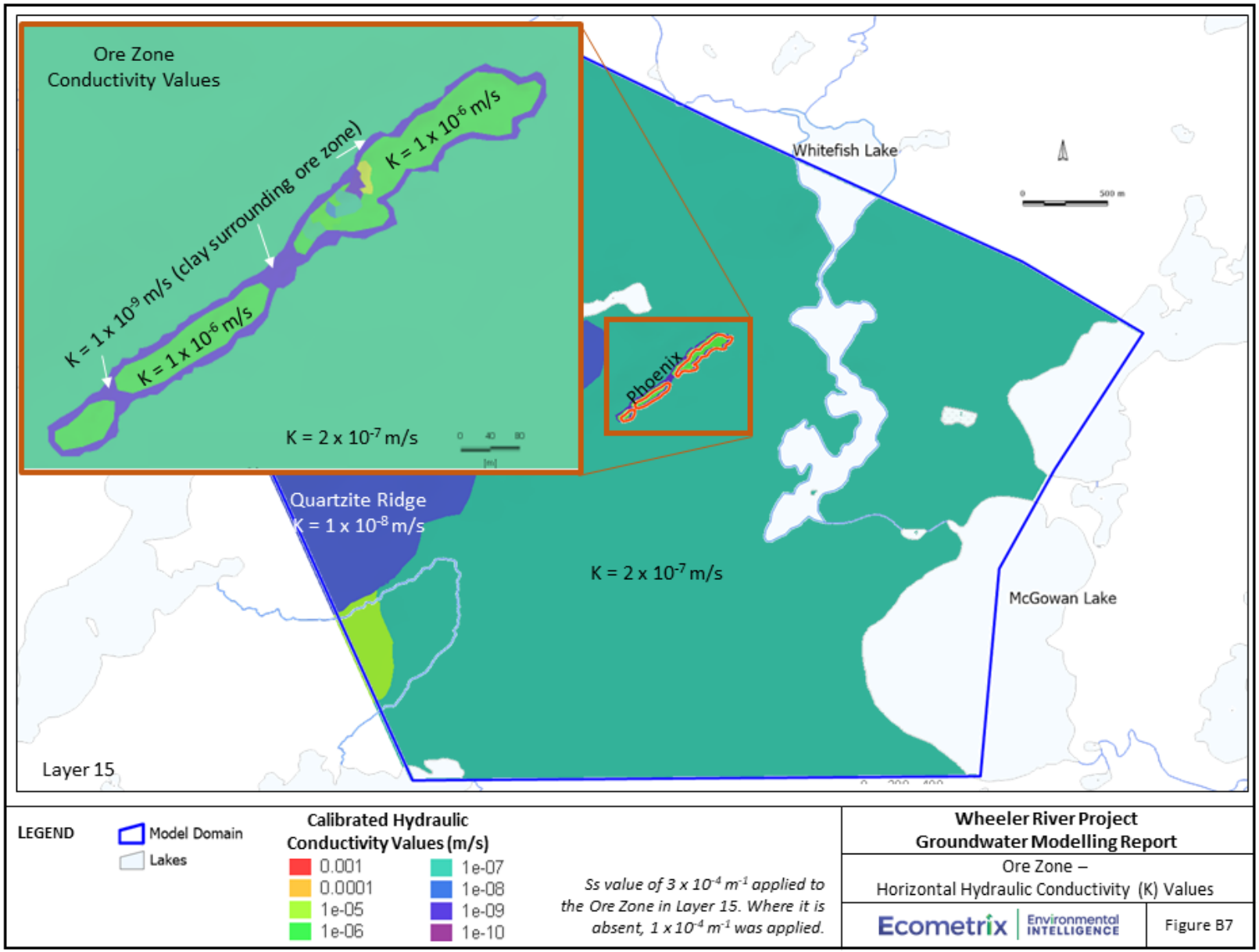
Ore Zone
Conductivity Values
K = 1 x 10-6 m/s
K = 1 x 10-9 m/s (clay surrounding ore zone)
K = 1 x 10-6 m/s
K = 2 x 10-7 m/s
Whitefish Lake
Phoenix
Quartzite Ridge
K = 1 x 10-8 m/s
K = 2 x 10-7 m/s
McGowan Lake
Layer 15
LEGEND
Model Domain
Lakes
Calibrated Hydraulic Conductivity Values (m/s)
0.001
0.0001
1e-05
1e-06
1e-07
1e-08
1e-09
1e-10
Ss value of 3 x 10-4 m-1 applied to the Ore Zone in Layer 15. Where it is absent, 1 x 10-4 m-1 was applied.
Wheeler River Project
Groundwater Modelling Report
Ore Zone –
Horizontal Hydraulic Conductivity (K) Values
Ecometrix Environmental INTELLIGENCE
Figure B7

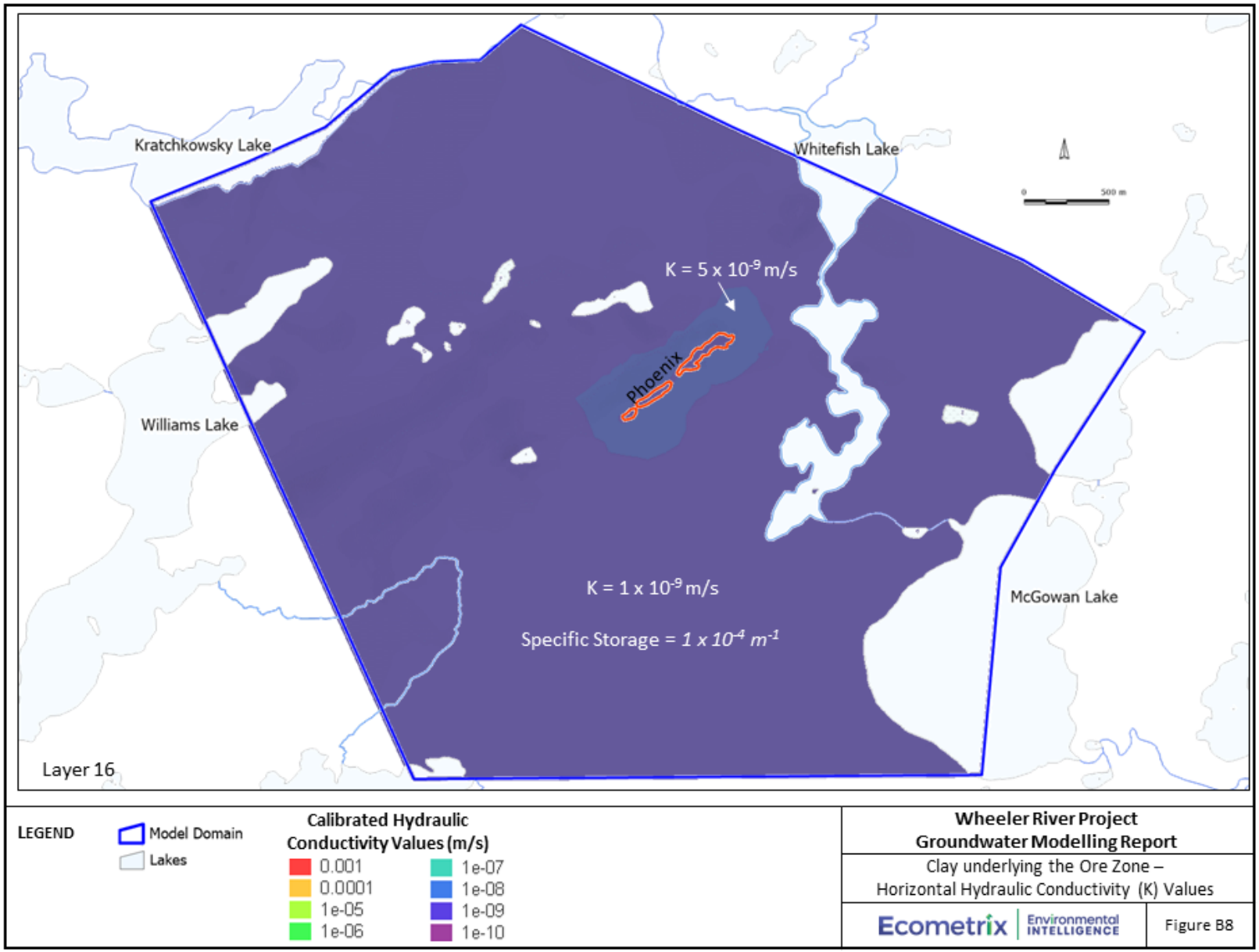
Kratchkowsky Lake
Whitefish Lake
0
500 m
K = 5 x 10-9 m/s
Phoenix
Williams Lake
K = 1 x 10-9 m/s
Specific Storage = 1 x 10-4 m-1
McGowan Lake
Layer 16
LEGEND
Model Domain
Lakes
Calibrated Hydraulic Conductivity Values (m/s)
0.001
0.0001
1e-05
1e-06
1e-07
1e-08
1e-09
1e-10
Wheeler River Project
Groundwater Modelling Report
Clay underlying the Ore Zone –
Horizontal Hydraulic Conductivity (K) Values
Ecometrix Environmental INTELLIGENCE
Figure B8

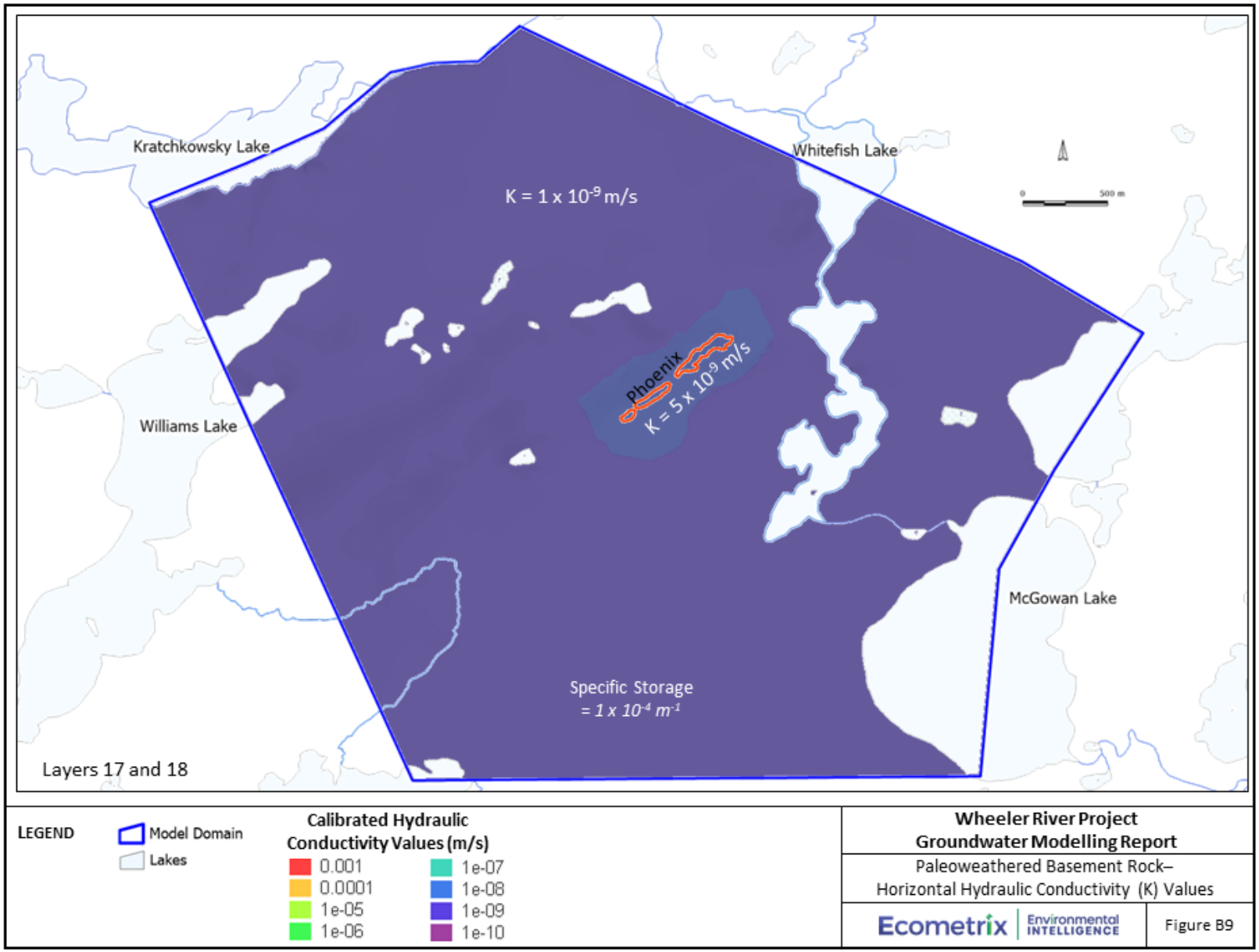
Kratchkowsky Lake
Whitefish Lake
K = 1 x 10-9 m/s
Phoenix
K = 5 x 10-9 m/s
Williams Lake
McGowan Lake
Specific Storage
= 1 x 10-4 m-1
Layers 17 and 18
LEGEND
Model Domain
Lakes
Calibrated Hydraulic Conductivity Values (m/s)
0.001
0.0001
1e-05
1e-06
1e-07
1e-08
1e-09
1e-10
Wheeler River Project
Groundwater Modelling Report
Paleoweathered Basement Rock–
Horizontal Hydraulic Conductivity (K) Values
Ecometrix Environmental INTELLIGENCE
Figure B9

Appendix C Model Layer Elevations

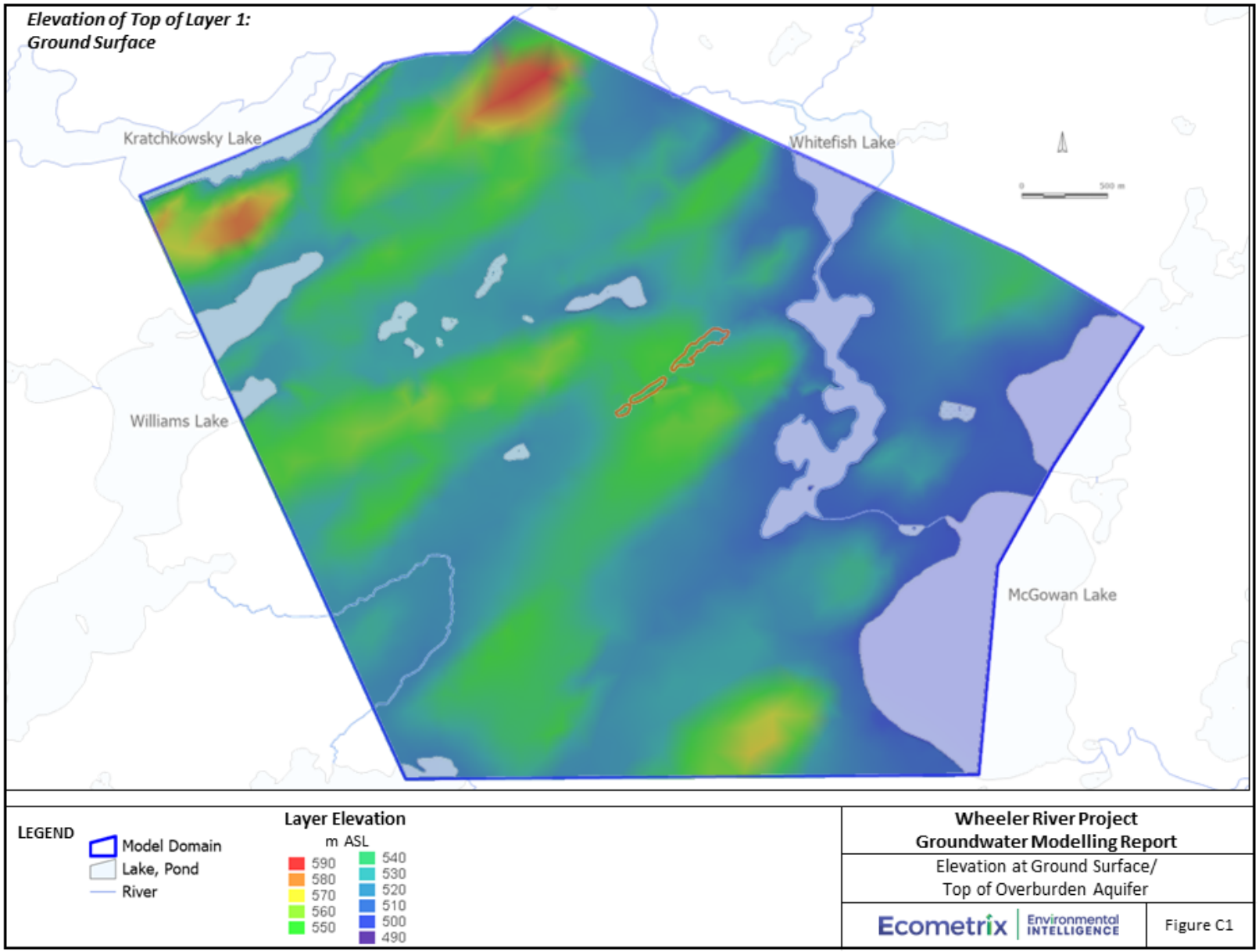
Elevation of Top of Layer 1:
Ground Surface
Kratchkowsky Lake
Whitefish Lake
Williams Lake
McGowan Lake
LEGEND
Model Domain
Lake, Pond
River
Layer Elevation
m ASL
590
580
570
560
550
540
530
520
510
500
490
Wheeler River Project
Groundwater Modelling Report
Elevation at Ground Surface/
Top of Overburden Aquifer
Ecometrix Environmental INTELLIGENCE
Figure C1

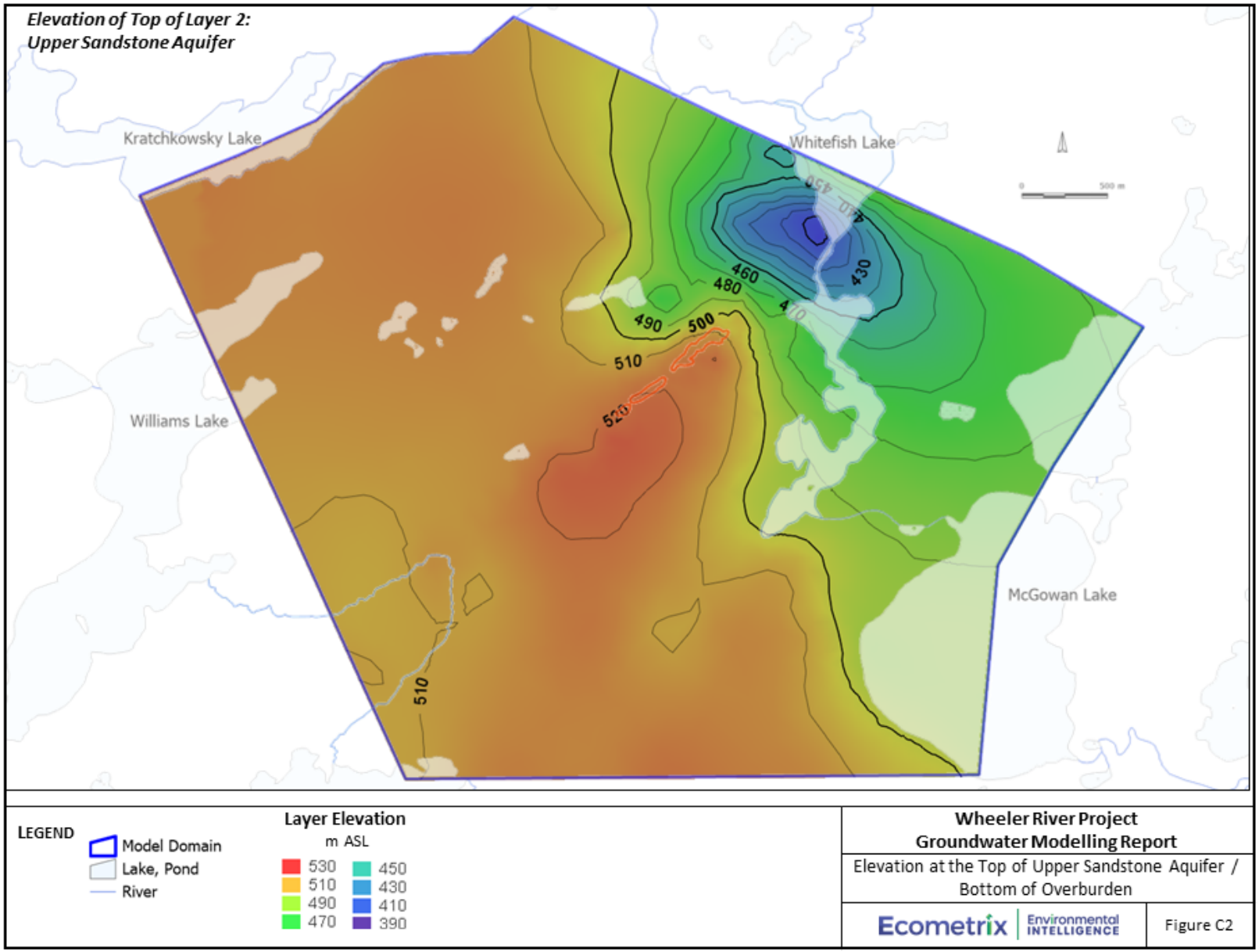
Elevation of Top of Layer 2:
Upper Sandstone Aquifer
Kratchkowsky Lake
Whitefish Lake
Williams Lake
McGowan Lake
430
460
480
490
500
510
520
510
LEGEND
Model Domain
Lake, Pond
River
Layer Elevation
m ASL
530
510
490
470
450
430
410
390
Wheeler River Project
Groundwater Modelling Report
Elevation at the Top of Upper Sandstone Aquifer / Bottom of Overburden
Ecometrix Environmental INTELLIGENCE
Figure C2

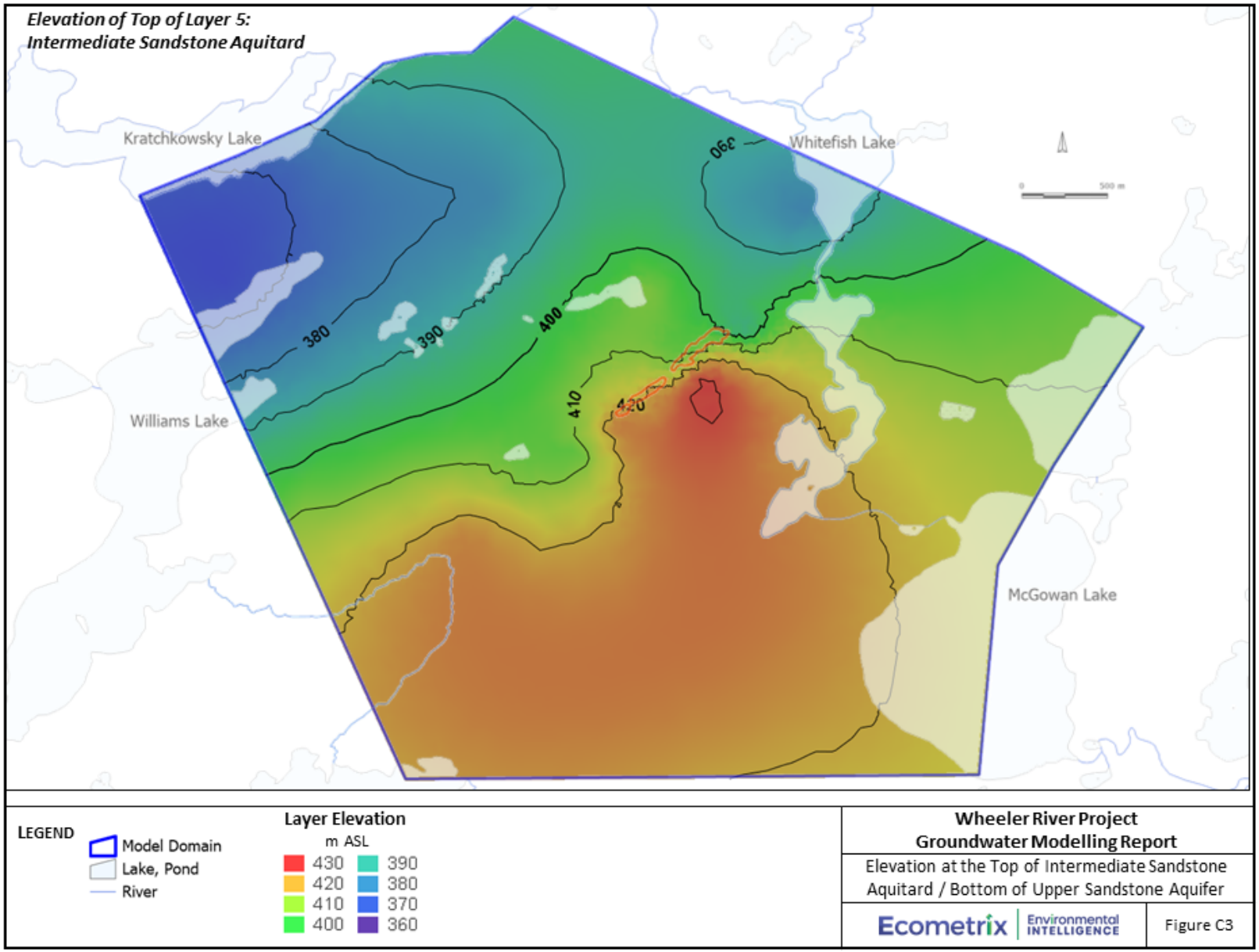
Elevation of Top of Layer 5:
Intermediate Sandstone Aquitard
Kratchkowsky Lake
Whitefish Lake
Williams Lake
McGowan Lake
380
390
400
410
420
430
0
500 m
LEGEND
Model Domain
Lake, Pond
River
Layer Elevation
m ASL
430
420
410
400
390
380
370
360
Wheeler River Project
Groundwater Modelling Report
Elevation at the Top of Intermediate Sandstone Aquitard / Bottom of Upper Sandstone Aquifer
Ecometrix
Environmental INTELLIGENCE
Figure C3

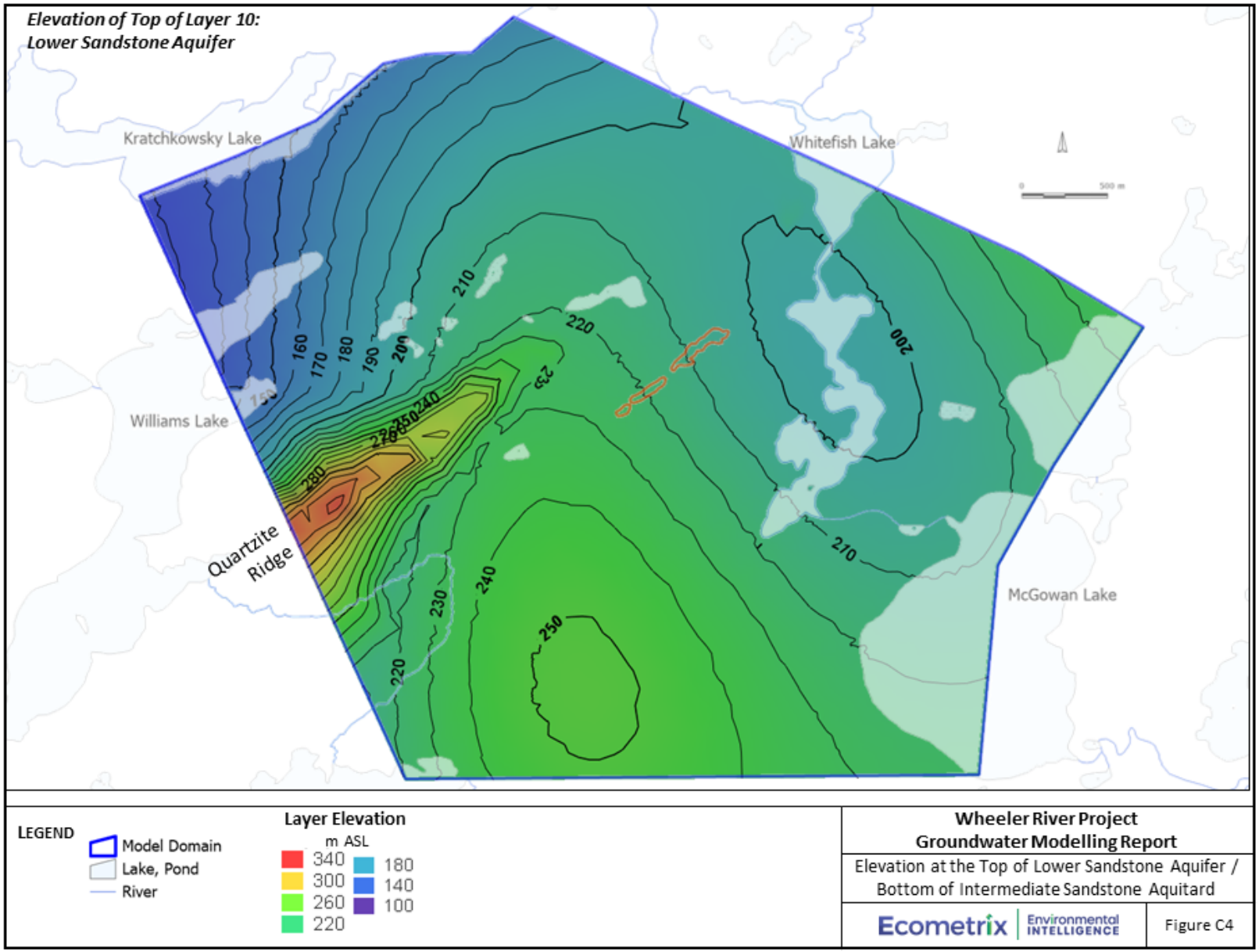
Elevation of Top of Layer 10:
Lower Sandstone Aquifer
Kratchkowsky Lake
Whitefish Lake
Williams Lake
Quartzite Ridge
McGowan Lake
160
170
180
190
200
210
220
230
240
250
260
270
280
LEGEND
Model Domain
Lake, Pond
River
Layer Elevation
m ASL
340
300
260
220
180
140
100
Wheeler River Project
Groundwater Modelling Report
Elevation at the Top of Lower Sandstone Aquifer / Bottom of Intermediate Sandstone Aquitard
Ecometrix Environmental INTELLIGENCE
Figure C4

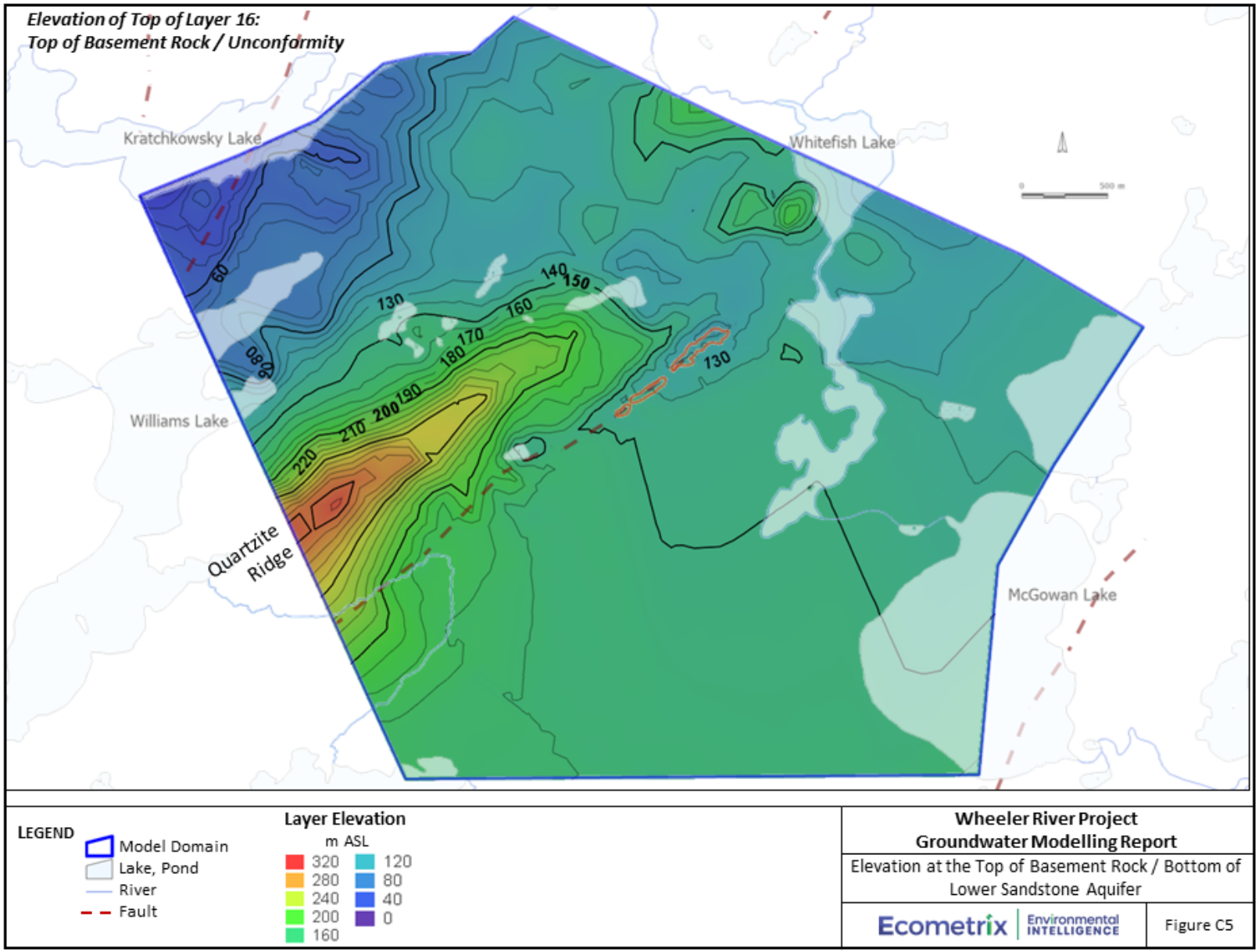
Elevation of Top of Layer 16:
Top of Basement Rock / Unconformity
Kratchkowsky Lake
Whitefish Lake
Williams Lake
Quartzite Ridge
McGowan Lake
60
130
140
150
160
170
180
190
200
210
220
130
LEGEND
Model Domain
Lake, Pond
River
Fault
Layer Elevation
m ASL
320
280
240
200
160
120
80
40
0
Wheeler River Project
Groundwater Modelling Report
Elevation at the Top of Basement Rock / Bottom of Lower Sandstone Aquifer
Ecometrix Environmental INTELLIGENCE
Figure C5

Appendix D Groundwater Chemistry

Hydrochemistry results for five (5) groundwater wells (GWR-038 through GWR-042) is included in the groundwater chemistry summary tables presented in this Appendix, but these wells do not appear in Table 3-4 or in the hydrochemistry discussion in Section 3.2.2. The groundwater quality results for those wells have been included herein for completeness, and borehole logs are provided for those wells in the Baseline Geology and Hydrogeology Report (Ecometrix, 2024a). However, water quality in those wells was compromised by inadvertent introduction of KCl. Groundwater quality associated with these wells was thus not used in modelling or in the calculation of summary statistics.

Table D-1: Existing, Pre-Mining, Groundwater Chemistry

Well Cluster	Units	Upgradient Cluster				NW Cluster[b]				SE Cluster[c]				WR-607 Cluster[d]						Downgradient Cluster					
Groundwater Monitoring Well		GWR-006		GWR-029		GWR-003		GWR-025		GWR-008		GWR-009		GWR-033		GWR-034		GWR-035		GWR-005		GWR-014		GWR-012	
Lithology		OB		Mfa		OB		MFa		MFa		MFb		MFa		MFb		OB / MFd		OB		MFc		MFa	
Hydrostratigraphic Unit		OB		LSA		OB		LSA		LSA/DSZ		ISA/DSZ		LSA		ISA		USA		OB		USA/DSZ		LSA/DSZ	
Sampling Date		2020-08-22	2021-04-14	2020-08-30	2021-04-12	2020-08-16	2021-04-18	2020-08-22	2021-04-17	2020-09-06	2021-04-09	2020-09-14	2021-04-10	2020-11-03	2021-05-25	2020-10-30	2021-05-24	2020-11-03	2021-05-24	2020-08-29	2021-05-22	2020-08-29	2021-05-21	2020-08-29	2021-05-23
Field Parameters																									
Field pH	pH units	6.75	6.90	6.46	7.30	6.35	5.86	6.49	7.06	6.92	7.42	10.87	7.67	7.02	7.32	8.77	7.57	6.48	6.30	7.49	6.8	11.38*	9.77	6.94	7.17
Field Temp.	°C	6.7	4.8	6.5	3.6	14.6	5.1	9.6	4.1	9.1	3.9	5.9	3.3	6.5	7.5	2.8	7.2	4.3	5.4	10.4	6.3	8.4	6.2	11.5	7.9
Field Conductivity	µS/cm	53.1	92.8	56.7	108	28.2	17.2	668	1392	71.9	98.9	153	362.1	229.9	461.9	303.3	666	40.3	71	68.2	97.5	275.6	270.3	351.8	602
ORP	mV	-	-	-	-	-	-	-	-	-	-	-	-	-	-	-	-	-	-	-	-	-	-	-	-
Field SPC	µS/cm	80.4	150.9	87.6	183.1	35.3	27.8	946	2315	102	165.7	241	618	351.4	694	520	1007	66.7	113.6	93.4	150.5	397.2	421.5	470.5	896
Field TDS	mg/L	52	98	57	119	23	18	615	1505	66	108	157	402	231	451	343	654	43	74	61	98	259	274	306	582
Diss. O2	mg/L	3.76	4.70	2.48	12.83	9.05	3.82	3.15	12.35	7.53	12.56	3.00	12.47	3.22	6.09	9.52	5.16	3.87	8.01	2.33	11.82	1.07	12.20	1.63	11.61
Fe2+	mg/L	1.0	1.3	2.0	-	0.0	0.0	2.0	1.0	2.5	1.5	0	1.5	2.0	1.0	0.0	0.0	0.5	0.0	2.0	1.5	0.0	0.0	2.0	1.5
Analytical Results																									
Bicarbonate	mg/L	35	35	33	29	12	17	51	35	55	39	<1	188	43	51	166	156	22	27	34	26	115	76	112	77
Carbonate	mg/L	<1	<1	<1	<1	<1	<1	<1	<1	<1	<1	49	<1	<1	<1	<1	<1	<1	<1	<1	<1	<1	18	<1	<1
Chloride	mg/L	10	1.4	6.1	6.1	0.1	<0.1	233	319	3	2.7	0.3	0.4	57	67	<1	<1	5.8	5.7	3.3	3.3	0.4	0.4	81	86
Hydroxide	mg/L	<1	<1	<1	<1	<1	<1	<1	<1	<1	<1	2	<1	<1	<1	<1	<1	<1	<1	<1	<1	<1	<1	<1	<1
P. alkalinity	mg/L	<1	<1	<1	<1	<1	<1	<1	<1	<1	<1	46	<1	<1	<1	<1	<1	<1	<1	<1	<1	<1	15	<1	<1
pH	pH units	7.04	7.32	7.14	7.36	6.76	6.88	6.9	6.96	7.44	7.16	10.06	7.59	7.48	7.43	8.07	7.63	7.04	6.79	6.99	6.8	7.68	9.05	7.62	7.24
Specific conductivity	µS/cm	71	61	72	68	27	19	918	1110	86	69	215	289	331	334	481	480	54	46	70	49	190	175	452	416
Sum of ions	mg/L	75	64	56	54	20	23	488	610	78	56	127	252	191	194	329	318	44	44	57	43	190	138	284	245
Total alkalinity	mg/L	29	29	27	24	10	14	42	29	45	32	87	154	35	42	136	128	18	22	28	21	94	92	92	63
Total hardness	mg/L	30	32	21	21	12	8	222	283	24	17	53	104	59	73	21	19	14	12	11	9	84	45	121	106
Ammonia as nitrogen	mg/L	0.15	0.17	0.03	0.05	0.09	<0.01	0.08	0.14	0.05	0.08	0.96	0.07	0.12	0.27	0.08	0.19	<0.01	0.03	<0.01	0.01	3.4	1.9	0.35	0.33
Nitrate (calc. from NO2+NO3-N)	mg/L	0.09	0.09	<0.04	<0.04	<0.04	0.13	<0.04	<0.04	<0.04	<0.04	0.04	<0.04	<0.04	<0.04	<0.04	0.09	<0.04	0.04	<0.04	<0.04	0.09	<0.04	<0.04	<0.04
Nitrite	mg/L	<0.03	0.05	<0.03	<0.03	<0.03	<0.03	<0.03	<0.03	<0.03	<0.03	0.11	<0.03	<0.03	<0.03	<0.03	0.25	<0.03	<0.03	<0.03	<0.03	0.23	0.11	<0.03	<0.03
Nitrite+Nitrate as nitrogen	mg/L	0.02	0.02	<0.01	<0.01	<0.01	0.03	<0.01	<0.01	<0.01	<0.01	0.01	<0.01	<0.01	<0.01	<0.01	0.02	<0.01	0.01	<0.01	<0.01	0.02	<0.01	<0.01	<0.01
Ortho-phosphate as P	mg/L	0.13	0.14	0.08	0.02	0.05	0.01	0.08	<0.01	0.12	0.16	0.04	0.2	<0.01	0.01	26	62	<0.01	0.01	0.05	0.02	<0.01	0.06	0.08	0.04
Organic carbon, dissolved	mg/L	2.4	1.3	1.6	1.2	1.4	0.8	2.2	1.1	7	1	10	33	3.4	2	8.7	7.9	2.1	0.4	0.5	0.7	18	8.3	4.1	1.9
Iron (II)	mg/L	-	0.04	-	0.02	-	<0.02	-	0.09	-	-	-	<0.02	-	-	-	-	-	-	-	0.07	-	<0.02	-	-
Fluoride	mg/L	0.14	0.14	0.09	0.1	0.04	0.03	0.21	0.21	0.07	0.17	0.08	0.1	0.09	0.12	0.02	0.02	<0.01	0.02	0.09	0.11	0.08	0.18	0.01	0.24
Total dissolved solids	mg/L	199	178	71	82	64	63	566	653	72	59	139	264	132	209	375	402	50	45	75	51	160	142	274	250
Total suspended solids	mg/L	838	413	<1	6	133	<1	7	17	3	4	9	13	10	8	3	6	3	<1	18	20	13	24	10	26
Calcium	mg/L	4.9	5.2	5.6	5.3	2.9	2.4	66	84	6.8	4.7	20	29	18	23	7.7	6.7	3.5	3	2.9	2.3	33	17	37	31
Magnesium	mg/L	4.3	4.7	1.7	1.9	1.1	0.5	14	18	1.8	1.2	0.8	7.6	3.4	3.8	0.5	0.5	1.3	1	1	0.8	0.4	0.7	7	6.9
Potassium	mg/L	1.8	1.5	1.6	1.5	1	0.3	3.5	4.1	1.7	1.5	8.6	1.2	2.1	2.1	149	148	1.1	0.7	1.1	1.2	6.3	4.4	4.4	3.7
Sodium	mg/L	12	9	5.3	5.5	2.1	1.7	68	83	8.6	5.4	21	23	36	30	3.7	3.9	4.9	3.9	10	6.1	21	15	36	32
Sulfate	mg/L	6.4	7	2.4	4.2	1	0.9	52	67	0.7	0.9	24	2.5	31	17	1.8	2.2	5.9	3	4.5	3	10	4.2	5.9	8.1

Notes

a Monitoring Well GWR-028, completed in the MFb and part of the Upgradient Cluster, could not be sampled because it is damaged

a Monitoring Well GWR-027, completed in the MFb and part of the Upgradient Cluster, could not be sampled because it is damaged

c Monitoring Well GRW-007, completed in Overburden, and part of the SE cluster, could not be sampled because it was dry

d The water quality in GRW-034 is considered to reflect influence from drilling fluids and additves, and is not considered reliable. Analysitcal well for this data is not used further in this baseline report.

e Monitoring Well GRW-002, completed in Overburden, and part of the SE cluster, could not be sampled because it was dry

f Radon-222 concentration estimated based on the daughter products of Lead-214 and Bismuth-214

g Samples sent to the A.E. Lalonde AMS Laboratory, University of Ottawa for Tritium analysis are in tritium units (TU) where 1TU=0.1191Bq/L. The final results are converted to Bq/L.

h Sample was taken at the end of a 48 hour long pumping test on GWR-032. 5,680 gallons were pumped from the well during the test before sampling and no field parameters available.

i The water quality in compromised by inadvertent introduction of KCl. Groundwater quality not used in model or to calculate summary statistics.

TableD-2: Existing, Pre-Mining, Groundwater Chemistry

Well Cluster	Units	LA-5 Cluster				Paloeweathered Zone		Phoenix Ore Zone[e]														
Groundwater Monitoring Well		GWR-036		GWR-037		GWR-031		GWR-011		GWR-013		GWR-032			GWR-038[i]	GWR-039[i]	GWR-040[i]		GWR-041[i]	GWR-042[i]	GWR-046	GWR-047	GWR-048
Lithology		OB		MFd		PWZ		MFa		MFb		OZ			OZ	OZ	OZ		OZ	OZ	MFc	MFb	Mfa
Hydrostratigraphic Unit		OB		USA/DSZ		PWZ		LSA/DSZ		ISA/DSZ		OZ			OZ	OZ	OZ		OZ	OZ	ISA	ISA/DSZ	LSA
Sampling Date		2020-11-05	2021-04-08	2020-10-24	2021-04-09	2020-08-09	2021-06-04	2020-08-08	2021-06-01	2020-08-09	2021-06-02	2019-11-14[i]	2020-08-08	2021-06-04	2021-09-04	2021-09-05	2021-09-01	2021-09-01 DUP	2021-09-06	2021-09-07	2021-09-14	2021-09-10	2021-09-10
Field Parameters																							
Field pH	pH units	6.45	6.62	6.13	6.02	7.03	7.21	8.70	6.82	9.68	7.35	-	6.79	6.83	7.54	6.74	6.84	6.84	6.88	6.71	6.37	6.47	6.08
Field Temp.	°C	4.4	3.4	4.8	4.1	11.3	16.8	17.5	7.2	10.5	7.8	-	8.0	18.5	7.7	8.9	11.3	11.3	8	8.6	10.24	9.51	8.44
Field Conductivity	µS/cm	18.3	42.8	26.4	49.1	588	1162	98.5	144.8	174.8	182.7	-	737	1486	7233	23173	11290	11290	9996	16567	136	97	111
ORP	mV	-	-	-	-	-	-	-	-	-	-	-	-	-	-	-	-	-	-	-	51.1	-84.5	-57.5
Field SPC	µS/cm	30.5	73.1	43.1	81.1	789	1374	114	219.2	238.4	271.5	-	958	1683	10811	33458	15302	15302	14820	24146	192	138	163
Field TDS	mg/L	20	48	57	53	513	893	74	142	155	176	-	623	1094	7027	21748	9947	9947	9633	15695	123	90	106
Diss. O2	mg/L	9.80	8.36	4.01	3.00	4.62	3.65	4.64	11.91	3.60	11.83	-	1.16	2.26	5.57	4.59	2.57	2.57	6.69	6.28	12.2	3.14	1.74
Fe2+	mg/L	0.0	0.0	0.5	1.0	0.5	0.0	0.0	1.0	0.0	1.0	-	1.5	1.5	-	-	-	-	-	-	-	-	-
Analytical Results																							
Bicarbonate	mg/L	30	16	15	16	167	160	54	41	105	85	155	174	118	104	40	76	76	80	61	86.3	75.2	57
Carbonate	mg/L	<1	<1	<1	<1	<1	<1	<1	<1	24	<1	<1	<1	<1	<1	<1	<1	<1	<1	<1	<1	<1	<1
Chloride	mg/L	0.2	<0.1	0.4	0.1	151	145	7.4	7.2	0.6	1.3	202	234	220	1600	4760	2560	2580	2270	3590	8.63	6.13	4.14
Hydroxide	mg/L	<1	<1	<1	<1	<1	<1	<1	<1	<1	<1	<1	<1	<1	<1	<1	<1	<1	<1	<1	<1	<1	<1
P. alkalinity	mg/L	<1	<1	<1	<1	<1	<1	<1	<1	20	<1	<1	<1	<1	<1	<1	<1	<1	<1	<1	-	-	-
pH	pH units	6.96	6.91	6.57	6.38	7.36	7.83	7.83	7.34	9.3	7.76	7.52	7.33	7.4	7.56	6.49	6.98	7.39	6.91	6.51	7.06	7.37	7.08
Specific conductivity	µS/cm	21	35	32	39	810	686	115	99	248	141	965	1000	860	5380	16100	7530	7530	7050	11530	277	160	139
Sum of ions	mg/L	47	28	32	29	504	439	92	71	210	126	566	598	504	3130	9220	4360	4350	4130	6760	-	-	-
Total alkalinity	mg/L	25	13	12	13	137	131	44	34	126	70	127	143	97	85	33	62	62	66	50	70.7	61.6	46.7
Total hardness	mg/L	16	14	8	6	190	148	38	26	57	48	267	256	182	614	2470	1830	1830	1340	1900	89.5	29.4	43.4
Ammonia as nitrogen	mg/L	<0.01	<0.01	0.04	0.02	0.05	0.35	0.26	0.13	0.68	0.02	-	0.31	0.73	-	44	12	12	18	-	0.026	<0.005	<0.005
Nitrate (calc. from NO2+NO3-N)	mg/L	0.49	0.49	<0.04	<0.04	<0.04	<0.04	<0.04	<0.04	0.04	0.13	<0.4	0.04	<0.04	0.04	<0.04	<0.04	<0.04	<0.04	<0.04	<0.02	<0.02	<0.02
Nitrite	mg/L	<0.03	<0.03	<0.03	<0.03	<0.03	<0.03	<0.03	<0.03	0.05	<0.03	-	<0.03	<0.03	-	<0.03	<0.03	<0.03	0.04	-	<0.01	<0.01	<0.01
Nitrite+Nitrate as nitrogen	mg/L	0.11	0.11	<0.01	<0.01	<0.01	<0.01	<0.01	<0.01	0.01	0.03	-	0.01	<0.01	0.01	<0.01	<0.01	<0.01	<0.01	<0.01	<0.05	<0.05	<0.05
Ortho-phosphate as P	mg/L	0.09	0.08	0.02	0.04	<0.01	0.01	0.11	0.12	0.03	0.06	-	<0.01	0.01	-	0.04	0.02	<0.01	0.02	-	-	-	-
Organic carbon, dissolved	mg/L	1.1	0.5	3.9	2	68	6.2	3.6	1	7.9	2	-	36	5.8	-	40	19	19	21	-	34.6	8.95	15.6
Iron (II)	mg/L	-	-	-	<0.02	-	<0.02	-	-	-	-	-	-	0.04	-	0.07	-	-	0.05	-	7.77	<0.02	2.3
Fluoride	mg/L	0.01	0.06	<0.01	0.01	0.32	0.42	0.2	0.18	0.13	0.08	0.22	0.19	0.23	0.27	0.14	0.21	0.21	0.21	0.18	0.059	0.074	0.142
Total dissolved solids	mg/L	112	66	90	55	536	393	101	98	182	177	639	628	599	3280	10400	4640	4080	4510	7830	188	132	122
Total suspended solids	mg/L	180	71	<1	<1	5	41	171	34	28	208	-	11	17	-	68	28	26	31	-	-	-	-
Calcium	mg/L	1.2	2.7	2	1.8	58	43	13	7.9	21	14	84	78	55	190	843	590	590	431	665	29.4	8.24	13.1
Magnesium	mg/L	3.2	1.8	0.7	0.4	11	9.9	1.3	1.6	1.1	3.1	14	15	11	34	90	88	88	64	58	3.91	2.14	2.6
Potassium	mg/L	5.3	2.8	1.9	1.8	5.5	5.3	2.4	2	6.7	1.8	5.6	5.4	4.6	955	3000	767	732	975	2000	6.77	4.46	1.89
Sodium	mg/L	3.9	2.9	3.6	2.8	71	69	8.4	6.1	34	15	75	83	81	137	189	203	205	154	152	8.96	18.6	8.87
Sulfate	mg/L	2.6	1.9	8	6.5	40	6.6	5.5	4.7	17	5.2	30	8	13	110	300	71	67	160	230	10.1	2.28	6.26

Notes

a	Monitoring Well GWR-028, completed in the MFb and part of the Upgradient Cluster, could not be sampled because it is damaged
a	Monitoring Well GWR-027, completed in the MFb and part of the Upgradient Cluster, could not be sampled because it is damaged
c	Monitoring Well GRW-007, completed in Overburden, and part of the SE cluster, could not be sampled because it was dry
d	The water quality in GRW-034 is considered to reflect influence from drilling fluids and additves, and is not considered reliable. Analysitcal well for this data is not used further in this baseline report.
e	Monitoring Well GRW-002, completed in Overburden, and part of the SE cluster, could not be sampled because it was dry
f	Radon-222 concentration estimated based on the daughter products of Lead-214 and Bismuth-214
g	Samples sent to the A.E. Lalonde AMS Laboratory, University of Ottawa for Tritium analysis are in tritium units (TU) where 1TU=0.1191Bq/L. The final results are converted to Bq/L.
h	Sample was taken at the end of a 48 hour long pumping test on GWR-032. 5,680 gallons were pumped from the well during the test before sampling and no field parameters available.
i	The water quality in compromised by inadvertent introduction of KCl. Groundwater quality not used in model or to calculate summary statistics.

Table D-3: Existing, Pre-Mining, Groundwater Chemistry

Well Cluster	Units	Upgradient Cluster[a]				NW Cluster[b]				SE Cluster[c]				WR-607 Cluster[d]						Downgradient Cluster					
Groundwater Monitoring Well		GWR-006		GWR-029		GWR-003		GWR-025		GWR-008		GWR-009		GWR-033		GWR-034		GWR-035		GWR-005		GWR-014		GWR-012	
Lithology		OB		Mfa		OB		MFa		MFa		MFb		MFa		MFb		OB / MFd		OB		MFc		MFa	
Hydrostratigraphic Unit		OB		LSA		OB		LSA		LSA/DSZ		ISA/DSZ		LSA		ISA		USA		OB		USA/DSZ		LSA/DSZ	
Sampling Date		2020-08-22	2021-04-14	2020-08-30	2021-04-12	2020-08-16	2021-04-18	2020-08-22	2021-04-17	2020-09-06	2021-04-09	2020-09-14	2021-04-10	2020-11-03	2021-05-25	2020-10-30	2021-05-24	2020-11-03	2021-05-24	2020-08-29	2021-05-22	2020-08-29	2021-05-21	2020-08-29	2021-05-23
Aluminum, dissolved	mg/L	0.0096	0.016	0.014	<0.0005	0.0065	0.0055	0.0024	<0.0005	0.0081	0.0023	0.012	0.21	0.025	0.0013	0.035	0.2	0.013	0.0058	0.0022	<0.0005	0.02	0.003	0.0038	<0.0005
Antimony, dissolved	mg/L	<0.0002	<0.0002	<0.0002	<0.0002	<0.0002	<0.0002	0.0003	<0.0002	0.0005	<0.0002	0.0055	<0.0002	<0.0002	<0.0002	0.0003	0.0007	<0.0002	<0.0002	<0.0002	<0.0002	0.002	<0.0002	<0.0002	<0.0002
Arsenic, dissolved	ug/L	1.3	0.8	0.3	<0.1	0.2	0.1	<0.1	<0.1	0.1	0.1	3.3	11	2.2	1.8	0.2	0.4	0.2	0.2	1.1	1.4	0.6	0.5	0.2	<0.1
Barium, dissolved	mg/L	0.0081	0.0095	0.0082	0.0053	0.0082	0.0056	0.12	0.11	0.1	0.042	0.059	0.22	0.059	0.059	0.011	0.018	0.015	0.016	0.024	0.015	0.15	0.11	0.25	0.15
Beryllium, dissolved	mg/L	<0.0001	<0.0001	<0.0001	<0.0001	<0.0001	<0.0001	<0.0001	<0.0001	<0.0001	<0.0001	<0.0001	<0.0001	<0.0001	<0.0001	<0.0001	<0.0001	<0.0001	<0.0001	<0.0001	<0.0001	<0.0001	<0.0001	<0.0001	<0.0001
Bismuth, dissolved	mg/L	<0.0002	<0.0002	<0.0002	<0.0002	<0.0002	<0.0002	<0.0002	<0.0002	<0.0002	<0.0002	<0.0002	<0.0002	<0.0002	<0.0002	<0.0002	<0.0002	<0.0002	<0.0002	<0.0002	<0.0002	<0.0002	<0.0002	<0.0002	<0.0002
Boron, dissolved	mg/L	0.01	0.01	0.04	0.04	<0.01	<0.01	0.32	0.4	0.03	0.03	<0.01	<0.01	0.04	0.05	<0.01	<0.01	<0.01	<0.01	0.03	0.03	0.02	0.02	0.15	0.15
Bromine	ug/L	22	18	85	79	<5	<5	2900	3600	40	34	<5	5	750	860	12	12	76	79	46	47	5	7	1000	1100
Cadmium, dissolved	mg/L	<0.00001	<0.00001	<0.00001	<0.00001	0.00001	0.00001	<0.00001	<0.00001	<0.00001	<0.00001	0.00001	0.00001	0.00001	<0.00001	0.00003	0.00006	0.00002	0.00001	<0.00001	<0.00001	<0.00001	<0.00001	<0.00001	<0.00001
Chromium, dissolved	mg/L	<0.0005	<0.0005	<0.0005	<0.0005	<0.0005	<0.0005	<0.0005	<0.0005	<0.0005	<0.0005	<0.0005	0.0058	<0.0005	<0.0005	0.0048	0.0019	<0.0005	<0.0005	<0.0005	<0.0005	<0.0005	<0.0005	<0.0005	<0.0005
Cobalt, dissolved	mg/L	0.0002	0.0002	<0.0001	<0.0001	0.0009	0.0003	<0.0001	<0.0001	<0.0001	<0.0001	<0.0001	0.0047	0.0005	0.0005	0.0003	0.0003	0.001	0.0012	<0.0001	<0.0001	<0.0001	<0.0001	<0.0001	<0.0001
Copper, dissolved	mg/L	0.0008	<0.0002	<0.0002	<0.0002	0.0017	0.0007	<0.0002	<0.0002	<0.0002	0.0007	0.0008	0.0011	0.0003	<0.0002	0.016	0.025	0.0005	0.0003	<0.0002	<0.0002	0.0004	0.0009	<0.0002	<0.0002
Iron, dissolved	mg/L	0.49	0.53	4.86	2.16	0.039	0.16	16	9.7	3.55	2.81	0.21	15.3	0.47	0.66	0.61	0.75	0.32	0.16	3.71	4.84	0.055	0.064	5.6	1.32
Lead, dissolved	mg/L	<0.0001	<0.0001	<0.0001	<0.0001	0.0001	<0.0001	<0.0001	<0.0001	<0.0001	<0.0001	<0.0001	0.0003	0.0002	<0.0001	0.011	0.0054	<0.0001	<0.0001	<0.0001	<0.0001	<0.0001	<0.0001	<0.0001	<0.0001
Lithium, dissolved	ug/L	8.5	9.1	11	13	0.8	0.8	32	40	12	9.9	9	6.3	14	15	0.4	0.7	4	3.1	11	11	12	14	26	28
Manganese, dissolved	mg/L	0.14	0.16	0.23	0.24	0.14	0.073	0.97	1.14	0.4	0.33	0.021	2.75	0.21	0.27	0.019	0.037	0.14	0.23	0.17	0.2	0.0018	0.0037	0.57	0.59
Molybdenum, dissolved	mg/L	0.0012	0.0007	0.0001	<0.0001	0.0012	<0.0001	0.0005	0.0002	0.0003	0.0002	0.0087	0.0038	0.003	0.0026	0.0007	0.0004	0.0008	0.0009	0.0023	0.0007	0.0024	0.0034	0.0023	0.0007
Nickel, dissolved	mg/L	0.0004	0.0004	0.0002	<0.0001	0.0021	0.0017	0.0002	<0.0001	0.0004	0.0002	0.0012	0.0053	0.0011	0.0008	0.0035	0.002	0.005	0.01	0.0003	<0.0001	0.0027	0.0015	0.0006	0.0002
Selenium, dissolved	mg/L	<0.0001	<0.0001	0.0011	<0.0001	<0.0001	<0.0001	<0.0001	<0.0001	<0.0001	<0.0001	<0.0001	<0.0001	0.0001	<0.0001	0.0001	<0.0001	<0.0001	<0.0001	<0.0001	<0.0001	<0.0001	0.0001	0.0002	<0.0001
Silica, soluble, dissolved	mg/L	23	24.2	17.4	17.2	16.5	17.6	17.8	16.8	25.8	23.9	19.5	30.3	10.9	12.2	5.2	6.9	20.3	19.1	19.9	20.4	15.5	16.3	24.4	21.2
Silver, dissolved	mg/L	<0.00005	<0.00005	<0.00005	<0.00005	<0.00005	<0.00005	<0.00005	<0.00005	<0.00005	<0.00005	<0.00005	<0.00005	<0.00005	<0.00005	<0.00005	<0.00005	<0.00005	<0.00005	<0.00005	<0.00005	<0.00005	<0.00005	<0.00005	<0.00005
Strontium, dissolved	mg/L	0.034	0.029	0.12	0.12	0.02	0.02	1.88	2.19	0.12	0.1	0.24	0.21	0.3	0.36	0.021	0.022	0.033	0.031	0.057	0.059	0.26	0.15	0.61	0.59
Sulfur	mg/L	2.1	2.3	0.8	1.4	0.33	0.3	17	22	0.23	0.3	8	0.8	10.3	5.7	0.6	0.7	1.97	1	1.5	1	3.3	1.4	2	2.7
Thallium, dissolved	mg/L	<0.0002	<0.0002	<0.0002	<0.0002	<0.0002	<0.0002	<0.0002	<0.0002	<0.0002	<0.0002	<0.0002	<0.0002	<0.0002	<0.0002	<0.0002	<0.0002	<0.0002	<0.0002	<0.0002	<0.0002	<0.0002	<0.0002	<0.0002	<0.0002
Tin, dissolved	mg/L	<0.0001	<0.0001	0.0002	<0.0001	<0.0001	<0.0001	<0.0001	<0.0001	<0.0001	<0.0001	<0.0001	<0.0001	<0.0001	<0.0001	0.0017	0.0032	<0.0001	<0.0001	<0.0001	<0.0001	<0.0001	<0.0001	<0.0001	<0.0001
Titanium, dissolved	mg/L	<0.0002	0.0003	<0.0002	<0.0002	<0.0002	<0.0002	<0.0002	0.0004	<0.0002	<0.0002	<0.0002	0.0034	<0.0002	<0.0002	0.0011	0.0051	<0.0002	<0.0002	<0.0002	<0.0002	<0.0002	<0.0002	<0.0002	<0.0002
Vanadium, dissolved	mg/L	<0.0001	<0.0001	<0.0001	<0.0001	0.0001	<0.0001	<0.0001	<0.0001	<0.0001	<0.0001	<0.0001	0.0018	<0.0001	<0.0001	<0.0001	0.0004	<0.0001	<0.0001	<0.0001	<0.0001	<0.0001	<0.0001	<0.0001	<0.0001
Zinc, dissolved	mg/L	0.0009	0.0041	0.001	0.0016	0.01	0.009	0.003	0.0026	0.0029	0.0016	0.0014	0.017	0.015	0.004	0.14	0.12	0.0025	0.0045	0.0064	0.0014	0.0007	0.0008	0.0007	0.002
Phosphorus, dissolved	mg/L	0.06	0.02	0.06	<0.01	<0.01	<0.01	0.09	<0.01	0.06	0.1	0.05	0.19	<0.01	0.01	58.4	61	<0.01	<0.01	<0.01	<0.01	0.03	0.07	0.1	<0.01
Radionuclides																									
Uranium, dissolved	ug/L	1.4	0.2	0.2	0.2	0.5	<0.1	0.8	<0.1	2.4	0.7	5.3	22	3.6	0.8	136	87	0.2	<0.1	0.5	0.5	0.3	1.2	0.5	<0.1
Uranium-234 calculated	Bq/L	0.043	0.002	0.004	0.002	0.1	0.001	0.024	0.001	0.043	0.009	0.13	0.27	0.047	0.011	2.4	1.2	0.002	0.003	0.037	0.01	0.037	0.017	0.011	0.002
Uranium-238 calculated	Bq/L	0.043	0.002	0.004	0.002	0.1	0.001	0.024	0.001	0.043	0.009	0.13	0.27	0.047	0.011	2.4	1.2	0.002	0.003	0.037	0.01	0.037	0.017	0.011	0.002
Lead-210	Bq/L	0.09	0.08	0.1	0.07	0.6	0.03	0.08	0.08	<0.02	0.66	0.3	1.1	0.14	0.04	22	5.7	0.03	<0.02	0.28	<0.02	0.08	0.3	0.15	0.1
Polonium-210	Bq/L	0.13	0.22	0.02	0.34	0.2	0.05	0.02	0.18	0.05	0.67	0.07	0.73	0.16	0.12	6.3	4.4	0.06	0.03	0.11	0.02	0.03	0.52	0.03	0.26
Radium-226	Bq/L	0.36	0.06	0.07	0.09	0.27	0.02	0.26	0.29	0.81	0.32	0.33	0.3	1.6	0.13	3.6	0.9	0.14	0.04	0.16	0.03	0.08	0.06	0.17	0.12
Radon-222	Bq/L	32	20	35	<10	86	18	7	<4	38	<4	<3	<4	20	<3	25	8	30	20	15	<5	11	<6	23	<4
Thorium-230	Bq/L	0.12	<0.02	<0.01	0.04	0.08	<0.01	<0.01	0.03	0.01	0.02	0.03	0.22	0.03	<0.01	2.6	0.44	<0.01	<0.01	0.04	<0.01	0.01	<0.01	<0.01	<0.01
Tritium	Bq/L	<15	0.1	<15	0.1	<15	1.1	<15	0.4	<15	0.5	16	1.2	<15	0.5	<15	1.2	<15	0.8	<15	<0.1	19	0.1	<15	<0.1

Notes

a	Monitoring Well GWR-028, completed in the MFb and part of the Upgradient Cluster, could not be sampled because it is damaged
a	Monitoring Well GWR-027, completed in the MFb and part of the Upgradient Cluster, could not be sampled because it is damaged
c	Monitoring Well GRW-007, completed in Overburden, and part of the SE cluster, could not be sampled because it was dry
d	The water quality in GRW-034 is considered to reflect influence from drilling fluids and additves, and is not considered reliable. Analysitcal well for this data is not used further in this baseline report.
e	Monitoring Well GRW-002, completed in Overburden, and part of the SE cluster, could not be sampled because it was dry
f	Radon-222 concentration estimated based on the daughter products of Lead-214 and Bismuth-214
g	Samples sent to the A.E. Lalonde AMS Laboratory, University of Ottawa for Tritium analysis are in tritium units (TU) where 1TU=0.1191Bq/L. The final results are converted to Bq/L
h	Sample was taken at the end of a 48 hour long pumping test on GWR-032. 5,680 gallons were pumped from the well during the test before sampling and no field parameters available.
i	The water quality in compromised by inadvertent introduction of KCl. Groundwater quality not used in model or to calculate summary statistics.

Table D-4: Existing, Pre-Mining, Groundwater Chemistry

Well Cluster	Units	LA-5 Cluster				Paloeweathered Zone		Phoenix Ore Zone[e]														
Groundwater Monitoring Well		GWR-036		GWR-037		GWR-031		GWR-011		GWR-013		GWR-032			GWR-038[i]	GWR-039[i]	GWR-040[i]		GWR-041[i]	GWR-042[i]	GWR-046	GWR-047	GWR-048
Lithology		OB		MFd		PWZ		MFa		MFb		OZ			OZ	OZ	OZ		OZ	OZ	MFc	MFb	Mfa
Hydrostratigraphic Unit		OB		USA/DSZ		PWZ		LSA/DSZ		ISA/DSZ		OZ			OZ	OZ	OZ		OZ	OZ	ISA	ISA/DSZ	LSA
Sampling Date		2020-11-05	2021-04-08	2020-10-24	2021-04-09	2020-08-09	2021-06-04	2020-08-08	2021-06-01	2020-08-09	2021-06-02	2019-11-14[h]	2020-08-08	2021-06-04	2021-09-04	2021-09-05	2021-09-01	2021-09-01 DUP	2021-09-06	2021-09-07	2021-09-14	2021-09-10	2021-09-10
Aluminum, dissolved	mg/L	0.15	0.037	0.48	0.06	<0.005	<0.0005	0.0082	0.052	0.025	0.011	0.21	0.0057	0.0006	-	0.005	<0.005	<0.005	0.01	-	0.8	0.0065	0.001
Antimony, dissolved	mg/L	<0.0002	<0.0002	<0.0002	<0.0002	<0.002	0.0003	0.0014	<0.0002	0.0008	<0.0002	0.0003	<0.0002	<0.0002	-	<0.002	<0.002	<0.002	<0.002	-	0.00024	<0.0001	<0.0001
Arsenic, dissolved	ug/L	0.2	0.3	0.4	1	1	1.2	4.1	1.3	3.1	0.9	3.4	0.3	0.2	-	<1	<1	<1	<1	-	4.75	3.71	0.85
Barium, dissolved	mg/L	0.0095	0.0057	0.0073	0.0087	0.052	0.035	0.21	0.054	0.041	0.11	0.088	0.083	0.063	-	0.96	0.52	0.52	0.35	-	0.241	0.0626	0.0577
Beryllium, dissolved	mg/L	0.0001	<0.0001	<0.0001	<0.0001	<0.001	<0.0001	<0.0001	<0.0001	<0.0001	<0.0001	0.0002	<0.0001	<0.0001	-	<0.001	<0.001	<0.001	<0.001	-	0.000167	<0.00002	<0.00002
Bismuth, dissolved	mg/L	<0.0002	<0.0002	<0.0002	<0.0002	<0.002	<0.0002	<0.0002	<0.0002	<0.0002	<0.0002	-	<0.0002	<0.0002	-	<0.002	<0.002	<0.002	<0.002	-	<0.00005	<0.00005	<0.00005
Boron, dissolved	mg/L	<0.01	<0.01	<0.01	<0.01	0.5	0.55	0.04	0.04	0.02	<0.01	0.58	0.59	0.43	-	0.4	0.5	0.5	0.5	-	0.023	0.018	0.041
Bromine	ug/L	<5	<5	<5	<5	1100	1500	100	100	8	<5	-	2300	2000	-	15800	9800	9800	6800	-	11	34	57
Cadmium, dissolved	mg/L	0.00001	<0.00001	0.00002	<0.00001	<0.0001	<0.00001	<0.00001	<0.00001	<0.00001	<0.00001	0.00001	<0.00001	<0.00001	-	<0.0001	<0.0001	<0.0001	<0.0001	-	0.0000336	<0.000005	<0.000005
Chromium, dissolved	mg/L	<0.0005	<0.0005	<0.0005	<0.0005	0.009	0.0008	<0.0005	<0.0005	<0.0005	<0.0005	0.013	0.0011	<0.0005	-	<0.005	<0.005	<0.005	<0.005	-	0.00169	<0.0005	0.00068
Cobalt, dissolved	mg/L	0.0004	0.0002	0.0005	0.0004	0.002	0.0002	<0.0001	<0.0001	<0.0001	0.0001	0.0007	<0.0001	<0.0001	-	0.003	0.001	0.001	0.002	-	0.00584	0.00025	0.00036
Copper, dissolved	mg/L	0.002	0.0006	0.0013	0.0009	<0.002	<0.0002	0.0006	0.0018	0.0006	0.0008	<0.0002	<0.0002	<0.0002	-	<0.002	<0.002	<0.002	<0.002	-	0.00629	<0.0002	<0.0002
Iron, dissolved	mg/L	0.12	0.014	1.64	1.38	3.6	0.09	0.012	0.86	0.086	0.014	3.83	6.4	4.2	-	23	8.2	7.7	18.2	-	6.03	11.9	9.62
Lead, dissolved	mg/L	0.0001	<0.0001	0.0002	<0.0001	0.001	<0.0001	<0.0001	0.0001	<0.0001	<0.0001	0.0003	0.0005	<0.0001	-	<0.001	<0.001	<0.001	<0.001	-	0.00157	<0.00005	<0.00005
Lithium, dissolved	ug/L	3	2.8	9.2	9	89	90	10	13	8.8	6.2	-	75	65	-	470	250	250	210	-	8.3	9.6	15.5
Manganese, dissolved	mg/L	0.048	0.039	0.12	0.16	0.22	0.13	0.085	0.36	0.026	0.22	0.2	0.24	0.22	-	1.8	0.85	0.83	0.87	-	3.91	2.14	2.6
Molybdenum, dissolved	mg/L	0.0003	0.0007	<0.0001	0.0028	0.062	0.012	0.028	0.0042	0.018	0.0054	0.078	0.0059	0.0038	-	0.008	0.011	0.011	0.045	-	0.00389	0.00374	0.00298
Nickel, dissolved	mg/L	0.0023	0.0018	0.0037	0.0023	0.04	0.0019	0.0003	0.0001	0.0024	0.0018	0.012	0.0014	0.001	-	0.056	0.019	0.02	0.024	-	0.0487	0.00062	0.00066
Selenium, dissolved	mg/L	0.0007	0.0008	0.0001	0.0004	<0.001	<0.0001	0.0001	<0.0001	0.0001	<0.0001	0.0001	<0.0001	<0.0001	-	0.003	0.002	0.002	0.002	-	0.000359	<0.00005	<0.00005
Silica, soluble, dissolved	mg/L	25.5	26.2	33.4	35.3	10	9.1	22.5	24.1	19.2	22.7	-	13.5	13.3	-	55.7	50.5	51.2	70.2	-	13.1	11.8	11.6
Silver, dissolved	mg/L	<0.00005	<0.00005	0.0001	0.00011	<0.0005	<0.00005	<0.00005	<0.00005	<0.00005	<0.00005	<0.00005	<0.00005	<0.00005	-	<0.0005	<0.0005	<0.0005	<0.0005	-	0.000046	<0.00001	<0.00001
Strontium, dissolved	mg/L	0.012	0.012	0.014	0.012	1.4	1.17	0.13	0.12	0.16	0.08	2.37	2.51	1.66	-	23.5	16.1	16.1	11.2	-	0.115	0.0796	0.169
Sulfur	mg/L	0.87	0.6	2.7	2.1	13	2.2	1.8	1.6	5.7	1.7	-	2.7	4.3	-	100	24	22	53.3	-	8.69	1.34	3.58
Thallium, dissolved	mg/L	<0.0002	<0.0002	<0.0002	<0.0002	<0.002	<0.0002	<0.0002	<0.0002	<0.0002	<0.0002	<0.0002	<0.0002	<0.0002	-	<0.002	<0.002	<0.002	<0.002	-	<0.00001	<0.00001	<0.00001
Tin, dissolved	mg/L	<0.0001	<0.0001	<0.0001	<0.0001	<0.001	<0.0001	<0.0001	<0.0001	0.0001	<0.0001	<0.0001	<0.0001	<0.0001	-	<0.001	<0.001	<0.001	<0.001	-	0.00033	<0.0001	<0.0001
Titanium, dissolved	mg/L	0.0009	0.0004	0.0048	0.0006	<0.002	<0.0002	<0.0002	<0.0002	<0.0002	<0.0002	0.0003	<0.0002	<0.0002	-	<0.002	<0.002	<0.002	<0.002	-	0.00897	<0.0003	<0.0003
Vanadium, dissolved	mg/L	0.0001	0.0004	<0.0001	<0.0001	<0.001	<0.0001	0.0005	<0.0001	0.0019	<0.0001	0.0074	0.0004	<0.0001	-	<0.001	<0.001	<0.001	<0.001	-	0.0012	<0.0005	<0.0005
Zinc, dissolved	mg/L	0.0061	0.0044	0.0067	0.0041	18.4	0.69	0.0018	0.012	0.001	0.0016	2.94	5	2.62	-	0.09	0.01	0.011	0.065	-	0.0125	0.0011	0.0031
Phosphorus, dissolved	mg/L	0.04	0.04	0.01	0.03	<0.1	<0.01	0.15	0.01	0.1	0.01	-	<0.01	<0.01	-	<0.1	<0.1	<0.1	<0.1	-	<0.05	0.13	0.289
Radionuclides																							
Uranium, dissolved	ug/L	0.9	0.1	5.8	0.8	17	50	9	0.7	14	55	299	5.7	11	504	38	10	10	10	564	22.6	0.752	0.488
Uranium-234 calculated	Bq/L	0.042	0.002	0.08	0.01	0.46	10.7	0.36	0.008	0.29	10.5	-	0.21	1.69	-	15.9	0.24	0.56	1	-	-	-	-
Uranium-238 calculated	Bq/L	0.042	0.002	0.08	0.01	0.46	10.7	0.36	0.008	0.29	10.5	-	0.21	1.69	-	15.9	0.24	0.56	1	-	-	-	-
Lead-210	Bq/L	0.14	0.07	0.08	0.05	1100	7300	0.6	0.3	0.4	8	1200	3300	2200	-	2700	5000	5000	2300	-	0.9	1.1	0.46
Polonium-210	Bq/L	0.08	0.05	0.14	0.11	460	650	0.4	0.3	0.4	13	120	260	110	-	460	700	600	420	-	0.65	0.14	1.3
Radium-226	Bq/L	0.22	0.06	0.19	0.03	120	76	1	0.5	0.5	17	300	400	180	-	6200	1500	1100	10000	-	0.93	0.24	0.75
Radon-222	Bq/L	17	20	64	57	5900	12000000	90	<8	34	41	400000[f]	2700000	3800000	-	6000000	6000000	6000000	4000000	-	11	1800	620
Thorium-230	Bq/L	<0.01	0.02	<0.01	<0.01	1.1	30	0.3	<0.1	0.2	4.7	14	2	7	-	21	6	10	6	-	0.2	<0.01	0.01
Tritium	Bq/L	<15	0.8	<15	0.1	<15	910	<15	0.1	<15	0.8	-	950	1800	-	RTR	<15	<15	RTR	-	<40	<40	<40

Notes

a	Monitoring Well GWR-028, completed in the MFb and part of the Upgradient Cluster, could not be sampled because it is damaged
a	Monitoring Well GWR-027, completed in the MFb and part of the Upgradient Cluster, could not be sampled because it is damaged
c	Monitoring Well GRW-007, completed in Overburden, and part of the SE cluster, could not be sampled because it was dry
d	The water quality in GRW-034 is considered to reflect influence from drilling fluids and additves, and is not considered reliable. Analysitcal well for this data is not used further in this baseline report.
e	Monitoring Well GRW-002, completed in Overburden, and part of the SE cluster, could not be sampled because it was dry
f	Radon-222 concentration estimated based on the daughter products of Lead-214 and Bismuth-214
g	Samples sent to the A.E. Lalonde AMS Laboratory, University of Ottawa for Tritium analysis are in tritium units (TU) where 1TU=0.1191Bq/L. The final results are converted to Bq/L.
h	Sample was taken at the end of a 48 hour long pumping test on GWR-032. 5,680 gallons were pumped from the well during the test before sampling and no field parameters available.
i	The water quality in compromised by inadvertent introduction of KCl. Groundwater quality not used in model or to calculate summary statistics.

Appendix E 1D Model Supporting Information

Elemental Concentrations in Rock for the Project

Table E-1: Solid Phase Elemental Concentrations

Median Metal/Trace Element Concentrations (mg/kg)	MFd (n= 2754-3077)	MFc (n= 7116-8532)	MFb (n= 5279-6086)	Mfa (n=9415-10,436)	Ore Zone			Paleoweathered Basement (n=108)
					Black or Brown Friable High Grade U Zone (n=95)	Brown Redox U Zone (n=46)	Sulphide or Hematite Cemented U Zone (n=34)	
Total Digestion								
As	-	-	-	-	-	-	-	-
Co	0.16	0.37	0.49	0.58	105	85	91	28
Cr	8	9	13	11	119	150	180	155
Cu	1.5	1.2	1.3	3.7	2.32E+03	5.79E+03	1.11E+03	228
Mo	0.1	0.17	0.24	0.18	86	101.5	258.5	5
Ni	1.5	3.4	2.4	4.7	343.5	288.5	239	167
Pb	2.65	3.16	3.56	3.14	4055	3455	4205	83
Se	-	-	-	-	-	-	-	-
Sr	43	87	178	112	279	281	218	169
Th	3.36	11.9	23.2	11.4	73.5	131.5	96	25
U	1	1.16	1.4	2.24	4.18E+04	5.02E+04	7.58E+04	403
V	3	5.2	10.3	8.3	779	1.37E+03	713	310
Zn	2	2	2	3	333	185.5	247	31
Partial Digestion								
As	0.18	0.42	0.71	0.46	176	147	78.5	24
Co	0.06	0.12	0.16	0.22	90.5	63.5	75.5	16
Cr	-	-	-	-	-	-	-	-
Cu	0.65	0.58	0.665	2.02	2.18E+03	5.40E+03	1.05E+03	219
Mo	0.05	0.06	0.07	0.08	76	73	182	3
Ni	0.41	0.88	0.68	1.48	314	257	179	79
Pb	0.506	0.667	0.851	0.6905	3.71E+03	3.14E+03	3.72E+03	46
Se	0.1	0.1	0.1	0.1	4.5	12.5	5	1
Sr	-	-	-	-	-	-	-	-
Th	0.68	2.14	5.36	2.39	-	-	-	-
U	0.21	0.26	0.33	0.58	4.07E+04	4.88E+04	7.49E+04	335
V	0.4	0.9	1.8	1.2	561	892	507	104
Zn	0.6	0.7	0.6	0.7	262	119	77.5	14

Notes:
n= number of samples used to calculated median values; Median values calculated using value of detection limit where value <DL
"-" indicates element not analyzed following digestion by method indicated

Surface Complexation Binding Constants

The sources of binding constants for uranium, metals and radionuclides to adsorbing phases, including goethite, illite and quartz are provided in Table E-2. As is shown in Table E-2, binding constants for all elements/constituents could not always be associated with adsorbing phases.

Table E-2: Summary of Compiled Surface Complexation Constants

Aqueous-phase element/species being	Goethite	Reference	Quartz	Reference	Clay	Reference
Al	X	1	X	8		
As(III)						
As(V)	X	2			X	12
Cd	X	2	X	9	X	13
Co	X	2	X	10	X	13
Cr(III)	X	3				
Cu	X	2			X	13
Mo	X	2				
Ni	X	2			X	13
Pb	X	2			X	13
Se(IV)	X	2			X	14
Se(VI)	X	2			X	14
Zn	X	2			X	13
U	X	2	X	8	X	13
U-carbonate	X	4	X	8	X	15
V	X	5				
Ra	X	6	X	11	X	13
Th	X	7			X	13
Ca	X	2				
Ba	X	2				
Sr	X	2				
Mg	X	2				
PO4	X	2				
SO4	X	2				
Mn	X	2				
Fe2+						

References:

1. Lövgren et al., 1990
2. Mathur and Dzombak, 2006
3. Dzombak and Morel, 1991
4. Wazne et al., 2003
5. Peacock and Sherman, 2004
6. Chen and Kocar, 2018
7. LaFlamme and Murray, 1987
8. Dong and Wan, 2014
9. Schaller et al., 2009
10. Landry et al., 2009
11. Riese, 1982
12. Manning and Goldberg, 1996
13. Bradbury and Baeyens, 2009a
14. Goldberg, 2014
15. NRC, 1995

Adsorption Behaviour – Supporting Information

In Figure E1, a sorption isotherm for uranium to the solid assemblage conceptualized for the Desilicified Zone is shown (at pH 6.4; pH value used the model for this hydrostratigraphic unit). At the high end of dissolved uranium concentrations shown, the sorption is non-linear with lower relative ratios of concentrations in the solids to those in the water. This behaviour of lower apparent K_d values at higher concentrations in water is common to many chemical constituents. The figure shows that at higher uranium concentrations, similar to those that are being modelled in association with the Recovered solutions, the sorptive capacity of the solid becomes depleted. This is an important reason rationalizing the use of a more complex geochemical approach versus applying K_d values for this work.

At lower uranium concentrations, the sorption isotherm is linear, and the K_d (slope of the line) in this linear region is approximately $1.07x10^2$ L/kg as shown in the insert/enlargement area and (very closely) corresponds to that shown in Table 3-11 ($1.04x10^2$ L/kg).

Figures E2 through E8 demonstrate that the sorption behavior of constituents to the different sorbing phases (quartz, illite and goethite) in the Desilicified Zone and Paleoweathered Zone (illite) is aligned with the studies from which the binding constants were taken as well as with results from other literature studies. In E2 through E8 there are two "panels" in each figure. Panel "a)" shows the sorption behaviour predicted in this in the geochemical model developed in this assessment and Panel "b)" shows the sorption behaviour in the literature. The following in shown:

- Figure E2: Sorption behaviour of U to quartz follows literature behaviour.
- Figure E3 and E4: Sorption behaviour of U to illite in the absence and presence of aqueous carbonate species, respectively, follows literature behaviour.
- Figure E5: Sorption behaviour of U to goethite in the presence of aqueous carbonate species, follows literature behaviour.
- Figure E6: Sorption behaviour of Cd to goethite shows a good alignment with literature behaviour but may overestimate sorption at low pH.
- Figure E7: Vanadium sorption to goethite does not follow literature behaviour; sorption in the literature is stronger and occurs over a broader pH range (compare the Kd values shown on both panels a) and b)). The difference is that the thermodynamic database developed for this project contains several vanadium complexes, shown in Figure E8, that limit the sorption, as the surface complexation constant is for the species VO_4^{-3}. The high Kd values observed in Table 3-11 for vanadium, suggest that some of these complexes may not be valid. In any case, the approach used in this work was conservative, in that vanadium sorption is underestimated.

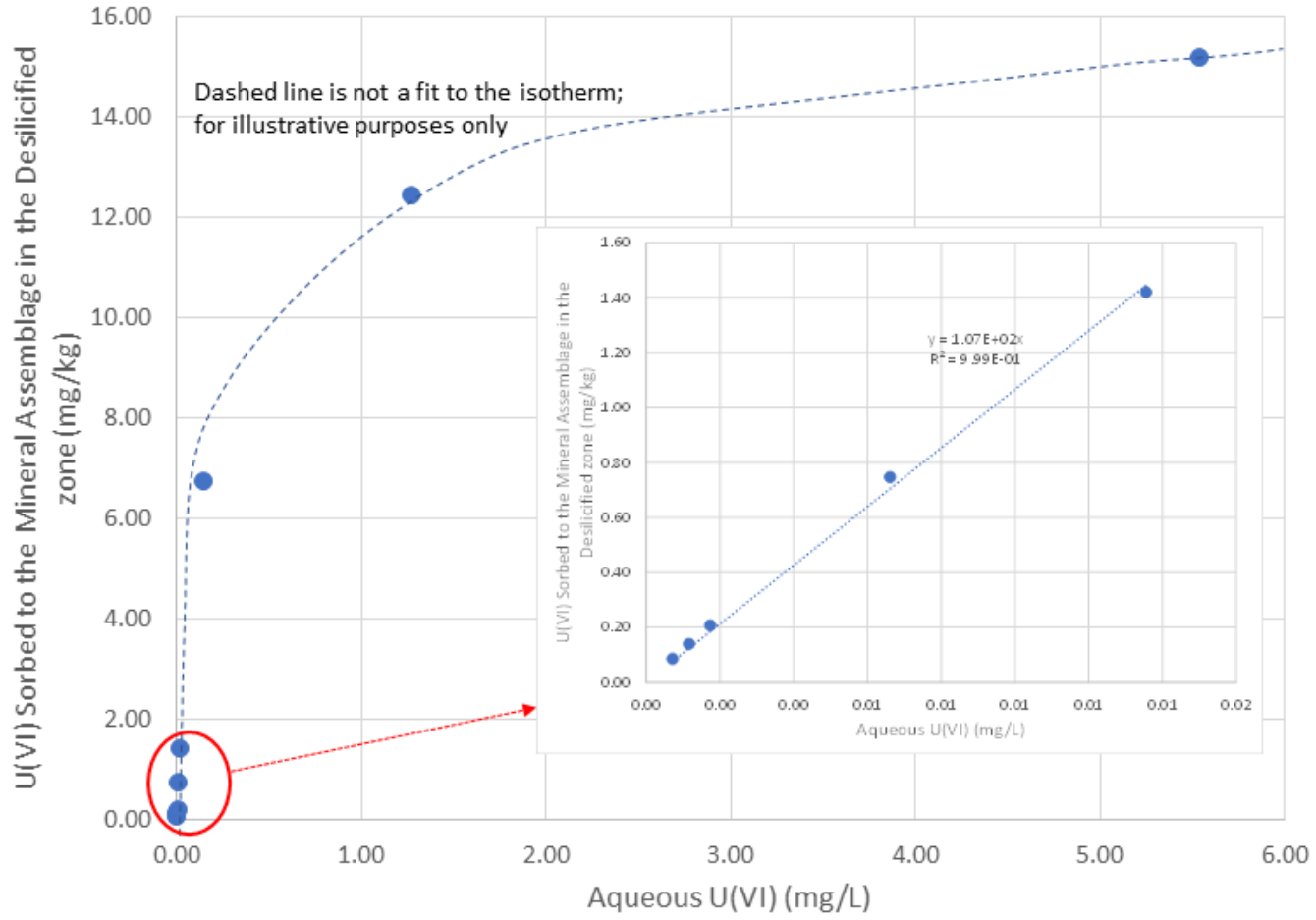

Legend

Blue markers dots in the plot show the information derived from PHREEQC modelling.

Wheeler River Project Advanced Exploration Feasibility Field Test	
U(VI) Sorption Isotherm at pH 6.4	
Ecometrix Environmental INTELLIGENCE	Figure E1

a) This work: U(VI) Sorption to Quartz; reproduces experimental sorption curve in Dong and Wan (2014)

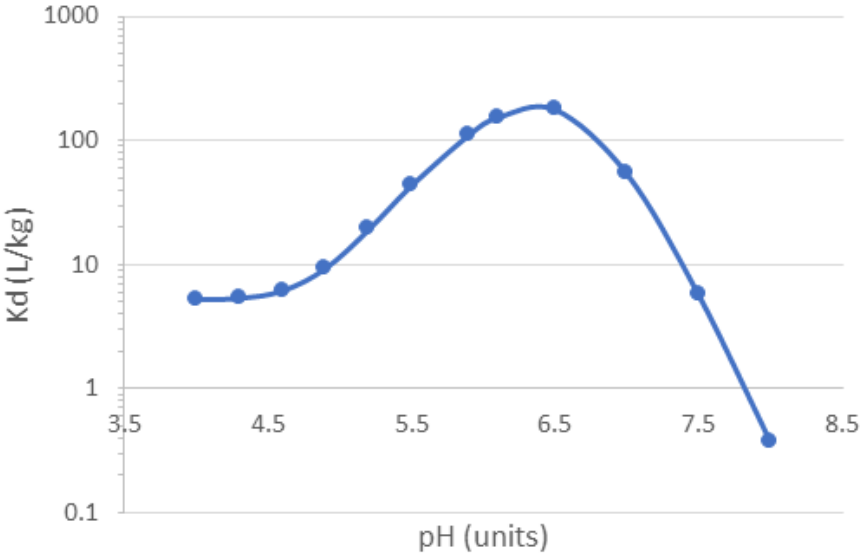

SSA (0.036 m^2/g) from Don and Wang, 2014; moles of reactive sites (mol/kg solid) from Prikryl et al., 2001.

b) From Dong and Wan, 2014

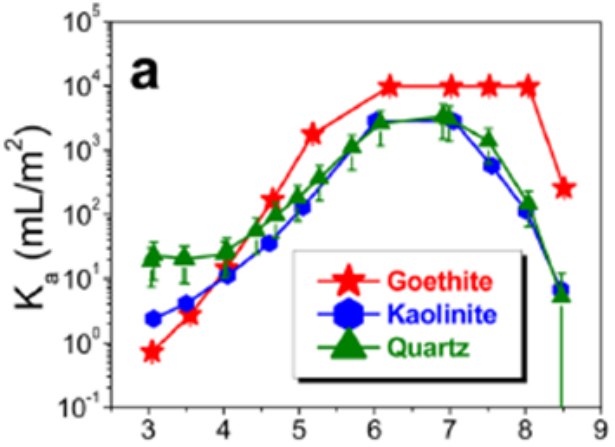

Figure 3. Comparison of U(VI) adsorption onto reference goethite, kaolinite and quartz (a). Surface complexation modeling of U(VI) adsorption onto goethite (b), kaolinite (c), and quartz (d). Symbols are experimental data points with estimated uncertainties. The solid lines are the overall model fits and the dashed lines are the fitted distribution of specific surface species: 1 = $(>FeOH)_2UO_2^+$, 2 = $(>FeOH)_2UO_2CO_3^-$, 3 = $>X_2UO_2$, 4 = $(>SOH)_2UO_2^+$, and 5 = $(>SOH)_2UO_2CO_3^-$, 6 = $(>QOH)_2UO_2^{2+}$, and 7 = $(>QOH)_2UO_2CO_3$.

Surface area of quartz used in Don and Wang, 2014 is 0.036 m^2/g

Legend

Blue markers/dots in the plot show the information derived from PHREEQC modelling. The blue line is not a fit to the data; for illustrative purposes only

Wheeler River Project Advanced Exploration Feasibility Field Test	
U(VI) Sorption to Quartz	
Ecometrix Environmental INTELLIGENCE	Figure E2

a) This work: U(VI) Sorption to illite; no carbonate species

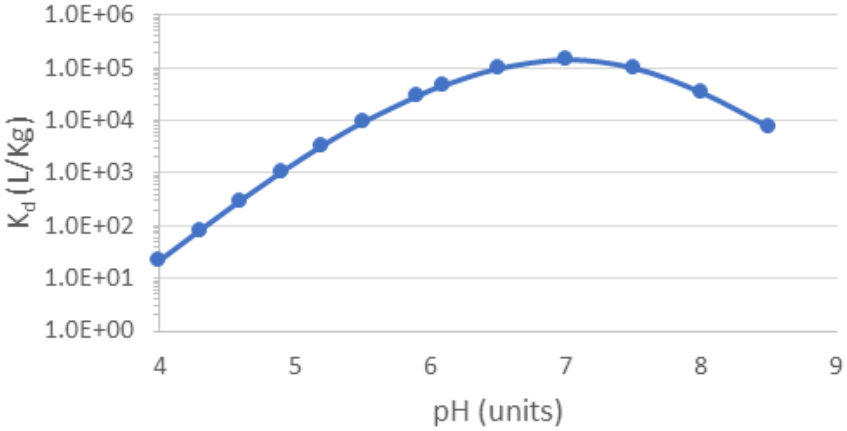

SSA (m^2/g) and moles of reactive sites (mol/kg solid) from Bradbury and Baeyens, 2009

b) From Bradbury and Baeyens, 2009

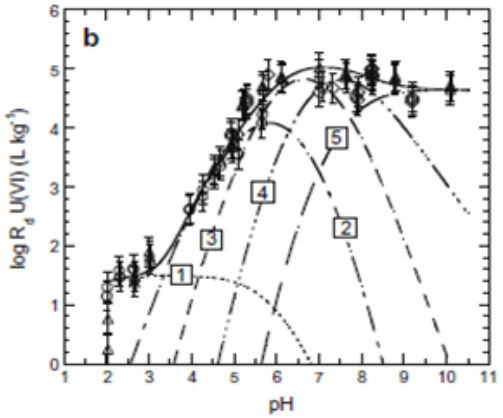

Fig. 4. (a) Aqueous speciation of U(VI) in 0.1 M $NaClO_4$. The hydrolysis constants are taken from Table 3, (b) U(VI) sorption edge measurements on conditioned Na-illite in 0.1 M $NaClO_4$ (symbols) and the modelled sorption (continuous line). (The different symbols represent different series of experiments.) The contributions to the overall sorption of the individual U(VI) surface species are shown by the different curves: (1) UO_2^{2+} cation exchange; (2) $\equiv S^sOUO_2^+$; (3) $\equiv S^sOUO_2OH^0$; (4) $\equiv S^sOUO_2(OH)_2^-$; (5) $\equiv S^sOUO_2(OH)_3^{2-}$. The continuous curves are the calculated U(VI) sorption edges using the 2SPNE SC/CE model and the parameters given in Tables 2–5.

Legend

Panel a: Blue markers/dots dots in the plot show the information derived from PHREEQC modelling. The blue line is not a fit to the data; for illustrative purposes only

Wheeler River Project Advanced Exploration Feasibility Field Test	
U(VI) Sorption to Illite, no carbonate species	
Ecometrix Environmental INTELLIGENCE	Figure E3

a) This work: U(VI) Sorption to illite; equilibrated with atmosphere (log CO_2(g) partial pressure = -3.5)

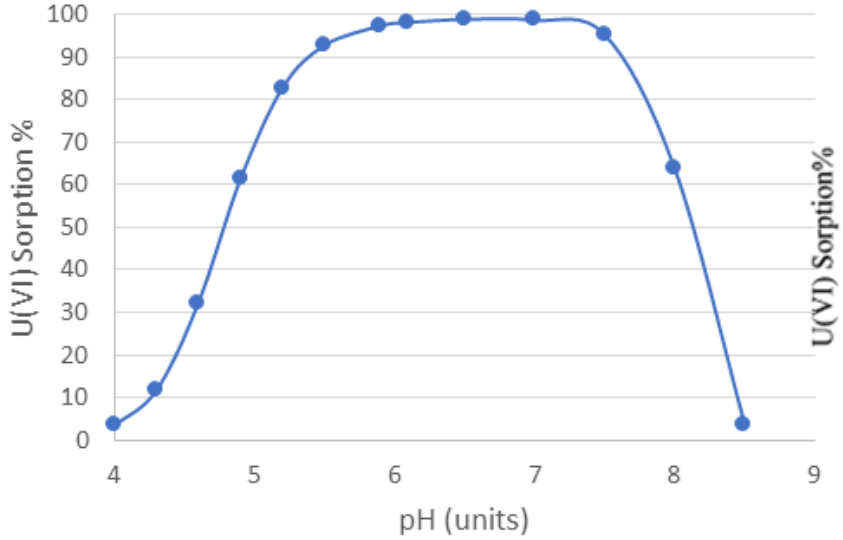

SSA (m^2/g) and moles of reactive sites (mol/kg solid) from Bradbury and Baeyens, 2009

b) From Bachmaf and Merkel, 2010; Sorption of U(VI) to Montmorillonite

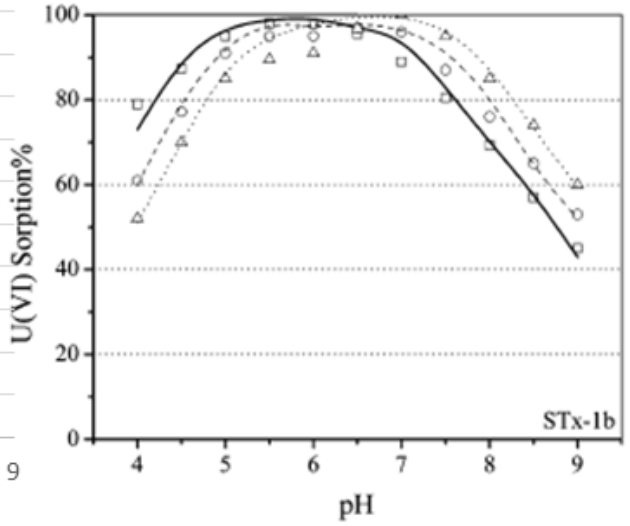

Fig. 3 Comparison of uraniumsorption data on kaolinite (KGa-1b), kaolinite (KGa-2), montmorillonite (STx-1b), montmorillonite (SWy-2), and natural bentonite (IBECO) and the surface complexation model (SCM). Experimental conditions: $\Sigma U = 100\ \mu g\ L^{-1}$, suspension density = 1.66 g L^{-1}, $Pco_2 = 10^{-3.5}$ hPa, 25°C, $I = 0.001$,

Legend

Panel a: Blue markers/dots in the plot show the information derived from PHREEQC modelling. The blue line is not a fit to the data; for illustrative purposes only

** Change to draft, right panel needs to be updated to correct source – does not change intent/conclusion

Wheeler River Project Advanced Exploration Feasibility Field Test	
U(VI) Sorption to Illite, carbonate species present	
Ecometrix Environmental INTELLIGENCE	Figure E4

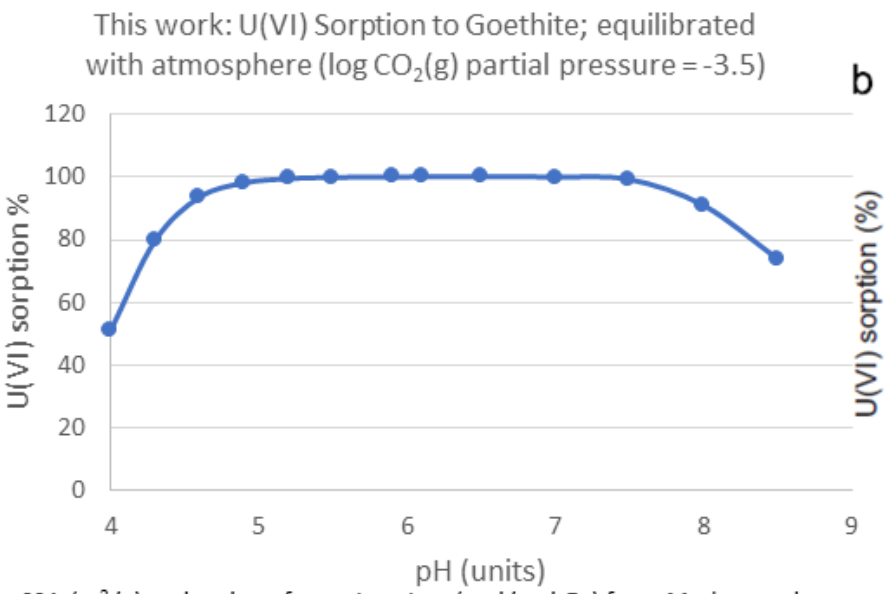

SSA (m^2/g) and moles of reactive sites (mol/mol Fe) from Mathur and Dzombak, 2006

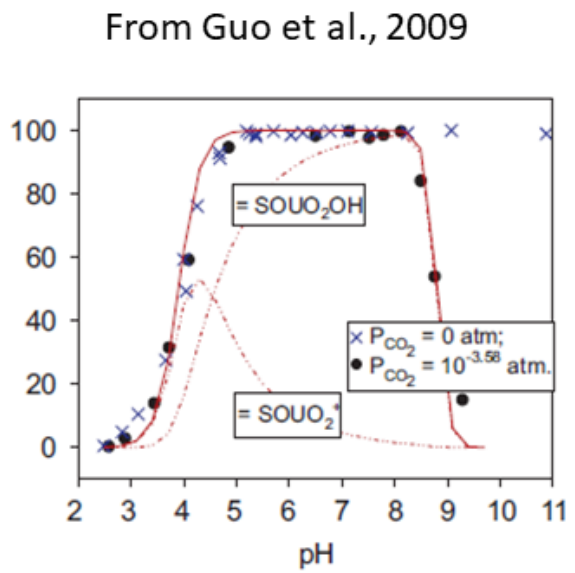

Fig. 4. pH sorption edges of U(VI) on goethite; (a) effect of phosphate; (b) effect of carbonate; (c) effect of FA; (d) FA sorption as a function of pH in the presence and absence of U(VI). Symbols in Fig. 4(a)–(c) represent the experimental data collected at [U(VI)] = 5.16e−5 mol/L, [NaCl] = 0.1 mol/l and m/V = 5 g/L; symbols in Fig. 4(d) represent the experimental data collected at [FA] = 20 mg/L, [NaCl] = 0.1 mol/L and m/V = 5 g/L; lines in Fig. 4(b) are the results calculated by model 2.

Legend

Panel a: Blue markers/dots in the plot show the information derived from PHREEQC modelling. The blue line is not a fit to the data; for illustrative purposes only

Wheeler River Project Advanced Exploration Feasibility Field Test	
U(VI) Sorption to goethite, carbonate species present	
Ecometrix Environmental INTELLIGENCE	Figure E5

This work: Cd sorbed to Goethite; experimental conditions as modelled in Mathur and Dzombak, 2006

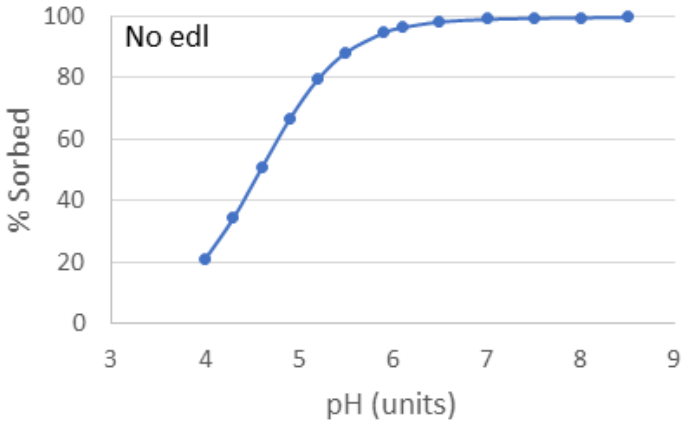

SSA (m^2/g) and moles of reactive sites (mol/mol Fe) from Mathur and Dzombak, 2006

From Mathur and Dzombak, 2006

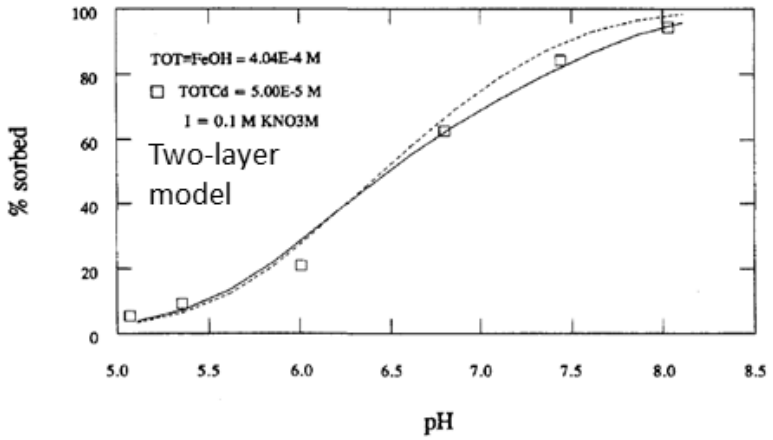

Fig. 1. Example fit of cation sorption data: cadmium sorption on goethite. Data from Barrow et al. [46]. FeOOH = 2.0 g L^{-1}, TOT≡FeOH = 4.04 x 10^{-4}M, TOTCd = 5 x 10^{-5} M, I = 0.1 M KNO_3. Model fits shown are from Mathur [24], Fig. 2ECD16, and include optimal fit for the particular data set (—) and fit provided by the best overall estimate surface complexation constants for cadmium given in Table 3 (- - -) for the same experimental conditions.

Legend

Panel a: Blue markers/dots in the plot show the information derived from PHREEQC modelling. The blue line is not a fit to the data; for illustrative purposes only

Wheeler River Project Advanced Exploration Feasibility Field Test	
Cd Sorption to Goethite	
Ecometrix Environmental INTELLIGENCE	Figure E6

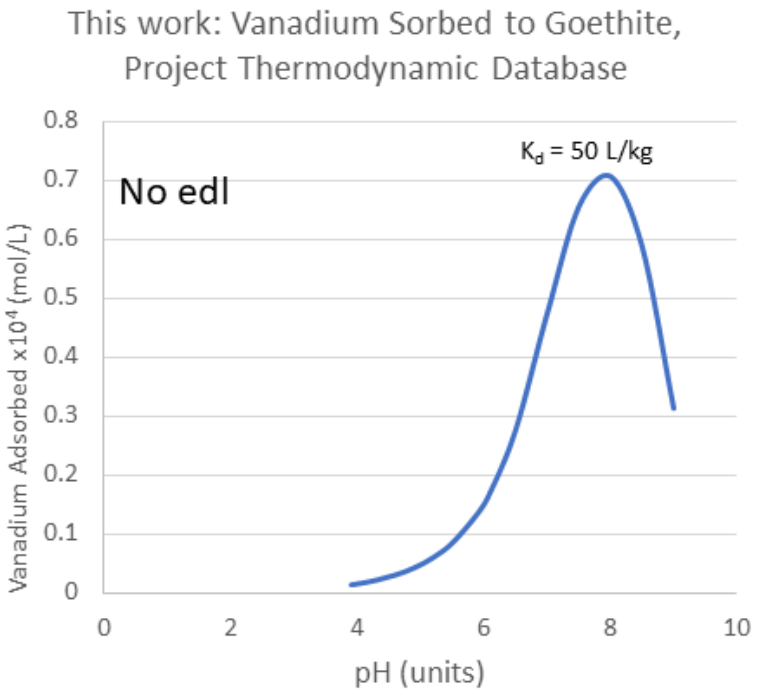

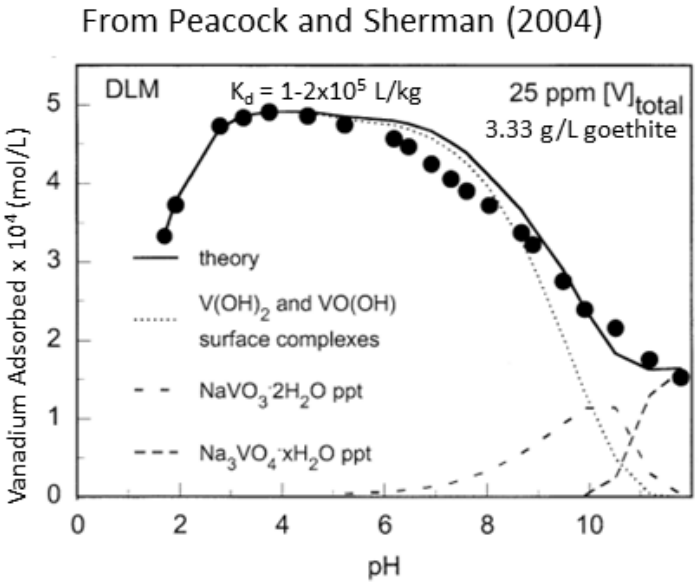

SSA (m^2/g) and moles of reactive sites (mol/mol Fe) from Mathur and Dzombak, 2006. [V]Tot = 25 mg/L; 3.33 g/L goethite.

Legend

Panel a: The blue line in the plot is a smoothed line derived from discrete points in the PHREEQC modelling. The line is not a fit to the data; for illustrative purposes only

Wheeler River Project
Advanced Exploration Feasibility Field Test

Vanadium Sorption to Geothite

Ecometrix Environmental INTELLIGENCE | Figure E7

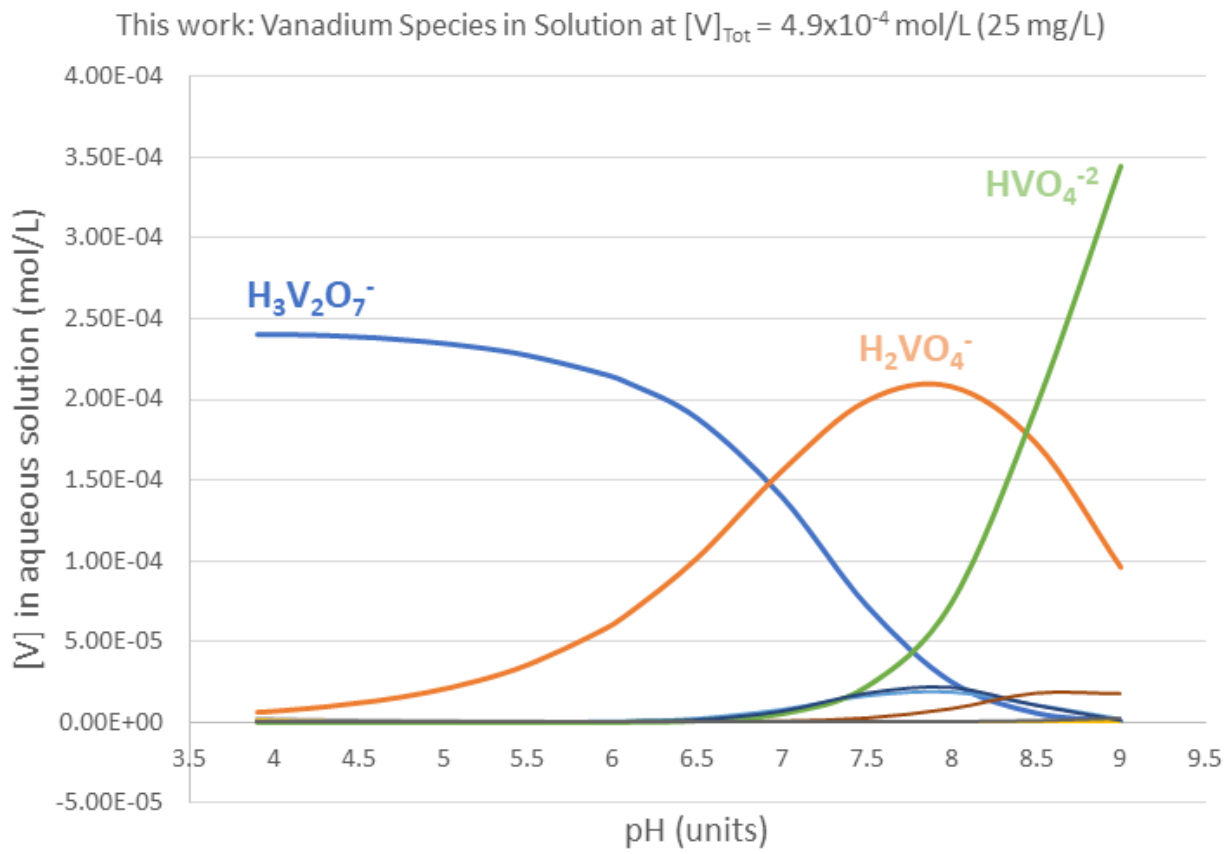

Wheeler River Project
Advanced Exploration Feasibility Field Test

Vanadium Speciation in Solution using the Thermodynamic Database for the Project

Ecometrix Environmental INTELLIGENCE | Figure E8

Radioactive Decay of ^{226}Radium and ^{230}Thorium and Production of Daughter Products

Radioactive decay was implemented in the 1D reactive transport model to account for decay and production of daughter products. The following radioactive decay chain was included in the model, following the work of Pique et al. (2013).

Th-230	→	Ra-226	→	Rn-222
	α		α	
$t_{1/2}$ 77,000 yr		$t_{1/2}$ 1,600 yr		$t_{1/2}$ 3.82 d

The 1D reactive transport model used was the 'Desilicified Zone Pathway' model (Figure 3-6b of the main text) and the low solids scenario was evaluated. The low solids scenario was evaluated because this is conservative for ^{226}Ra, as it will migrate more quickly along the groundwater flow path (i.e., less time for radioactive decay). Radioactive decay of ^{230}Th, resulting production of ^{226}Ra-226, and decay of ^{226}Ra was implanted in PHREEQC using the RATES and KINETICS keywords. The elements Th and Ra were used to represent ^{230}Th and ^{226}Ra, because the groundwater chemistry data collection for Th and Ra was limited to the radioactivity of these isotopes. This allowed for the modelling to be done without the need to specifically define these isotopes in PHREEQC. The decay rates for ^{230}Th and ^{226}Ra were calculated in the model as follows:

$$\partial C/\partial t = -\lambda \cdot C$$

$$\lambda = \ln(2) / t_{1/2}$$

where C is the concentration of ^{230}Th and ^{226}Ra (mol/L), λ is the decay constant (seconds^{-1}), and $t_{1/2}$ is the half-life (seconds). Decay of ^{230}Th was modelled to produce ^{226}Ra with stoichiometry of 1:1, and Ra-226 was modelled to produce ^{222}Rn with stoichiometry of 1:1. The production of ^{226}Rn from the decay of ^{230}Th was modelled at each time step (3.9 years) in PHREEQC using this stoichiometry, such that the rate expression for ^{226}Rn did not need to account for this production.

Results of modelling radioactive decay are shown in groundwater at the point of discharge to Whitefish Lake for ^{226}Ra and ^{230}Th in Figures E9 and E10, respectively. Accounting for radioactive decay results in modest decrease in the maximum ^{226}Ra concentration in groundwater (3.9×10^{-7} mg/L with decay versus 4.8×10^{-7} mg/L without decay), which was modelled to occur after approximately 3,200 years due to sorption and de-sorption processes. Decay of ^{230}Th results in negligible loss of ^{230}Th and production of ^{226}Ra due to the slow decay rate evident in its long half-life (77,000 years). Due to the long half-life of ^{230}Th decay and similarity of initial ^{230}Th and ^{226}Ra concentrations (within an order of magnitude), radioactive decay results in decreases in ^{226}Ra rather than increases from the ^{230}Th decay.

To provide a check on the model calculations for the radioactive decay, an arbitrary high concentration of ^{226}Ra (1.29 mol/L) was input to the model as the initial concentration, and the

model was evaluated at the discharge location, 1,000 m downgradient of the ore zone. In this model simulation, the concentration of ^{226}Ra decreased exponentially for 460 years, when the concentration then decreased rapidly due to the flushing out of the initial waters by the infiltrating fresh water. The rate of decrease of ^{226}Ra during the initial 460 years was forecast out to 1,600 years, which is the half-life of ^{226}Ra (Figure E-11). The ^{226}Ra concentration forecasted using the initial decay rate was equal to half of the initial ^{226}Ra concentration. This check demonstrates that the radioactive decay was modelled correctly.

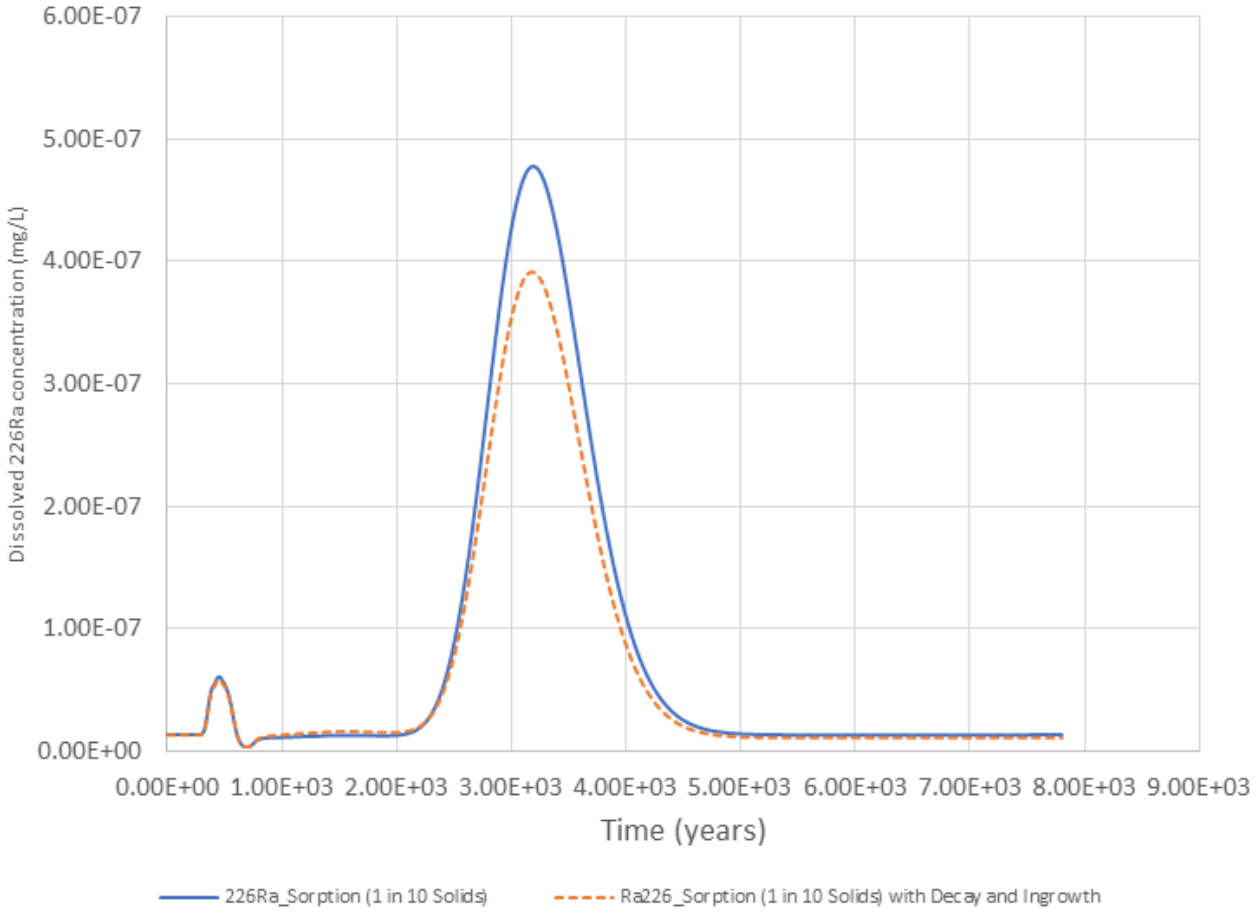

Wheeler River Project
Advanced Exploration Feasibility Field Test

Radium-226 Dissolved Phase Concentrations with Sorption, Decay and Ingrowth, 1 in 10 Solids

Ecometrix Environmental INTELLIGENCE | Figure E9

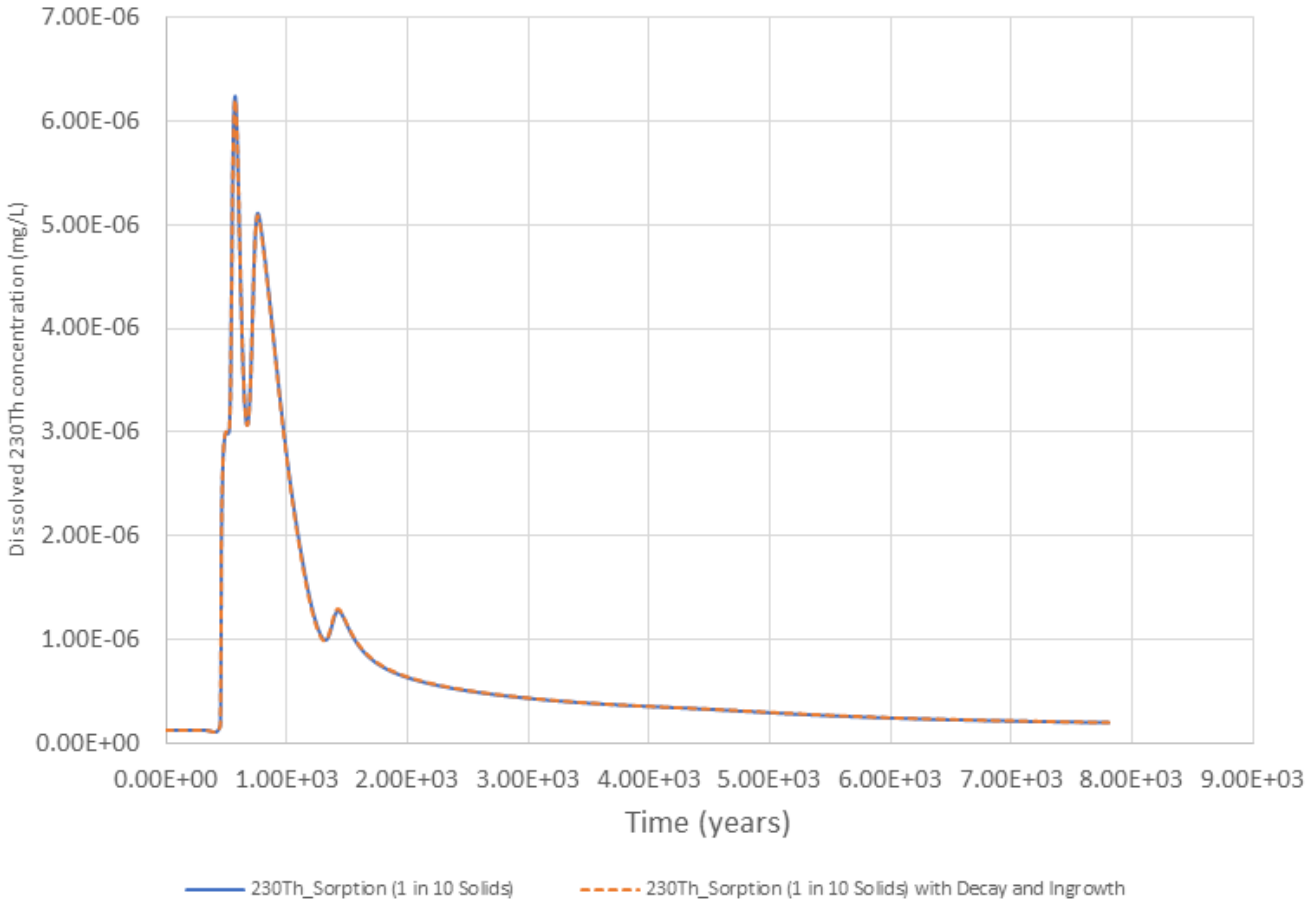

Wheeler River Project
Advanced Exploration Feasibility Field Test

Thorium-230 Dissolved Phase Concentrations with Sorption and Decay, 1 in 10 Solids

Ecometrix Environmental INTELLIGENCE | Figure E10

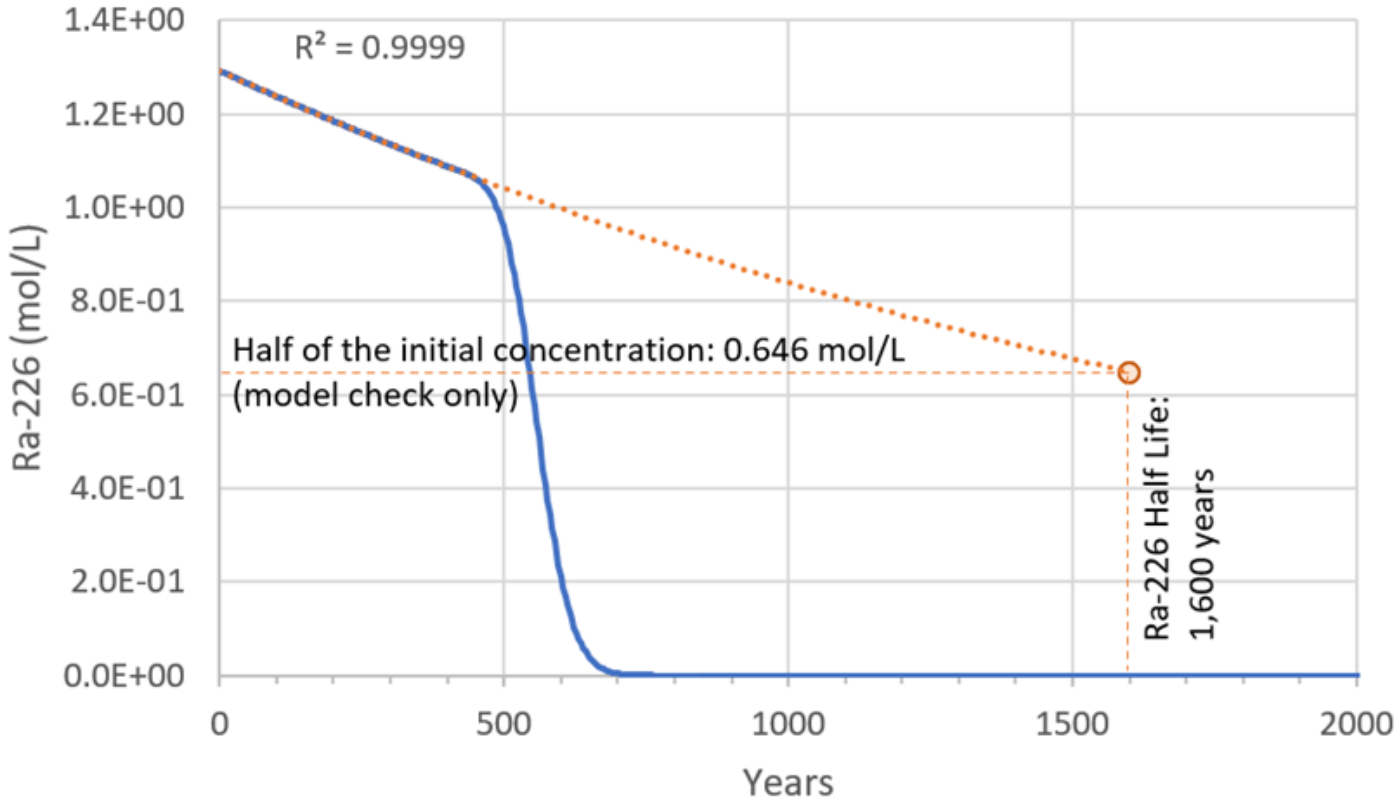

	Wheeler River Project **Advanced Exploration Feasibility Field Test**
	Model Check: 226Ra Decay
	Ecometrix Environmental INTELLIGENCE — Figure E11

Example PHREEQC and PiChem Input Files

#PHREEQC Input File_Transport_PWZ_DSZ and Sediments2_Chlorite2.phr

```
DATABASE C:\PHREEQC OLD COMPUTER\phreeqc\database\Enhanced
PHREEQC4_Unified_May2022_Chlorite.dat

TITLE water quality evolution at Pheonix during gw restoration
# Authors: Elizabeth Haack; ehaack@ecometrix.ca
# Reactive Transport Model_Remediated Groundwater from Mining Area to below Lake
# Paleoweathered, Desilicified zones and Lake Bottom Sediments
# Natural groundwater from upgradient

EXCHANGE_MASTER_SPECIES

Y          Y-   # X- = Illite Exchange Site

SURFACE_MASTER_SPECIES
Hfo_     Hfo_OH# Goethite surface reactive site
Hao_s    Hao_sOH #Illite surface reactive sites
Hao_w    Hao_wOH
Hao_ww           Hao_wwOH
Q          QOH     # Quartz surface reactive sites
Hco_     Hco_OH           # chlorite

Linear Linear

SURFACE_SPECIES
Linear = Linear
Linear + H2AsO4- = LinearH2AsO4-
     -log_k -96.02
Linear + Cd+2 = LinearCd+2
          -log_k -96.82
Linear + Co+2 = LinearCo+2
     -log_k -97.60
Linear + Cr(OH)+2 = LinearCr(OH)+2
     -log_k -96.94
Linear + Cu+2 = LinearCu+2
    -log_k -97.52
Linear + MoO4-2 = LinearMoO4-2
     -log_k -97.50
Linear + Ni+2 = LinearNi+2
     -log_k -97.05
Linear + Pb+2 = LinearPb+2
     -log_k -95.92
Linear + Ra+2 = LinearRa+2
     -log_k -96.92
Linear + SeO4-2 = LinearSeO4-2
```

```
    -log_k -96.70
Linear + Th(OH)3(CO3)- = LinearTh(OH)3(CO3)-
    -log_k -97.64
Linear + Th(OH)2(CO3) = LinearTh(OH)2(CO3)
    -log_k -97.64
Linear + UO2CO3 = LinearUO2CO3
    -log_k -96.70
Linear + H2VO4- = LinearH2VO4-
    -log_k -96.40
Linear + Zn+2 = LinearZn+2
    -log_k -96.82

############################################################

SOLUTION 0 #Groundwater Sweep;
units   mg/L
pH      6.467 charge
pe      15.535
Temperature     7
Al      5.20E-02
As      1.30E-03
Ba      5.40E-02
C(4)    8.66E+01
Ca      9.78E+00
Cd      1.00E-05
Cl      7.20E+00
Co      1.00E-04
Cr      5.00E-04
Cu      1.80E-03
F       1.80E-01
Fe      8.60E-01
K       8.60E-01
Mg      2.00E+00
Mn      3.60E-01
Mo      4.20E-03
Na      6.10E+00
Ni      1.00E-04
Pb      1.00E-04
S(6)    4.70E+00
Se      1.00E-04
Si      2.41E+01
Sr      1.20E-01
Zn      1.20E-02
P       1.00E-01
U       7.00E-04
V       1.00E-04
Ra      1.37E-08
Th      1.30E-07
```

END

SOLUTION 1-45 #EA Solution #1
units mg/L
pH 4.3 charge
pe 14
Temp 7
Al 7
As 0.06
Ba 0.05
C(4) 58
Ca 110
Cd 0.015
Cl 200
Co 2
Cr 0.05
Cu 0.17
#F
Fe 100
K 9
Mg 6
Mn 3.4
Mo 0.1
Na 190
Ni 9.7
Pb 3.1
S(6) 703
Se 0.08
Si 40
Sr 4.4
Zn 1.4
P 4
U 100
V 0.51
Ra 5.47E-06
Th 3.93E-06

END

SOLUTION 46-55 #PWZ
units mg/L
pH 6.7 charge
pe 14
temp 7
Al 0.034
As 0.05
Ba 0.036

```
C(4)    154
Ca      6.76
Cd      0.00001
Cl      86.5
Co      0.01
Cr      0.0045
Cu      0.005
F       0.53
Fe      0.49
K       5.6
Mg      3.09
Mn      0.7
Mo      0.0128
Na      76.1
Ni      0.015
Pb      0.0001
S(6)    4.55
Se      0.0001
Si      9.18
Sr      1.17
Zn      0.00425
P       0.01
U       0.01239
V       0.0001
Ra      5.47E-09
Th      1.00E-06

END

SOLUTION 56-145 #DSZ
units   mg/L
pH      6.46 charge
pe      14
Temperature     7
Al      0.052
As      0.0013
Ba      0.054
C(4)    86.6
Ca      9.78
Cd      0.00001
Cl      7.2
Co      0.0001
Cr      0.0005
Cu      0.0018
F       0.18
Fe      0.86
K       2
Mg      1.6
```

```
Mn      0.36
Mo      0.0042
Na      6.10
Ni      0.0001
Pb      1.00E-04
S(6)    4.7
Se      1.00E-04
Si      24.1
Sr      0.12
Zn      0.012
P       0.1
U       0.0007
V       0.0001
Ra      1.37E-08
Th      1.31E-07

END

solution 146 # Lake Bottom Sediments
units   mg/L
pH      6.45
pe      14
Temp    7
Al      0.037
As      0.0003
Ba      0.0057
C(4)    33.9
Ca      2.7
Cd      0.00001
Cl      6.86
Co      0.0004
Cr      0.0005
Cu      0.0006
F       0.06
Fe      0.405
K       2.8
Mg      1.8
Mn      0.14
Mo      0.0007
Na      2.9
Ni      0.0018
Pb      0.0001
S(6)    1.9
Se      0.0008
Si      26.2
Sr      0.012
Zn      0.0044
P       0.04
```

```
U          0.0005
V          0.0001
Ra         1.64117E-09
Th         2.61966E-08

Surface 1-45 #Chlorite in the mining area
-equilibrate with solution 1-45
Hco_     2.10E-02 0.5       795
-no_edl

EXCHANGE 46-55 #Illite in the paleoweathered zone
-equilibrate with solution 46-95
Y          0.483

EXCHANGE 56-145 #Illite in the desilicified zone
-equilibrate with solution 96-145
Y          0.093015

Surface 46-55 #Mineral Assemblage, reactive sites, paleoweathered zone
-equilibrate with solution 46-95
Hao_s    0.004293          97        2147
Hao_w    0.08586
Hao_ww             0.08586
-no_edl

QOH      7.06E-03          0.31      5963
-no_edl

Surface 56-145 #Mineral Assemblage, reactive sites, Desilicified zone
-equilibrate with solution 96-145
Hfo_     0.00693 60        34.2
-no_edl

Hao_s    0.0008268         97        413.4
Hao_w    0.0165
Hao_ww             0.0165
-no_edl

QOH      0.0119   0.31      10017
-no_edl

SURFACE 146 #Reactive sites, Lake bottom sediments
-equilibrate 146
    Linear 1e100 1 1
-no_edl

EQUILIBRIUM_PHASES 1-45 #Mining Area
O2(g) -0.68
```

```
Gibbsite 1.2 0
Gypsum          0 0

EQUILIBRIUM_PHASES 46-146 #Paleoweathered, Desilicified zones and Lake Bottom Sediments
O2(g) -0.68
Gibbsite 1.2 0

SOLID_SOLUTIONS 46-146 ##Paleoweathered, Desilicified zones and Lake Bottom Sediments
Ba(x)Ra(1-x)SO4
-comp1 Barite 0
-comp2 Ra(SO4)(s) 0

PRINT
-reset false

KNOBS
        -diagonal_scale
        -step 10
        -pe   5
        -iterations 200
        -tolerance 1e-15
        -convergence_tolerance  1e-8

SELECTED_OUTPUT
-file Full Solids_Chlorite Cell 146.sel
-reset false
-solution true
-distance true
-time true
-pH true
-pe true
-alkalinity true
-solid_solutions Barite Ra(SO4)(s)
totals U Al As Cu Cd Co Cr Ni Pb Mo Se Sr Zn V Ra Th S P Ba Mn Fe(2) Cl Ca Mg Na K Fe Br Si C(4) Se(4)
Se(6) As(3) As(5)
-equilibrium_phases     Gibbsite
-molalities Hfo_O- Hfo_OH Hfo_OH2+ QO- QOH QOH2+ Hao_sO- Hao_sOH Hao_sOH2+ Hao_wO-
Hao_wOH Hao_wOH2+ Hao_wwO- Hao_wwOH Hao_wwOH2+ YH CaY2 MgY2 YNa KY RaY2
USER_PUNCH
-head U_G U_Q U_C Al_G Al_Q Al_C As_G As_Q As_C Cu_G Cu_Q Cu_C Cd_G Cd_Q Cd_C Co_G Co_Q Co_C
Cr_G Cr_Q Cr_C Ni_G Ni_Q Ni_C Pb_G Pb_Q Pb_C Mo_G Mo_Q Mo_C Se_G Se_Q Se_C Sr_G Sr_Q Sr_C Zn_G
Zn_Q Zn_C V_G V_Q V_C Ra_G Ra_Q Ra_C Th_G Th_Q Th_C SO4_G SO4_Q SO4_C Phos_G Phos_Q Phos_C
Ba_G Ba_Q Ba_C Mn_G Mn_Q Mn_C Fe(II)_G Fe(II)_Q Fe(II)_C SO4_ppm U_ppm porevolumes years
mol_U(VI) Soln_density ULinear AsLinear CuLinear CdLinear CoLinear CrLinear NiLinear PbLinear MoLinear
SeLinear ZnLinear VLinear RaLinear ThLinear
50 PUNCH        SURF("U(6)","Hfo")
51 PUNCH        SURF("U(6)","Q")
52 PUNCH        SURF("U(6)","Hao")
```

```
60 PUNCH      SURF("Al","Hfo")
61 PUNCH      SURF("Al","Q")
62 PUNCH      SURF("Al","Hao")
70 PUNCH      SURF("As","Hfo")
71 PUNCH      SURF("As","Q")
72 PUNCH      SURF("As","Hao")
80 PUNCH      SURF("Cu","Hfo")
81 PUNCH      SURF("Cu","Q")
82 PUNCH      SURF("Cu","Hao")
90 PUNCH      SURF("Cd","Hfo")
91 PUNCH      SURF("Cd","Q")
92 PUNCH      SURF("Cd","Hao")
95 PUNCH      SURF("Co","Hfo")
96 PUNCH      SURF("Co","Q")
97 PUNCH      SURF("Co","Hao")
100 PUNCH     SURF("Cr","Hfo")
101 PUNCH     SURF("Cr","Q")
102 PUNCH     SURF("Cr","Hao")
110 PUNCH     SURF("Ni","Hfo")
111 PUNCH     SURF("Ni","Q")
112 PUNCH     SURF("Ni","Hao")
120 PUNCH     SURF("Pb","Hfo")
121 PUNCH     SURF("Pb","Q")
122 PUNCH     SURF("Pb","Hao")
130 PUNCH     SURF("Mo","Hfo")
131 PUNCH     SURF("Mo","Q")
132 PUNCH     SURF("Mo","Hao")
140 PUNCH     SURF("Se","Hfo")
141 PUNCH     SURF("Se","Q")
142 PUNCH     SURF("Se","Hao")
145 PUNCH     SURF("Sr","Hfo")
146 PUNCH     SURF("Sr","Q")
147 PUNCH     SURF("Sr","Hao")
150 PUNCH     SURF("Zn","Hfo")
151 PUNCH     SURF("Zn","Q")
152 PUNCH     SURF("Zn","Hao")
155 PUNCH     SURF("V","Hfo")
156 PUNCH     SURF("V","Q")
157 PUNCH     SURF("V","Hao")
160 PUNCH     SURF("Ra","Hfo")
161 PUNCH     SURF("Ra","Q")
162 PUNCH     SURF("Ra","Hao")
165 PUNCH     SURF("Th","Hfo")
166 PUNCH     SURF("Th","Q")
167 PUNCH     SURF("Th","Hao")
170 PUNCH     SURF("S","Hfo")
171 Punch     SURF("S","Q")
172 PUNCH     SURF("S","Hao")
```

```
175 PUNCH       SURF("P","Hfo")
176 Punch       SURF("P","Q")
177 PUNCH       SURF("P","Hao")
180 PUNCH       SURF("Ba","Hfo")
181 Punch       SURF("Ba","Q")
182 PUNCH       SURF("Ba","Hao")
185 PUNCH       SURF("Mn","Hfo")
186 Punch       SURF("Mn","Q")
187 PUNCH       SURF("Mn","Hao")
190 PUNCH       SURF("Fe(2)","Hfo")
191 Punch       SURF("Fe(2)","Q")
192 PUNCH       SURF("Fe(2)","Hao")
200 SO4_ppm = TOT("S(6)")*96.066* 1000
201 PUNCH       SO4_ppm
205 U_ppm = TOT("U")*238.02891*1000
206 PUNCH       U_ppm
210 PUNCH       (STEP_NO + .5) / 100
215 PUNCH       (total_time/365/24/60/60)
220 PUNCH       TOT("U(6)")
225 PUNCH       RHO
300 PUNCH       SURF("U","Linear")
301 PUNCH       SURF("As","Linear")
302 PUNCH       SURF("Cu","Linear")
303 PUNCH       SURF("Cd","Linear")
304 PUNCH       SURF("Co","Linear")
305 PUNCH       SURF("Cr","Linear")
306 PUNCH       SURF("Ni","Linear")
307 PUNCH       SURF("Pb","Linear")
308 PUNCH       SURF("Mo","Linear")
309 PUNCH       SURF("Se","Linear")
310 PUNCH       SURF("Zn","Linear")
311 PUNCH       SURF("V","Linear")
312 PUNCH       SURF("Ra","Linear")
313 PUNCH       SURF("Th","Linear")

TRANSPORT
-cells 146
-shifts 1500
-lengths 45*3.6 10*10 90*3.6 1*0.36
-time_step        3.46E+8
-boundary_conditions    3 3
-diffc 0.0e-9
-disp 45*1.79 10*5 90*1.79 1*0.179 #5
-correct_disp true
-punch_cells      146
-punch_frequency 1
-dump dump.file
-dump_frequency 10
```

```
USER_GRAPH 1
      -headings  mol_U(VI) Fe pH
      -chart_title "Uranium with years"
      -axis_scale x_axis 0 5000 auto
      -axis_scale y_axis 1e-8 1e-3 auto auto log
          -axis_scale sy_axis 4 7 auto auto
      -axis_titles "Years", "Concentration U(VI)", "pH"
      -initial_solutions false
 -start
 10 x =  (total_time/365/24/60/60)
 20 PLOT_XY x, TOT("U(6)"), color = Red, symbol = Square, symbol_size = 6, y-axis = 1
 30 PLOT_XY x, TOT("Fe(2)"), color = Blue, symbol = Square, symbol_size = 6, y-axis = 1
 40 PLOT_XY x, -LA("H+"), color = Green, symbol = Square, symbol_size = 6, y-axis = 2
 -end

USER_GRAPH 2
      -headings  YH       YNa      CaY2     MgY2    KY RaY2
      -chart_title "Exchange Species"
      -axis_scale x_axis 0 5000 auto
      -axis_scale y_axis 1e-10 1e-2 auto auto log
          -axis_scale sy_axis 1e-17 1e-10 auto auto log
          #-axis_scale sy_axis 4 7 auto auto
      -axis_titles "Years", "Equivalents of Exchangers"
      -initial_solutions false
 -start
 10 x =  (total_time/365/24/60/60)
 20 PLOT_XY x, MOL("YH"), color = Red, symbol = Square, symbol_size = 6, y-axis = 1
 30 PLOT_XY x, MOL("YNa"), color = Green, symbol = Square, symbol_size = 6, y-axis = 1
 40 PLOT_XY x, MOL("CaY2"), color = Blue, symbol = Square, symbol_size = 6, y-axis = 1
 50 PLOT_XY x, MOL("MgY2"), color = Yellow, symbol = Square, symbol_size = 6, y-axis = 1
 60 PLOT_XY x, MOL("KY"), color = Black, symbol = Square, symbol_size = 6, y-axis = 1
 70 PLOT_XY x, MOL("RaY2"), color = Brown, symbol = Square, symbol_size = 6, y-axis = 2
 -end

USER_GRAPH 3
      -headings  Goethite          Gibbsite          Barite    Ra(SO4)(s) UonGoethite UonQuartz
         UonClay
      -chart_title "Solid Phases and Sorbed species"
      -axis_scale x_axis 0 5000 auto
      -axis_scale y_axis 1e-10 1e-1 auto auto log
          -axis_scale sy_axis 1e-10 1e-3 auto auto log
      -axis_titles "Years", "Moles Solid Phases"      "Moles Sorbed Species"
      -initial_solutions false
 -start
 10 x =  (total_time/365/24/60/60)
 20 PLOT_XY x, EQUI("Goethite"), color = Brown, symbol = Square, symbol_size = 6, y-axis = 1
```

```
 30 PLOT_XY x, EQUI("Gibbsite"), color = Red, symbol = Square, symbol_size = 6, y-axis = 1
 40 PLOT_XY x, S_S("Barite"), color = orange, symbol = Square, symbol_size = 6, y-axis = 1
 50 PLOT_XY x, S_S("Ra(SO4)(s)"), color = Black, symbol = Square, symbol_size = 6, y-axis = 1
 60 PLOT_XY x, SURF("U(6)","Hfo"), color = Green, symbol = Square, symbol_size = 6, y-axis = 2
 70 PLOT_XY x, SURF("U(6)","Q"), color = Blue, symbol = Square, symbol_size = 6, y-axis = 2
 80 PLOT_XY x, SURF("U(6)","Hao"), color = Yellow, symbol = Square, symbol_size = 6, y-axis = 2
  -end


USER_GRAPH 4
       -headings  mol_Cu mol_Co mol_Pb mol_Ra mol_SO4 mol_Th mol_Cd
       -chart_title "COPCs with years"
       -axis_scale x_axis 0 5000 auto
       -axis_scale y_axis 1e-8 1e-3 auto auto log
           -axis_scale sy_axis 1e-8 1e-3 auto auto log
       -axis_titles "Years", "Concentration COPCs", "Concentration Ra and Th"
       -initial_solutions false
  -start
 10 x =  (total_time/365/24/60/60)
 20 PLOT_XY x, TOT("Cu"), color = Red, symbol = Square, symbol_size = 6, y-axis = 1
 30 PLOT_XY x, TOT("Co"), color = Yellow, symbol = Square, symbol_size = 6, y-axis = 1
 40 PLOT_XY x, TOT("Pb"), color = Blue, symbol = Square, symbol_size = 6, y-axis = 1
 50 PLOT_XY x, TOT("Ra"), color = Black, symbol = Square, symbol_size = 6, y-axis = 2
 60 PLOT_XY x, TOT("S(6)"), color = Green, symbol = Square, symbol_size = 6, y-axis = 1
 70 PLOT_XY x, TOT("Th"), color = Orange, symbol = Square, symbol_size = 6, y-axis = 2
 80 PLOT_XY x, TOT("Cd"), color = Brown, symbol = Square, symbol_size = 6, y-axis = 1
  -end

USER_GRAPH 5
       -headings  mol_Se mol_As mol_Se(4) mol_Se(6) mol_As(3) mol_As(5)
       -chart_title "COPCs with years"
       -axis_scale x_axis 0 5000 auto
       -axis_scale y_axis 1e-10 1e-1 auto auto log
       -axis_titles "Years", "Concentrations Se and As"
       -initial_solutions false
  -start
10 x =   (total_time/365/24/60/60)
 20 PLOT_XY x, TOT("Se"), color = Red, symbol = Square, symbol_size = 6, y-axis = 1
 30 PLOT_XY x, TOT("As"), color = Yellow, symbol = Square, symbol_size = 6, y-axis = 1
 40 PLOT_XY x, TOT("Se(4)"), color = Blue, symbol = Square, symbol_size = 6, y-axis = 1
 50 PLOT_XY x, TOT("Se(6)"), color = Black, symbol = Square, symbol_size = 6, y-axis = 1
 60 PLOT_XY x, TOT("As(3)"), color = Green, symbol = Square, symbol_size = 6, y-axis = 1
 70 PLOT_XY x, TOT("As(5)"), color = Orange, symbol = Square, symbol_size = 6, y-axis = 1
   -end

USER_GRAPH 6
       -headings  mol_Mo mol_Se mol_V Mo_onSediment Se_onSediment V_onSediment
       -chart_title "Species on Sediment"
```

```
      -axis_scale x_axis 0 5000 auto
      -axis_scale y_axis 1e-10 1e-1 auto auto log
          -axis_scale sy_axis 1e-10 1e-1 auto auto log
      -axis_titles  "Years", "Concentrations Species", "Concentrations Sorbed on Sediment"
      -initial_solutions false
 -start
10 x =   (total_time/365/24/60/60)
 20 PLOT_XY x, TOT("Mo"), color = Red, symbol = Square, symbol_size = 6, y-axis = 1
 30 PLOT_XY x, TOT("Se"), color = Orange, symbol = Square, symbol_size = 6, y-axis = 1
 40 PLOT_XY x, TOT("V"), color = Blue, symbol = Square, symbol_size = 6, y-axis = 1
 50 PLOT_XY x, SURF("Mo","Linear"), color = Green, symbol = Square, symbol_size = 6, y-axis = 2
 60 PLOT_XY x, SURF("Se","Linear"), color = Black, symbol = Square, symbol_size = 6, y-axis = 2
 70 PLOT_XY x, SURF("V","Linear"), color = Brown, symbol = Square, symbol_size = 6, y-axis = 2
  -end

END
```

#Restored Solution 1_Minimal__ClayProtons_PWZonly_071922.phr

```
PRINT
-reset false

KNOBS
        -diagonal_scale
        -step 10
        -pe   5
        -iterations 200
        -tolerance 1e-15
        -convergence_tolerance  1e-8

SELECTED_OUTPUT
   -high_precision       true
   -time                 true
   -ionic_strength       true
   -percent_error        true
-pH       true
-pe       true
-alkalinity          true
-totals U Al As Cd Co Ni Pb Se S(6) Fe(2) Cl Ca Mg Na K Fe C(4) Charge_Dummy
-equilibrium_phases       Gibbsite Gypsum
-molalities YH CaY2 MgY2 YNa KY Hco_OH Hco_OH2+ Hco_O-

USER_PUNCH
-head U_G U_Q U_C Al_G Al_Q Al_C As_G As_Q As_C Cd_G Cd_Q Cd_C Co_G Co_Q Co_C Ni_G Ni_Q Ni_C
Pb_G Pb_Q Pb_C Se_G Se_Q Se_C SO4_G SO4_Q SO4_C Fe(II)_G Fe(II)_Q Fe(II)_C SO4_ppm U_ppm
porevolumes years mol_U(VI) Soln_density ULinear AsLinear CdLinear CoLinear NiLinear PbLinear SeLinear
50 PUNCH        SURF("U(6)","Hfo")
51 PUNCH        SURF("U(6)","Q")
52 PUNCH        SURF("U(6)","Hao")
60 PUNCH        SURF("Al","Hfo")
61 PUNCH        SURF("Al","Q")
62 PUNCH        SURF("Al","Hao")
70 PUNCH        SURF("As","Hfo")
71 PUNCH        SURF("As","Q")
72 PUNCH        SURF("As","Hao")
90 PUNCH        SURF("Cd","Hfo")
91 PUNCH        SURF("Cd","Q")
92 PUNCH        SURF("Cd","Hao")
95 PUNCH        SURF("Co","Hfo")
96 PUNCH        SURF("Co","Q")
97 PUNCH        SURF("Co","Hao")
110 PUNCH       SURF("Ni","Hfo")
111 PUNCH       SURF("Ni","Q")
112 PUNCH       SURF("Ni","Hao")
120 PUNCH       SURF("Pb","Hfo")
```

```
121 PUNCH       SURF("Pb","Q")
122 PUNCH       SURF("Pb","Hao")
140 PUNCH       SURF("Se","Hfo")
141 PUNCH       SURF("Se","Q")
142 PUNCH       SURF("Se","Hao")
170 PUNCH       SURF("S(6)","Hfo")
171 Punch       SURF("S(6)","Q")
172 PUNCH       SURF("S(6)","Hao")
190 PUNCH       SURF("Fe(2)","Hfo")
191 Punch       SURF("Fe(2)","Q")
192 PUNCH       SURF("Fe(2)","Hao")
200 SO4_ppm = TOT("S(6)")*96.066* 1000
201 PUNCH       SO4_ppm
205 U_ppm = TOT("U")*238.02891*1000
206 PUNCH       U_ppm
210 PUNCH       (STEP_NO + .5) / 100
215 PUNCH       (total_time/365/24/60/60)
220 PUNCH       TOT("U(6)")
225 PUNCH       RHO
300 PUNCH       SURF("U","Linear")
301 PUNCH       SURF("As","Linear")
303 PUNCH       SURF("Cd","Linear")
304 PUNCH       SURF("Co","Linear")
306 PUNCH       SURF("Ni","Linear")
307 PUNCH       SURF("Pb","Linear")
309 PUNCH       SURF("Se","Linear")

SOLUTION 1 #Restored EA Solution 1
units     mg/L
pH        4.3 charge
pe        14
temperature     7
Al        7
As        0.06
C(4)      58
Ca        110.0
Cd        0.0150
Co        2
Cl        200.0
Fe        100.0
K         9.0
Mg        6.0
Na        190.0
Ni        9.7
Pb        3.1
S(6)      696
Se        0.08
Si        40.0
```

```
U          100.0

surface
-equilibrate 1
Hco_     0.0197   0.5        882
-no_edl

EQUILIBRIUM_PHASES
O2(g) -0.68
Gibbsite 1.2 0
Gypsum          0 0
```

#Restored Solution 1_Minimal__ClayProtonsOreZone_071922.phr

```
PRINT
-reset false

KNOBS
        -diagonal_scale
        -step 10
        -pe   5
        -iterations 200
        -tolerance 1e-15
        -convergence_tolerance  1e-8

SELECTED_OUTPUT
   -high_precision       true
   -time                 true
   -ionic_strength       true
   -percent_error        true
-pH       true
-pe       true
-alkalinity          true
-totals U Al As Cd Co Ni Pb Se S(6) Fe(2) Cl Ca Mg Na K Fe C(4) Charge_Dummy
-equilibrium_phases       Gibbsite Gypsum
-molalities YH CaY2 MgY2 YNa KY Hco_OH Hco_OH2+ Hco_O-

USER_PUNCH
-head U_G U_Q U_C Al_G Al_Q Al_C As_G As_Q As_C Cd_G Cd_Q Cd_C Co_G Co_Q Co_C Ni_G Ni_Q Ni_C
Pb_G Pb_Q Pb_C Se_G Se_Q Se_C SO4_G SO4_Q SO4_C Fe(II)_G Fe(II)_Q Fe(II)_C SO4_ppm U_ppm
porevolumes years mol_U(VI) Soln_density ULinear AsLinear CdLinear CoLinear NiLinear PbLinear SeLinear
50 PUNCH        SURF("U(6)","Hfo")
51 PUNCH        SURF("U(6)","Q")
52 PUNCH        SURF("U(6)","Hao")
60 PUNCH        SURF("Al","Hfo")
61 PUNCH        SURF("Al","Q")
62 PUNCH        SURF("Al","Hao")
70 PUNCH        SURF("As","Hfo")
71 PUNCH        SURF("As","Q")
72 PUNCH        SURF("As","Hao")
90 PUNCH        SURF("Cd","Hfo")
91 PUNCH        SURF("Cd","Q")
92 PUNCH        SURF("Cd","Hao")
95 PUNCH        SURF("Co","Hfo")
96 PUNCH        SURF("Co","Q")
97 PUNCH        SURF("Co","Hao")
110 PUNCH       SURF("Ni","Hfo")
111 PUNCH       SURF("Ni","Q")
112 PUNCH       SURF("Ni","Hao")
120 PUNCH       SURF("Pb","Hfo")
```

```
121 PUNCH       SURF("Pb","Q")
122 PUNCH       SURF("Pb","Hao")
140 PUNCH       SURF("Se","Hfo")
141 PUNCH       SURF("Se","Q")
142 PUNCH       SURF("Se","Hao")
170 PUNCH       SURF("S(6)","Hfo")
171 Punch       SURF("S(6)","Q")
172 PUNCH       SURF("S(6)","Hao")
190 PUNCH       SURF("Fe(2)","Hfo")
191 Punch       SURF("Fe(2)","Q")
192 PUNCH       SURF("Fe(2)","Hao")
200 SO4_ppm = TOT("S(6)")*96.066* 1000
201 PUNCH       SO4_ppm
205 U_ppm = TOT("U")*238.02891*1000
206 PUNCH       U_ppm
210 PUNCH       (STEP_NO + .5) / 100
215 PUNCH       (total_time/365/24/60/60)
220 PUNCH       TOT("U(6)")
225 PUNCH       RHO
300 PUNCH       SURF("U","Linear")
301 PUNCH       SURF("As","Linear")
303 PUNCH       SURF("Cd","Linear")
304 PUNCH       SURF("Co","Linear")
306 PUNCH       SURF("Ni","Linear")
307 PUNCH       SURF("Pb","Linear")
309 PUNCH       SURF("Se","Linear")

SOLUTION 1 #Restored EA Solution 1
units     mg/L
pH        4.3 charge
pe        14
temperature     7
Al        7
As        0.06
C(4)      58
Ca        110.0
Cd        0.0150
Co        2
Cl        200.0
Fe        100.0
K         9.0
Mg        6.0
Na        190.0
Ni        9.7
Pb        3.1
S(6)      696
Se        0.08
Si        40.0
```

```
U          100.0

surface
-equilibrate 1
Hco_     0.00355 0.5        159
-no_edl

EQUILIBRIUM_PHASES
O2(g) -0.68
Gibbsite 1.2 0
Gypsum          0 0
```

#50% Restored Solution 1_Minimal_ClayProtons_071922.phr

```
PRINT
-reset false

KNOBS
        -diagonal_scale
        -step 10
        -pe   5
        -iterations 200
        -tolerance 1e-15
        -convergence_tolerance  1e-8

SELECTED_OUTPUT
   -high_precision       true
   -time                 true
   -ionic_strength       true
   -percent_error        true
-pH       true
-pe       true
-alkalinity          true
-totals U Al As Cd Co Ni Pb Se S(6) Fe(2) Cl Ca Mg Na K Fe C(4) Charge_Dummy
-equilibrium_phases       Gibbsite Gypsum
-molalities YH CaY2 MgY2 YNa KY Hco_OH Hco_OH2+ Hco_O-

USER_PUNCH
-head U_G U_Q U_C Al_G Al_Q Al_C As_G As_Q As_C Cd_G Cd_Q Cd_C Co_G Co_Q Co_C Ni_G Ni_Q Ni_C
Pb_G Pb_Q Pb_C Se_G Se_Q Se_C SO4_G SO4_Q SO4_C Fe(II)_G Fe(II)_Q Fe(II)_C SO4_ppm U_ppm
porevolumes years mol_U(VI) Soln_density ULinear AsLinear CdLinear CoLinear NiLinear PbLinear SeLinear
50 PUNCH        SURF("U(6)","Hfo")
51 PUNCH        SURF("U(6)","Q")
52 PUNCH        SURF("U(6)","Hao")
60 PUNCH        SURF("Al","Hfo")
61 PUNCH        SURF("Al","Q")
62 PUNCH        SURF("Al","Hao")
70 PUNCH        SURF("As","Hfo")
71 PUNCH        SURF("As","Q")
72 PUNCH        SURF("As","Hao")
90 PUNCH        SURF("Cd","Hfo")
91 PUNCH        SURF("Cd","Q")
92 PUNCH        SURF("Cd","Hao")
95 PUNCH        SURF("Co","Hfo")
96 PUNCH        SURF("Co","Q")
97 PUNCH        SURF("Co","Hao")
110 PUNCH       SURF("Ni","Hfo")
111 PUNCH       SURF("Ni","Q")
112 PUNCH       SURF("Ni","Hao")
120 PUNCH       SURF("Pb","Hfo")
```

```
121 PUNCH       SURF("Pb","Q")
122 PUNCH       SURF("Pb","Hao")
140 PUNCH       SURF("Se","Hfo")
141 PUNCH       SURF("Se","Q")
142 PUNCH       SURF("Se","Hao")
170 PUNCH       SURF("S(6)","Hfo")
171 Punch       SURF("S(6)","Q")
172 PUNCH       SURF("S(6)","Hao")
190 PUNCH       SURF("Fe(2)","Hfo")
191 Punch       SURF("Fe(2)","Q")
192 PUNCH       SURF("Fe(2)","Hao")
200 SO4_ppm = TOT("S(6)")*96.066* 1000
201 PUNCH       SO4_ppm
205 U_ppm = TOT("U")*238.02891*1000
206 PUNCH       U_ppm
210 PUNCH       (STEP_NO + .5) / 100
215 PUNCH       (total_time/365/24/60/60)
220 PUNCH       TOT("U(6)")
225 PUNCH       RHO
300 PUNCH       SURF("U","Linear")
301 PUNCH       SURF("As","Linear")
303 PUNCH       SURF("Cd","Linear")
304 PUNCH       SURF("Co","Linear")
306 PUNCH       SURF("Ni","Linear")
307 PUNCH       SURF("Pb","Linear")
309 PUNCH       SURF("Se","Linear")

SOLUTION 1 #50% of Restored Solution #1 and GRW-011
units     mg/L
pH        5.1 charge
pe        1.40E+01
temperature       7.00E+00
Al        3.53E+00
As        3.07E-02
C(4)      7.23E+01
Ca        6.01E+01
Cd        7.52E-03
Co        1.00E+00
Cl        1.04E+02
Fe        5.05E+01
K         5.51E+00
Mg        3.80E+00
Na        9.82E+01
Ni        4.86E+00
Pb        1.55E+00
S(6)      3.51E+02
Se        4.01E-02
Si        3.21E+01
```

```
U          5.01E+01

surface
-equilibrate 1
Hco_     0.00355 0.5        159
-no_edl

EQUILIBRIUM_PHASES
O2(g) -0.68
Gibbsite 1.2 0
Gypsum          0 0
```

#BackgroundGroundwater_USS_OB_bnd_071922.phr

```
PRINT
-reset false

KNOBS
        -diagonal_scale
        -step 10
        -pe   5
        -iterations 200
        -tolerance 1e-15
        -convergence_tolerance  1e-8

SELECTED_OUTPUT
   -high_precision      true
   -time              true
   -ionic_strength      true
   -percent_error       true
-pH      true
-pe      true
-alkalinity        true
-totals U Al As Cd Co Ni Pb Se S(6) Fe(2) Cl Ca Mg Na K Fe C(4) Charge_Dummy
-equilibrium_phases      Gibbsite Gypsum
-molalities YH CaY2 MgY2 YNa KY Hco_OH Hco_OH2+ Hco_O-

USER_PUNCH
-head U_G U_Q U_C Al_G Al_Q Al_C As_G As_Q As_C Cd_G Cd_Q Cd_C Co_G Co_Q Co_C Ni_G Ni_Q Ni_C
Pb_G Pb_Q Pb_C Se_G Se_Q Se_C SO4_G SO4_Q SO4_C Fe(II)_G Fe(II)_Q Fe(II)_C SO4_ppm U_ppm
porevolumes years mol_U(VI) Soln_density ULinear AsLinear CdLinear CoLinear NiLinear PbLinear SeLinear
50 PUNCH       SURF("U(6)","Hfo")
51 PUNCH       SURF("U(6)","Q")
52 PUNCH       SURF("U(6)","Hao")
60 PUNCH       SURF("Al","Hfo")
61 PUNCH       SURF("Al","Q")
62 PUNCH       SURF("Al","Hao")
70 PUNCH       SURF("As","Hfo")
71 PUNCH       SURF("As","Q")
72 PUNCH       SURF("As","Hao")
90 PUNCH       SURF("Cd","Hfo")
91 PUNCH       SURF("Cd","Q")
92 PUNCH       SURF("Cd","Hao")
95 PUNCH       SURF("Co","Hfo")
96 PUNCH       SURF("Co","Q")
97 PUNCH       SURF("Co","Hao")
110 PUNCH      SURF("Ni","Hfo")
111 PUNCH      SURF("Ni","Q")
112 PUNCH      SURF("Ni","Hao")
120 PUNCH      SURF("Pb","Hfo")
121 PUNCH      SURF("Pb","Q")
```

```
122 PUNCH       SURF("Pb","Hao")
140 PUNCH       SURF("Se","Hfo")
141 PUNCH       SURF("Se","Q")
142 PUNCH       SURF("Se","Hao")
170 PUNCH       SURF("S(6)","Hfo")
171 Punch       SURF("S(6)","Q")
172 PUNCH       SURF("S(6)","Hao")
190 PUNCH       SURF("Fe(2)","Hfo")
191 Punch       SURF("Fe(2)","Q")
192 PUNCH       SURF("Fe(2)","Hao")
200 SO4_ppm = TOT("S(6)")*96.066* 1000
201 PUNCH       SO4_ppm
205 U_ppm = TOT("U")*238.02891*1000
206 PUNCH       U_ppm
210 PUNCH       (STEP_NO + .5) / 100
215 PUNCH       (total_time/365/24/60/60)
220 PUNCH       TOT("U(6)")
225 PUNCH       RHO
300 PUNCH       SURF("U","Linear")
301 PUNCH       SURF("As","Linear")
303 PUNCH       SURF("Cd","Linear")
304 PUNCH       SURF("Co","Linear")
306 PUNCH       SURF("Ni","Linear")
307 PUNCH       SURF("Pb","Linear")
309 PUNCH       SURF("Se","Linear")

SOLUTION 1
units     mg/L
pH        6.45 charge
pe        15.5481
temperature     7
Al        3.70E-02
As        3.00E-04
C(4)      33.9
Ca        2.70E+00
Cd        1.00E-05
Co        4.00E-04
Cl        7.08E+00
Fe        4.05E-01
K         2.80E+00
Mg        1.80E+00
Na        2.90
Ni        1.80E-03
Pb        1.00E-04
S(6)      1.90E+00
Se        8.00E-04
Si        2.62E+01
U         5.00E-04
```

```
# BackgroundGroundwater_LSS_bnd_071922.phr
PRINT
-reset false

KNOBS
        -diagonal_scale
        -step 10
        -pe   5
        -iterations 200
        -tolerance 1e-15
        -convergence_tolerance  1e-8

SELECTED_OUTPUT
   -high_precision      true
   -time              true
   -ionic_strength      true
   -percent_error       true
-pH      true
-pe      true
-alkalinity        true
-totals U Al As Cd Co Ni Pb Se S(6) Fe(2) Cl Ca Mg Na K Fe C(4) Charge_Dummy
-equilibrium_phases      Gibbsite Gypsum
-molalities YH CaY2 MgY2 YNa KY Hco_OH Hco_OH2+ Hco_O-

USER_PUNCH
-head U_G U_Q U_C Al_G Al_Q Al_C As_G As_Q As_C Cd_G Cd_Q Cd_C Co_G Co_Q Co_C Ni_G Ni_Q Ni_C
Pb_G Pb_Q Pb_C Se_G Se_Q Se_C SO4_G SO4_Q SO4_C Fe(II)_G Fe(II)_Q Fe(II)_C SO4_ppm U_ppm
porevolumes years mol_U(VI) Soln_density ULinear AsLinear CdLinear CoLinear NiLinear PbLinear SeLinear
50 PUNCH       SURF("U(6)","Hfo")
51 PUNCH       SURF("U(6)","Q")
52 PUNCH       SURF("U(6)","Hao")
60 PUNCH       SURF("Al","Hfo")
61 PUNCH       SURF("Al","Q")
62 PUNCH       SURF("Al","Hao")
70 PUNCH       SURF("As","Hfo")
71 PUNCH       SURF("As","Q")
72 PUNCH       SURF("As","Hao")
90 PUNCH       SURF("Cd","Hfo")
91 PUNCH       SURF("Cd","Q")
92 PUNCH       SURF("Cd","Hao")
95 PUNCH       SURF("Co","Hfo")
96 PUNCH       SURF("Co","Q")
97 PUNCH       SURF("Co","Hao")
110 PUNCH      SURF("Ni","Hfo")
111 PUNCH      SURF("Ni","Q")
112 PUNCH      SURF("Ni","Hao")
120 PUNCH      SURF("Pb","Hfo")
121 PUNCH      SURF("Pb","Q")
```

```
122 PUNCH       SURF("Pb","Hao")
140 PUNCH       SURF("Se","Hfo")
141 PUNCH       SURF("Se","Q")
142 PUNCH       SURF("Se","Hao")
170 PUNCH       SURF("S(6)","Hfo")
171 Punch       SURF("S(6)","Q")
172 PUNCH       SURF("S(6)","Hao")
190 PUNCH       SURF("Fe(2)","Hfo")
191 Punch       SURF("Fe(2)","Q")
192 PUNCH       SURF("Fe(2)","Hao")
200 SO4_ppm = TOT("S(6)")*96.066* 1000
201 PUNCH       SO4_ppm
205 U_ppm = TOT("U")*238.02891*1000
206 PUNCH       U_ppm
210 PUNCH       (STEP_NO + .5) / 100
215 PUNCH       (total_time/365/24/60/60)
220 PUNCH       TOT("U(6)")
225 PUNCH       RHO
300 PUNCH       SURF("U","Linear")
301 PUNCH       SURF("As","Linear")
303 PUNCH       SURF("Cd","Linear")
304 PUNCH       SURF("Co","Linear")
306 PUNCH       SURF("Ni","Linear")
307 PUNCH       SURF("Pb","Linear")
309 PUNCH       SURF("Se","Linear")

SOLUTION 1
units     mg/L
pH        6.45926 charge
pe        15.5388
temperature     7
Al        4.60E-02
As        1.30E-03
C(4)      8.66E+01
Ca        9.82E+00
Cd        9.89E-06
Co        9.75E-05
Cl        7.20E+00
Fe        8.60E-01
K         2.00E+00
Mg        1.59E+00
Na        6.10E+00
Ni        9.99E-05
Pb        9.91E-05
S(6)      4.70E+00
Se        9.98E-05
Si        2.41E+01
U         6.95E-04
```

#Lake Bottom Sediments_071922.phr

```
SOLUTION_MASTER_SPECIES
Charge_dummy Charge_dummy- 0 Charge_dummy- 1

SOLUTION_SPECIES
Charge_dummy- = Charge_dummy-
log_k 0

SURFACE_MASTER_SPECIES
Linear Linear

SURFACE_SPECIES
Linear = Linear
Linear + H2AsO4- = LinearH2AsO4-
    -log_k -96.02
Linear + Cd+2 = LinearCd+2
        -log_k -96.82
Linear + Co+2 = LinearCo+2
    -log_k -97.60
Linear + Ni+2 = LinearNi+2
    -log_k -97.05
Linear + Pb+2 = LinearPb+2
    -log_k -95.92
Linear + SeO4-2 = LinearSeO4-2
    -log_k -96.70
Linear + UO2CO3 = LinearUO2CO3
    -log_k -96.70

solution
units   mg/L
pH      6.45
pe      14
temp    7
Al      0.037
As      0.0003
C(4)    33.9
Ca      2.7
Cd      0.00001
Co      0.0004
Cl      6.86
Fe      0.405
K       2.8
Mg      1.8
Na      2.9
Ni      0.0018
Pb      0.0001
S(6)    1.9
Se      0.0008
```

```
Si        26.2
U         0.0005
Charge_dummy 1000     charge

SURFACE
-equilibrate 1
    Linear 1e100 1 1
-no_edl

EQUILIBRIUM_PHASES
O2(g) -0.68
Gibbsite 1.2 0
```

#OB_Porosity 0.18_Minimal_071922.phr

```
solution
units   mg/L
pH      6.45 charge
pe      14
temp    7
Al      0.037
As      0.0003
C(4)    33.9
Ca      2.7
Cd      0.00001
Co      0.0004
Cl      6.86
Fe      0.405
K       2.8
Mg      1.8
Na      2.9
Ni      0.0018
Pb      0.0001
S(6)    1.9
Se      0.0008
Si      26.2
U       0.0005

exchange
Y 0.0190
-equilibrate 1

surface
-equilibrate 1
Hfo_    0.00142 60      7.01
-no_edl

Hao_s   0.000169        97      84.7
Hao_w   0.00339
Hao_ww          0.00339
-no_edl

QOH     0.00243         0.31    2053
-no_edl

EQUILIBRIUM_PHASES
O2(g) -0.68
Gibbsite 1.2 0
```

#OB_Porosity 0.22_Minimal_071922.phr

```
solution
units     mg/L
pH        6.45 charge
pe        14
temp      7
Al        0.037
As        0.0003
C(4)      33.9
Ca        2.7
Cd        0.00001
Co        0.0004
Cl        6.86
Fe        0.405
K         2.8
Mg        1.8
Na        2.9
Ni        0.0018
Pb        0.0001
S(6)      1.9
Se        0.0008
Si        26.2
U         0.0005

exchange
Y 0.0181
-equilibrate 1

surface
-equilibrate 1
Hfo_      0.00135 60          6.67
-no_edl

Hao_s     0.000161            97          80.6
Hao_w     0.00322
Hao_ww              0.00322
-no_edl

QOH       0.00231             0.31        1953
-no_edl

EQUILIBRIUM_PHASES
O2(g) -0.68
Gibbsite 1.2 0
```

#OB_Porosity 0.25_Minimal_071922.phr

```
solution
units   mg/L
pH      6.45 charge
pe      14
temp    7
Al      0.037
As      0.0003
C(4)    33.9
Ca      2.7
Cd      0.00001
Co      0.0004
Cl      6.86
Fe      0.405
K       2.8
Mg      1.8
Na      2.9
Ni      0.0018
Pb      0.0001
S(6)    1.9
Se      0.0008
Si      26.2
U       0.0005

exchange
Y 0.0174
-equilibrate 1

surface
-equilibrate 1
Hfo_    0.00130 60      6.41
-no_edl

Hao_s   0.000155        97      77.5
Hao_w   0.00310
Hao_ww          0.00310
-no_edl

QOH     0.00222         0.31    1878
-no_edl

EQUILIBRIUM_PHASES
O2(g) -0.68
Gibbsite 1.2 0
```

#USS_Porosity 0.02_Minimal_042522.phr

```
solution
units   mg/L
pH      6.45 charge
pe      14
temp    7
Al      0.037
As      0.0003
C(4)    33.9
Ca      2.7
Cd      0.00001
Co      0.0004
Cl      6.86
Fe      0.405
K       2.8
Mg      1.8
Na      2.9
Ni      0.0018
Pb      0.0001
S(6)    1.9
Se      0.0008
Si      26.2
U       0.0005

exchange
Y 0.00160
-equilibrate 1

surface
-equilibrate 1
Hfo_    0.000119        60      0.59
-no_edl

Hao_s   0.0000142       97      7.09
Hao_w   0.000284
Hao_ww          0.000284
-no_edl

QOH     0.000203        0.31    172
-no_edl

EQUILIBRIUM_PHASES
O2(g) -0.68
Gibbsite 1.2 0
```

#DSZ_Porosity0.2_Minimal_071922.phr

```
solution
units     mg/L
pH        6.46 charge
pe        14
temperature     7
Al        0.052
As        0.0013
C(4)      86.6
Ca        9.82
Cd        0.00001
Co        0.0001
Cl        7.2
Fe        0.86
K         2
Mg        1.6
Na        6.10
Ni        0.0001
Pb        1.00E-04
S(6)      4.7
Se        1.00E-04
Si        24.1
U         7.00E-04

exchange
Y 0.0186
-equilibrate 1

surface
-equilibrate 1
Hfo_      0.00138 60        6.84
-no_edl

Hao_s     0.000165          97        82.68
Hao_w     0.0033
Hao_ww          0.0033
-no_edl

QOH       0.00237           0.31      2003
-no_edl

EQUILIBRIUM_PHASES
O2(g) -0.68
Gibbsite 1.2 0
```

#LSS and ISS_Porosity0.01_Minimal_071922.phr

```
solution
units     mg/L
pH        6.46 charge
pe        14
temperature     7
Al        0.052
As        0.0013
C(4)      86.6
Ca        9.82
Cd        0.00001
Co        0.0001
Cl        7.2
Fe        0.86
K         2
Mg        1.6
Na        6.10
Ni        0.0001
Pb        1.00E-04
S(6)      4.7
Se        1.00E-04
Si        24.1
U         7.00E-04

exchange
Y 0.000806
-equilibrate 1

surface
-equilibrate 1
Hfo_      0.0000600       60        0.296
-no_edl

Hao_s     0.00000716      97        3.58
Hao_w     0.000143
Hao_ww          0.000143
-no_edl

QOH       0.000103        0.31      86.8
-no_edl

EQUILIBRIUM_PHASES
O2(g) -0.68
Gibbsite 1.2 0
```

#Paleoweathered_NewAq_Minimal_071922.phr

```
solution
units     mg/L
pH        6.7 charge
pe        14
temperature     7
Al        0.034
As        0.05
C(4)      154
Ca        6.76
Cd        0.00001
Co        0.01
Cl        86.5
Fe        0.49
K         5.6
Mg        3.09
Na        76.1
Ni        0.015
Pb        0.0001
S(6)      4.55
Se        0.0001
Si        9.18
U         0.01239

exchange
Y 0.0483
-equilibrate 1

surface
-equilibrate 1

Hao_s   0.0004293         97        215
Hao_w   0.0086
Hao_ww          0.0086
-no_edl

QOH     7.06E-04          0.31      596
-no_edl

EQUILIBRIUM_PHASES
O2(g) -0.68
Gibbsite 1.2 0
```

References

Bachmaf, S., Merkel, B., 2010. Sorption of Uranium (VI) at the Clay Mineral-Water Interface. Environmental Earth Sciences 63, 925–934. July. **https://doi.org/10.1007/s12665-010-0761-6**

Bradbury M.H., Baeyens B., 2009. Sorption Modelling on Illite Part I: Titration Measurements and the Sorption of Ni, Co, Eu and Sn. Geochimica et Cosmochimica Acta.; 73:990–1003. doi: 10.1016/j.gca.2008.11.017

Chen, M.A., Kocar, B.D., 2018. Radium Sorption to Iron (Hydr)oxides, Pyrite, and Montmorillonite: Implications for Mobility. Environ. Sci. Technol. 52, 4023–4030. **https://doi.org/10.1021/acs.est.7b05443**

Dong, W., Wan, J., 2014. Additive Surface Complexation Modeling of Uranium (VI) Adsorption onto Quartz-Sand Dominated Sediments. Environmental Science & Technology 48, 6569–6577. **https://doi.org/10.1021/es0606327**

Dzombak, D.A., Morel, F.M.M., 1991. Surface Complexation Modeling: Hydrous Ferric Oxide. Wiley.

Goldberg S. 2014. Macroscopic Experimental and Modeling Evaluation of Selenite and Selenate Adsorption Mechanisms on Gibbsite. Soil Sci. Soc. Am. J. 78:473–479.

Guo, Z., Li, Y., Wu, W., 2009. Sorption of U(VI) on goethite: Effects of pH, Ionic Strength, Phosphate, Carbonate and Fulvic Acid. Applied Radiation and Isotopes 67, 996–1000. **https://doi.org/10.1016/j.apradiso.2009.02.001**

LaFlamme, B.D., Murray, J.W., 1987. Solid / Solution Interaction: The Effect of Carbonate Alkalinity on Adsorbed Thorium. Geochimica et Cosmochimica Acta 51, 243–250. February. **https://doi.org/10.1016/0016-7037(87)90235-3**

Landry, C.J., Koretsky, C.M., Lund, T.J., Schaller, M.S., 2009. Surface complexation modeling of Co(II) adsorption on mixtures of hydrous ferric oxide, quartz and kaolinite. Geochimica et Cosmochimica Acta 73, 3723–3737. July. **https://doi.org/10.1016/j.gca.2009.03.028**

Lövgren, L., Sjöberg, S., Schindler, P.W., 1990. Acid/Base Reactions and Al(III) Complexation at the Surface of Goethite. Geochimica et Cosmochimica Acta 54, 1301–1306. May. **https://doi.org/10.1016/0016-7037(90)90154-D**

Manning, B.A., Goldberg, S., 1996. Modeling Competitive Adsorption of Arsenate with Phosphate and Molybdate on Oxide Minerals. Soil Science Society of America Journal, 60, 121-131.

Mathur, S.S. and Dzombak, D.A. 2006. Surface Complexation: Goethite. In, Surface Complexation Modelling, J. Lutzenkirchen (editor). Elsevier. p443.

NRC (Nuclear Regulatory Commission), 1995. A Uniform Approach to Surface Complexation Modeling of Radionuclide Sorption. Report No. CNWRA 95-001. January.

Peacock, C.L., Sherman, D.M., 2004. Vanadium (V) Adsorption onto Goethite (α-FeOOH) at pH 1.5 to 12: A Surface Complexation Model Based on ab Initio Molecular Geometries and EXAFS Spectroscopy. Geochimica et Cosmochimica Acta 68, 1723–1733. **https://doi.org/10.1016/j.gca.2003.10.018**

Piqué, A., Pekala, M., Molinero, J., Duro, L., Trinchero, P., de Vries, L.M. 2013. Updated model for radionuclide transport in the near-surface till at Forsmark: Implementation of decay chains and sensitivity analyses. Amphos[21] Consulting S.L. Report prepared for Svensk Kärnbränslehantering AB, Swedish Nuclear Fuel and Waste Management Co. Document R-13-02. February 2013.

Prikryl, J.D., Jain, A., Turner, D.R., Pabalan, R.T., 2001. Uranium VI Sorption Behavior on Silicate Mineral Mixtures. Journal of Contaminant Hydrology, 47, 241–253.

Riese, A.C., 1982. Adsorption of Radium and Thorium onto Quartz and Kaolinite: A Comparison of Solution/Surface Equilibria Models. Ph.D. Submission. Colorado School of Mines, Golden, Colorado. September.

Schaller, M.S., Koretsky, C.M., Lund, T.J., Landry, C.J., 2009. Surface Complexation Modeling of Cd(II) Adsorption on Mixtures of Hydrous Ferric Oxide, Quartz and Kaolinite. J Colloid Interface Sci 339, 302–309. **https://doi.org/10.1016/j.jcis.2009.07.053**

Wazne, M., Korfiatis, G.P., Meng, X., 2003. Carbonate Effects on Hexavalent Uranium Adsorption by Iron Oxyhydroxide. Environmental Science and Technology 37, 3619–3624. **https://doi.org/10.1021/es034166m**

Appendix F Summary of Results from Metallurgical Testing

F.1 Summary of Metallurgical Test Work

This summary of results is focused on the metallurgical test work done to support an understanding of the:

a) mineralogy and hydrogeochemical changes in the ore and barrier zones as a result of the lixiviant (mining solution) injections;

b) the composition of the uranium bearing solution (UBS) at the end of mining and prior to any remediation; and

c) water quality and secondary mineral phases formed during remediation of the ore zone.

Metallurgical testing completed, the objectives and results of the work, and the information carried forward for discussion in this response are summarized in Table F-1.

Further details on the metallurgical testing, including the sample information for cores (e.g., mineralogy, location, U content, depth), test conditions (e.g., duration, # of iterations, column length, flow rate, temperature, pressure, sample frequency, influent/effluent composition) are provided in the sections below. All data presented herein are from the metallurgical test programs used to support the 2018 Prefeasibility Study (Denison 2018) and the Feasibility Study (Denison 2023).

Table F-1: Summary of Metallurgical Testing

Years	Description	Objective	Results	Information informing IR-20, IR-67 and IR-69
2017-2018	Batch leach tests and bottle roll/agitation leach tests	Early testing of leaching with alkaline and acidic based lixiviants	Supported decision for Acid Leaching	No discussion herein; very preliminary testing.
	A column leach test conducted using sulfuric acid followed, which also included simulated groundwater restoration tests.	Initial column test with acid leaching and evaluation of groundwater remediation	Early indication of groundwater remediation needs	Water Quality of UBS at the end of mining and Restoration Phase/flushing solution (groundwater remediation)
2021	Column leach tests on blended crushed ore	Test leach recoveries on a range of feed grades. Determine potential recovery and generate a representative sample for process plant testing.	Operationally, the feed sample for Column 1 is was verified as a reasonable blend to represent ISR wellfield production of UBS. Groundwater remediation with groundwater and alkaline solutions	Water Quality of UBS at the end of mining and Restoration Phase/flushing solution (groundwater remediation). Mineralogy.
2022	Column leach and remediation tests on crushed and screened core from individual hydrogeologic units	• Develop information to support geochemical modelling of the deposit, including leaching and neutralization phases. • Generate a detailed chemical and mineralogical characterization of the dominant hydrogeological units(HGUs) within the ore zone • Evaluate behaviour of different HGUs during ISR and neutralization, in particular those hosting the majority of the resource. • Compare the efficacy of neutralization of different HGUs, with the use of dilute sodium hydroxide	Uranium leachability was found to vary amongst the HGUs. Also, there were some indications of an HGU ("2A") to be avoided during operations to prevent clay mobilization.	Water Quality of UBS at the end of mining.
2018	Static uranium ore dissolution (jar) test on intact core	Room temperature, 1,138 hours (48 days) exposure of drill core to concentrated sulphuric acid (35 g/L) in a very slow-motion shaker.	Provided visual indication that with sufficient soak time, lixiviant will penetrate into intact high grade uranium pieces. The incomplete recoveries at the end of the tests can be attributed largely to requiring longer residence time	No discussion herein; testing limited to visual information.
2018-2022	Coreflood tests on intact core in 2018 to 2022	Simulate the in situ field conditions, to understand and develop the lixiviant conditions necessary for successful full-scale ISR. Objectives were to: evaluate the rate of uraninite dissolution and changes in permeability of the core with leaching; generate laboratory scale test results applicable to planning the 2022 field test; and delineate a life-of-well-pattern production profile.	Results were inconsistent in the early work (Coreflood 1 to 3C) due to highly variable reagent dosages in this pioneering work. Coreflood 4 and 5 (2021-ongoing). In Coreflood 4, as uranium mass gradually leached away, there was a mild trend of increasing flow rate at the same pressure, indicating permeability increase. Lessons learned from past testing, particularly with respect to reagent adjustments, were put into practice with this testing to enable completion of the longest test run to support the feasibility work. In total, 51.8% of the initial dry mass of the sample was removed by leaching; 50% of this was the result of uranium leaching. Feed grade was 26.66% U_3O_8. In Coreflood 5 is ongoing and is focused on HGU 2B, which has the majority of contained uranium, highest grade and highest natural permeability. The methodology was different from the other coreflood tests in that the flow was directed through a pencil hole in core. Cumulative recovery at end of February 2023 was 33%.	Water Quality of UBS at the end of mining and Restoration Phase/flushing solution (groundwater remediation). Mineralogy.
2022	Feasibility field test (FFT) leaching and remediation in 2022	The FFT was a full-scale proof of concept in an ISR method; to demonstrate injection of lixiviant and recovery of UBS from the CSW test pattern. Injection was into 1 well (GWR-041).	After pH below 3 was achieved in GWR-041, active leaching of uranium began. UBS grade from GWR-041 rose while pH declined. Uranium grade trended upwards to 25 g/L over four days, while injection pressure decreased. This suggests that leaching played a role in reducing resistance to flow. A peak sample grade of 43 g/L U was collected from GWR-041 after a further three days, so the acid injection phase was ended (on October 12). A global leaching recovery curve could be developed using the field testing and coreflood tests.	No discussion included herein.

F.2 2018 Column Leach and Groundwater Restoration Test

In early 2018, a column leach test with acid lixiviant was performed. The core material used for testing came from three drill holes. Select intervals of overlying very low-grade sandstone was blended with very high-grade intervals to create a composite feed grade of 24.2% U. Details on the core material used in the leach tests are provided in Appendix A to this response, in Table F-A1.

A total of 137 pore volumes (PVs) of uranium bearing solution (UBS) was generated at flow rate ranging between 2 to 4 PV/d. A 90% recovery was achieved with a peak individual sample uranium grade of 27.4 g/L and average UBS grade of 8.4 g/L U. Following the leaching, the column was flushed with simulated groundwater to simulate groundwater restoration. Analytical results from the first pore volume of water removed from the column during the restoration phase are incorporated into the range in UBS composition at the end of mining presented in Table F-2.

Flushing of the column with simulated groundwater (Phase 1 of restoration) was continued for 84 pore volumes. Phase 2 (RPV 84-108) circulated simulated ore zone water quality fortified with 1 g/L Bicarbonate [from $NaHCO_3$]. The test simulated the operation of a Reverse Osmosis (RO) water treatment step where solution exiting the column would be treated prior to being re-introduced. Phase 3 (RPV 108-114) re-established injection of simulated groundwater quality. The objective of this phase was to displace the bicarbonate and to ensure ground water stability once the circulation of fluid is halted. Analytical results for groundwater collected during this restoration process are shown in Table F-9 and Table F-10. Information presented in those tables is discussed further in Section F-9.

F.3 Column and Coreflood Tests

The following were common to all column and coreflood tests performed**:**

- The pore volume was determined by pumping water (deionized water, site groundwater) into each column or core until filled.
- Temperature was controlled to 10°C by placing the apparatus in a walk-in cooler.
- An online UBS or Remediation/Flushing Solution sample was taken daily.

Table F-2: UBS Chemistry at end of Leaching (Mining)

Test	Units	Coreflood 2B (2021)	Coreflood 3C	Number of Samples	Range of Values of UBS constituent concentrations across Metallurgical tests from 2018-2021 representative of End of mining conditions		Baseline Ore Zone Groundwater Chemistry
Sample Name		**D-CF2B-57**	**D-CF3C-142**		**Minimum**	**Maximum**	**GWR-032 (2021-06-04)**
Acidity	mg/L			5	65000	87000	
Bicarbonate	mg/L	-	-	6	0	<1	118
Carbonate	mg/L			5	<1	<1	<1
Chloride	mg/L			1	<10	1220	220
Hydroxide	mg/L			0	<1	<1	<1
P. alkalinity	mg/L			0	<1	<1	<1
pH	pH units	2.1	1.1	13	0.63	2.10	6.83
Specific Conductance	uS/cm			9	52100	303000	860
Eh	mV			10	580	870	
Sum of ions	mg/L			5	52700	70100	504
Total alkalinity	mg/L			5	<1	<1	97
Total hardness	mg/L			5	202	1480	182
Nitrate	mg/L			5	<4	<40	<0.04
Fluoride	mg/L			5	1	34	0.23
Total dissolved solids	mg/L			5	8970	47900	599
Calcium	mg/L	557	723	13	58	723	55
Magnesium	mg/L	47	<63	13	<10	240	11
Potassium	mg/L	148.8	<86	13	6.2	149	4.6
Sodium	mg/L	17.9	<77	13	6.0	12300	81
Aluminum, dissolved	mg/L	1738	71	13	69	4609	0.0006
Antimony, dissolved	mg/L			5	0.040	1	<0.0002
Arsenic, dissolved	mg/L	<0.1	<1	13	<0.1	21	0.2
Barium, dissolved	mg/L	<0.1	<1	13	<0.05	<0.5	0.063
Beryllium, dissolved	mg/L			5	0.07	0.4	<0.0001
Boron, dissolved	mg/L			1	<1	<10	0.43
Cadmium, dissolved	mg/L	<0.1	<1	13	0.018	1.809	<0.00001
Chromium, dissolved	mg/L	9.1403	<1	13	<0.1	9.140	<0.0005
Cobalt, dissolved	mg/L	5.41	<1	12	0.5	15	<0.0001
Copper, dissolved	mg/L	5.16	10.23	13	5.2	964	<0.0002
Iron, dissolved	mg/L	3309	4094	13	820	4094	4.2
Lead, dissolved	mg/L	0.97	19.45	13	0.20	19	<0.0001
Manganese, dissolved	mg/L	16.35	<81	13	2.70	41	0.22
Molybdenum, dissolved	mg/L	1.65	59.57	13	1.65	60	0.0038
Nickel, dissolved	mg/L	15.7	<1	13	<1	27	0.001
Selenium, dissolved	mg/L	18.4	<1	13	<0.025	26	<0.0001
Silver, dissolved	mg/L			5	<0.005	<0.05	<0.00005
Strontium, dissolved	mg/L	5.2	<1	7	0.60	5	1.66
Thallium, dissolved	mg/L	-	-	5	0.05	<0.2	<0.0002
Tin, dissolved	mg/L	-	-	5	0.07	0.30	-
Titanium, dissolved	mg/L			5	2.80	32	<0.0002
Uranium, dissolved	mg/L	7.45E+03	3.88E+04	13	7.70E+02	3.88E+04	1.10E-02
Vanadium, dissolved	mg/L	160.88	62.57	13	6.16	161	<0.0001
Zinc, dissolved	mg/L	134.37	4.03	13	2.30	331	2.62
Sulfur	mg/L	9,263	22,877	13	5211	209411	4.3
Phosphorous	mg/L	-	75.4	13	2	75	<0.01
Silica, soluble, dissolved	mg/L	-	-	6	31	192	13.3
Radium-226*	Bq/L	-	-	4	230	3000	180
Radium-228*	Bq/L	-	-	1	5	5	-
Lead-210*	Bq/L	-	-	4	600	1700	2200
Polonium-210*	Bq/L	-	-	4	290	2000	110
Thorium-230*	Bq/L	-	-	4	21000	220000	7
Thorium-232*	Bq/L	-	-	4	2	12	-
Radium-226*	mg/L	-	-	4	6.29E-06	8.21E-05	4.92E-06
Thorium-230*	mg/L	-	-	4	2.75E-02	2.88E-01	9.17E-06

Notes

* Analytical results for radionuclides are limited. The ranges of radionuclide concentrations (Bq/L) provided are considered conservative because they reflect composite samples collected over the ISR leaching period in the 2021 column samples, not UBS at the end of mining

Analytical results for Coreflood 2B and 3C are provided (in addition to the range of UBS Constituent Concentrations) because results from the remediation portion of these tests was used for development of the Restored Solutions modelled in the draft EIS (Appendix 7-C)

Used to highlight baseline groundwater quality in the ore zone for comparison with UBS Composition at end of mining.

F.4 2021 UBS Column Tests

The objective of the 2021 column tests was to test leach recoveries on a range of feed grades. Four samples were generated from nine drill holes, all proximal to the WS Shear where most of the resource lies. The samples contain varying amounts of uraninite, sulphides, clay and iron and represent blends of the various hydrogeologic units within the deposit (HGUs). Samples were crushed to -10 mm. Columns with a diameter of ~100 mm were packed with the samples. Four column tests were conducted, with details for each sample listed in Table F-3.

The 2021 column tests used the full-size distribution of crushed core and achieved relatively high mineral liberation in contact with lixiviant. This results in relatively rapid leach kinetics compared to intact core. The initial flow rate was calculated based on a retention time of eight hours (3 column pore volumes per day (PV/d)).

Table F-3: Summary of Samples for Column Test 1 to 4

Column No.	Sample ID	Mass (g)	Feed U_3O_8 (wt%)[a]	HGUs in Blend[b]	Hole IDs	Number of PVs - Leaching	Number of PVs - Remediation
1	Sample A	27,338	48.1	2A/B/C/D	GWR-10, 16, 19, 21	116	6.7 (D.I. Water)
2	Sample B	18,619	46.1	2B	GWR-10, 19, 23, 26	120.4	16.5 (Site GW, 10g/L NaOH Solution)
3	Sample D	9,180	1.8	2A/C/D/E	GWR-15, 16, 19, 26	14.7	15.5 (Site GW, 10g/L NaOH Solution)
4	Samples C&E	8,742	26.9	2A/C/D/E	GWR-01, 19, 22	29.7	11.2 (Site Water, 1.5g/L NaHCO3)

Notes

[a] Back Calculated

[b] HGUs = Hydrogeological Units in the Ore Zone

A single pass flow of dilute sulfuric acid and hydrogen peroxide lixiviant was run between 22 to 38 days. Lixiviant strength was generally decreased over the course of each run. UBS composition from each of the column leach tests at the end of leaching is shown in Table F-2.

On completion of the leaching tests, each column was flushed with water (de-ionized water or groundwater) and for columns #2, #3 and #4, neutralization of groundwater was evaluated using alkaline solutions. Solutions used and porewater volumes flushed are summarized in Table F-3. Analytical results for solution composition during the remediation phase are included in Table F-9 and Table F-10.

Mineralogy of the column samples pre-testing were analyzed by XRD and QEMSCAN; the mineral assemblages aligned with the overall understanding of the ore zone mineralogy as presented in Table 3-1. XRD results for the fine particles are provided as Table F-4. These results show the formation of secondary sulphate minerals during the uranium ore leaching process. The other mineral phases are associated with the (pre-mining) ore zone mineralogy (Table 3-1).

Table F-4: XRD Results for Fine Particles in UBS, Column Experiments #1 to #4 (2021)

Mineral Phase	Column #1	Column # 2	Column #3	Column #4
Anglesite	18.1	9.8	-	6.6
Anhydrite	7	-	-	-
Biotite	-	38	24.2	8.3
Chlinochlore	62.6	21.2	20.3	20.1
Gypsum	-	4.4	-	-
Kaolinite	-	22	41.1	57
Quartz	-	-	5.4	-
Pyrite	12.3	4.6	8.9	7.1

Notes

Secondary Minerals

F.5 2022 Column Leaching and Remediation Tests

A suite of 5 column leaching tests was undertaken to support remediation planning. Whereas core flood testing may more realistically represent the ISR conditions with respect to operational conditions (i.e., using intact core and pressure applied), this phase of column testing used crushed material to accelerate the testing process and, thus, provide key information on the remediation phase and prepare for the (2022) field feasibility study.

The 2022 column testing program consisted of five 100mm diameter columns loaded with samples from different HGUs providing characterization of ore variability. The samples were selected from a blend of assay sample splits of fresh core from GWR-054 through GWR-061, supplemented by preserved core from GWR-016, GWR-022 and GWR-024 stored frozen by Denison. The hole locations are shown Figure F-1 ranging along the length of the deposit. Intervals from five to eight different drill holes were composited to meet required sample mass and/or to meet representativeness for each HGU.

The samples were hand crushed to minimize fines generation, to a maximum size of 30 mm. Minimum size fraction was +0.212 mm by wet screening out fines. This was designed to promote flow through the column and minimize exposed mineral surface area. Overall procedures were like 2021 column tests. The lixiviant was a mixture of sulphuric acid and hydrogen peroxide and was prepared using Wheeler River groundwater. Lixiviant was injected upwards in essentially flooded plug flow conditions. The flow rate was calculated based on ~0.67 measured column

PV/d. Test parameter variables were minimized, so the differences between HGUs could be distinguished.

Initially, all five columns were fed lixiviant from a common tank. The low-grade columns 2A and 2E were run until fully leached. From that point forward, 2A and 2E were fed from a separate tank to perform groundwater flush and neutralization. A summary of details of the column tests including pore volumes during leaching, during post-leaching flushing with groundwater, and during neutralization are provided in Table F-5.

UBS composition at the end of the leaching period is provided in Table F-2, and groundwater quality following the groundwater flushing and neutralization is provided in Table F-9 and Table F-10.

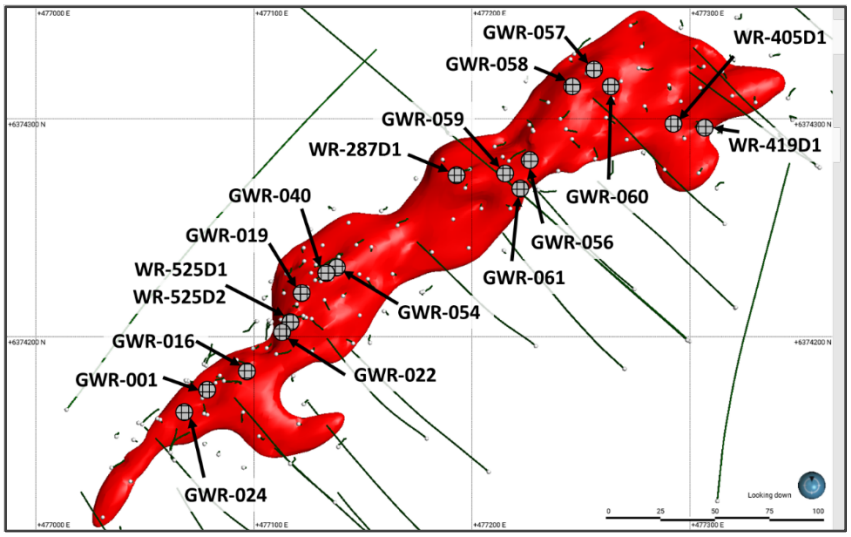

Figure F-1: Metallurgical Hole Locations for 2022 Column Leach Testing

Table F-5: 2022 Column Leach Testing Details

Columns	2a	2b	2c	2d	2e
Estimated Grade (wt % U3O8)	5.0%	58.3%	41.3%	46.1%	1.6%
	Numbers of Pore Volumes				
Phase 1: Groundwater equilibration	2.9	3.1	3.0	2.8	3.1
Phase 2: In-Situ Recovery (ISR)	20.8	66.7	64.1	62.4	19.4
Phase 3: Groundwater Flushing	15.0	16.2	15.1	11.6	14.9
Phase 4: Neutralization	4.4	4.2	11.0	2.6	3.7
Total Pore Volumes	43.1	90.3	93.1	79.4	41.1
pH at end of Phase 2	0.93	0.95	0.91	0.91	0.95
pH at end of Phase 4	9.53	7.1	3.8	7.22	7.87

QEMSCAN was done on the column pre-testing and at the end of the flushing period. The results are presented as Table F-6. Mineral phases that reflect basement-derived materials in the ore zone residuals include biotite, spodumene, petalite and garnet.

Table F-6: 2022 Column Leach Test QEMSCAN results

QEMSCAN	Column 2a		Column 2b		Column 2c		Column 2d		Column 2e	
	Pre-Test (Feed)	Post-Test (Residuals)	Pre-Test (Feed)	Post-Test (Residuals)	Pre-Test (Feed)	Post-Test (Residuals)	Pre-Test (Feed)	Post-Test (Residuals)	Pre-Test (Feed)	Post-Test (Residuals)
Mineral	**2A-BATCH-1**	**DCL-2a-R**	**2B-BATCH-1**	**DCL-2b-R**	**2C-BATCH-1**	**DCL-2c-R**	**2D-BATCH-1**	**DCL-2d-R**	**2E-BATCH-1**	**DCL-2e-R**
Anglesite		3.84		3.28		3.99		14.18		1.15
Biotite	4.84	1.38	0.25	0.44	4.26	0.83	1.16	1.41	2.96	1.98
Bornite	0.36	0.07					0.70	1.15	0.43	0.20
Calcite			0.42	0.69		0.14				
Chalcocite (CuS)			1.54		0.28		0.31		1.28	
Chalcopyrite	12.37	13.03	0.71	2.27	0.11	0.16		0.25	8.76	3.48
Chlorite				3.15						
Clinochlore-(Fe)		11.34				0.8		9.39		52.26
Covellite (CuS)	0.35	0.38	0.19	2.61	0.39	1.34	0.06	0.18	0.10	0.20
Fe-oxide		0.03				1.15		0.53		0.03
Galena	0.63	0.40	0.43	1.23	0.25	0.3	0.53	3.06	0.10	0.02
Garnet	0.25				2.52		1.47		0.43	
Goethite-Clay mix	4.31	0.03	0.35	0.10	7.37	16.78	10.95	1.66	1.52	0.41
Illite	0.21	0.52		0.05					0.32	0.67
Ilmenite		0.08				0.09				0.47
Kaolinite	42.04	40.41	1.52	3.28	7.12	11.67	0.75	2.09	62.20	28.63
Muscovite	9.46	6.09	0.79	3.35	0.81	1.2	0.15	2.06	13.69	8.79
Petalite		0.15		0.05				0.03		0.02
Pyrite	8.48	10.44	1.49	3.38	0.98	1.58	0.12	0.09		0.84
Quartz	4.40	9.11		1.05	0.05	0.42		1.74	1.01	0.12
Rutile	0.61	0.58	0.07	0.04	0.04	0.04			0.44	0.32
Sphalerite	0.56	0.41		0.04	0.03			0.02		
Spodumene		0.17		0.05		0.16				0.05
Uraninite	10.70	1.07	92.10	74.89	75.74	58.72	83.73	61.93	6.67	0.29
Zircon	0.36	0.45	0.06	0.02		0.04				
Siderite						0.54				

F.6 2018-2022 Coreflood Tests

Core testing machines (CTM) were typically used to study in situ oil recovery processes, for flooding uranium deposit drill core with lixiviant to simulate ISR conditions on a micro scale which are referred to as coreflood tests. All drill cores tested were from vertically oriented drill holes allowing the flow from end to end of the coreholder to simulate flow in the vertical direction of the deposit. This is tangential to the intended predominantly horizontal flow path between wells in situ.

From late 2019 to mid-2021, coreflood tests numbered 1, 2A, 2B, 3A, and 3C were performed. The main objective was to simulate the in situ field conditions, to understand and develop the lixiviant conditions necessary for successful full-scale ISR. Priority was placed on testing a large number of samples over short durations. Tests were ended early, so, uranium recoveries were low relative to later testing (generally < 10%). Results for Coreflood 2B and 3C are discussed further herein.

Coreflood 2B and 3C

Details for the testing of Coreflood 2B and 3C are provided in Table F-7.

Table F-7: 2021 Coreflood Test Details

Coreflood	**2B**		**3C**	
Corehole	GWR-024		GWR-019	
Core Dimensions (average diameter, average length), in mm	60 x100		78*70	
Core Pore volume (mL)	36.9		53.1	
Estimated Grade (wt % U3O8)	24		70.7	
	Number of Pore Volume	pH (at end of Leaching or Remediation Phase)	Number of Pore Volume	pH (at end of Leaching or Remediation Phase)
In-Situ Recovery (ISR)	34.4	2.1	82.7	0.98
Groundwater Flushing	22.7	1.91	91.6	2.83
Neutralization with NaOH	55.6	11.92	-	-
Neutralization with $NaHCO_3$	-	-	62.4	6.87
Post-Neutralization Groundwater Flush	9.3	11.47	17.2	6.43
Total Pore Volumes	122	-	253.9	-

The UBS composition at the end of leaching for Coreflood 2B and 3C is provided in Table F-2. The analytical results for these samples were provided in Table F-2 because Corefloods 2B and 3C were the primary basis for the development of the restored solutions. UBS composition during

flushing for these coreflood tests is discussed further in Section F-9 and is summarized in Table F-9 and Table F-10.

At the end of testing, the core from Coreflood 2B was frozen. The frozen core was cut in the middle into two sides. XRD, QEMSCAN and SEM was done on one half of the sample, on the inside cut. The XRD results indicated:

- 19.5 wt% Kaolinite
- 26.7 wt % Montmorillonite
- 45.3 wt % Dickite
- 2.9 % Fluorite
- 5.6 % Pyrite

The cumulative uranium recovery for core 2B was low, and thus the sample (post-leaching) has a mineralogical composition comparable to that of the unmined ore zone. The portion of the sample that underwent mineralogical analysis was also rich in clay minerals. The QEMSCAN results are shown in Figure F-2. The SEM image (not shown) shows the presence of uraninite, pyrite, and sphalerite.

The QEMScan shows a minor amount of mineral phase suggestive of a small amount of jarosite ("Fe-Al-Si-S") closely associated with pyrite. This suggests formation of oxidation products/secondary minerals in the core with exposure to lixiviant.

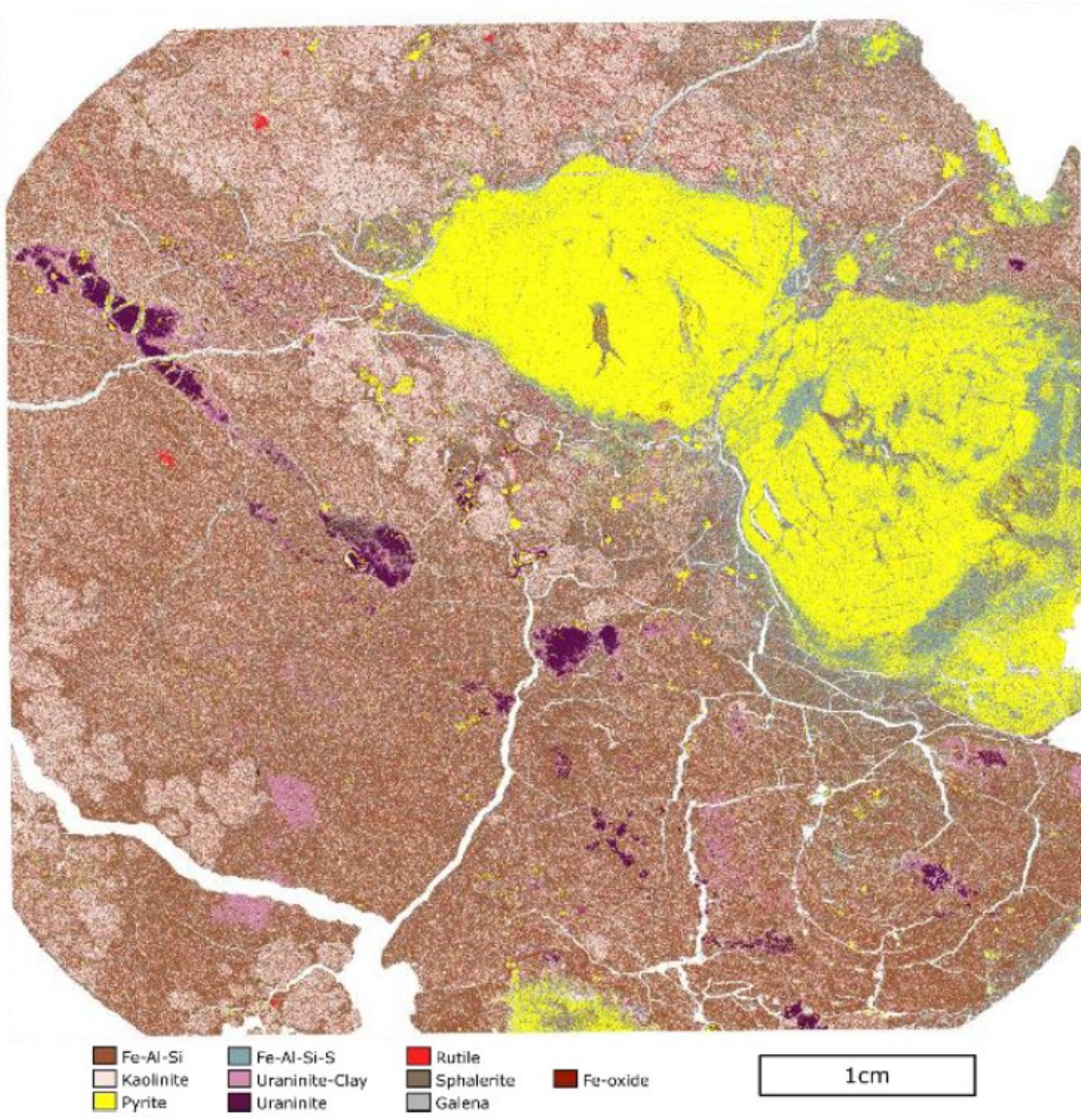

Figure F-2: Coreflood 2, QEMSCAN

Coreflood 4

The Coreflood 4 sample was taken from a high-grade segment of HGU 2C from hole GWR-040, which is the middle CSW in the planned field feasibility test (FFT) well pattern. Thus, it was an excellent candidate to correlate with subsequent FFT results.

Coreflood 4 feed sample side view is shown in Figure F-3Figure. Near-horizontal mineral banding is evident.

Figure F-3: Coreflood 4 Feed Sample Side View, Prior to Placement in Coreflood Machine

Coreflood 4 ran for a total of 113 PVs over 391 days, with life-of-test average UBS grade of 18.7 g/L U and reagent consumptions of 2.78 kg H_2SO_4 and 0.35 kg H_2O_2 per kg U. Part of the difficulty of production ramp-up of Coreflood 4 was due to the flow constraint of low micro scale permeability through the intact core, particularly with generally lower permeability in the vertical flow direction of coreflood samples. As uranium mass gradually leached away, there was a mild trend of increasing flow rate at the same pressure, indicating permeability increase.

In total, 51.8% of the initial dry mass of the sample was removed by leaching. Just over half of the mass loss is accounted for by uranium leaching, and the remainder is accounted for by gangue mineralization leaching. The feed grade was back calculated from measurements of the total uranium in UBS collected throughout the test plus leach residue sections. Feed grade was 26.66% U_3O_8, and final recovery was 97.1%. Coreflood 4 is the most comprehensive simulation of ISR for the Phoenix FS, with the highest recovery demonstrated from an intact core to date.

Coreflood 4 provides the most information about the mineralogical and hydrogeochemical changes that are occurring in the ore zone during mining. Post-leaching, the core leached in Coreflood 4 was cut into segments, as shown in Figure F-4, assayed and visually examined (photographed) for changes to the core due to leaching. The mineralogy of each section was determined.

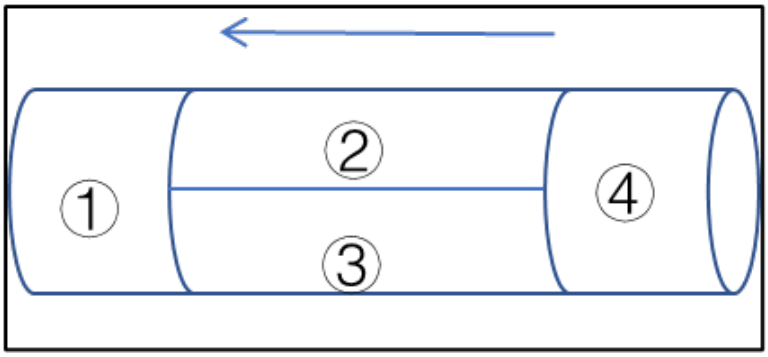

Figure F-4: Coreflood 4 Cut Sections and Direction of Flow

Coreflood 4 feed side puck (Section 4), inlet face view is shown in Figure F-5. The feed end was deeply eroded, nearly through to the discharge side of the section.

Figure F-5: Coreflood 4 Feed Side Puck (Section 4), Inlet Face View

Coreflood 4 middle (Section 2), centre longitudinal cut face view is shown in Figure F-6. It was strongly bleached throughout, with cracks that appeared after drying.

Figure F-6: Coreflood 4 Middle (Section 2), Centre Longitudinal Cut Face View

Coreflood 4 discharge end puck (Section 1), inlet face view, dried, is shown in Figure H-7. It was strongly bleached across the entire cross-section.

Figure F-7: Coreflood 4 Discharge End Puck (Section 1), Inlet Face View, Dried

XRD for each of the sections is given in Table F-8. Mineral phases that reflect basement-derived materials in the ore zone residuals include anorthite.

Table F-8: XRD Results for Coreflood 4 Core Sections

Mineralogical Composition Post-Extraction	D-CF4A-1	D-CF4A-2	D-CF4A-3	D-CF4A-4
Location/section in the coreflood column	Discharge End	Midsection	Midsection	Feed End
Kaolinite (Al2Si2O9H4)	74.7	22.1	38.3	43.8
Pyrite (FeS2)	17.9	20	12.4	16
Chamosite (Mg2.518Fe2.482)Al1.2Si3.8O18H10) (Chlorite Group)	7.3	5.8	1.4	--
Gypsum (CaSO6H4)	--	7.5	4.5	4.8
Barite (BaSO4)	--	1.6	0.7	--
Anorthite (CaSiAl2O8)	--	30.7	31.8	--
Goethite (FeO2H)	--	12.4	10.9	4.3
Anglesite (PbSO4)	--	--	--	31.1

F.7 Composition of the UBS remaining in the Ore Zone at the end of Mining

The analytical results for the UBS composition in Coreflood 2B and 3C are shown in Table F-2, along with a range of UBS composition that was developed from the relevant analytical results for a total of 13 samples from across the column and coreflood tests. The ranges of values for constituents of potential concern (COPCs), as defined in Appendix 7-C of the draft EIS, are provided in Table F-2. Uranium and other COPC concentrations generally vary by 2-3 orders of magnitude. There is expected variability in the UBS composition because of the nature of the deposit, which has been captured in the conditions of the metallurgical testing, and the nature of the testing (e.g., core vs. crushed rock, test duction, lixiviant composition, etc.,). The analytical results were given explicitly for Coreflood 2B and 3C because of the use of results from these coreflood tests to develop the restored solutions, which is discussed further in Section F-9.

F.8 Mineralogical and Hydrogeochemical Changes to the Ore Zone with Mining

Understanding of changes in the mineralogy of the ore zone with mining are informed by the XRD results from Coreflood 4, as this test was terminated at the completion of the ISR process, and QEMSCAN results for the 2022 columns, because these tests provide quantitative information on the mineral assemblage following mining and with remediation. The following conclusions are made with respect to changes in the mineralogy in the ore zone with mining:

- The mining process is effective as leaching uraninite from the ore zone and also results in partial dissolution of sulphide minerals (pyrite, sphalerite, galena, etc.,);

- Secondary sulphate minerals are formed as a result of the mining process. The associated equations are shown in Appendix A. Jarosite minerals were suggested surrounding pyrite particles in the QEMSCAN of Coreflood 2, but were not detected in any of the other post-mining residuals. Gypsum and barite were detected in XRD but not present at quantifiable levels in association with the 2022 column residuals. Formation of anglesite is shown by XRD and QEMSCAN in post-mining residuals.

- The elevated concentration of aluminum in solution evidences clay mineral dissolution, but overall the relative abundance of clays in the ore zone increases with ISR mining, as would be expected with ore dissolution.

The hydrochemistry of the ore zone post-mining is presented in Appendix F, Table F-2. Consistent with the dissolution of parent minerals and the pH of the UBS, most COPCs concentrations in the UBS at the end of mining are elevated with respect to baseline groundwater conditions in the ore zone.

F.9 Composition of the Restored Solutions

The restored solutions were developed using the metallurgical data that were available when conditions in Post-Decommissioning were being conceptualized in 2020-2021 for numerical modelling (presented herein) and effects assessment. This included the early results on acid leaching of the core (2018) and Coreflood 2B and 3C results. At that time, the coreflood tests provided the most detailed information from which to develop the chemistry of the Restored Solutions #1 and #2, using the remediation portion of the tests. From the results of that testing, "Restored Solution #1" and "Restored Solution #2" (Table 3-5) were developed to represent the bounding scenarios for groundwater quality considered in the reactive transport model to evaluate the potential for environmental effects following remediation of the mining area. As is discussed further below, these solution compositions were developed to reflect remediation of the ore zone through flushing and neutralization, without over-neutralization – meaning, base addition past circumneutral conditions to alkaline conditions.

Since that time, more information from the column and coreflood tests has become available that supports the composition of the Restored Solutions put forward in the draft EIS as being representative of porewater within the mining zone with remediation.

When developing the restored solutions for the draft EIS, the approach was generally to select concentrations for any given element/parameter that represented a low to mid-range value for the COPC from the metallurgical testing solutions, to be conservative with respect to evaluating potential effect, but also to reflect the goal of the remediation (to align with ALARA, as is discussed below). For dissolved uranium, the concentration in Restored Solutions #1 and #2 were set to upper bounds of 100 mg/L and 30 mg/L, respectively. In some cases, like Co and Ni, the values selected for modelling were identified to be on the high end upon subsequent metallurgical testing. Thus, the concentrations for these elements modelled are conservative with respect to anticipated pore water concentrations of these elements post-remediation. The basis of the selected concentrations for Restored Solution #1, which was the solution modelled in this report, is provided below in Table F-9. As Restoration Solution #1 contains the higher remaining concentrations, and lower pH (i.e., differs more from baseline conditions in the ore zone), this solution was carried forward for geochemical reactive transport modelling to evaluate environmental effects.

Table F-9: Groundwater Chemistry basis for Restored Solution #1

Metallurgical Test		2018 Pre-Feasibility; Restoration Phase Data	Coreflood 2B	Coreflood 2B	Coreflood 2B	Coreflood 3C	2021 Column, 2	2021 Column, 3	2021 Column, 4	2022 Column, 2a	2022 Column, 2c	2022 Column, 2d	2022 Column, 2e	2022 Column, 2e	Restored Solution #1	Notes on Value Carried Forward in Restored Solution for Model
Sample Name		RPV30-23	D-CF2B-121-143	D-CF2B-134-144,146	D-CF2B-COMBINED-1 (D-CF2B-134-144,146)	D-CF3C-225-237	D-CL2-FW-2	D-CL3-FW-2	D-CL4-FW-2	D-CL2A-68	D-CL2C-114	D-CL2D-111	D-CL2E-63	D-CL2E-68		
Statistic		-	Average Value[a]	Average Value[a]	-	Average Value[a]				-	-	-	-	-		
Remediation Method		GW Flush	NaOH Neutralization	NaOH Neutralization	NaOH Neutralization	Bicarbonate Neutralization	Groundwater	Groundwater	NaOH Neutralization	NaOH Neutratlization	GW Flush	GW Flush	GW Flush	NaOH Neutratlization		
pH	pH units	3.87	4.4	4.42	Same as adjacent (D-CF3C-238-256)	2.97	2.6	2.44	2.66	3.80	2.58	2.46	2.48	4.05	4.3	High end of observed
Eh	mV		520	525		598					570	542	426	648	-	Set in model to reflect oxidized conditions
Pore Volumes of remediation	-	30-32	59-74	69-76		109-130				19.4	15.1	11.6	14.9	18.6	-	
Aluminum, dissolved	mg/L	5.6	9.7	10.3	7.0	<5	5.4	26	9.1	9.0	9.9	12	32.8	15.6	7	Low end of observed
Arsenic, dissolved	mg/L	<0.010	0.17	0.22	0.03	0.48	0.15	0.31	0.1	0.02	0.14	0.06	0.4	0.012	0.06	Low end of observed
Barium, dissolved	mg/L	<0.05	0.10	<0.1	<0.05	<0.1	<0.005	<0.05	<0.05	<0.05	<0.05	<0.05	0.006	0.018	0.05	Mid range of observed
Total Inorganic Carbon (C(4))	mg/L		-	-	-										58	Assumed to be approximately equivalent to GW values and considers some bicabonate
Calcium	mg/L	109	228	210	-	81.7	11	43	23	21	22	380	20	35	110	Mid range of observed
Cadmium, dissolved	mg/L	<0.001	<0.1	<0.1	0.015	<0.1	0.061	0.033	0.020	0.051	0.001	0.004	0.0004	0.0003	0.015	Mid range of observed
Chloride	mg/L	37			-		1	<1	1	33	<1	6	3	9	200	Very limited information available. Set to a higher value to consider potential for values closer to baseline ore zone water quality
Cobalt, dissolved	mg/L		2.8	2.1	2.0	<0.1				0.15	0.03	0.16	0.53	0.42	2	High end of observed
Chromium, dissolved	mg/L	0.04	0.22	0.14	<0.05	<0.1	0.18	0.76	0.16	<0.05	<0.05	<0.05	0.17	0.013	0.05	Mid range of observed
Copper, dissolved	mg/L	2.23	0.21	0.24	0.17	<0.1	6.2	5.8	9.2	25	3.1	3.2	20.1	4.7	0.17	Low end of observed
Fluoride	mg/L	NA	-	-	-		2.4	0.32	1.6	3	6.0	4.2	2	3		No data available at time of developing Restored Solution
Iron, dissolved	mg/L	54.1	378	334	324	13.0	23.2	92	40	124	33	75	74	57	100	Mid range of observed
Potassium	mg/L	<1	10.1	9.5	-	<8	3.5	4.7	1.5	3.7	1.5	5.6	1.9	1.4	9	High end of observed
Magnesium	mg/L	3.7	-	-	-	<6	0.6	11	0.2	3.0	0.4	4.4	38	43	6	Mid range of observed
Manganese, dissolved	mg/L	0.68	9.3	-	3.4	<8	0.57	0.63	0.85	2.0	0.98	4.1	0.31	0.30	3.4	Mid range of observed
Molybdenum, dissolved	mg/L	0.05	0.22	0.22	0.10	<0.1	0.16	2.1	0.10	0.05	0.05	0.03	0.58	0.019	0.1	Mid range of observed
Sodium	mg/L	221	283.2	351.0	-	120	3.1	4.1	2.8	760	3.0	4.3	3.7	378	190	Mid range of observed
Nickel, dissolved	mg/L	0.20	12.8	10.0	9.7	<0.1	0.56	3.2	0.75	0.55	0.06	0.35	1.04	0.92	9.7	High end of observed
Lead, dissolved	mg/L	3.08	2.9	3.41	3.1	1.8	4.97	0.68	0.96	1.3	0.22	0.10	2.64	0.50	3.1	Mid-high range of observed
Sulfate	mg/L	860	2700	2724	-	679	300	750	480	2180	470	1460	690	1220	620	Mid range of observed
Selenium, dissolved	mg/L	<0.025	0.31	0.23	0.08	<0.1	0.39	0.10	0.13	0.01	0.02	0.05	0.042	0.098	0.08	Mid range of observed
Si	mg/L	71.9	-	-	-										40	limited information available; value similar to available data assumed
Strontium, dissolved	mg/L		4.5	4.4	4.4	3.2	0.32	0.70	0.22	0.62	0.43	0.58	0.67	0.76	4.4	Upper range of observed
Zinc, dissolved	mg/L	1.48	1.6	1.4	1.4	0.14	1.7	3.6	3.0	10	0.14		0.20	0.13	1.4	Mid-range of observed
P	mg/L		-	-		<4									4	applied limited information
Uranium	mg/L	105	586	334	338	45.2	92	217	579	145	288	328	38.1	30.8	100	Mid-low end of observed; value set as upper bound in the EIS
Vanadium, dissolved	mg/L	0.09	2.9	0.8	0.51	0.32	0.35	2.8	1.1	0.13	0.70	0.51	1.8	0.006	0.51	Low end of observed
Polonium-210	Bq/L	6.3+/-0.5	-	-	1600	-	-	-	-	-	-	-	-	-		Not modelled (lack of thermodynamic constants)
Radium-228	Bq/L	-	-	-	<10	-	-	-	-	-	-	-	-	-		Not modelled
Thorium-228	Bq/L	-	-	-	<3	-	-	-	-	-	-	-	-	-		Not modelled
Thorium-230	Bq/L	105+/-9.6	-	-	<500	-	-	-	-	-	-	-	-	-		See Below for values in mg/L
Radium-226	Bq/L	65.8+/-0.3	-	-	<200	-	-	-	-	-	-	-	-	-		See Below for values in mg/L
Lead-210	Bq/L	530+/-1.3	-	-	2400	-	-	-	-	-	-	-	-	-		Not modelled (transport behaviour taken into account with Pb
Thorium-232	Bq/L	0.2+/-0.04	-	-	0.05	-	-	-	-	-	-	-	-	-		Not modelled
Radium-226	mg/L	1.80E-06	-	-	<5.47E-06	-	-	-	-	-	-	-	-	-	5.47E-06	Limited data, high end value[b]
Thorium-230	mg/L	1.38E-04	-	-	<6.55E-04	-	-	-	-	-	-	-	-	-	3.93E-06	Limited data set[b]

Notes

Data Available when developing the Restored Solutions for the modelling in Appendix 7-C of the EIS

[a] Arithmetic average values, calculated using detected measurements or where all values were non-detect, assumed the detection limit. pH value is the median, not the arithmetic average.

[b] Limited data set meant that PFS groundwater flushing data at pH 5.8 was also considered in setting this value, with a Th-230 concentration of 2.62E-07 mg/L and a Ra-226 value of 1E-05 mg/L (see Table IR-67-10)

Table F-10: Groundwater Chemistry basis for Restored Solution #2

Metallurgical Test		2018 Pre-Feasibility; Restoration Phase Data			Coreflood 3C	Coreflood 3C	2021 Column, 4	2022 Column, 2b	Restored Solution #2	Notes on Value Carried Forward in Restored Solution for Model
Sample Name		RPV 38-42	RPV 42-53	RPV 54-57	D-CF3C-238-256	D-CF3C-COMBINED-1 (D-CF3C-238-256)	D-CL4-FW-3	D-CL2b-116		
Statistic		-	-	-	Average[a]	-		-		
Remediation Method		GW Flush	Neutralization ($NaHCO_3$)	GW Flush	Bicarbonate Neutralization	Bicarbonate Neutralization	Distilled Water Flush Post NaOH Neutralization	NaOH Neutratlization		
pH	pH units	5.8	8.5	8.3	6.51	Same as adjacent (D-CF3C-238-256)	7.48	6.51	6.1	Low end of Observed
Eh	mV				402		-	387	-	Set in model to reflect oxidized conditions
Pore Volumes of remediation	-	76-84	82-108	-	131-162		-	18.70	-	
Aluminum, dissolved	mg/L	0.27	1.32	4.4	<5	0.56	0.70	10	0.56	Low end of observed
Arsenic, dissolved	mg/L	0.10	0.04	0.06	0.25	0.1	<0.01	0.000259	0.1	Upper end of observed
Barium, dissolved	mg/L	<0.05	0.05	0.04	<0.1	0.05	<0.05	0.2	0.05	Mid range of observed
Total Inorganic Carbon (C(4))	mg/L	-	-	-	-				105	Assumed to be approximately equivalent to GW values and considers some bicabonate neutralization
Calcium	mg/L	28	13	5	48.1		16	127	10	Low end of observed
Cadmium, dissolved	mg/L	0.002	<0.001	<0.001	<0.1	0.004	0.004	<0.1	0.004	Mid range of observed
Chloride	mg/L	15	2	12			6	-	50	Set to a higher value to consider potential for values closer to baseline ore zone water quality
Cobalt, dissolved	mg/L				0.11	<0.01		<0.1	0.01	Low end of observed
Chromium, dissolved	mg/L	<0.01	<0.01	<0.01	<0.1	<0.05	0.05	<0.1	0.05	Mid range of observed
Copper, dissolved	mg/L	0.04	<0.01	<0.01	0.12	<0.02	0.33	0.2	0.02	Low end of observed
Fluoride	mg/L	0.5	1.2	0.8			1.4	-	0.8	Mid range of observed
Iron, dissolved	mg/L	6.13	0.44	1.23	9.1	4.7	1.7	10	4.7	Mid range of observed
Potassium	mg/L	<1	<1	2	<8		1.2	<8	3.5	Mid range of observed
Magnesium	mg/L	<1	<1	<1	6.7		1.2	<6	3	Mid range of observed
Manganese, dissolved	mg/L	0.07	0.02	0.05	<8	0.48	0.28	<8	0.48	Mid range of observed
Molybdenum, dissolved	mg/L	0.03	0.05	<0.005	0.47	0.13	<0.01	0.4	0.13	Mid range of observed
Sodium	mg/L	36	235	87	251		351	887	90	Low range of observed
Nickel, dissolved	mg/L	0.03	<0.01	<0.01	0.10	<0.01	0.21	0.1	0.01	Low end of observed
Lead, dissolved	mg/L	2.13	0.36	0.39	0.20	0.32	0.25	10.0	0.32	Mid range of observed
Sulfate	mg/L	174	117	100	718.7		440	2480	136	Low end of observed
Selenium, dissolved	mg/L	<0.025	<0.025	0.026	0.86	<0.01	0.09	<0.1	0.01	Low end of observed
Si	mg/L	43.7	43.8	44.4				132.6	40	Mid range of observed
Strontium, dissolved	mg/L				2.0	2.4	0.20	0.7	2.4	Upper end of observed
Zinc, dissolved	mg/L	0.08	<0.01	<0.01	0.10	<0.05	0.46	0.1	0.05	Mid-range of observed
P	mg/L				<4			<5	4	applied limited information available
Uranium (mg/L)	mg/L	3.5	4.1	0.5	19.3	26.4	187	38.7	30	Upper End of Observed
Vanadium, dissolved	mg/L	<0.01	0.007	0.03	0.13	0.16	0.03	0.2	0.16	Upper end of observed
Polonium-210	Bq/L	14.9+/-0.3	1.9+/-0.1	2.7+/-0.1	-	280	-	-		Not modelled (lack of thermodynamic constants)
Radium-228	Bq/L	-	-	-	-	<2	-	-		Not modelled
Thorium-228	Bq/L	-	-	-	-	<1	-	-		Not modelled
Thorium-230	Bq/L	0.2+/-0.03	1.36+/-0.14	3.2+/-0.4	-	<100	-	-		See Below for values in mg/L
Radium-226	Bq/L	389+/-0.7	262+/-0.5	129+/-0.4	-	370	-	-		See Below for values in mg/L
Lead-210	Bq/L	301+/-0.7	40+/-0.3	22+/-0.2	-	660	-	-		Not modelled (transport behaviour taken into account with Pb modelled)
Thorium-232	Bq/L	<0.01	<0.01	<0.01	-	0.007	-	-		Not modelled
Radium-226	mg/L	1.06E-05	7.17E-06	3.53E-06	-	1.01E-05	-	-	1.01E-05	Limited data, high end value
Thorium-230	mg/L	2.62E-07	1.78E-06	4.19E-06	-	<1.31E-04	-	-	1.31E-06	Limited data set ; Low end of observed

Notes

Data Available when developing the Restored Solutions for the modelling in Appendix 7-C of the EIS

Data Available when developing the Restored Solutions for the modelling in Appendix 7-C of the EIS, but not considered in the development of Restored Solution #2 as pH was alkaline

[a] Arithmetic average values, calculated using detected measurements or where all values were non-detect, assumed the detection limit. pH value is the median, not the arithmetic average.

F.10 _Remediation of Mining Area within the context of ALARA

Decommissioning of the mining area will continue until recovered water reaches and is demonstrated to be stabilized (maintained) at acceptable mining area decommissioning objectives (Section 2.3.3.1.1 of the Revised Draft EIS). Such decommissioning objectives consider protection of plausible downgradient water uses. For the purpose of the assessment "plausible use" has been determined to be the protection of aquatic life in Whitefish Lake, since the numeric 3D groundwater modelling presented herein has indicated that Whitefish Lake is where groundwater associated with the remediated mining area will discharge to. It is within this frame of reference therefore that the ALARA concept should be considered. That is, ALARA can be defined for the purpose of the remediation of the mining area to the extent that subsequent discharge of groundwater to Whitefish Lake does not adversely affect aquatic biota in the lake.

The metallurgical testing done to date evidences an amelioration of UBS quality post-mining with flushing using groundwater and base (hydroxide or bicarbonate) to a restored solution of pH in the range of 4.5-5.5. The intent of the remediation approach is to raise the pH consistently but incrementally, so as to avoid over-neutralizing and yielding an alkaline solution. Alkaline pH conditions favour the formation of precipitates that are not desired from a physical (clogging) or chemical standpoint (secondary solids formed in place of removal of COPCs in the dissolved-phase from the subsurface). Potential environmental effects were thus evaluated based on plausible use, as defined above, at a pH and groundwater conditions that were shown to be achievable through groundwater flushing and addition of base without the risk of over-neutralization. Restored Solution #1 contains the higher remaining concentrations, and lower pH (i.e., differs more from baseline conditions in the ore zone) and was carried forward for geochemical reactive transport modelling to evaluate environmental effects.

It is noted that the freeze wall will remain in place during mining area remediation (Section 2.3.3.1.1 of the Revised Draft EIS), until decommissioning objectives are achieved to ensure there is no loss of tertiary control of the mining fluid (even in a diluted state). Refinement of the mining area decommissioning objectives and associated modelling will be done as the Project progresses through updates to the Decommissioning Plan; nevertheless, the objectives as they may evolve will be bound by the objectives evaluated in the EIS, which as shown are protective of aquatic biota in Whitefish Lake. The final acceptable mining area decommissioning objectives will be developed prior to initiation of groundwater remediation, as part of the Detailed Decommissioning Plan (DDP).

F.11 References

Denison (Denison Mines Corp), 2018. Prefeasibility Study Report for the Wheeler River Uranium Project, Saskatchewan, Canada. Report dated: September 24, 2018.

Denison (Denison Mines), 2023. Feasibility Study.

Appendix A

2018 Column Leach Testing

Table F-A1: Sample Inventory for 2018 ISR Column Leach Test

Original Sample Purpose	Sample I.D.	WR Hole No.	Lithology	Est. U%	Mass (g)	Mass U (g)
Porosity/Perm.	S066906	419D1	BSMT	0.22	320	0.61
Porosity/Perm.	S066907	525D2	SDST	0.06	323	0.17
Porosity/Perm.	S066908	405D1	SDST	0.06	270	0.14
Porosity/Perm.	S066909	405D1	BSMT	0.08	299	0.21
Porosity/Perm.	S066910	525D1	BSMT	51.72	843	375
Leach Testing	S066911	525D1	SDST	0.06	282	0.17
Leach Testing Composite Sample	S066912-S066916	525D1 525D2	SDST & BSMT	29.4	1,090	276
Leach Testing Total Composite Sample	S066906-S066916	405D1 419D1 525D1 525D2	SDST & BSMT	19.03 (wet)	3,427 (wet)	652.3

Reactions forming secondary sulphate minerals

K-Jarosite

$KFe3(SO4)2(OH)6 + 6H+ = K+ + 3Fe+3 + 2SO4-2 + 6H2O$

Barite

$BaSO4 = Ba+2 + SO4-2$

Anglesite

$PbSO4 = Pb+2 + SO4-2$

Gypsum

$CaSO4:2H2O = Ca+2 + SO4-2 + 2H2O$